

**International Doctorate Program
in Molecular Oncology
and Endocrinology**

**XVI cycle - 2001–2004
Coordinator: Prof. Giancarlo Vecchio**

**“Construction and characterization of a fully human antitumor
immunoRNase selective for ErbB2-positive carcinomas”**

**“Analysis of the role of the membrane transporter
ABCC2/MRP2 in multidrug resistance (MDR)”**

Candidate: Dr Angela Arciello

**University of Naples Federico II
Dipartimento di Biologia e Patologia Cellulare e Molecolare
“L. Califano”**

Administrative Location

Dipartimento di Biologia e Patologia Cellulare e Molecolare “L. Califano”
Università degli Studi di Napoli Federico II

Partner Institutions

Italian Institutions

Università di Napoli Federico II, Naples, Italy

Istituto di Endocrinologia ed Oncologia Sperimentale 'G. Salvatore', CNR, Naples, Italy

Seconda Università di Napoli, Naples, Italy

Università del Sannio, Benevento, Italy

Università di Genova, Genoa, Italy

Università di Padova, Padua, Italy

Foreign Institutions

Johns Hopkins University, Baltimore, MD, USA

Thomas Jefferson University, Philadelphia, PA, USA

National Institutes of Health, Bethesda, MD, USA

Supporting Institutions

Università di Napoli Federico II

Ministero dell'Istruzione, dell'Università e della Ricerca

Istituto Superiore di Oncologia (ISO)

Fondazione Italiana per la Ricerca sul Cancro (FIRC)

Polo delle Scienze e delle Tecnologie per la Vita, Università di Napoli Federico II

Polo delle Scienze e delle Tecnologie, Università di Napoli Federico II

Faculty

Italian Faculty

Giancarlo Vecchio, MD, Co-ordinator

Francesco Beguinot, MD

Francesca Carlomagno, MD

Gabriella Castoria, MD

Pietro Formisano, MD

Antonio Leonardi, MD

Rosa Marina Melillo, MD

Giuseppe Palumbo, PhD

Silvio Parodi, MD

Renata Piccoli, PhD

Antonio Rosato, MD

Massimo Santoro, MD

Donatella Tramontano, PhD

Giancarlo Troncone, MD

Foreign Faculty

National Institutes of Health (USA)

Ettore Appella, MD

Luigi M. De Luca, PhD

Michael M. Gottesman, MD

Silvio Gutkind, PhD

Derek LeRoith, MD

Stephen Marx, MD

Ira Pastan, MD

Johns Hopkins University (USA)

Vincenzo Casolaro, MD

Pierre Coulombe, PhD

James G. Herman MD

Lawrence Lichtenstein, MD

Robert Schleimer, PhD

Thomas Jefferson University (USA)

Carlo M. Croce, MD

Renato L. Baserga, MD

To my parents and Elio

Chapter 1

Construction and characterization of a fully human antitumor immunoRNase selective for ErbB2-positive carcinomas

Chapter 2

Analysis of the role of the membrane transporter ABCC2/MRP2 in multidrug resistance (MDR)

TABLE OF CONTENTS

Chapter 1

Construction and characterization of a fully human antitumor immunoRNase selective for ErbB2-positive carcinomas	6
1. ABSTRACT	7
2. BACKGROUND	8
3. AIMS OF THE STUDY	16
4. MATERIALS AND METHODS	17
4.1 Bacterial Strains	17
4.2 Expression Vectors	17
4.3 Culture Media for Bacterial Strains	17
4.4 Antibodies	20
4.5 Cell lines and Culture Conditions	20
4.6 Preparation of Bacterial Competent Cells and Transformation	20
4.7 Construction of the Chimeric cDNA Encoding hERB-hRNase	21
4.8 Expression of hERB-hRNase	23
4.9 Preparation of Periplasmic Extract for the Isolation of hERB-hRNase	23
4.10 Purification of hERB-hRNase	24
4.10.1 Isolation of hERB-hRNase by two Steps of Affinity Chromatography	24
4.10.2 Isolation of hERB-hRNase by Hydrophobic Interaction Chromatography, Followed by Affinity Chromatography	25
4.10.3 Isolation of hERB-hRNase from the Insoluble Fraction of Bacterial Cells	25
4.11 Gel Electrophoresis (SDS-PAGE)	26
4.11.1 Coomassie Staining	26
4.11.2 Western Blot Analyses	26
4.11.3 RNase Activity	27
4.12 RNase Activity Assays	27
4.13 Binding Assays	27
4.14 Internalization of hERB-hRNase	28
4.15 Cytotoxicity Assays	28
4.16 Stability of the IR	28
4.17 <i>In Vivo</i> Antitumor Activity	29

5. RESULTS AND DISCUSSION	30
5.1 Construction of the Chimeric cDNA Encoding hERB-hRNase	30
5.2 Expression of hERB-hRNase	33
5.3 Purification of hERB-hRNase	35
5.3.1 Isolation of hERB-hRNase by two Steps of Affinity Chromatography	35
5.3.2 Isolation of hERB-hRNase by Hydrophobic Interaction Chromatography (HIC), Followed by Affinity Chromatography	37
5.4 Isolation of hERB-hRNase from the Insoluble Fraction of Bacterial Cells	39
5.5 Analysis of the Ribonucleolytic Activity of hERB-hRNase	41
5.6 Analysis of the Ability of hERB-hRNase to Specifically Recognize ErbB2 Receptor	41
5.7 Internalization of hERB-hRNase by Target Cells	44
5.8 Cytotoxic Effects of hERB-hRNase on Tumor Cells	45
5.9 Stability of hERB-hRNase	48
5.10 <i>In vivo</i> Antitumor Activity of hERB-hRNase	50
6. CONCLUSIONS	51
7. BIBLIOGRAPHY	52

Chapter 2

Analysis of the role of the membrane transporter ABCC2/MRP2 in multidrug resistance (MDR)	57
1. ABSTRACT	58
2. BACKGROUND	59
2.1 Multidrug Resistance (MDR) and ATP-Binding Cassette (ABC) Transporters	59
2.2 Screening for ABC Transporters Involved in MDR	66
2.3 Prostaglandins, as a New Class of Compounds Interacting with ABC Transporters	70
3. AIMS OF THE STUDY	73
4. MATERIALS AND METHODS	74
4.1 Cell Lines and Culture Conditions	74

4.2 Antibodies, Drugs and Chemicals	74
4.3 siRNA Preparation and Transfection	75
4.4 Western Blot Analyses	77
4.5 Analysis of Drug Sensitivity	78
5. RESULTS AND DISCUSSION	80
5.1 Overexpression of the ABC Transporter ABCC2/MRP2 in the Resistant Tumor Cell Line RC0.1	80
5.2 Analysis of the Effect of the MDR-Reversing Agent MK571 on the Resistance Phenotype of RC0.1 Tumor Cell Line	82
5.3 Inhibition of MRP2 Protein Expression by RNA Interference	83
5.4 Analysis of the Effects of siRNA-Mediated MRP2 Silencing on the Resistance Phenotype of RC0.1 Tumor Cell Line	89
5.5 Identification of New Substrates for the ABC Transporter ABCC2/MRP2	91
5.6 Identification of the Cyclopentenone Prostaglandin 15-Deoxy- $\Delta^{12,14}$ -Prostaglandin J ₂ (15-d-PGJ ₂) as a New Substrate of the ABC Transporter MRP2	95
6. CONCLUSIONS	102
7. BIBLIOGRAPHY	103
ACKNOWLEDGEMENTS	114
LIST OF PUBLICATIONS	5/115

LIST OF PUBLICATIONS

- 1) Spalletti-Cernia D, Sorrentino R, Di Gaetano S, Arciello A, Garbi C, Piccoli R, D'Alessio G, Vecchio G, Laccetti P, Santoro M. Antineoplastic ribonucleases selectively kill thyroid carcinoma cells via caspase-mediated induction of apoptosis. *J Clin Endocrinol Metab.* 2003;88:2900-7.
- 2) De Lorenzo C, Arciello A, Cozzolino R, Palmer DB, Laccetti P, Piccoli R, D'Alessio G. A fully human antitumor immunoRNase selective for ErbB-2-positive carcinomas. *Cancer Res.* 2004;64:4870-4.
- 3) Szakács G, Annereau JP, Lababidi S, Shankavaram U, Arciello A, Bussey KJ, Reinhold W, Guo Y, Kruh GD, Reimers M, Weinstein JN, Gottesman MM. Predicting drug sensitivity and resistance: profiling ABC transporter genes in cancer cells. *Cancer Cell.* 2004;6:129-37.
- 4) Annereau JP, Szakács G, Tucker CJ, Arciello A, Cardarelli C, Collins J, Grissom S, Zeeberg B, Reinhold W, Weinstein J, Pommier Y, Paules RS, Gottesman MM. Analysis of ABC transporter expression in drug-selected cell lines by a microarray dedicated to multidrug resistance. *Mol Pharmacol.* 2004.[Epub ahead of print]

Chapter 1

Construction and characterization of a fully human antitumor immunoRNase selective for ErbB2-positive carcinomas

1. ABSTRACT

The aim of the study was the construction and characterization of a novel, fully human immunoRNase (IR). IRs, chimeric proteins made up of a ribonuclease (RNase) molecule fused to an antibody moiety, represent a valid alternative to immunotoxins (ITs). ITs directed to cell surface molecular targets have shown to have a therapeutic potential. However, they also have limitations, mainly represented by nonspecific toxicity and by the immunogenicity of their bacterial or plant toxins. To circumvent some of these problems, toxins have been replaced by mammalian RNases, molecules *per se* not cytotoxic, which become toxic when internalized by target cells. In particular, the use of human RNases, physiologically present in extracellular fluids and tissues, has allowed the construction of immunoconjugates potentially less immunogenic. Obviously, the preparation of fully human IRs is highly desirable to obtain effective and tumor-selective, but also immunocompatible immunoagents.

A novel, fully human IR was prepared in the present study. It is made up of human pancreas RNase (HP-RNase), fused to a human single chain variable fragment (scFv) directed to the ErbB2 receptor. This scFv, named Erbicin, has been isolated in our laboratory from a large human scFv phagemid library. ErbB2, a tyrosine kinase receptor, represents one of the most specific tumor associated antigens (TAA), since this receptor is overexpressed in clinically significant tumors, such as breast, ovary and lung carcinomas. On the other hand, in normal tissues it is expressed only in certain epithelial cell types.

The novel, fully human anti-ErbB2 IR, named hERB-hRNase, was successfully expressed in bacterial cells and isolated from the periplasmic fraction. The characterization of its biological properties showed that the human IR retains the enzymatic activity of the wild-type ribonuclease (HP-RNase) and specifically binds to ErbB2-positive cells with high affinity, as the parental scFv. Furthermore, our studies showed that the human IR undergoes receptor-mediated endocytosis in target cells. In fact, the IR behaves as an immunoprototoxin and upon internalization by target cells becomes selectively cytotoxic in a dose-dependent manner at nanomolar concentrations. Administered in five doses of 1.5 mg/kg to mice bearing an ErbB2-positive tumor, hERB-hRNase induced a dramatic reduction of tumor volume.

The immunoconjugate hERB-hRNase is the first fully human antitumor IR produced so far, with a high potential as a poorly immunogenic human drug devoid of nonspecific toxicity, directed against ErbB2-positive malignancies.

2. BACKGROUND

Conventional anticancer treatments, such as radiation and systemic drugs, are characterized by the lack of tumor cell specificity and the appearance of multidrug resistance (MDR) phenotype (Biedler and Riehm 1970). Immunotherapy represents an alternative and effective strategy to fight cancer, mainly based on antibodies specifically directed to cancer cells expressing a tumor associated antigen (TAA) (Trikha *et al.* 2002; Ross *et al.* 2003). The Food and Drug Administration has approved several monoclonal antibodies as therapeutic agents to treat tumors, and an increasing number are undergoing clinical evaluation (Brekke and Sandlie 2003). Examples of approved antibodies are humanized or human-mouse chimeric monoclonal antibodies, such as anti-ErbB2 trastuzumab (Herceptin) and anti-CD20 rituximab (Rituxan), widely used against breast cancer and non-Hodgkin's lymphoma, respectively (Milenic 2002). To enhance their clinical potential, antibodies also have been coupled to cytotoxic agents or radionuclides (Allen 2002).

Immunotoxins (ITs), made up of antibodies or miniantibodies, such as single chain variable fragments (scFvs), fused to toxins, have been proposed as anticancer drugs during the past two decades (Pastan and FitzGerald 1991; Reiter and Pastan 1998). These chimeric proteins combine the potent toxicity of toxins with the antigen specificity of antibodies. They have been shown to kill cancer cells with IC_{50} values (the concentration for 50% cytotoxicity) in the 0.01-1 nM range (Reiter *et al.* 1994; Wels *et al.* 1995). However, obstacles to full success of ITs in the treatment of cancer include: 1) immunogenicity due to the murine nature of the immunomoieties and the plant or bacterial nature of the toxin moieties; 2) high aspecific toxicity; 3) their large size, which hinders their diffusion into bulky tumors.

These three factors have greatly limited the therapeutic potential of ITs (Weiner *et al.* 1989; Schindler *et al.* 2001), especially because of the occurrence of vascular leak syndrome (Schnell *et al.* 2000; Soler-Rodriguez *et al.* 1993; Baluna and Vitetta 1999). Some of these effects have been alleviated by the development of humanized antibodies and the use of scFvs (single chain variable fragments), consisting of the antigen-binding domains of Ig heavy (V_H) and light (V_L) chain regions connected by a flexible peptide linker (Huston *et al.* 1988), all encoded by a single gene (Fig. 1). scFvs have proved particularly useful, since they can easily penetrate solid tumors, fully preserving the specificity of the parental antibody. However, the toxins themselves remain a problem.

An alternative and more recent strategy in anticancer immunotherapy is that based on immunoconjugates in which the toxin is replaced by a ribonuclease (RNase) molecule (Rybak and Newton 1999) (Fig. 1). The key to this strategy is that mammalian RNases, although *per se* not cytotoxic, become cytotoxic when they are internalized by the target cell, *i.e.* the cell that displays on its surface the epitope recognized by the antibody moiety (Rybak and Newton 1999). This is why the most suitable epitopes for the selection of an antibody for these immunoconjugates are cell receptors, since the anti-receptor antibody can mimic the receptor ligand and be internalized. Thus, these fusion proteins are not ITs but rather immunoprototoxins. They have been called immunoRNases (IRs) (De Lorenzo *et al.* 2002a).

IRs were prepared with various RNases, each fused to a monoclonal antibody raised against a cell receptor (De Lorenzo *et al.* 2002a; Zewe *et al.* 1997; Suwa *et al.* 1999; Stocker *et al.* 2003). The first IR was prepared with bovine pancreatic RNase A (Newton *et al.* 1992) fused to an anti-transferrin receptor antibody, and shown to be cytotoxic to tumor cells expressing the antigen in the 200-500 nM range. Another IR was prepared by fusing onconase, an amphibian RNase isolated from *Rana Pipiens* oocytes, with an anti-CD22 monoclonal antibody against B-cell lymphoma (Newton *et al.* 2001). Satisfactory results were obtained with this immunoconjugate in the treatment of human lymphomas. IRs were also prepared using bovine seminal RNase (BS-RNase). This RNase was shown to possess *per se* a selective anti-tumor activity *in vitro* and *in vivo* (Matousek 1973; Laccetti *et al.* 1994; Pouckova *et al.* 1998; Soucek *et al.* 1996), since it is the only mammalian RNase to be selectively internalized by tumor cells. Immunoconjugates were prepared by fusing BS-RNase with a single chain variable fragment (scFv) specific for the oncofetal antigen placental alkaline phosphatase (Deonarain and Epenetos 1998).

The immunocompatibility of IRs as anticancer agents can be greatly improved by the use of human RNases, as they are physiologically present in extracellular fluids and tissues, and are expected to be much less immunogenic than xenogeneic proteins, if not immunogenic at all (Fig. 1). Human RNases used for the construction of IRs include eosinophil-derived RNase (EDN) (Newton *et al.* 1994), angiogenin (Newton *et al.* 1996), and human pancreas ribonuclease (HP-RNase) (Russo *et al.* 1993). IRs, made up of human RNases fused to an anti-transferrin receptor scFv, were prepared (Rybak and Newton 1999). These IRs were cytotoxic to tumor cells with IC₅₀ values in the 5-20 nM range. However, the abundance of the transferrin receptor at the blood-brain barrier (Zewe *et al.* 1997), which can result in the uptake of high amounts of these immunoconjugates by the brain, and the non human origin of the scFv set a limit to the use of these reagents as therapeutic drugs.

A scheme of the IRs produced so far is reported in Table 1.

ImmunoRNases		
TARGET	RNase	AUTHORS
Transferrin receptor	RNase A	Newton <i>et al.</i> 2002
Placental alkaline phosphatase	Bovin seminal RNase (BS-RNase)	Deonarain and Epenetos 1998
CD 22	Onconase	Newton and Rybak 2001
Transferrin receptor	Angiogenin	Newton <i>et al.</i> 1996
Transferrin receptor	Eosinophil-derived RNase (EDN)	Zewe <i>et al.</i> 1997
Transferrin receptor	Human pancreas RNase (HP-RNase)	Zewe <i>et al.</i> 1997
ErbB2 receptor	Human pancreas RNase (HP-RNase)	De Lorenzo <i>et al.</i> 2002
<p>Table 1. Scheme of the IRs produced so far. Human RNases are indicated in red.</p>		

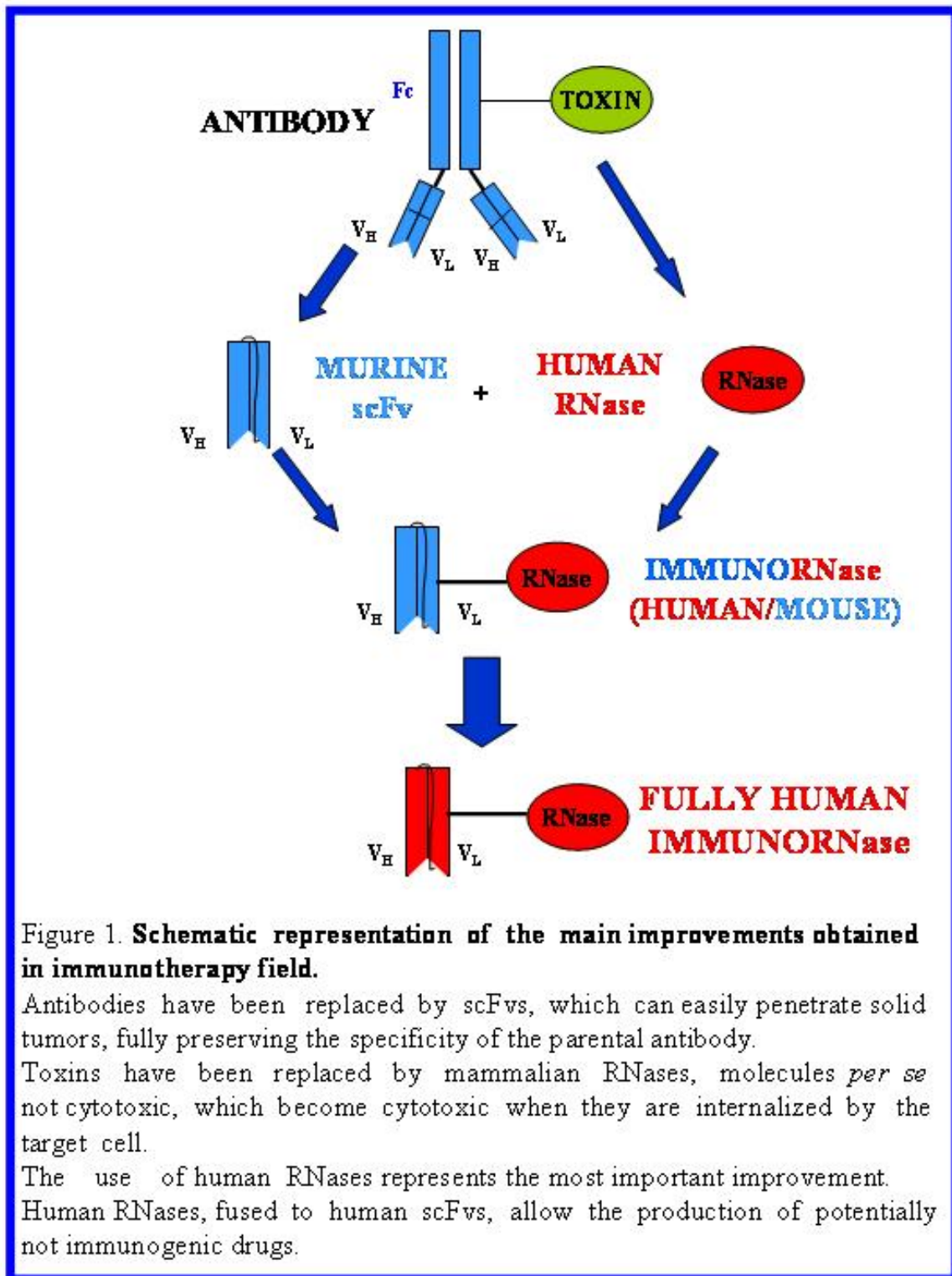


Figure 1. **Schematic representation of the main improvements obtained in immunotherapy field.**

Antibodies have been replaced by scFvs, which can easily penetrate solid tumors, fully preserving the specificity of the parental antibody.

Toxins have been replaced by mammalian RNases, molecules *per se* not cytotoxic, which become cytotoxic when they are internalized by the target cell.

The use of human RNases represents the most important improvement.

Human RNases, fused to human scFvs, allow the production of potentially not immunogenic drugs.

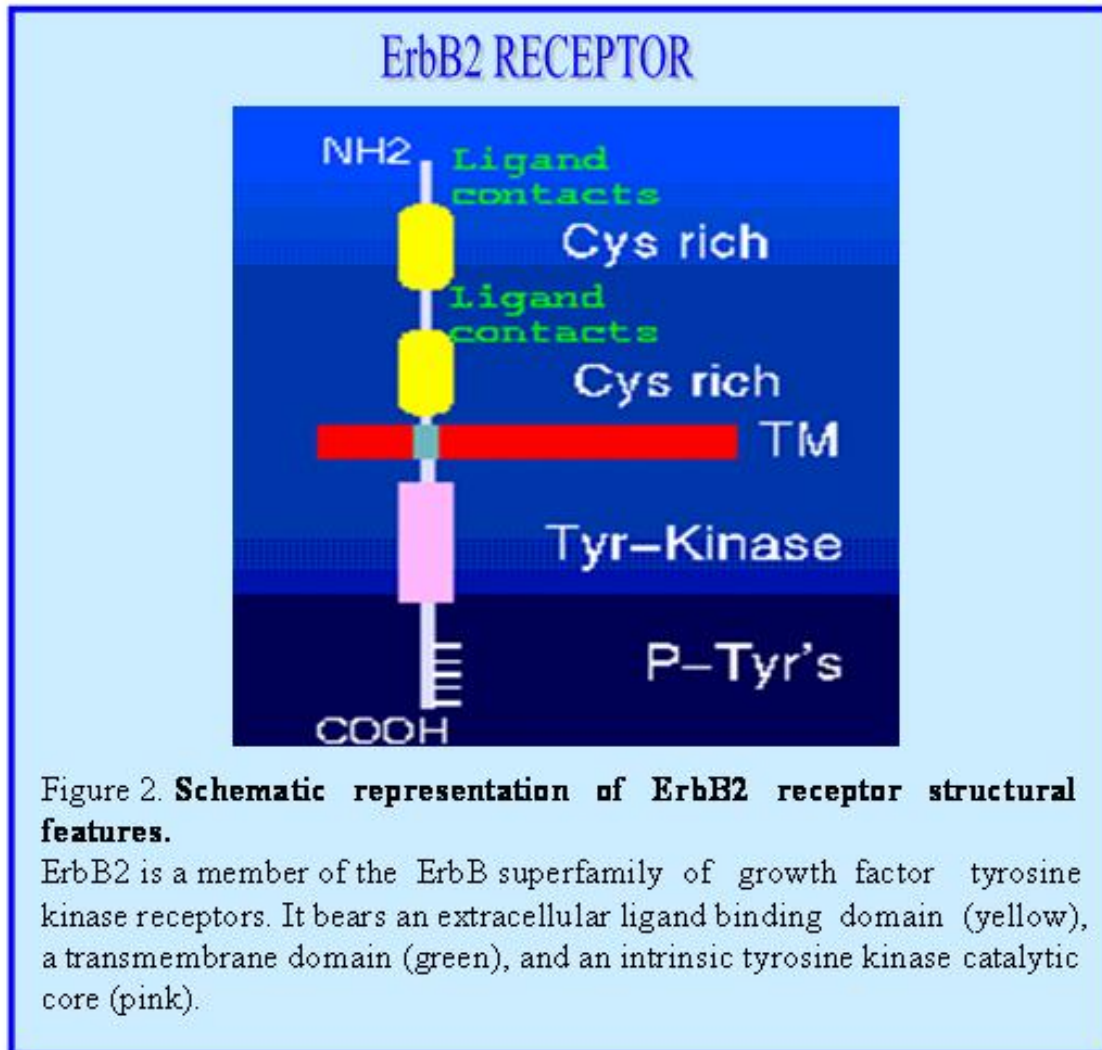
An attractive target for IR-based, directed tumor therapy is the ErbB2 transmembrane receptor. It is a member of the ErbB superfamily of growth factor tyrosine kinase receptors (King *et al.* 1985), homologous to the EGF receptor (King *et al.* 1985, Yamamoto *et al.* 1986). Typical to other tyrosine kinase receptors, ErbB2 bears an extracellular ligand binding domain capable of transmitting a signal that results in the activation of the intracellular portion of the protein (Klapper *et al.* 2000). Central to this activation is an intrinsic tyrosine kinase catalytic core showing close resemblance between the receptors, but wide variety in the flanking sequences enabling diversity of interactions with receptor-specific effector proteins (Klapper *et al.* 2000). Receptor activation results in phosphorylation of specific tyrosine residues located within the receptor's cytoplasmic region, which leads to the recruitment of phosphotyrosine-binding effector proteins, and subsequent simultaneous stimulation of multiple signaling pathways (Klapper *et al.* 2000). The monomeric molecule is inactive but a dimeric form is fully active. The EGF-like ligands act as allosteric modifiers by promoting rapid receptor dimerization (Yarden and Schlessinger 1987). A specific ligand for ErbB2 is still unknown (Klapper *et al.* 2000).

A schematic representation of ErbB2 receptor structural features is reported in Fig. 2.

ErbB2 is highly expressed on several tumor cells, especially in breast, ovary and lung carcinomas (Slamon *et al.* 1989; Tagliabue *et al.* 1991), as well as in salivary gland and gastric tumor-derived cell lines (Fukushige *et al.* 1986; Semba *et al.* 1985). Its overexpression, which occurs most commonly via gene amplification, can reach as many as 2×10^6 molecules/cell. In normal tissues it is expressed at low levels, and only in certain epithelial cell types (Press *et al.* 1990), so we can define this receptor as one of the most specific TAA. ErbB2 plays a key role in the development of malignancy, since it potentiates and prolongs the signal transduction cascades elicited by ligand activation of other ErbB tyrosine kinase receptors (Graus-Porta *et al.* 1997; Ullrich and Schlessinger 1990). Furthermore, overexpression of ErbB2 may also increase resistance of tumor cells to host defenses through the evasion of immune surveillance exerted by activated macrophages (Hudziak *et al.* 1988).

The accessibility of ErbB2 on cell surface and its implication in the development of malignancy make it an attractive target for immunotherapy, since it is internalized upon ligand binding, an event which can be mimicked by an antibody directed towards the receptor that can deliver an RNase into ErbB2-overexpressing tumor cells. Such a strategy has been successfully tested using a murine scFv fused to human pancreas RNase (HP-RNase) (Russo *et al.* 1993). This immunoconjugate, named ERB-HPR (De Lorenzo *et al.* 2002a), was found to be active as a ribonuclease and able to bind and selectively kill ErbB2-positive cells. However, the non human origin of the scFv sets a limit to the therapeutic

potential of this IR. The use of antibody and RNase moieties of human origin for the preparation of fully human IRs is highly desirable to obtain effective and tumor-selective but also immunocompatible immunoagents.



A clear progress in this area of research consisted of the development of the antibody humanization technology with the production of humanized versions of rodent antibodies (Carter *et al.* 1992) with reduced immunogenic potential. A humanized version of an anti-ErbB2 murine antibody (Herceptin) is currently in use for treatment of advanced breast cancer (Milenic 2002). Fully human scFvs have recently been generated with the phage display technology through the expression of large repertoires of antibody variable regions on filamentous phages after their fusion to a phage coat protein (Griffiths *et al.* 1994; Vaughan *et al.* 1996; Sheets *et al.* 1998). Human scFvs specific to ErbB2 have been produced, using for their selection the isolated recombinant extracellular domain (Sheets *et al.* 1998; Schier *et al.* 1995) or more recently breast tumor cells (Poul *et al.* 2000). Given their high affinity for the receptor, these immunoreagents may be considered precious tools as delivery vehicles for specifically directing cytotoxic agents to antigen-bearing tumor cells. However, none of these exhibit antitumor activity.

Taking advantage of phage display technology, a novel human anti-ErbB2 scFv (De Lorenzo *et al.* 2002b) was isolated in our laboratory from a large human scFv phagemid library (Griffiths *et al.* 1994). A double-selection strategy was used and performed on live cells either expressing high levels of the receptor antigen or virtually lacking the antigen. Such a strategy is represented in Fig. 3. The isolated scFv, named Erbicin, specifically binds to ErbB2-positive cells, inhibits receptor autophosphorylation, is internalized in target cells, and strongly inhibits their proliferation (De Lorenzo *et al.* 2002b). These biological properties make the human scFv Erbicin a very promising immunoagent for the diagnosis of specific tumors and also the ideal candidate to deliver cytotoxic molecules specifically to ErbB2-overexpressing tumor cells.

My research project was aimed at the construction and the characterization of a fully human antitumor IR made up of the available human scFv Erbicin fused to human pancreas RNase (HP-RNase). This IR, to our knowledge the first human IR to be produced (De Lorenzo *et al.* 2004), has been termed hERB-hRNase. It has a high potential as a new antitumor drug against ErbB2-positive malignancies, being strong and selective as an anticancer agent, poorly immunogenic and devoid of nonspecific toxicity.

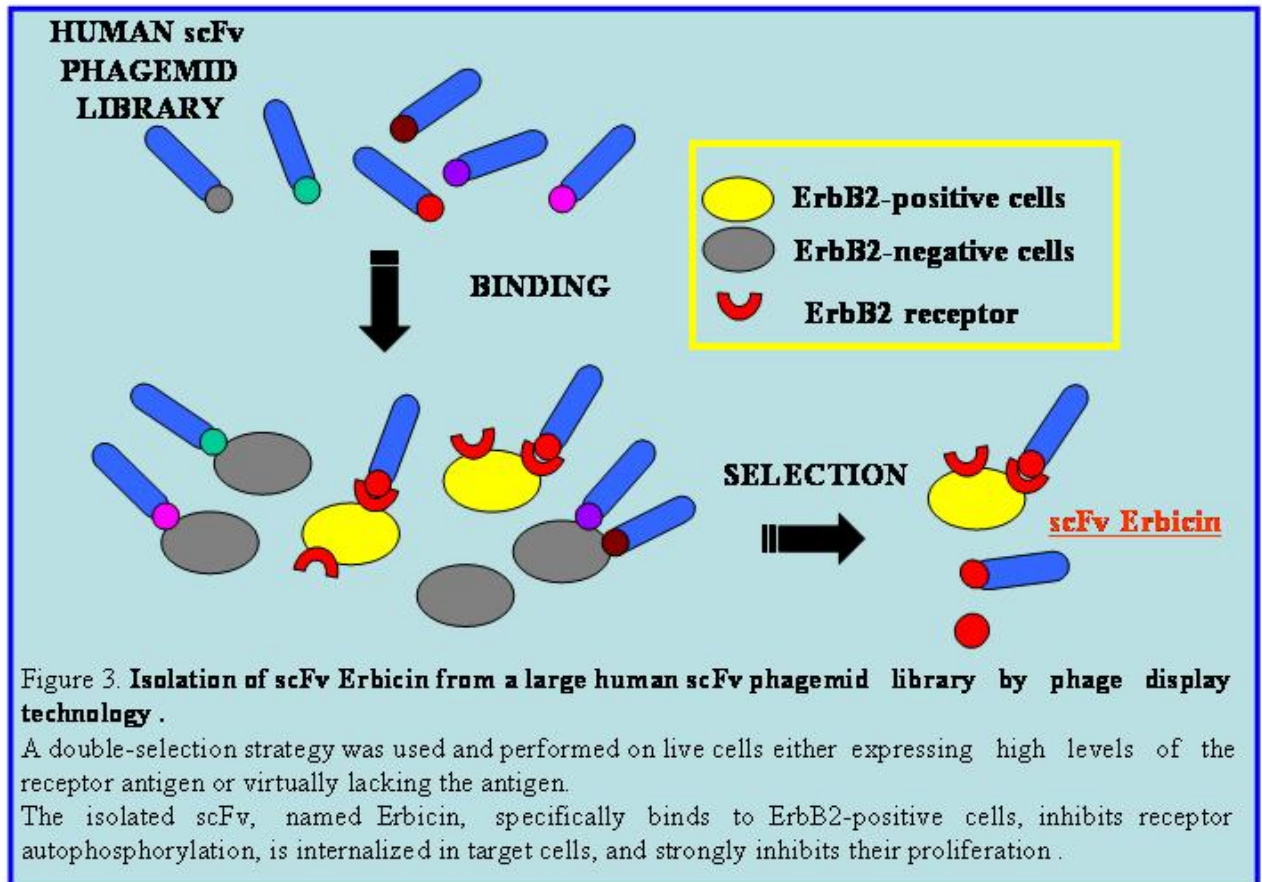


Figure 3. Isolation of scFv Erbicin from a large human scFv phagemid library by phage display technology .

A double-selection strategy was used and performed on live cells either expressing high levels of the receptor antigen or virtually lacking the antigen.

The isolated scFv, named Erbicin, specifically binds to ErbB2-positive cells, inhibits receptor autophosphorylation, is internalized in target cells, and strongly inhibits their proliferation .

3. AIMS OF THE STUDY

The aim of the study was the construction, isolation and characterization of a novel, fully human IR.

The first step of the research project was the construction of the cDNA encoding the chimeric protein, composed by the human anti-ErbB2 scFv Erbicin (De Lorenzo *et al.* 2002b) fused to human pancreas ribonuclease (HP-RNase) (Russo *et al.* 1993). The cDNA was then used to express the immunoconjugate in bacterial cells. The recombinant IR was then isolated from the periplasmic space following an appropriate purification protocol.

The second step of the research project was aimed at the characterization of the functional properties of the IR. In particular, analyses were performed to test the preservation of the enzymatic activity in the fusion protein, as well as the ability of the immunoconjugate to recognize and bind with high affinity ErbB2-positive tumor cells, and to undergo receptor-mediated endocytosis in target cells.

In vitro experiments were performed to test the effects of the IR on the proliferation of a panel of ErbB2-positive and ErbB2-negative tumor cells. In parallel experiments, the cytotoxic activity of hERB-hRNase was compared to that of Herceptin, a humanized version of an anti-ErbB2 murine antibody, currently in use for treatment of advanced breast cancer (Milenic 2002).

Experiments were then aimed at testing the stability of hERB-hRNase at 37°C, which is a critical factor for its potential as a therapeutic agent.

Finally, *in vivo* studies were performed to test the effects of the IR on the growth of tumors induced in mice by inoculation of ErbB2-positive tumor cells.

4. MATERIALS AND METHODS

4.1 Bacterial Strains

Escherichia coli strains SF110 (Meerman and Georgiou 1994) and BL21 (DE3) (purchased from EMD Biosciences, Inc., Novagen Brand, Madison, WI) were used.

4.2 Expression Vectors

The expression vector pET22b(+) (Novagen) (Fig. 4), containing the sequence encoding the human IR hERB-hRNase, was used to transform *E. coli* BL21 (DE3) strain.

The phagemid expression vector pHEN2 (Fig. 5) (Nissim *et al.* 1994), available in our laboratory, containing the sequence encoding the human IR hERB-hRNase, was used to transform *E. coli* SF110 strain.

4.3 Culture Media for Bacterial Strains

LB (Luria-Bertani) and 2x YT media were prepared as described by Sambrook and Russel 2001.

Culture media were supplemented with antibiotics. Ampicillin (100 µg/ml) and tetracycline (10 µg/ml), both purchased from Sigma Chemical Co. (St. Louis, MO), were added to 2x YT medium, used for *E. coli* SF110 strain transformed with the recombinant pHEN2 expression vector. Ampicillin (100 µg/ml) was added to LB medium, used for *E. coli* BL21 (DE3) strain transformed with the recombinant pET22b(+) expression vector.

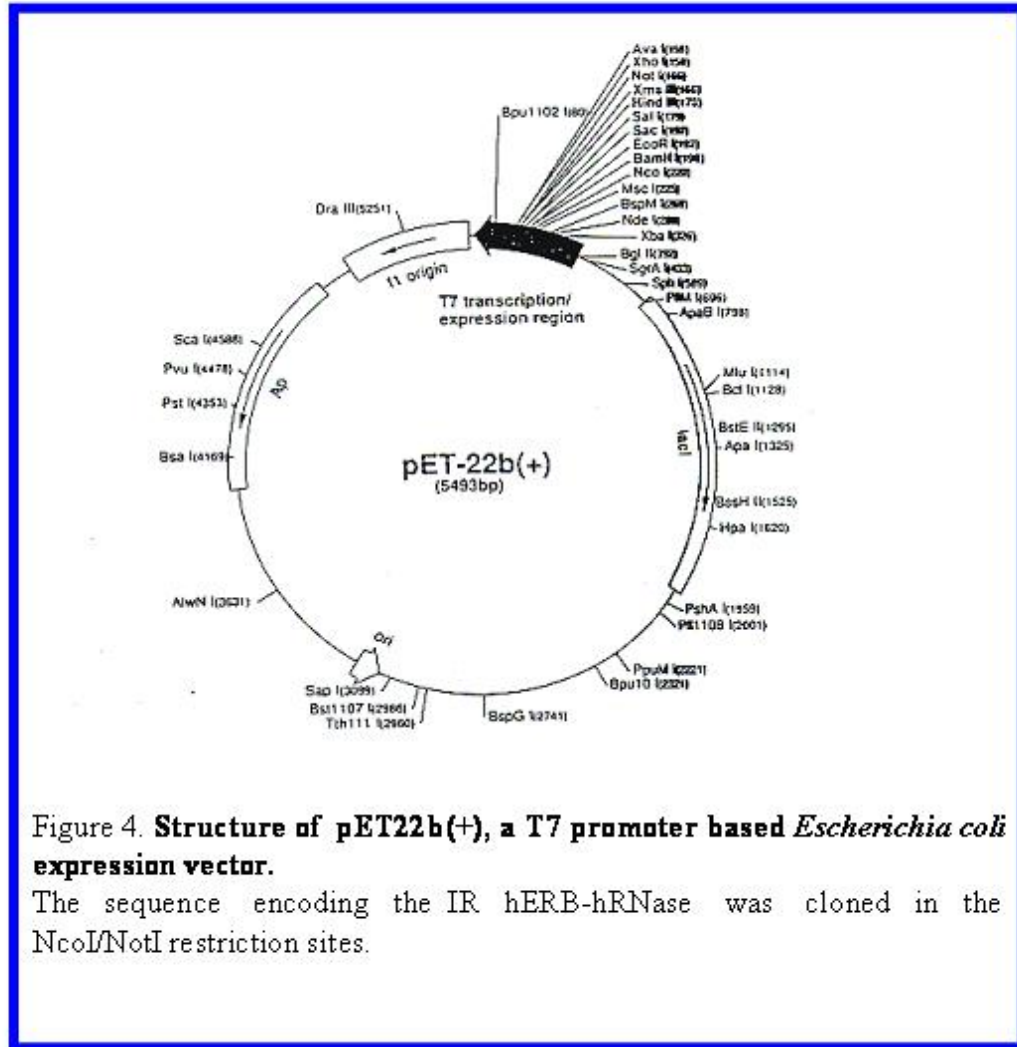


Figure 4. **Structure of pET22b(+), a T7 promoter based *Escherichia coli* expression vector.**

The sequence encoding the IR hERB-hRNase was cloned in the NcoI/NotI restriction sites.

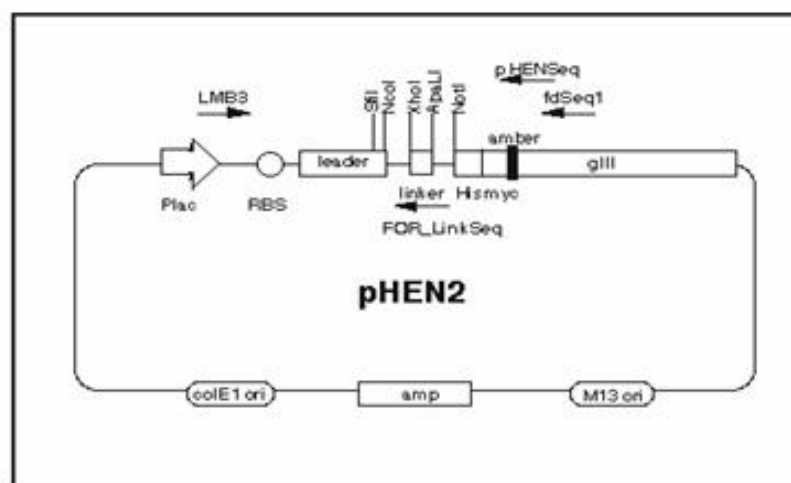


Figure 5. **Structure of the phagemid expression vector pHEN2.**

The sequence encoding the IR hERB-hRNase was cloned in the NotI restriction site.

P lac: β -galactosidase gene promoter.

RBS: ribosomal binding site.

Leader: signal peptide.

Linker: sequence encoding a linker peptide of 15 residues (SSGGGSGGGGSGGS) interposed between V_H and V_L chains of the scFv.

His: sequence encoding a hexahistidine tag.

Myc: sequence encoding a myc tag.

Amber: UAG stop codon.

gIII: sequence encoding the phagemid protein III.

colE1 ori: origin of replication from bacterial genome.

Amp: sequence encoding β -lactamase, responsible for ampicillin resistance.

M13 ori: origin of replication from bacteriophage M13 genome.

4.4 Antibodies

The antibodies used in the current study were the following: Herceptin (Genentech, South San Francisco, CA); murine mAb 9E10 directed against the myc tag protein (Evan *et al.* 1985); the IgG fraction from a rabbit anti-HP-RNase antiserum (Igtech, Salerno, Italy) purified by affinity chromatography of the antiserum on protein A-Sepharose CL-4B (Amersham Biosciences AB, Uppsala, Sweden); horseradish peroxidase-conjugated anti-His antibody (Qiagen, Valencia, CA); horseradish peroxidase-conjugated goat anti-rabbit immunoglobulin antibody (Pierce, Rockford, IL); horseradish peroxidase-conjugated rabbit anti-mouse immunoglobulin antibody (Pierce); FITC-conjugated sheep anti-rabbit immunoglobulin antibody (Dako, Cambridgeshire, UK).

4.5 Cell lines and Culture Conditions

The MDA-MB361 (kindly provided by Dr N. Normanno, Cancer Institute of Naples), the SKBR3 cell line from human breast tumor (from American Type Culture Collection, Rockville, MD) and the A431 cell line from human epidermoid carcinoma (from American Type Culture Collection, Rockville, MD) were cultured in RPMI 1640 (Gibco BRL, Life Technologies, Paisley, UK). The MDA-MB453 cell line from human breast tumor (a gift of H. C. Hurst, ICRF, London), and the AG12 (TUBO) cell line from a BALB-neu T mouse-derived mammary lobular carcinoma (kindly provided by Dr G. Forni, University of Turin, Italy) were grown in DMEM (Gibco BRL). Media were supplemented with 10% fetal bovine serum (20% for TUBO cells), 2 mM L-glutamine, 50 Units/ml penicillin, and 50 µg/ml streptomycin (all from Life Technologies). Cells were grown at 37°C in a humidified atmosphere containing 5% CO₂/95% air. All of the cell lines were discarded after 3 months and new lines were obtained from frozen stocks.

4.6 Preparation of Bacterial Competent Cells and Transformation

Single clones of SF110 *E. coli* strain, grown at 37°C in LB agar containing tetracycline (10 µg/ml), were inoculated into 5 ml of 2x YT medium containing the same antibiotic and 1% glucose. In the same manner, single clones of BL21 (DE3) *E. coli* strain, grown at 37°C in LB agar, were inoculated into 5 ml of LB medium.

Cells of both bacterial strains were incubated at 37°C on a shaker, and grown to an O.D.₆₀₀ of 0.5. At this point, cells (1.5 ml for each transformation) were incubated at 0°C for 10 minutes, and harvested by centrifugation at 5,000

rpm for 5 minutes at 4°C. Cell pellet was then dissolved in 750 µl of ice-cold 50 mM CaCl₂, and incubated for 20 minutes at 0°C. Following the incubation, cells were again harvested by centrifugation at 5,000 rpm for 5 minutes at 4°C. Cell pellet was then dissolved in 150 µl of the same solution (50 mM CaCl₂).

At this point, competent cells (150 µl) were transformed with plasmidic DNA and incubated at 4°C for 40 minutes. Following the incubation, heat shock was performed by incubation of the cells at 42°C for 2 minutes, followed by incubation at 4°C for 2 minutes. Following the addition of 1 ml of medium (LB or 2x YT, depending on the bacterial strain), cells were incubated at 37°C for 1 hour. Cells were then harvested by centrifugation at 5,000 rpm for 3 minutes at room temperature. Medium (1 ml) was then removed and cell pellet was dissolved in the remaining solution (about 100 µl) and plated on LB agar containing tetracycline (10 µg/ml) and ampicillin (100µg/ml), in the case of *E. coli* SF110 strain, or ampicillin (100 µg/ml), in the case of BL21 (DE3) *E. coli* strain.

4.7 Construction of the Chimeric cDNA Encoding hERB-hRNase

A cDNA encoding HP-RNase (Russo *et al.* 1993) was engineered by two successive PCR. Upstream primers (termed A and B) were used to incorporate the NotI restriction site at the 5' end, as well as a spacer sequence, whereas a downstream primer (C) was employed to introduce a NotI site at the 3' end. In the first reaction, primers B and C were used.

The sequences of primers A, B and C are reported in Table 2.

Oligonucleotide A	5'-ATAAGAATGCGGCCGCAAGCGGCGGCCCGGAAGGCGG-3'
Oligonucleotide B	5'-GGCCCGGAAGGCGGCAGCAAAGAATCTAGAGCTAAAAA-3'
Oligonucleotide C	5'-ATAAGAATGCGGCCGCAAGAGTCTTCAACAGACG-3'
Table 2. Sequences of the oligonucleotides employed to engineer the cDNA encoding HP-RNase.	

The oligonucleotide B sequence encodes the C-terminal half of the spacer. The oligonucleotide C sequence contains the NotI restriction site. In the second reaction, primers A and C were used. The oligonucleotide A encodes the N-terminal half of the spacer preceded by the NotI site sequence.

PCR reactions were performed in a final volume of 50 μ l, using 20 ng of plasmidic DNA as template. The reaction mixture contained the 2 primers (20 μ M each), dNTPs mixture (0.2 mM), MgSO₄ (1 mM), amplification buffer (Invitrogen Life Technologies, Inc., Carlsbad, CA) and Pfx enzyme from Pyrococcus (5 U) (Invitrogen Life Technologies, Inc., Carlsbad, CA).

Polymerase chain reaction (PCR) was performed as indicated below:

- Denaturation step: 2 minutes at 95°
- Amplification step (30 cycles): 2 minutes at 95°C
2 minutes at 55°C
2 minutes at 37°C
- Elongation step (1 cycle): 10 minutes at 73°C

Following the reaction, the amplified fragment was purified using a DNA purification system (Promega Biosciences Inc., San Luis Obispo, CA), and digested with NotI restriction enzyme (New England Biolabs, Hertfordshire, UK). Digestion of 6 μ g of amplified fragment with 20 U of NotI restriction enzyme was performed by incubation at 37°C for 2 hours. Following the digestion, the fragment was cloned into the corresponding site of pHEN2 vector (Nissim *et al.* 1994), downstream to the sequence encoding the available human anti-ErbB2 scFv (De Lorenzo *et al.* 2002b). To this purpose, ligation was performed using a kit purchased from Promega Biosciences Inc. (San Luis Obispo, CA). The phagemid expression vector pHEN2 was previously digested with NotI restriction enzyme, and treated with shrimp alkaline phosphatase (SAP) (Roche Applied Science, Indianapolis, IN). Digested vector (4 μ g) was incubated with 20 U of SAP at 37°C for 15 minutes. SAP enzyme was then inactivated by incubation at 65°C for 10 minutes.

Following the ligation, the correct directional insertion of the RNase gene in the NotI restriction site was assessed by PCR, using the forward primer A in combination to a reverse oligonucleotide corresponding to a vector sequence positioned downstream to the NotI site (5'-TGAATTTTCTGTATGAGG-3').

Sequence analyses confirmed the expected DNA sequence. The assembled gene was then cloned in pET22b(+), a T7 promoter based *E. coli* expression vector, in the NcoI/NotI restriction sites.

4.8 Expression of hERB-hRNase

Single clones of *E. coli* SF110 strain, previously transformed with the recombinant pHEN2 expression vector, and grown at 37°C on LB agar containing 100 µg/ml ampicillin and 10 µg/ml tetracycline, were inoculated into 5 ml of 2x YT medium containing the same antibiotics and 1% glucose. In a similar manner, single clones of *E. coli* BL21 (DE3) strain, previously transformed with the recombinant expression vector pET22b(+), and grown at 37°C on LB agar containing 100 µg/ml ampicillin, were inoculated into 5 ml of LB medium containing the same antibiotic. Following this step, cells of both *E. coli* strains were grown at 37°C on a shaker to an O.D.₆₀₀ of 0.6. At this point, cells were inoculated into 1 liter of the same medium containing the necessary antibiotics, and grown at 37°C on a shaker to an O.D.₆₀₀ of 1. Following bacterial growth, the expression of hERB-hRNase was induced by addition of isopropyl-β-D-thiogalactopyranoside (IPTG). IPTG activates both the T7 promoter of pET22b(+) vector, and the lac promoter of pHEN2 vector. In the case of SF110 *E. coli* strain, the addition of IPTG was performed after removal of glucose, present in the medium during bacterial growth. To this purpose, SF110 *E. coli* cells were harvested by centrifugation at 6,000 rpm for 20 minutes at room temperature, and then suspended in glucose-free medium. In both the expression systems, IPTG was added to the cultures to a final concentration of 1 mM, and cells were then grown at room temperature overnight on a shaker. Following overnight growth, cells were harvested by centrifugation at 6,000 rpm for 20 minutes at 4°C.

In order to verify hERB-hRNase expression, an aliquot of cell culture (5 ml) was removed before and after induction with IPTG. Cells of both aliquots (induced and not induced) were harvested by centrifugation at 6,000 rpm for 20 minutes at 4°C, and suspended in 100 µl of ice-cold phosphate-buffered saline (PBS), pH 8.0, containing 1M NaCl and a cocktail of proteases inhibitors (Roche Applied Science, Indianapolis, IN). Following an incubation of 30 minutes at 0°C, periplasmic extract was obtained by centrifugation at 12,000 rpm for 15 minutes at 4°C, and analyzed by SDS-PAGE 12%, followed by Coomassie staining, Western blot analyses with an anti-His and an anti-HP-RNase antibody, and zymogram analyses.

4.9 Preparation of Periplasmic Extract for the Isolation of hERB-hRNase

In order to obtain the periplasmic extract, cell pellet was dissolved in ice-cold 50 mM Tris-HCl, pH 7.4, containing 1 mM EDTA, 20% sucrose and a cocktail of proteases inhibitors (Roche Applied Science, Indianapolis, IN), and incubated for 1 hour on ice. Following the incubation, the periplasmic extract was

obtained by centrifugation at 12,000 rpm for 30 minutes at 4°C. At this point, the soluble fraction represented the periplasmic extract, whereas the insoluble fraction was solubilised with 4 M urea (Bayly *et al.* 2002), in order to recover a putative fraction of hERB-RNase associated to cell membranes. To this purpose, the insoluble fraction was dissolved in 4 M urea and TBS 1x (0.25 M Tris-HCl, pH 8.0, containing 1.4 M NaCl and 27 mM KCl), and incubated for 1 hour at 4°C on a shaker. Samples were then centrifuged at 22,000 x g for 1 hour at 4°C. A soluble fraction containing the IR was thus obtained.

4. 10 Purification of hERB-hRNase

Two alternative protocols were used to isolate hERB-hRNase.

4.10.1 Isolation of hERB-hRNase by two Steps of Affinity Chromatography

Periplasmic extract was loaded on an immobilized-metal affinity chromatography (IMAC) column, using a cobalt-chelating resin (TALON; Clontech, Palo Alto, CA). This kind of chromatography is based on the ability of the COOH-terminal hexahistidine tag of the recombinant protein to bind Co^{+2} ions. Sample was incubated with the resin for 2 hours at room temperature on a shaker. Wash and elution steps were performed according to the manufacturer's instructions. Following the incubation, the resin was washed with 50 mM NaH_2PO_4 , pH 7.0, containing 0.3 M NaCl and 20 mM imidazol. Elution step was performed in the presence of a high concentration of imidazol (250 mM), which compete with hERB-hRNase for the binding to the Co^{+2} ions of the resin.

Further purification was achieved by affinity chromatography using uridine 2',5'- and 3',5'-diphosphate agarose (pUp agarose, Sigma Chemical Co., St. Louis, MO). Briefly, the sample was diluted with sodium acetate buffer, pH 5.8, containing 0.15 M NaCl, and loaded on the column, previously equilibrated in 0.1 M sodium acetate buffer, pH 5.8, containing 0.15 M NaCl, 10% glycerol and 0.005% Tween 20. After extensive washing with the equilibrium buffer, the protein was eluted in PBS, pH 7.6, containing 0.5 M NaCl, 10% glycerol and 0.005% Tween 20. The purity of the final preparation was evaluated by SDS-PAGE 12%, followed by Coomassie staining, Western blot analyses with an anti-His and an anti-HP-RNase antibody, and zymogram analyses.

4.10.2 Isolation of hERB-hRNase by Hydrophobic Interaction Chromatography, Followed by Affinity Chromatography

Periplasmic extract was incubated with the MEP HyperCel matrix (BioSeptra, Cergy-Saint-Christophe, France) for two hours at room temperature. This kind of chromatography is based on the ability of the hydrophobic regions of the antibody portion of the immunoconjugate to bind 4-mercapto-ethyl-pyridine (MEP). After extensive washes with 50 mM Tris-HCl, pH 8.0, two additional wash steps were performed: the first with H₂O, and the second with 25 mM sodium caprylate in 50 mM Tris-HCl, pH 8.0. The MEP HyperCel resin was then equilibrated in 50 mM Tris-HCl, pH 8.0 before elution of the protein with 50 mM sodium acetate, pH 4.0. The sample was immediately adjusted to pH 7.0, diluted with BPER buffer (Bacterial Protein Extraction Buffer, Pierce, Rockford, IL), and loaded on an immobilized-metal affinity chromatography (IMAC) column by using a cobalt-chelating resin (TALON, Clontech, Palo Alto, CA) for achieving further purification. Wash and elution steps were performed according to the manufacturer's recommendations (for details see above). The purity of the final preparation was evaluated by SDS-PAGE 12%, followed by Coomassie staining, Western blot analyses with an anti-His and an anti-HP-RNase antibody, and zymogram analyses.

4.10.3 Isolation of hERB-hRNase from the insoluble fraction of bacterial cells

As previously described, a considerable amount of expressed hERB-hRNase is present in the insoluble fraction obtained from bacterial cells. Such immunoconjugate was efficiently recovered by solubilisation with urea (Bayly *et al.* 2002). The recovered IR was isolated by using the hydrophobic interaction chromatography (HIC) described above, followed by the affinity chromatography based on uridine 2',5'- and 3',5'-diphosphate agarose (pUp agarose, Sigma Chemical Co., St. Louis, MO) (for details see above).

4.11 Gel Electrophoresis (SDS-PAGE)

SDS-PAGE was performed as described by Laemmli 1970.

4.11.1 Coomassie Staining

Following gel electrophoresis, gel was incubated for 30 minutes at room temperature in 20% isopropanol, containing 10% acetic acid, and 0.1% Coomassie Brilliant Blue R250 (Applichem, Darmstadt, Germany). Following the incubation, gel was treated with 20% ethanol, containing 7% acetic acid. Such a solution was replaced by water when protein bands were detectable.

4.11.2 Western Blot Analyses

Following gel electrophoresis, proteins were transferred to PVDF membranes (Immobilon-P, Millipore, Billerica, MA) at 25 V overnight at 4°C. At this point, membranes were incubated in a blocking solution (5% non-fat milk in PBS buffer, containing 0.1% Tween 20) at room temperature for 1 hour. Membranes were then washed with PBS buffer containing 0.1% Tween 20, and incubated with the IgG fraction from a rabbit anti-HP-RNase antiserum (Igtech, Salerno, Italy), purified by affinity chromatography of the antiserum on protein A-Sepharose CL-4B (Amersham Pharmacia Biotech., Uppsala, Sweden), diluted 1:1000, or with murine mAb 9E10 directed against the myc tag protein (Evan *et al.* 1985) diluted 1:1000, or with horseradish peroxidase-conjugated anti-His antibody (Qiagen, Valencia, CA) diluted 1:1000. Primary antibodies were all diluted in PBS buffer containing 0.1% Tween 20 and 5% non-fat milk, and incubated with the membranes at room temperature for 1 hour on a shaker. Membranes were then washed with PBS buffer containing 0.1% Tween 20, and incubated with a horseradish peroxidase-conjugated goat anti-rabbit immunoglobulin antibody (Pierce, Rockford, IL), or with a horseradish peroxidase-conjugated rabbit anti-mouse immunoglobulin antibody (Pierce, Rockford, IL). Both the secondary antibodies were diluted 1:5000 in PBS buffer, containing 0.1% Tween 20 and 5% non-fat milk. Membranes were incubated with the secondary antibodies for 1 hour at room temperature on a shaker. Membranes were then washed with PBS buffer containing 0.1% Tween 20. Detection by enzyme-linked chemiluminescence (enhanced chemiluminescence: ECL) was performed according to the manufacturer's instructions (Super Signal[®]West-Pico Chemiluminescent Substrate, Pierce, Rockford, IL), using a Phosphorimager.

4.11.3 RNase Activity

RNase zymograms, carried out on SDS-PAGE electropherograms, were performed as described previously (Blank *et al.* 1982). Briefly, following electrophoresis, gel was incubated for 30 minutes in 50 mM Tris-HCl, pH 7.4, containing 25% isopropanol and then equilibrated in 50 mM Tris-HCl, pH 7.4. Gel was then incubated at 37°C for 10 minutes in the same buffer, containing 4 mg/ml RNA. Following the incubation, gel was washed with the equilibrium buffer and incubated for 15 minutes at room temperature in a solution of 0.2% toluidine blue, containing 0.1% acetic acid. Following the coloration step, gel was washed several times with water. At the end of the procedure, proteins endowed with enzymatic activity were visualized as white bands on a dark background. Bovine seminal ribonuclease (BS-RNase) (100-200 ng) was used as a positive control.

4.12 RNase Activity Assays

RNase activity was tested using a modified version of the procedure described by Bartholeyns *et al.* 1977, based on assaying acid-soluble products of RNA degradation. Yeast RNA (8mg/ml) was incubated for 30 minutes at 37°C with the enzyme under test in the reaction buffer (0.05 M Tris-HCl, pH 8.0, containing 0.15 M NaCl and 0.05 mg/ml RNase-free BSA). The reaction was stopped, and undegraded RNA was precipitated by addition of one volume of cold 10% perchloric acid, containing 0.25% uranyl acetate. After 15 minutes on ice, the A_{260} of the supernatant, diluted 1:20 with distilled water, was determined. A blank reaction was performed in the absence of the enzyme. In this assay, one unit of enzymatic activity is defined as the amount of enzyme that generates an increase of 1 absorbance unit at 260 nm.

4.13 Binding Assays

ErbB2-positive SKBR3, MDA-MB361, MDA-MB453 and AG12 (TUBO) cells, and ErbB2-negative A431 control cells, harvested in non-enzymatic dissociation solution (Sigma, St. Louis, MO), were washed with PBS and transferred to U-bottom microtiter plates (1×10^5 cells per well). After blocking with PBS containing 6% bovine serum albumin (BSA), the plates were incubated with purified immunoagents in ELISA buffer (PBS/BSA 3%) for 90 minutes. After centrifugation and removal of supernatants, harvested cells were washed twice in 200 μ l of ELISA buffer, suspended in 100 μ l of the same buffer and incubated for 1 hour with either rabbit anti-HP-RNase IgGs (for hERB-

hRNase detection), or with murine anti-myc mAb (for scFv detection), followed by peroxidase-conjugated anti-rabbit or anti-mouse IgGs (Pierce, Rockford, IL), respectively, according to the source of the primary antibody. After 1 hour, the plates were centrifuged, washed with ELISA buffer, and reacted with 3,3',5,5'-tetramethylbenzidine (TMB) (Sigma, St. Louis, MO). The reaction was stopped by addition of 1N HCl. Binding values were determined from the absorbance at 450 nm, and reported as the mean of at least three determinations (standard deviation $\leq 5\%$).

4.14 Internalization of hERB-hRNase

Cells grown on coverslips to 60% confluency were incubated with the immunoagent (20 $\mu\text{g/ml}$) for 16 hours at 37°C. Cells were then washed, fixed and permeabilized as described elsewhere (Becerril *et al.* 1999). Intracellular IR was detected with a rabbit anti-HP-RNase antibody, followed by FITC-conjugated sheep antirabbit antibody. Optical confocal sections were taken using a confocal microscope (LSM 510; Zeiss, Oberkochen, Germany).

4.15 Cytotoxicity Assays

Cells were seeded in 96-well plates (150 $\mu\text{l/well}$); SKBR3, MDA-MB361, AG12 (TUBO) and MDA-MB453 cells were seeded at a density of $1.5 \times 10^4/\text{well}$; A431 cells were seeded at a density of $5 \times 10^3/\text{well}$. Proteins under test were added, and after 72 hours cell counts were determined in triplicate using the trypan blue exclusion test. Cell survival was expressed as percentage of viable cells in the presence of the protein under test, with respect to control cultures grown in the absence of the protein.

4.16 Stability of the IR

The stability of hERB-hRNase was determined by incubating the IR at a concentration of 0.04 mg/ml in either human or murine serum at 37°C for 24 or 48 hours. Following the incubation, the samples were tested using the analytical tests described above: Western blot analyses, RNase activity assays, and binding assays (see above).

4.17 *In Vivo* Antitumor Activity

All of the experiments were performed with 6-week old female Balb/cAnNCrlBR mice (Charles River laboratories, Wilmington, MA). AG12 (TUBO) cells (5×10^5) were suspended in 0.2 ml sterile PBS and injected subcutaneously (day 0) in the right paw. At day 10, tumors were clearly detectable (at least 15 mm^3 in volume). At day 11, hERB-hRNase, dissolved in PBS, was administered 5 times at 72 hours intervals peritumorally or intraperitoneally to two groups of five mice at doses of 1,5 mg/kg of body weight. Equimolar doses of native HP-RNase or anti-ErbB2 scFv were administered peritumorally to other two groups as controls. Another group of control animals was treated with identical volumes of sterile PBS. At day 45, blood samples were taken and tested to obtain the main hematological parameters. During the treatment period, tumor volumes (V) were measured and calculated using the formula of rotational ellipsoid $V = A \times B^2 / 2$ (A is axial diameter and B is rotational diameter). All of the mice were maintained at the animal facility of the Department of Cellular and Molecular Biology and Pathology, University of Naples "Federico II". The experiments on animals described here were conducted in accordance with accepted standards of animal care and in accordance with the Italian regulations for the welfare of animals used in studies of experimental neoplasia. The School of Medicine Institutional Committee on animal care approved the study.

5. RESULTS AND DISCUSSION

5.1 Construction of the Chimeric cDNA Encoding hERB-hRNase

A cDNA encoding human pancreas ribonuclease (HP-RNase) (Russo *et al.* 1993) was available in our laboratory, inserted in the expression vector pET22b(+). It was engineered by two successive PCR (polymerase chain reaction) reactions which added a spacer sequence encoding a peptide of 11 residues designed to separate the RNase and scFv moieties in the fusion protein. It is known that the insertion of a spacer peptide is important to obtain a stable and biologically active immunoconjugate (Newton *et al.* 1996). During the two successive PCR reactions, upstream primers were used to incorporate the NotI restriction site at the 5' end, as well as the spacer sequence, whereas a downstream primer was employed to introduce a NotI restriction site at the 3' end (see Materials and Methods section for details). The PCR fragment was then digested and cloned into the corresponding restriction site of the phagemid expression vector pHEN2 (Nissim *et al.* 1994), downstream to the available sequence encoding the available human anti-ErbB2 scFv Erbicin (De Lorenzo *et al.* 2002b). The correct directional insertion of the RNase gene was assessed by PCR (see Materials and Methods section for details). Sequence analyses confirmed the expected DNA sequence. The cloning strategy is reported in Fig. 6.

The resulting construct encodes the immunoRNase (IR), henceforth called hERB-hRNase, whose structure is shown in Fig. 7 (De Lorenzo *et al.* 2004). It includes the scFv Erbicin at the NH₂-terminal end, followed by HP-RNase. A linker peptide of 15 residues (SSGGGGSGGGGSGGS) is interposed between V_H and V_L chains of the scFv, whereas a spacer peptide of 11 residues (AAASGGPEGGS) is inserted between the antibody fragment and the ribonuclease. Two COOH-terminal tags are located downstream to the ribonuclease: 1) a hexahistidine tag, useful for the isolation of the IR; 2) a myc tag, useful for its identification by Western blot analyses.

The assembled gene was then cloned in pET22b(+), a T7 promoter based *Escherichia coli* expression vector. This vector was chosen since it has been successfully used in our laboratory for the expression at satisfactory yields of other proteins, mainly ribonucleases. The resulting construct had the same structure of the one previously described (Fig. 7), with the only difference that the sequence encoding the myc tag is missing. It is important to mention that both the expression vectors, pET22b(+) and pHEN2, are equipped with an upstream pel B signal sequence, for the expression of hERB-hRNase as a soluble protein in the periplasmic space.

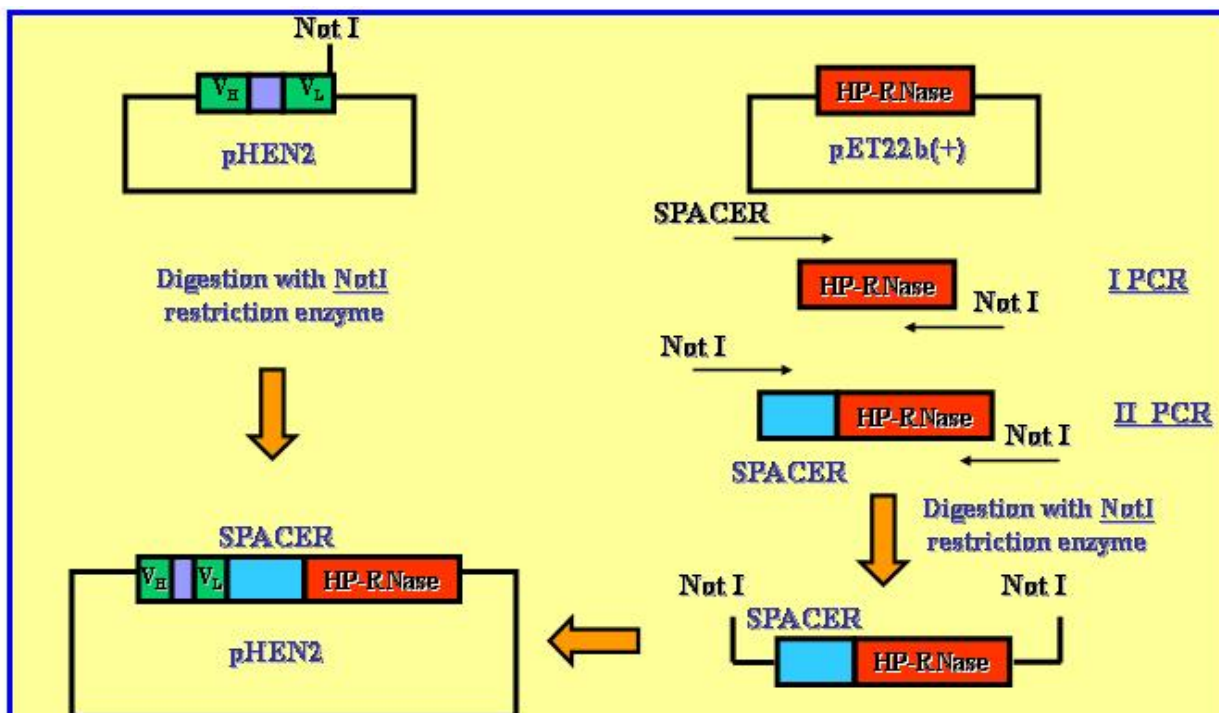


Figure 6. **Scheme of cloning strategy.**

A cDNA encoding human pancreas ribonuclease (HP-RNase), cloned in pET22b(+) expression vector, was engineered by two successive PCR, which introduced the required restriction sites and a spacer sequence encoding a peptide of 11 residues, designed to separate the RNase and scFv moieties in the fusion protein. The PCR fragment was digested with NotI restriction enzyme, and cloned into the corresponding restriction site of the phagemid expression vector pHEN2, containing the sequence encoding the scFv Erbicin.

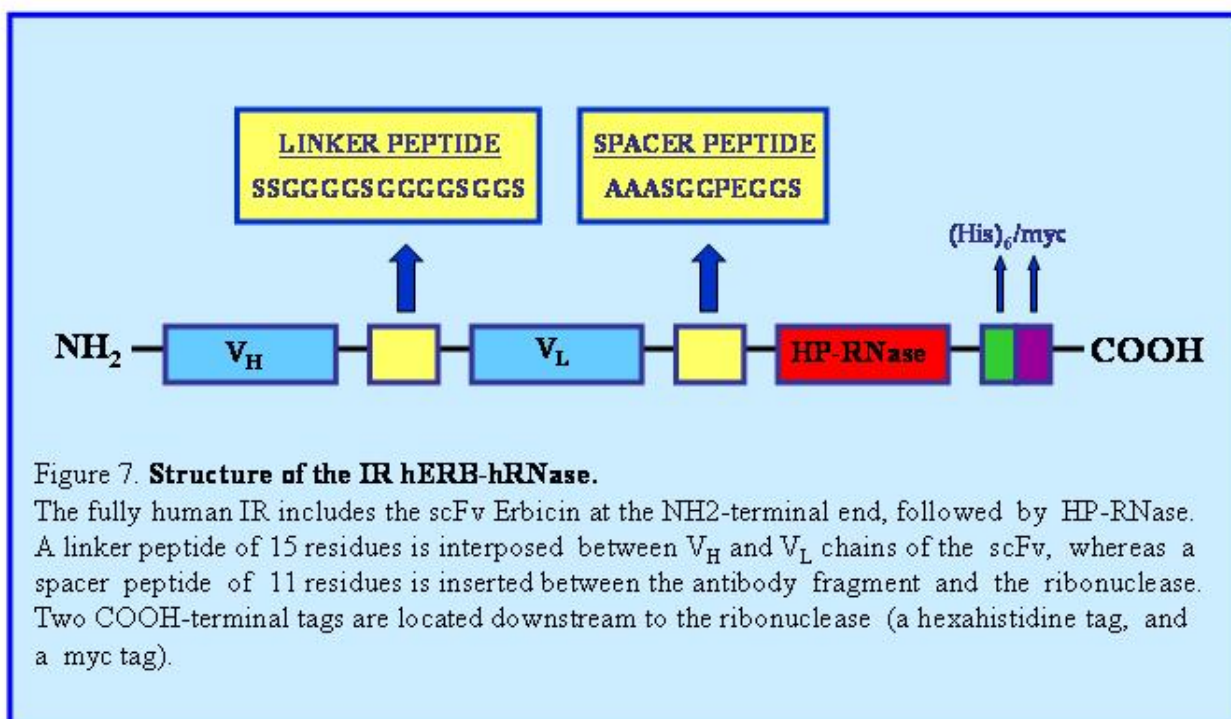


Figure 7. **Structure of the IR hERB-hRNase.**

The fully human IR includes the scFv ErbB at the NH₂-terminal end, followed by HP-RNase. A linker peptide of 15 residues is interposed between V_H and V_L chains of the scFv, whereas a spacer peptide of 11 residues is inserted between the antibody fragment and the ribonuclease. Two COOH-terminal tags are located downstream to the ribonuclease (a hexahistidine tag, and a myc tag).

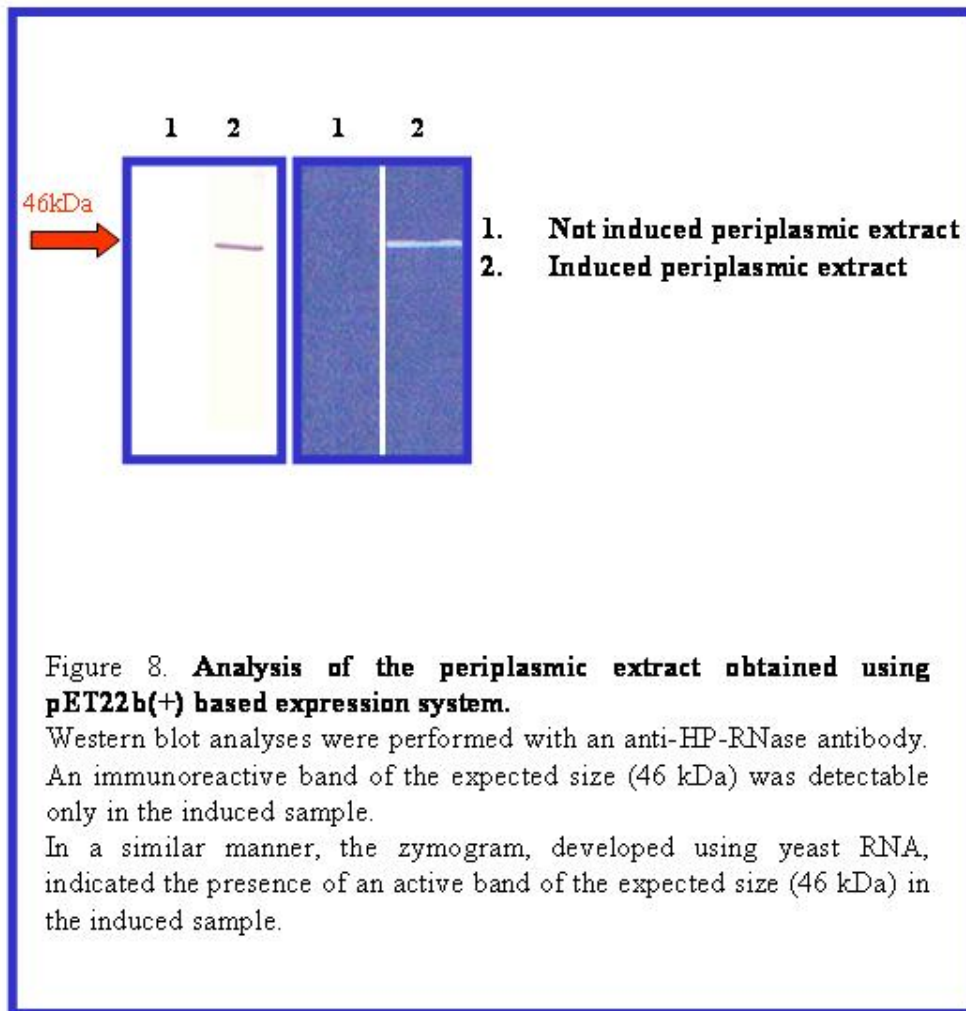
5.2 Expression of hERB-hRNase

Both the recombinant expression vectors pET22b(+) and pHEN2 were used to express hERB-hRNase in *E. coli*, with the purpose to compare the IR expression levels.

Cultures of *E. coli* BL21 (DE3) and SF110 were transformed with the recombinant expression vectors pET22b(+) and pHEN2, respectively. *E. coli* BL21 (DE3) cells were then grown at 37°C in LB medium containing ampicillin. Resistance to ampicillin is given by the recombinant vector pET22b(+), thus allowing to select transformed cells. On the other hand, *E. coli* SF110 cells were grown at 37°C in 2x YT medium containing 1% glucose, tetracycline and ampicillin, until the exponential phase of growth was reached. Resistance to tetracycline is a feature of SF110 *E. coli* strain, whereas resistance to ampicillin is given by the expression vector pHEN2, thus allowing to select transformed cells. In both cases, cells were grown until the exponential phase of growth was reached. The expression of hERB-hRNase was induced by addition of isopropyl- β -D-thiogalactopyranoside (IPTG). IPTG activates both the T7 promoter of pET22b(+) vector, and the lac promoter of pHEN2 vector. In the case of SF110 *E. coli* strain, the addition of IPTG was performed after removal of glucose, present in the medium during bacterial growth. In both the expression systems, IPTG was added to the cultures to a final concentration of 1 mM, and cells were then grown at room temperature overnight. Cells were then harvested by centrifugation. The IR was expected to be directed to the periplasmic space, because of the presence of the upstream pel B signal sequence in both the recombinant expression vectors, pET22b(+) and pHEN2. However, exogenous proteins, mainly if toxic, may be sequestered in inclusion bodies, when expressed at high levels in bacterial cells. For this reason, both periplasmic extracts and insoluble fractions of bacterial cells were prepared and analyzed by SDS-PAGE, followed by Western blot analyses with an anti-His and an anti-HP-RNase antibody. The results, obtained with both the expression vectors, were similar. In both cases, an immunoreactive band of the expected size, approximately Mr 46,000, was present in the periplasmic extracts, as well as in insoluble fractions. No bands were instead detected in the samples prepared from not induced cells. Such a result is reported for the expression vector pET22b(+) in Fig. 8, showing the analysis of the periplasmic extract with an anti-HP-RNase antibody.

In order to test the enzymatic activity of the IR present in the periplasmic space, a zymogram (Blank *et al.* 1982) was developed using yeast RNA as a substrate. An active band, corresponding to the size expected for hERB-hRNase (46,000 Da), was detected only in the samples prepared from induced bacteria, suggesting that the recombinant IR retains in the periplasmic space its enzymatic activity. Such a result is reported in Fig. 8 for the expression vector pET22b(+).

Since with the recombinant expression vector pET22b(+) the expression levels of hERB-hRNase were about 30% higher than those obtained using the expression vector pHEN2, further analyses were performed using the pET22b(+) based expression system.



5.3 Purification of hERB-hRNase

Two alternative protocols were used to isolate hERB-hRNase from the periplasmic space.

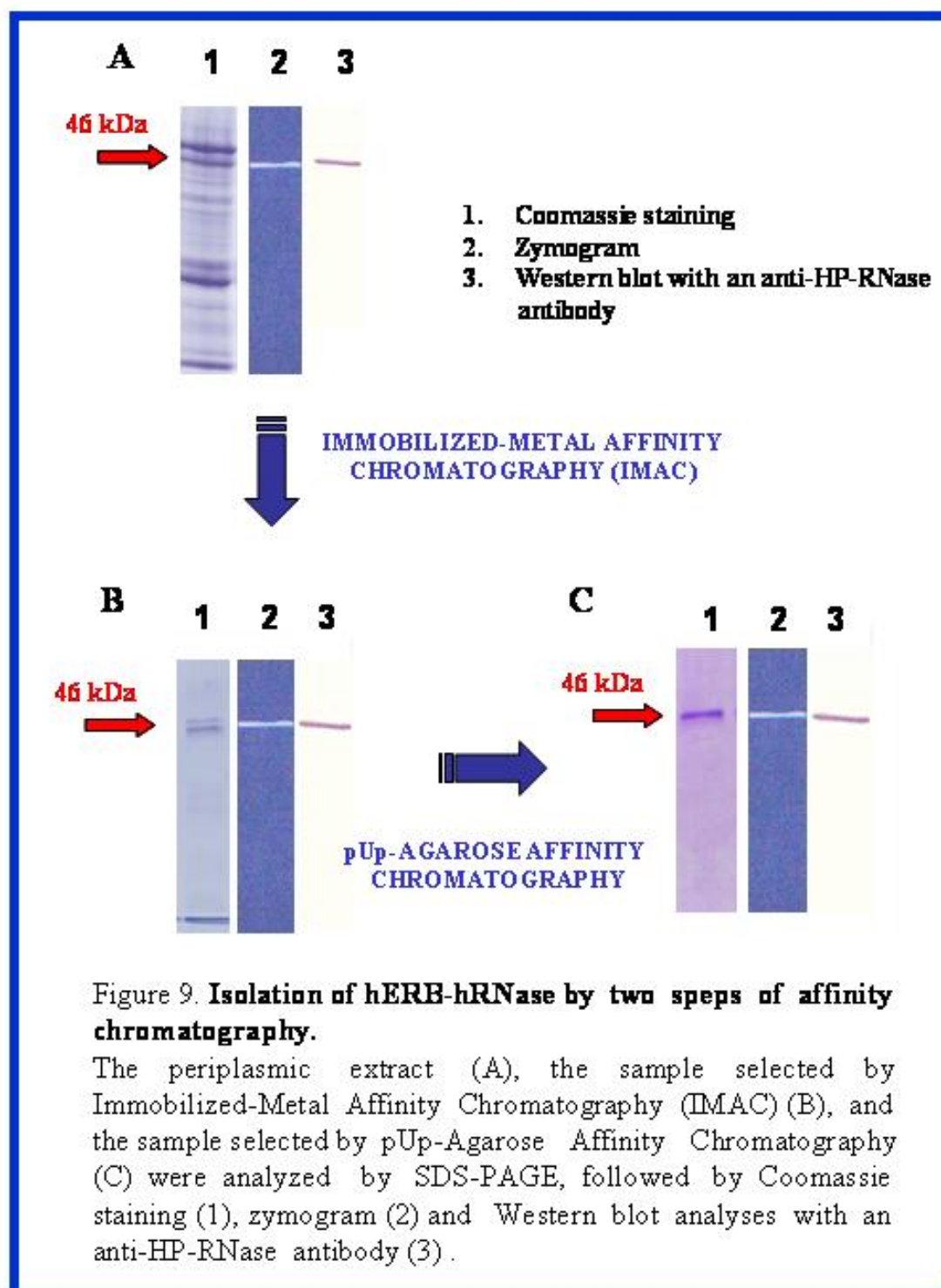
5.3.1 Isolation of hERB-hRNase by two Steps of Affinity Chromatography

The isolation of the IR was achieved by two steps of affinity chromatography. The first step is based on the ability of the COOH-terminal hexahistidine tag of the recombinant protein to bind Co^{+2} ions. The periplasmic extract was loaded on an immobilized-metal affinity chromatography (IMAC) column, using a cobalt-chelating resin (see Materials and Methods section for details). At the end of the chromatography, the selected sample was analyzed by SDS-PAGE, followed by Coomassie staining, Western blot analyses with an anti-HP-RNase antibody and an anti-His antibody, and zymogram. The latter was performed to test the ribonuclease activity of the immunoconjugate. The results are shown in Fig. 9. The resin selected few molecular species from the material present in the periplasmic fraction. Among these, only one immunoreactive band of the expected size, approximately Mr 46,000, was detectable by Western blot analyses, and demonstrated to be enzymatically active by zymogram (Fig. 9).

Further purification was achieved by a second affinity chromatography based on uridine 2',5'- and 3',5'-diphosphate agarose (pUp), which is able to bind to the active site of enzymatically active ribonucleases. This selection criterion was chosen to allow the isolation of immunoconjugate molecules containing an enzymatically active ribonuclease moiety, as inactive IRs are not able to bind the resin. After extensive washing with the equilibrium buffer, the protein was eluted in phosphate-buffered saline (PBS) containing 0.5 M NaCl (for details see Materials and Methods section). This buffer was chosen since it is compatible with the growth of eukaryotic cells, thus allowing the direct use of the purified IR in biological assays.

At the end of the second chromatographic step, the sample was analyzed by SDS-PAGE, followed by Coomassie staining, Western blot analyses with an anti-His and an anti-HP-RNase antibody, and zymogram (Fig. 9). The results indicated that the recombinant protein was homogeneous and endowed with ribonuclease activity.

The described protocol allowed the isolation of about 150 μg of purified IR from 2 liters of cultured cells. These results are quite satisfactory if one takes in consideration the difficulties to express chimeric proteins, composed by two moieties, which have to assume their correct folding.

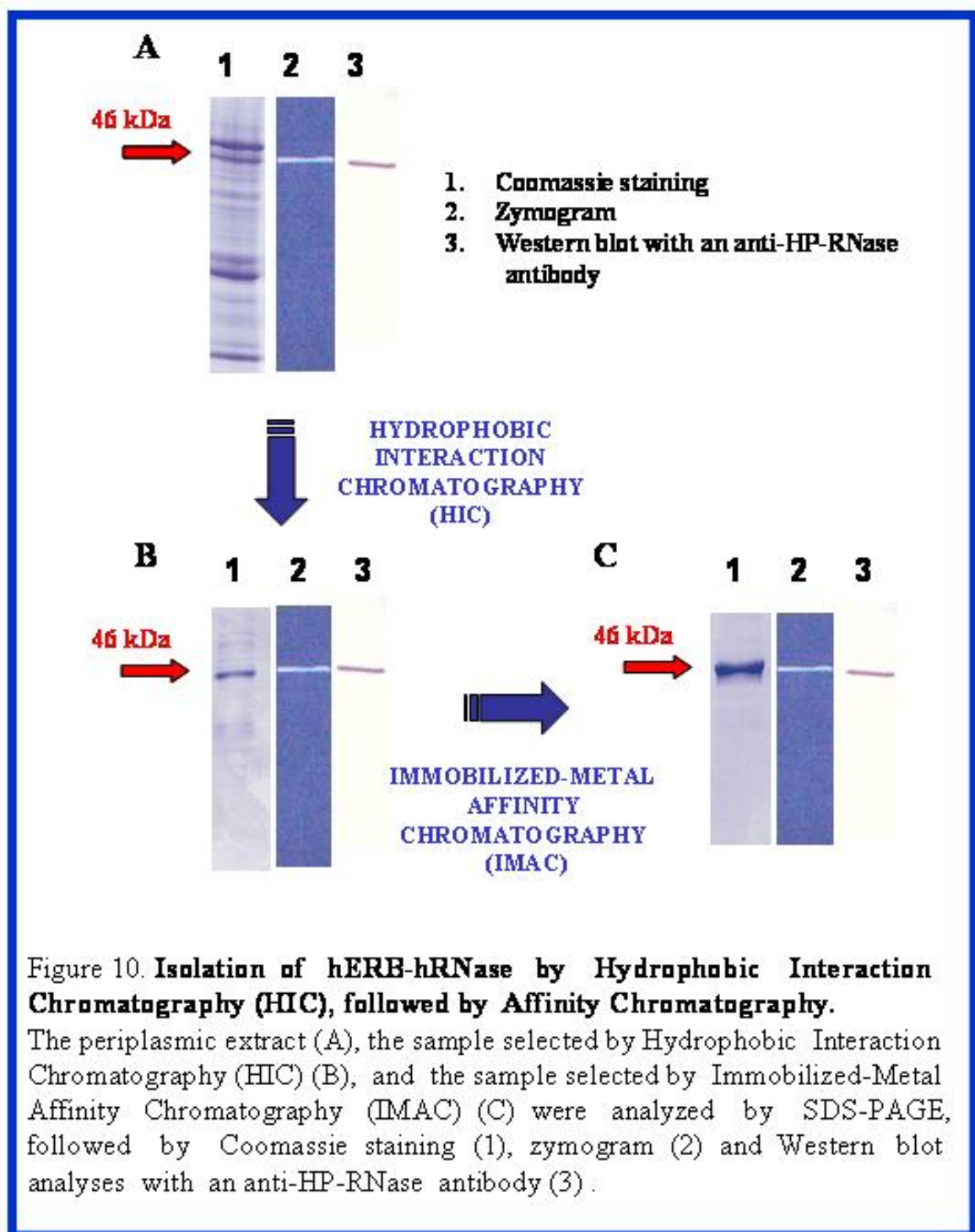


5.3.2 Isolation of hERB-hRNase by Hydrophobic Interaction Chromatography (HIC), Followed by Affinity Chromatography

An alternative protocol was used to isolate the IR from the periplasmic space. In such purification protocol, the first step was a hydrophobic interaction chromatography (HIC), based on the ability of the hydrophobic regions of the antibody portion of the immunoconjugate to bind 4-mercapto-ethyl-pyridine (MEP) HyperCel matrix (see Materials and Methods section for details). The sample selected by this kind of chromatography was immediately neutralized, and loaded on an immobilized metal-affinity chromatography (IMAC) column, using the previously described cobalt-chelating resin. The purity of the final preparation was evaluated by SDS-PAGE, followed by Coomassie staining, Western blot analyses with an anti-His and an anti-HP-RNase antibody, and zymogram to test the enzymatic activity of the purified IR (Fig. 10). The results indicated that the recombinant protein was homogeneous and endowed with ribonuclease activity.

The protein was then dialyzed against phosphate-buffered saline (PBS), containing 0.16 M NaCl, as this buffer is compatible with the growth of eukaryotic cells, thus allowing the direct use of the IR in biological assays.

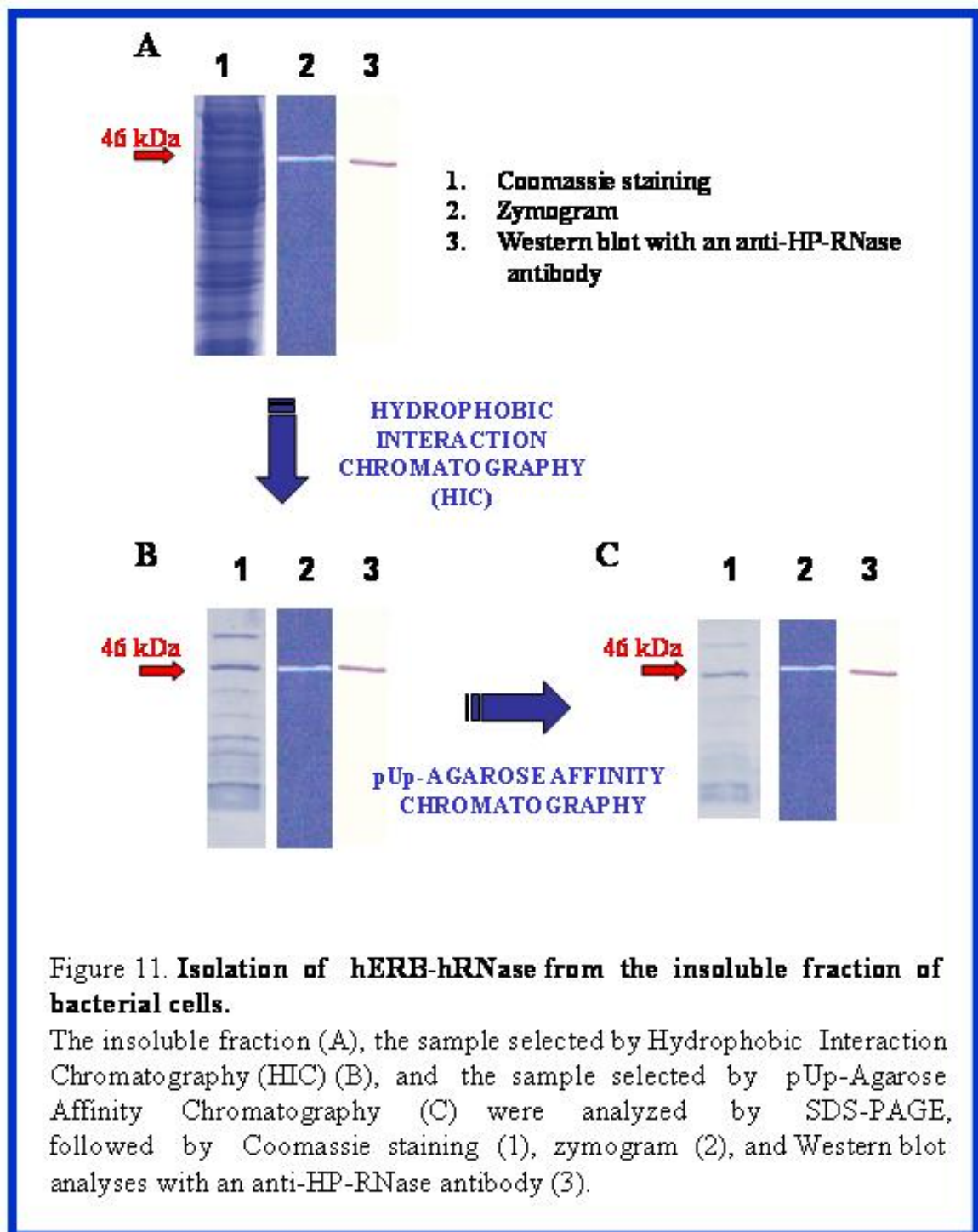
Both the described protocols of purification are valid to achieve purity. However, the latter protocol allows the isolation of slightly higher amounts of IR, about 200 μg of recombinant protein from 2 liters of cultured cells. This procedure was thus preferred to the other to isolate hERB-hRNase.



5.4 Isolation of hERB-hRNase from the Insoluble Fraction of Bacterial Cells

As previously described, a considerable amount of expressed hERB-hRNase is also present in the insoluble fraction obtained from bacterial cells. Such a fraction of expressed IR was efficiently recovered by solubilisation with urea (Bayly *et al.* 2002), and analyzed by SDS-PAGE, followed by Coomassie staining, and Western blot analyses with an anti-His and an anti-HP-RNase antibody. The results are shown in Fig. 11. The solubilised sample appeared to contain different molecular species. Among them, only one was found to be immunoreactive to an anti-HP-RNase antibody. This band corresponded to the expected size (46,000 Da). Furthermore, an active band of the same molecular mass was visualized by zymogram analyses (Fig. 11), suggesting that the solubilisation procedure did not affect the enzymatic activity of the IR.

The recovered IR was then isolated by using the hydrophobic interaction chromatography (HIC) described above, followed by the affinity chromatography based on uridine 2',5'- and 3',5'-diphosphate (pUp) agarose, which is able to bind to the active site of enzymatically active ribonucleases (see above). Such a second step of purification was chosen to select the molecules of immunoconjugate with an enzymatically active ribonuclease portion, since the enzymatic activity of a fraction of IR molecules could be affected by solubilisation with urea. The obtained sample was then analyzed as above (Fig. 11). The results indicated that although the recombinant protein was present, it was not homogeneous (Fig. 11), since contaminant bands were detectable, requiring further purification, with an expected loss of protein. For this reason, the isolation of hERB-hRNase from the insoluble fraction of bacterial cells was considered to be impracticable.



5.5 Analysis of the Ribonucleolytic Activity of hERB-hRNase

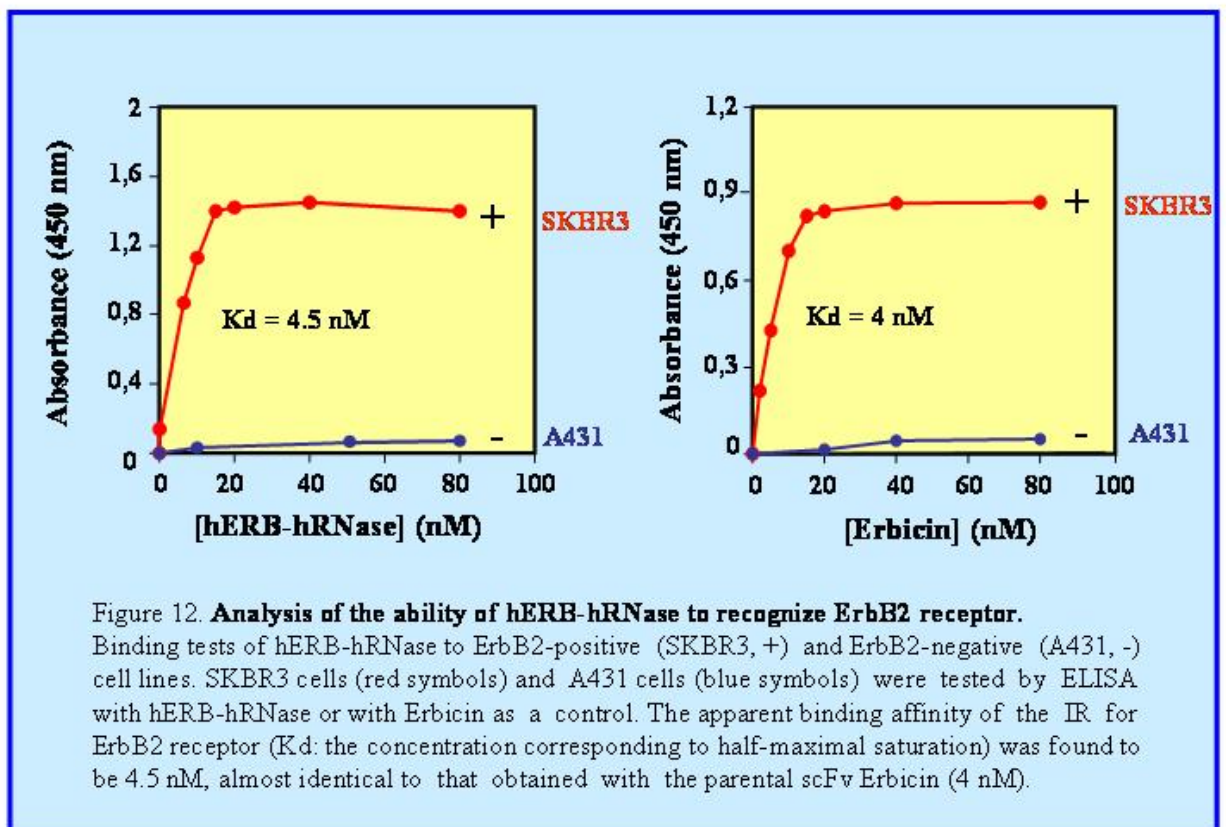
The enzymatic activity of the purified IR was further tested with the acid-insoluble RNA precipitation assay (Bartholeyns *et al.* 1977), by which the chimeric protein was found to have a specific activity of 950 ± 25 units/nmol. This value is the mean of data obtained with several preparations of the recombinant fusion protein (De Lorenzo *et al.* 2004). Since the specific activity of wild-type HP-RNase, tested in the same experimental conditions, was found to be approximately 1100 ± 20 units/nmol, we can conclude that the IR retains about 90% of the activity of the parental RNase (De Lorenzo *et al.* 2004). This result is of great interest, since most of the IRs prepared so far (Rybak and Newton 1999; Deonarain and Epenetos 1998) showed a consistent loss of enzymatic activity with respect to the native RNase.

5.6 Analysis of the Ability of hERB-hRNase to Specifically Recognize ErbB2 Receptor

The ability of the IR to specifically recognize ErbB2 receptor was evaluated by ELISA assays (see Materials and Methods section for details). The assays were performed using the following cell lines: SKBR3 cells, from human breast carcinoma, which express ErbB2 receptor at high levels, and A431 cells, from human epidermoid carcinoma, which express ErbB2 receptor at low levels, but are characterized by high expression levels of ErbB1 EGF receptor, belonging to the same ErbB family. It is worth noting that the use of intact cells, instead of the isolated antigen, allows the analysis of the ability of the immunoconjugate to bind the extracellular portion of ErbB2 receptor, in its native conformation.

The results of ELISA assays, shown in Fig. 12, indicate that hERB-hRNase binds with high affinity to SKBR3 cells, whereas no significant binding to A431 cells was detected. This clearly shows that the immunoconjugate is able to discriminate between ErbB2-positive and ErbB2-negative tumor cells, as well as among different receptors belonging to the same family. The apparent binding affinity of the IR for the ErbB2 receptor (*i.e.*, the concentration corresponding to half-maximal saturation) was found to be 4.5 nM, almost identical to that obtained with the parental scFv Erbicin (4 nM; Fig. 12) (De Lorenzo *et al.* 2004). Such a result clearly shows that the ability of the scFv Erbicin to recognize ErbB2 receptor is fully retained by the IR, and that the presence of the ribonuclease moiety in the immunoconjugate does not modify either the affinity of the scFv for ErbB2 or its ability to discriminate between ErbB2-positive and ErbB2-negative tumor cells.

ELISA assays were also performed using the following cell lines: MDA-MB361 cells, derived from human breast carcinomas, characterized by high expression levels of ErbB2 receptor; MDA-MB453 cells, derived from human breast carcinomas, and AG12 (TUBO) cells, from a BALB-neu T mouse-derived mammary lobular carcinoma (Rovero *et al.* 2000), both characterized by a lower level of ErbB2 expression, in comparison with SKBR3 and MDA-MB361 cells. The results of these assays, reported in Fig. 13, clearly show lower levels of ErbB2 immunoreactivity for MDA-MB453 and TUBO cells, compared with those obtained for SKBR3 and MDA-MB361 cells. These results are in agreement with previously reported data. In fact, the level of ErbB2 is reported six-fold lower in MDA-MB453 cells, compared with SKBR3 and MDA-MB361 cells (De Lorenzo *et al.* 2002a; Merlin *et al.* 2002). Thus, these results clearly indicate a positive correlation between ErbB2 expression levels on a particular cell type and the extent of binding of hERB-hRNase to those cells (De Lorenzo *et al.* 2004).



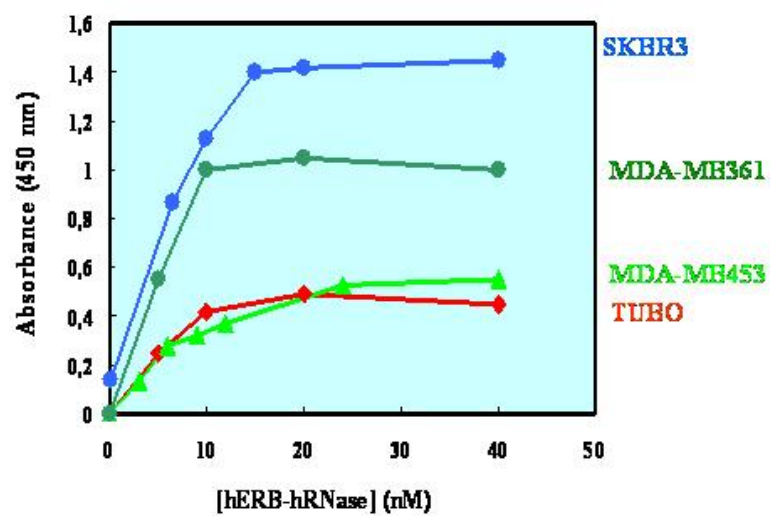
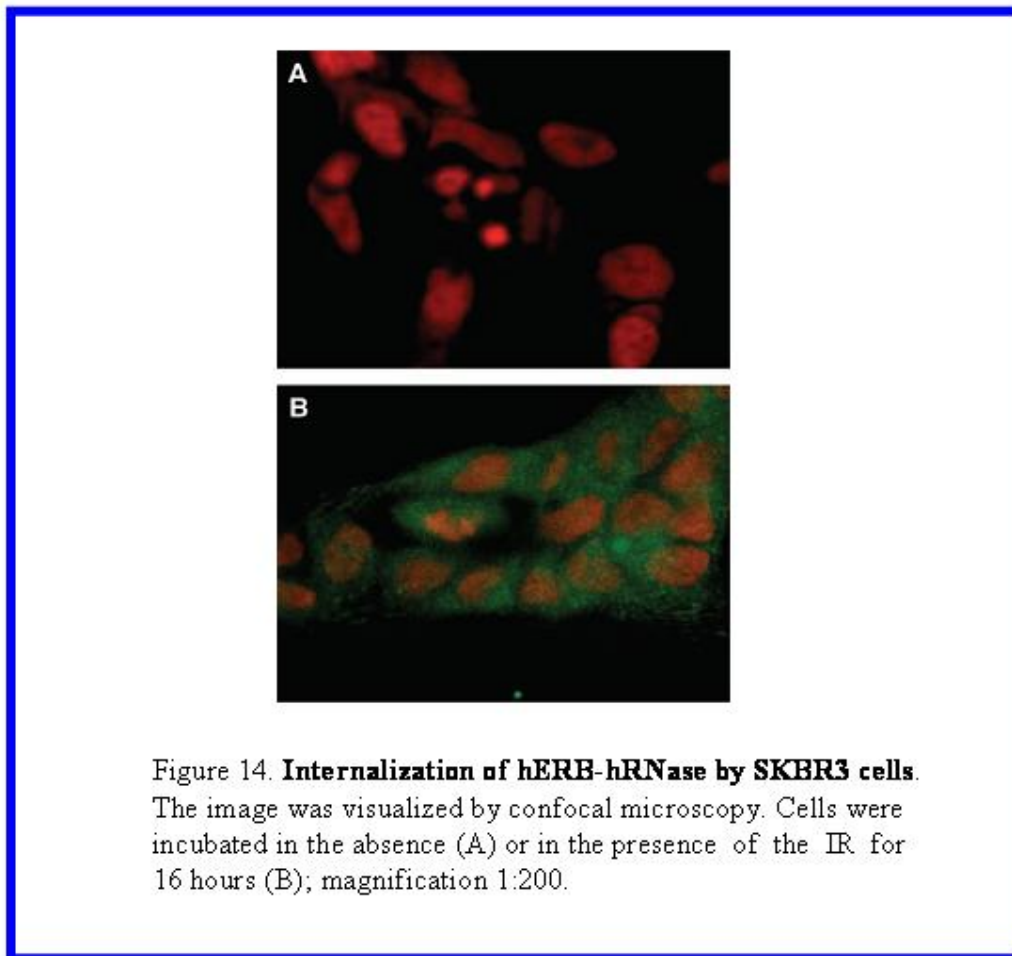


Figure 13. **Binding tests of hERB-hRNase to cells characterized by different ErbB2 expression levels.**

SKBR3 cells (●), MDA-MB361 cells (●), MDA-MB453 cells (▲), and TUBO cells (◆) were tested by ELISA assays with hERB-hRNase.

5.7 Internalization of hERB-hRNase by Target Cells

The human anti-ErbB2 scFv Erbicin undergoes receptor-mediated endocytosis in SKBR3 cells (De Lorenzo *et al.* 2002b). Experiments were aimed at testing whether the scFv retains this biological property in the fusion protein, thus providing a useful vehicle to deliver the RNase molecule into the cytosol of target cells. To this purpose, tumor target cells were incubated with hERB-hRNase for 16 hours at 37°C. After extensive washes, cells were fixed and permeabilized as described previously (De Lorenzo *et al.* 2002b). Internalized IR was visualized with an anti-HP-RNase antibody, followed by sheep antirabbit FITC-conjugated antibody. A strong intracellular staining was visualized by confocal microscopy in SKBR3 cells treated with hERB-hRNase (Fig. 14B), whereas no signal was detected in untreated SKBR3 cells (Fig. 14A) (De Lorenzo *et al.* 2004).



5.8 Cytotoxic Effects of hERB-hRNase on Tumor Cells

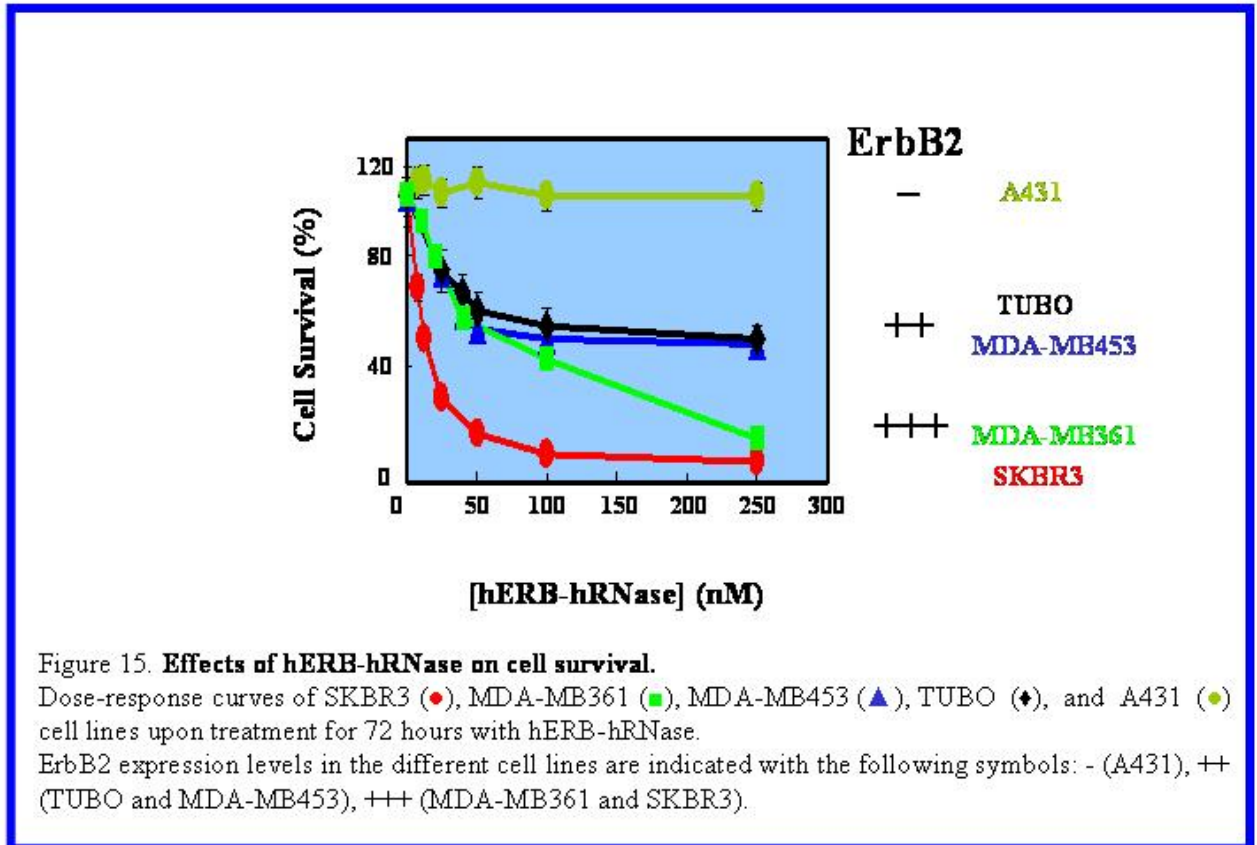
Purified hERB-hRNase was tested for cytotoxic activity on ErbB2-positive and ErbB2-negative tumor cells. The cytotoxicity assays were performed using the following cell lines: 1) SKBR3 and MDA-MB361 cells, derived from human breast carcinomas, characterized by high expression levels of ErbB2 receptor; 2) MDA-MB453 cells, from human breast carcinoma, and AG12 (TUBO) cells, from a BALB-neu T mouse-derived mammary lobular carcinoma (Rovero *et al.* 2000), characterized by a lower level of ErbB2 expression, with respect to SKBR3 and MDA-MB361 cells; 3) A431 cells, from human epidermoid carcinoma, characterized by very low levels of ErbB2 expression, but high levels of ErbB1 EGF receptor, belonging to the same ErbB family.

Cells were plated in the absence or in the presence of increasing amounts of hERB-hRNase. Following an incubation of 72 hours at 37°C, cell survival was measured by counting trypan blue-excluding cells and expressed as percentage of viable cells in the presence of the immunoconjugate, with respect to control cultures grown in the absence of the protein. The results of the assays are reported in Fig. 15. The IR was found to be cytotoxic in a dose-dependent manner on all of the antigen-positive cell lines tested, whereas no effects were observed on the proliferation of A431 cells. The values of IC₅₀ (*i.e.*, the concentration capable of reducing cell viability by 50%) were found to be 12.5, 47, 52, and 60 nM for SKBR3, MDA-MB361, MDA-MB453, and TUBO cells, respectively (De Lorenzo *et al.* 2004).

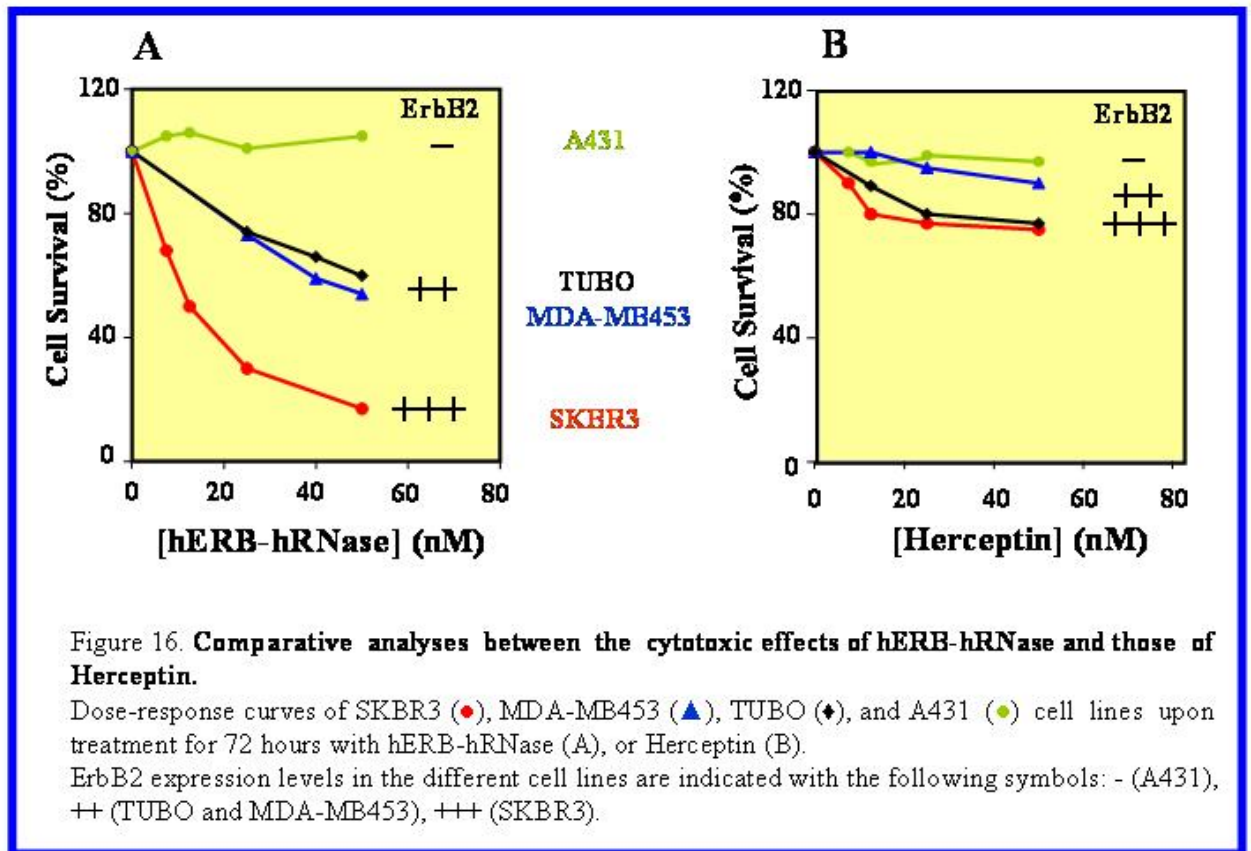
These results clearly indicate that the IR is able to finely discriminate between ErbB2-positive and ErbB2-negative cells and to selectively induce the death of target cells. Moreover, no effects on cell survival were detected when native HP-RNase was tested on ErbB2-positive cells at doses up to 20-fold higher than the highest dose of RNase present in the IR samples tested on cell cultures (data not shown). This clearly indicates that the RNase moiety has no effect on cell proliferation, unless driven inside the cells by the antibody moiety. It should be also noted that the scFv alone was found to inhibit the proliferation of SKBR3 cells with an IC₅₀ value of 200 nM (De Lorenzo *et al.* 2002b) (data not shown). This means that the IR, for which an IC₅₀ value of 12.5 nM was obtained, is much more effective as an anticancer agent than the isolated antibody moiety. The increased cytotoxic potential can only be attributed to the additional toxic action of the internalized RNase.

Furthermore, it is of interest to notice that the stronger cytotoxicity of hERB-hRNase on SKBR3 and MDA-MB361 cells compared with that observed on MDA-MB453 and AG12 (TUBO) cells is related to the different ErbB2 expression levels on these cell lines, assessed as described above. Thus, these results clearly indicate a strong positive correlation between ErbB2 expression

levels on a particular cell type, the extent of binding of hERB-hRNase to those cells, and their sensitivity to IR cytotoxic action.



Further studies were performed to compare the cytotoxic activity of hERB-hRNase and that of Herceptin, a humanized version of an anti-ErbB2 murine antibody, currently in use for treatment of advanced breast cancer (Milenic 2002). The results of these assays are reported in Fig. 16. Interestingly, in our hands the antiproliferative effects of Herceptin, tested for 72 hours on the previously described cell lines (SKBR3, MDA-MB453, TUBO and A431), were much weaker than those obtained with identical amounts of hERB-hRNase.



5.9 Stability of hERB-hRNase

The stability of immunoagents at 37°C is a critical factor for their potential as therapeutic agents. The stability of hERB-hRNase in human or murine serum at 37°C for up to 48 hours was analyzed by monitoring its integrity both as a protein and as functional bioeffector. Following an incubation in serum for 24 or 48 hours at 37°C, the percentage of undegraded and enzymatically active IR was determined by Western blot and zymogram analyses. By using a Phosphorimager, the intensity of the electrophoretic bands obtained with treated hERB-hRNase was expressed as the percentage of the signal given by the untreated protein. After 24 or 48 hours the percentage of undegraded and enzymatically active hERB-hRNase was $100 \pm 5\%$ (De Lorenzo *et al.* 2004) (Fig. 17).

The binding properties of the IR after incubation in serum were assessed by ELISA assays on ErbB2-positive cells and expressed as the concentration corresponding to half-maximal saturation (Fig. 17). The results showed that the protein, incubated in human or murine serum, conserved a value of half-maximal saturation of 5 nM, virtually identical to that measured for the protein before incubation (see above) (De Lorenzo *et al.* 2004).

Finally, hERB-hRNase was found to fully retain its cytotoxic activity after incubation at 37°C for up to 48 hours. The IC_{50} values of the incubated samples, tested on SKBR3 cells (see above), were within $\pm 10\%$ of the values measured before incubation (Fig. 17) (De Lorenzo *et al.* 2004).

These results clearly indicate that the IR is stable under the examined physiologic-like conditions.

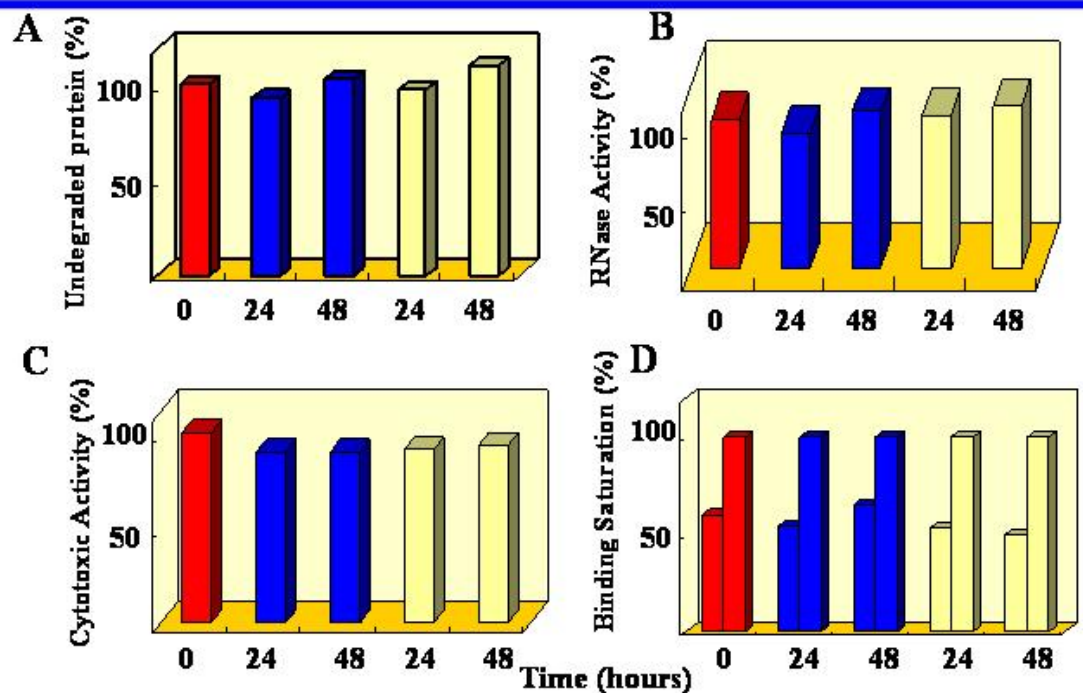
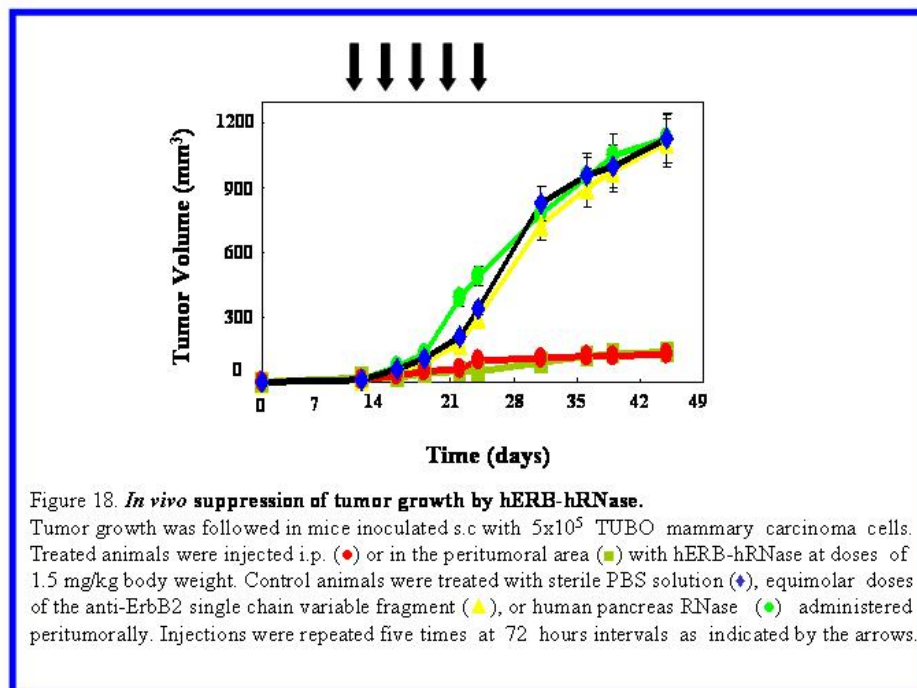


Figure 17. **Stability of hERB-hRNase in human (blue) or murine (yellow) serum at 37°C for up to 48 hours.** The percentage of undegraded IR was determined by Western blot analyses (A). The percentage of enzymatically active IR was determined by zymogram analyses (B). The percentage of cytotoxic activity was determined by cytotoxicity assays (IC_{50} values of the incubated samples tested on SKBR3 cells were compared to those measured before incubation) (C). The binding properties were assessed by ELISA assays on ErbB2-positive cells and expressed as the concentration corresponding to half-maximal saturation. For each time and for each experimental condition, two samples at a different concentration (5 and 20 nM) were tested (D).

5.10 *In vivo* Antitumor Activity of hERB-hRNase

The ErbB2-positive tumor cell line AG12 (TUBO), from a BALB-neu T mouse-derived mammary lobular carcinoma (Rovero *et al.* 2000), was used for *in vivo* studies. TUBO cells were used to induce the formation of tumors in BALB/cAnNCrIBR mice. The IR was administered five times at intervals of 72 hours, peritumorally or intraperitoneally, at doses of 1.5 mg/kg of body weight. Control animals were treated with identical volumes of sterile phosphate-buffered saline (PBS). A dramatic reduction in tumor volume was observed when hERB-hRNase was injected peritumorally (Fig. 18). Similar results were obtained when the protein was administered systemically by intra-peritoneal injections. This suggests that the protein is stable in the bloodstream and is able to permeate tumor masses. Contrarily, equimolar doses of the anti-ErbB2 scFv Erbicin and native HP-RNase, injected peritumorally, showed no significant effects on tumor growth (Fig. 18). Thus, these results clearly indicate that the effects on the growth of TUBO tumors can be attributed to the fusion protein as a whole. Moreover, during the period of treatment the animals did not show signs of wasting or other visible signs of toxicity, and their main haematological parameters were those of normal mice (data not shown).



6. CONCLUSIONS

In the present study, we report the construction, characterization and antitumor activity of a novel, fully human IR (De Lorenzo *et al.* 2004). Such IR is composed by the human pancreas ribonuclease (HP-RNase) and a human single chain variable fragment (scFv) directed to the ErbB2 receptor (De Lorenzo *et al.* 2002b). ErbB2 is an attractive tumor target because of its specific localization on many tumor cells of different origin, its extracellular accessibility, and its high expression levels in many carcinomas (Slamon *et al.* 1989; Klapper *et al.* 2000).

The novel fully human IR, named hERB-hRNase, was found to retain the enzymatic activity of native RNase and to bind to target cells as selectively and effectively as the parental, free scFv.

The fully human IR acts as an immunoprototoxin. This means that it is the ability of the scFv to be internalized by ErbB2-overexpressing cells, a feature fully preserved in the fusion protein, which allows the RNase to enter the cytosol and kill target cells. This was confirmed by experiments showing that HP-RNase is not *per se* a cytotoxic agent, neither *in vitro* nor *in vivo*. On the other hand, previous studies showed that the scFv alone is able to inhibit the proliferation of ErbB2-positive cells (De Lorenzo *et al.* 2002b). Here, we demonstrate that the IR is a more effective anticancer drug. Such a result can only be attributed to the additional toxic action of the internalized RNase.

Interestingly, the comparison between the cytotoxic effects of hERB-hRNase and those of Herceptin, a humanized version of an anti-ErbB2 murine antibody, currently in use for treatment of advanced breast cancer (Milenic 2002), indicated that the antiproliferative effects of Herceptin were much weaker than those obtained with the same amount of hERB-hRNase.

Furthermore, hERB-hRNase was found to be stable for at least 48 hours when incubated at 37°C in human or murine serum. Such a feature of the IR enhances its potential as a promising antitumor drug. Even more interesting are the results of *in vivo* assays of hERB-hRNase antitumor action carried out on mice inoculated with TUBO ErbB2-positive tumor cells, which produce tumors similar to the alveolar-type human lobular mammary carcinomas (Di Carlo *et al.* 1999). Treatment of mice inoculated with TUBO cells with only five doses of hERB-hRNase (1.5 mg/kg body weight) strongly inhibited tumor growth. These results can only be attributed to the fusion protein as a whole, as the two moieties, the anti-ErbB2 scFv and HP-RNase, when administered separately to tumor bearing mice, were not found to be effective in inhibiting tumor growth.

To our knowledge, hERB-hRNase is the first fully human IR to be constructed and tested with satisfactory results *in vitro* and *in vivo*. Its fully human nature, combined with its stability and its selective cytotoxic action on target cells, could make it a precious tool in the therapy of human mammary carcinomas.

7. BIBLIOGRAPHY

- Allen TM. Ligand-targeted therapeutics in anticancer therapy. *Nat Rev Cancer* 2002;2:750-63.
- Baluna R, Vitetta ES. An in vivo model to study immunotoxin-induced vascular leak in human tissue. *J Immunother* 1999;22:41-7.
- Bartholeyns J, Wang D, Blackburn P, Wilson G, Moore S, Stein WH. Explanation of the observation of pancreatic ribonuclease activity at pH 4.5. *Int J Pept Protein Res* 1977;10:172-5.
- Bayly AM, Kortt AA, Hudson PJ, Power BE. Large-scale bacterial fermentation and isolation of scFv multimers using a heat-inducible bacterial expression vector. *J Immunol Methods* 2002;262:217-27.
- Becerril B, Poul MA, Marks JD. Toward selection of internalizing antibodies from phage libraries. *Biochem Biophys Res Commun* 1999;255:386-93.
- Biedler JL, Riehm H. Cellular resistance to actinomycin D in Chinese hamster cells in vitro: cross-resistance, radioautographic, and cytogenetic studies. *Cancer Res* 1970;30:1174-84.
- Blank A, Sugiyama RH, Dekker CA. Activity staining of nucleolytic enzymes after sodium dodecyl sulfate-polyacrylamide gel electrophoresis: use of aqueous isopropanol to remove detergent from gels. *Anal Biochem* 1982;120:267-75.
- Brekke OH, Sandlie I. Therapeutic antibodies for human diseases at the dawn of the twenty-first century. *Nat Rev Drug Discov* 2003;2:52-62.
- Carter P, Presta L, Gorman CM, Ridgway JB, Henner D, Wong WL, Rowland AM, Kotts C, Carver, ME, Shepard HM. Humanization of an anti-p185HER2 antibody for human cancer therapy. *Proc Natl Acad Sci USA* 1992;89:4285-9.
- De Lorenzo C., Arciello A, Cozzolino R, Palmer DB, Laccetti P, Piccoli R, D'Alessio G. A fully human antitumor immunoRNase selective for ErbB-2-positive carcinomas. *Cancer Res* 2004;64:4870-4.
- De Lorenzo C, Nigro A, Piccoli R, D'Alessio G. A new RNase-based immunoconjugate selectively cytotoxic for ErbB2-overexpressing cells. *FEBS Lett* 2002a;516:208-12.
- De Lorenzo C, Palmer DB, Piccoli R, Ritter MA, D'Alessio G. A new human antitumor immunoreagent specific for ErbB2. *Clin Cancer Res* 2002b;8:1710-9.
- Deonarain MP, Epenetos AA. Design, characterization and anti-tumour cytotoxicity of a panel of recombinant, mammalian ribonuclease-based immunotoxins. *Br J Cancer* 1998;77:537-46.
- Di Carlo E, Diodoro MG, Boggio K, Modesti A, Modesti M, Nanni P, Forni G, Musiani P. Analysis of mammary carcinoma onset and progression in HER-2/neu oncogene transgenic mice reveals a lobular origin. *Lab Invest* 1999;79:1261-9.
- Evan GI, Lewis GK, Ramsay G, Bishop JM. Isolation of monoclonal antibodies specific for human c-myc proto-oncogene product. *Mol Cell Biol* 1985;5:3610-6.

Fukushige S, Matsubara K, Yoshida M, Sasaki M, Suzuki T, Semba K, Toyoshima K, Yamamoto T. Localization of a novel v-erbB-related gene, c-erbB-2, on human chromosome 17 and its amplification in a gastric cancer cell line. *Mol Cell Biol* 1986;6:955-8.

Graus-Porta D, Beerli RR, Daly JM, Hynes NE. ErbB-2, the preferred heterodimerization partner of all ErbB receptors, is a mediator of lateral signaling. *Embo J* 1997;16:1647-55.

Griffiths AD, Williams SC, Hartley O, Tomlinson IM, Waterhouse P, Crosby WL, Kontermann RE, Jones PT, Low NM, Allison TJ, *et al.* Isolation of high affinity human antibodies directly from large synthetic repertoires. *Embo J* 1994;13:3245-60.

Hudziak RM, Lewis GD, Shalaby MR, Eessalu TE, Aggarwal BB, Ullrich A, Shepard HM. Amplified expression of the HER2/ERBB2 oncogene induces resistance to tumor necrosis factor alpha in NIH 3T3 cells. *Proc Natl Acad Sci USA* 1988;85:5102-6.

Huston JS, Levinson D, Mudgett-Hunter M, Tai MS, Novotny J, Margolies MN, Ridge RJ, Bruccoleri RE, Haber E, Crea R, *et al.* Protein engineering of antibody binding sites: recovery of specific activity in an anti-digoxin single-chain Fv analogue produced in *Escherichia coli*. *Proc Natl Acad Sci USA* 1988;85:5879-83.

King CR, Kraus MH, Aaronson SA. Amplification of a novel v-erbB-related gene in a human mammary carcinoma. *Science* 1985;229:974-6.

Klapper LN, Kirschbaum MH, Sela M, Yarden Y. Biochemical and clinical implications of the ErbB/HER signaling network of growth factor receptors. *Adv Cancer Res* 2000;77:25-79.

Laccetti P, Spalletti-Cernia D, Portella G, De Corato P, D'Alessio G, Vecchio G. Seminal ribonuclease inhibits tumor growth and reduces the metastatic potential of Lewis lung carcinoma. *Cancer Res* 1994;54:4253-6

Laemmli UK. Cleavage of structural proteins during the assembly of the head of bacteriophage T4. *Nature* 1970;227:680-5.

Matousek J. The effect of bovine seminal ribonuclease (BS-RNase) on cells of Crocker tumour in mice. *Experientia* 1973;29:858-9.

Meerman HJ, Georgiou G. Construction and characterization of a set of *E. coli* strains deficient in all known loci affecting the proteolytic stability of secreted recombinant proteins. *Biotechnology (N Y)* 1994;12:1107-10.

Merlin JL, Barberi-Heyob M, Bachman N. In vitro comparative evaluation of trastuzumab (Herceptin) combined with paclitaxel (Taxol) or docetaxel (Taxotere) in HER2-expressing human breast cancer cell lines. *Ann Oncol* 2002;13:1743-8.

Milenic, DE. Monoclonal antibody-based therapy strategies: providing options for the cancer patient. *Curr Pharm Des* 2002;8:1749-64.

Newton DL, Hansen HJ, Mikulski SM, Goldenberg DM, Rybak SM. Potent and specific antitumor effects of an anti-CD22-targeted cytotoxic ribonuclease: potential for the treatment of non-Hodgkin lymphoma. *Blood* 2001;97:528-35.

Newton DL, Ilercil O, Laske DW, Oldfield E, Rybak SM, Youle RJ. Cytotoxic ribonuclease chimeras. Targeted tumoricidal activity in vitro and in vivo. *J Biol Chem* 1992;267:19572-8.

Newton DL, Nicholls PJ, Rybak SM, Youle RJ. Expression and characterization of recombinant human eosinophil-derived neurotoxin and eosinophil-derived neurotoxin-anti-transferrin receptor scFv. *J Biol Chem* 1994;269:26739-45

Newton DL, Xue Y, Olson KA, Fett JW, Rybak SM. Angiogenin single-chain immunofusions: influence of peptide linkers and spacers between fusion protein domains. *Biochemistry* 1996;35:545-53

Nissim A, Hoogenboom HR, Tomlinson IM, Flynn G, Midgley C, Lane D, Winter G. Antibody fragments from a 'single pot' phage display library as immunochemical reagents. *Embo J* 1994;13:692-8.

Pastan I, FitzGerald D. Recombinant toxins for cancer treatment. *Science* 1991;254:1173-7.

Pouckova P, Soucek J, Jelinek J, Zadinova M, Hlouskova D, Polivkova J, Navratil L, Cinatl J, Matousek J. Antitumor action of bovine seminal ribonuclease. Cytostatic effect on human melanoma and mouse seminoma. *Neoplasma* 1998;45:30-4

Poul MA, Becerril B, Nielsen UB, Morrison P, Marks, JD. Selection of tumor-specific internalizing human antibodies from phage libraries. *J Mol Biol* 2000;301:1149-61.

Press MF, Cordon-Cardo C, Slamon DJ. Expression of the HER-2/neu proto-oncogene in normal human adult and fetal tissues. *Oncogene* 1990;5:953-62.

Reiter Y, Brinkmann U, Jungh SH, Lee B, Kasprzyk PG, King CR, Pastan I. Improved binding and antitumor activity of a recombinant anti-erbB2 immunotoxin by disulfide stabilization of the Fv fragment. *J Biol Chem* 1994;269:18327-31.

Reiter Y, Pastan I. Recombinant Fv immunotoxins and Fv fragments as novel agents for cancer therapy and diagnosis. *Trends Biotechnol* 1998;16:513-20.

Ross J, Gray K, Schenkein D, Greene B, Gray GS, Shulok J, Worland PJ, Celniker A, Rolfe M. Antibody-based therapeutics in oncology. *Expert Rev Anticancer Ther* 2003;3:107-21.

Rovero S, Amici A, Carlo ED, Bei R, Nanni P, Quaglino E, Porcedda P, Boggio K, Smorlesi A, Lollini PL, Landuzzi L, Colombo MP, Giovarelli M, Musiani P, Forni G. DNA vaccination against rat her-2/Neu p185 more effectively inhibits carcinogenesis than transplantable carcinomas in transgenic BALB/c mice. *J Immunol* 2000;165:5133-42.

Russo N, de Nigris M, Ciardiello A, Di Donato A, D'Alessio G. Expression in mammalian cells, purification and characterization of recombinant human pancreatic ribonuclease. *FEBS Lett* 1993;333:233-7.

Rybak SM, Newton DL. Natural and engineered cytotoxic ribonucleases: therapeutic potential. *Exp Cell Res* 1999;253:325-35.

Sambrook and Russel. *Molecular cloning: a laboratory manual*. 3rd ed. New York: Cold Spring Harbor Laboratory Press; 2001. Appendix 2.

Schier R, Marks JD, Wolf, EJ, Apell G, Wong C, McCartney JE, Bookman MA, Huston JS, Houston LL, Weiner LM. In vitro and in vivo characterization of a human anti-c-erbB-2 single-chain Fv isolated from a filamentous phage antibody library. *Immunotechnology* 1995;1:73-81.

Schindler J, Sausville E, Messmann R, Uhr JW, Vitetta ES. The toxicity of deglycosylated ricin A chain-containing immunotoxins in patients with non-Hodgkin's lymphoma is exacerbated by prior radiotherapy: a retrospective analysis of patients in five clinical trials. *Clin Cancer Res* 2001;7:255-8.

Schnell R, Vitetta E, Schindler J, Borchmann P, Barth S, Ghetie V, Hell K, Drillich S, Diehl V, Engert A. Treatment of refractory Hodgkin's lymphoma patients with an anti-CD25 ricin A-chain immunotoxin. *Leukemia* 2000;14:129-35.

Semba K, Kamata N, Toyoshima K, Yamamoto T. A v-erbB-related protooncogene, c-erbB-2, is distinct from the c-erbB-1/epidermal growth factor-receptor gene and is amplified in a human salivary gland adenocarcinoma. *Proc Natl Acad Sci USA* 1985;82:6497-501.

Sheets MD, Amersdorfer P, Finnern R, Sargent P, Lindquist E, Schier R, Hemingsen G, Wong C, Gerhart JC, Marks, JD, Lindqvist E. Efficient construction of a large nonimmune phage antibody library: the production of high-affinity human single-chain antibodies to protein antigens. *Proc Natl Acad Sci USA* 1998;95:6157-62.

Slamon DJ, Godolphin W, Jones LA, Holt JA, Wong SG, Keith DE, Levin WJ, Stuart SG, Udove J, Ullrich A. Studies of the HER-2/neu proto-oncogene in human breast and ovarian cancer. *Science* 1989;244:707-12.

Soler-Rodriguez AM, Ghetie MA, Oppenheimer-Marks N, Uhr JW, Vitetta ES. Ricin A-chain and ricin A-chain immunotoxins rapidly damage human endothelial cells: implications for vascular leak syndrome. *Exp Cell Res* 1993;206:227-34.

Soucek J, Pouckova P, Matousek J, Stockbauer P, Dostal J, Zadinova M. Antitumor action of bovine seminal ribonuclease. *Neoplasma* 1996;43:335-40.

Stocker M, Tur MK, Sasse S, Krussmann A, Barth S, Engert A. Secretion of functional anti-CD30-angiogenin immunotoxins into the supernatant of transfected 293T-cells. *Protein Expr Purif* 2003;28:211-9.

Suwa T, Ueda M, Jino H, Ozawa S, Kitagawa Y, Ando N, Kitajima M. Epidermal growth factor receptor-dependent cytotoxic effect of anti-EGFR

antibody-ribonuclease conjugate on human cancer cells. *Anticancer Res* 1999;19:4161-5.

Tagliabue E, Centis F, Campiglio M, Mastroianni A, Martignone S, Pellegrini R, Casalini P, Lanzi C, Menard S, Colnaghi MI. Selection of monoclonal antibodies which induce internalization and phosphorylation of p185HER2 and growth inhibition of cells with HER2/NEU gene amplification. *Int J Cancer* 1991;47:933-7.

Trikha M, Yan L, Nakada MT. Monoclonal antibodies as therapeutics in oncology. *Curr Opin Biotechnol* 2002;13:609-14.

Ullrich A, Schlessinger J. Signal transduction by receptors with tyrosine kinase activity. *Cell* 1990;61:203-12.

Vaughan TJ, Williams AJ, Pritchard K, Osbourn JK, Pope AR, Earnshaw JC, McCafferty J, Hodits RA, Wilton J, Johnson KS. Human antibodies with sub-nanomolar affinities isolated from a large non-immunized phage display library. *Nat Biotechnol* 1996;14:309-14.

Weiner LM, O'Dwyer J, Kitson J, Comis RL, Frankel AE, Bauer RJ, Konrad MS, Groves ES. Phase I evaluation of an anti-breast carcinoma monoclonal antibody 260F9-recombinant ricin A chain immunoconjugate. *Cancer Res* 1989;49:4062-7.

Wels W, Beerli R, Hellmann P, Schmidt M, Marte BM, Kornilova ES, Hekele A, Mendelsohn J, Groner B, Hynes NE. EGF receptor and p185erbB-2-specific single-chain antibody toxins differ in their cell-killing activity on tumor cells expressing both receptor proteins. *Int J Cancer* 1995;60:137-44.

Yamamoto T, Ikawa S, Akiyama T, Semba K, Nomura N, Miyajima N, Saito T, Toyoshima K. Similarity of protein encoded by the human c-erb-B-2 gene to epidermal growth factor receptor. *Nature* 1986;319:230-4.

Yarden Y, Schlessinger J. Epidermal growth factor induces rapid, reversible aggregation of the purified epidermal growth factor receptor. *Biochemistry* 1987;26:1443-51.

Zewe M, Rybak SM, Dubel S, Coy JF, Welschof M, Newton DL, Little M. Cloning and cytotoxicity of a human pancreatic RNase immunofusion. *Immunotechnology* 1997;3:127-36.

Chapter 2

Analysis of the role of the membrane transporter ABCC2/MRP2 in multidrug resistance (MDR)

1. ABSTRACT

The ABC (ATP binding cassette) family of membrane transport proteins includes the best known mediators of resistance to anticancer drugs, such as the ABC transporters ABCB1 (MDR1/P-gp), ABCC1/MRP1, and ABCG2/MXR. However, although ABC transporters overexpression appears to be a major cause of failure in the treatment of cancer, acquired resistance to multiple anticancer drugs may also be multifactorial, involving alteration of detoxification processes, apoptosis, DNA repair and drug uptake.

The human prostate cancer cell line RC0.1 has been derived from the parental sensitive cell line DU145 by continuous exposure to the drug rubitecan (9-nitro-camptothecin), an inhibitor of topoisomerase I, now in phase III clinical trials. Several factors have been proposed to explain the phenotype of camptothecin resistance in RC0.1 cell line. Microarray analyses, performed using a novel ABC-ToxChip, indicated the overexpression of the ABC transporter MRP2 in the resistant cell line RC0.1. In order to establish the role of MRP2 in camptothecin resistance, different strategies were used in the present study to inhibit this ABC transporter. The inhibition of MRP2 expression was obtained by RNA interference technology, whereas the inhibition of its biological activity was achieved using the inhibitor MK571. In both cases, the resistance phenotype of RC0.1 tumor cells was not reverted. This indicated that MRP2 does not play a crucial role in the resistance mechanism. To explain MRP2 overexpression, we hypothesized that this represents an early adaptation of the cells to the drug, providing the background for the evolution of different resistance mechanisms.

The expression profile of the 48 ABC transporters has been characterized in a panel of 60 diverse cancer cell lines (the NCI-60), used by the National Cancer Institute (NCI) to screen for anticancer activity. By correlating the expression results with the growth inhibitory profiles of 1,429 candidate anticancer drugs tested against the cells, transporters able to confer resistance to anticancer drugs have been identified. In particular, 28 compounds were predicted to be less active in cells that expressed large amounts of MRP2. Such a prediction has been confirmed in the present study. Furthermore, the analysis of the chemical structures of the 28 identified MRP2 substrates led to the identification of common structural features, such as a cyclopentanone ring, an element structurally related to the cyclopentenone ring of prostaglandins. This observation led us to hypothesize a new role for MRP2 transporter, such as its involvement in the transport of cyclopentenone prostaglandins. Prostaglandins are involved in a wide variety of physiological and pathophysiological processes, but the mechanism of prostaglandin release from cells is not completely understood. Here we demonstrate an effective involvement of MRP2 in the transport of the cyclopentenone prostaglandin 15-deoxy- $\Delta^{12,14}$ -prostaglandin J₂ (15-d-PGJ₂).

2. BACKGROUND

2.1 Multidrug Resistance (MDR) and ATP-Binding Cassette (ABC) Transporters

Chemotherapy is still one of the most effective ways to treat metastatic tumors. Unfortunately, even when multiple agents are used simultaneously, the effectiveness of chemotherapy is limited by the multidrug resistance of cancer cells, a phenotype that makes tumor cells resistant to structurally and mechanistically unrelated drugs. Resistance to natural-product hydrophobic drugs, sometimes known as classical multidrug resistance (MDR), is generally associated with the decreased cellular accumulation of anti-cancer drugs and the elevated expression of an ATP-dependent drug-efflux pump, termed P-glycoprotein (P-gp), the MDR1 gene product (Gottesman *et al.* 2002).

Intrinsic or primary resistance is characteristic of cancers originating from tissues constitutively expressing high levels of P-gp, such as the epithelia of the kidney, liver and intestine, the endothelial cells of the brain, ovary, testis, the adrenal cortex and placenta (Gottesman *et al.* 2002). Since P-gp is also expressed in hematopoietic stem cells and other circulating blood cells, intrinsic resistance is also found in several hematological malignancies (Gottesman *et al.* 2002). These localizations are consistent with the concept that P-gp plays a major role in the normal uptake and excretion of many differential drugs and also serves as blood-brain, blood-testis, blood-ovary, and blood-fetus barriers for cytotoxic drugs. Furthermore, cells may increase P-gp expression as a consequence of a chronic environmental stress. This has been shown in experiments performed applying heat shock, or partial hepatectomy in various models (Chin *et al.* 1990; Thorgeirsson *et al.* 1987; Marino *et al.* 1990). In addition, molecular events occurring during malignant transformation (such as mutations in p53) may be sufficient to produce increased MDR1 expression (Chin *et al.* 1992; Zastawny *et al.* 1993; Thottassery *et al.* 1997). More importantly, due to their inherent genetic instability and heightened frequency of mutation, cancer cells are frequently heterogeneous with respect to MDR1 expression and such cells have a selective advantage during adaptation to stress, such as hypoxia or inflammation. As a result of these mechanisms, a significant portion of malignant cells may be already prepared for defense against chemotherapy at the time of diagnosis. In addition, cells may increase MDR1 expression in direct response to drug exposure (Szakács *et al.* 2004b).

Classical multidrug resistance P-gp mediated is due to increased drug efflux that lowers intracellular drug concentrations. Drugs that are affected by this kind of multidrug resistance include vinblastine and vincristine (Vinca Alkaloids),

doxorubicin and daunorubicin (Anthracyclines), the RNA transcription inhibitor actinomycin-D and the microtubule-stabilizing drug paclitaxel (Ambudkar *et al.* 1999).

However, resistance can also be mediated by reduced drug uptake. In fact, water-soluble drugs or agents that enter the cell by means of endocytosis, might fail to accumulate without evidence of increased efflux. Examples include the antifolate methotrexate, nucleotide analogues, such as 5-fluorouracil and 8-azaguanine, and cisplatin (Shen *et al.* 2000; Shen *et al.* 1998). Multidrug resistance can also result from activation of coordinately regulated detoxifying systems, such as DNA repair and the cytochrome P450 mixed-function oxidases. Indeed, coordinate induction of the multidrug transporter P-gp and cytochrome P4503A has been observed (Schuetz *et al.* 1996). This type of multidrug resistance can be induced after exposure to any drug. It has been shown that certain orphan nuclear receptors, such as SXR, might be involved in mediating this global response to environmental stress (Synold *et al.* 2001).

Finally, resistance can result from defective apoptotic pathways. This might occur as a result of malignant transformation; for example, in cancers with mutant or non-functional p53 (Lowe *et al.* 1993). Alternatively, cells might acquire changes in apoptotic pathways during exposure to chemotherapy, such as changes in cell-cycle machinery, which activate checkpoints and prevent initiation of apoptosis. An important principle in multidrug resistance is that cancer cells are genetically heterogeneous. Although the process that results in uncontrolled cell growth in cancer favours clonal expansion, tumor cells that are exposed to chemotherapeutic agents will be selected for their ability to survive and grow in the presence of cytotoxic drugs. These cancer cells are likely to be genetically heterogeneous because of the mutator phenotype. Thus, in any population of cancer cells, that is exposed to chemotherapy, more than one mechanism of multidrug resistance can be present. This phenomenon has been called multifactorial multidrug resistance (Gottesman *et al.* 2002).

In Fig. 1 a schematic representation of the mechanisms responsible for MDR is reported.

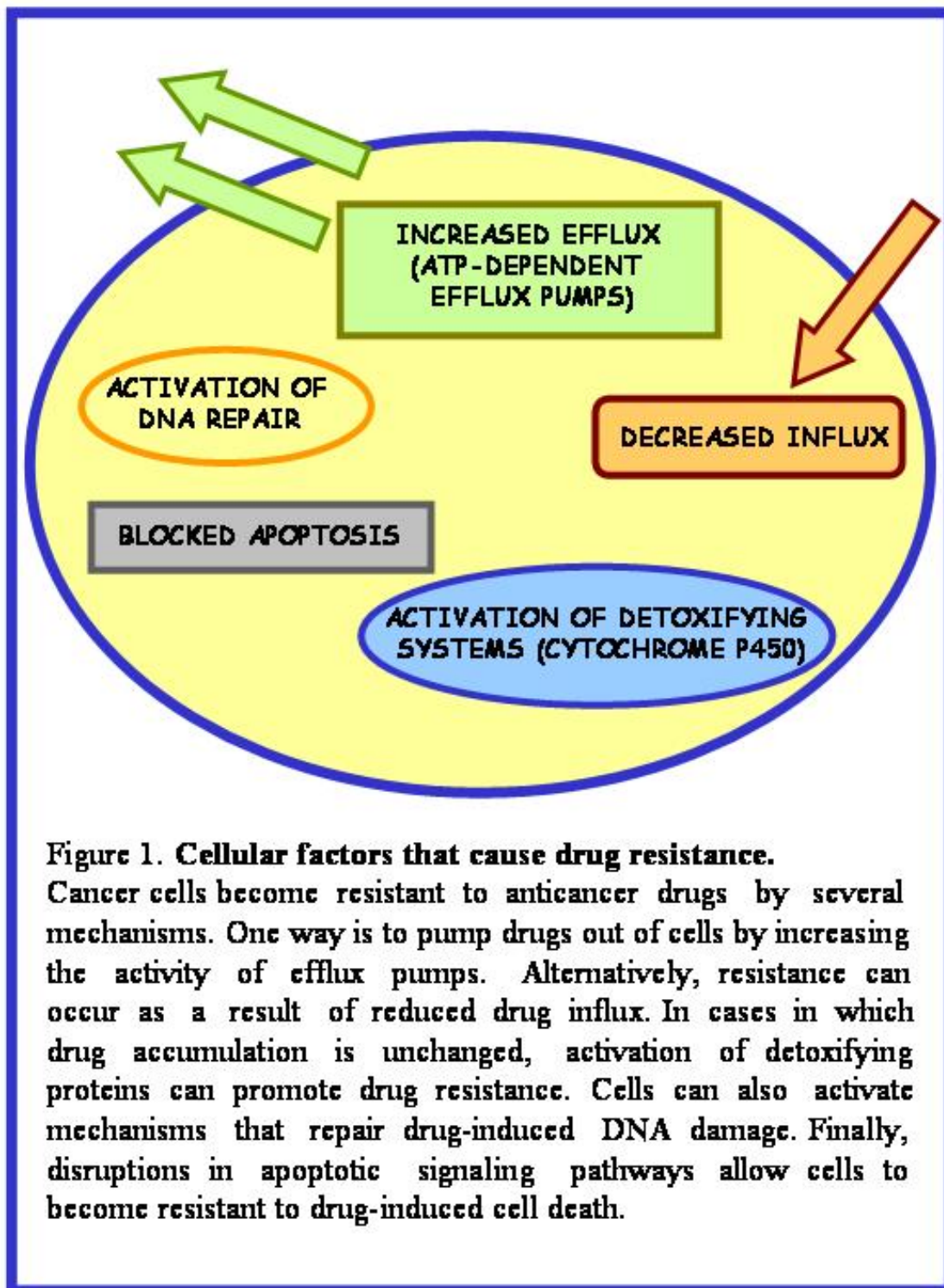


Figure 1. Cellular factors that cause drug resistance.

Cancer cells become resistant to anticancer drugs by several mechanisms. One way is to pump drugs out of cells by increasing the activity of efflux pumps. Alternatively, resistance can occur as a result of reduced drug influx. In cases in which drug accumulation is unchanged, activation of detoxifying proteins can promote drug resistance. Cells can also activate mechanisms that repair drug-induced DNA damage. Finally, disruptions in apoptotic signaling pathways allow cells to become resistant to drug-induced cell death.

P-gp, also known as ABCB1, belongs to the superfamily of ATP-binding cassette (ABC) transporters. ABC transporters are integral membrane proteins that transport a wide variety of substrates across cell membranes, including metabolic products, lipids, sterol and xenobiotics such as chemotherapeutic drugs. They share sequence and structural homology. Their functional significance is suggested by the observation that they form one of the largest protein families, found in various cellular membranes of organisms, from bacteria to mammals. So far, 48 human ABC genes have been identified and divided into 7 distinct subfamilies (ABCA-ABCG) on the basis of their sequence homology and domain organization (Dean *et al.* 2001).

P-gp is a broad-spectrum multidrug efflux pump that has 12 transmembrane regions and 2 ATP-binding sites (Chen *et al.* 1986) (Fig. 2). The transmembrane regions bind hydrophobic drugs that are either neutral or positively charged, and are probably presented to the transporter directly from the lipid bilayer (Ambudkar *et al.* 1999). Two ATP hydrolysis events, which do not occur simultaneously, are needed to transport one drug molecule (Senior and Bhagat 1998). Binding of substrate to the transmembrane regions stimulates the ATPase activity of P-gp, causing a conformational change that releases substrate to either the outer leaflet of the membrane (from which it can diffuse into the medium) or the extracellular space (Ramachandra *et al.* 1998). Hydrolysis at the second ATP site seems to be required to re-set the transporter so that it can bind substrate again, completing one catalytic cycle (Sauna ZE and Ambudkar SV 2000).

P-gp efficiently removes cytotoxic drugs and many commonly used pharmaceuticals from the lipid bilayer. Its broad substrate specificity presumably reflects a large, polymorphous drug-binding domain or domains within the transmembrane segments. As P-gp binds many different hydrophobic compounds, it has been easy to find potent P-gp inhibitors. Two inhibitors that are used in the laboratory and in clinical trials that attempted to reverse drug resistance are the calcium channel blocker verapamil and the immunosuppressant cyclosporin A (Gottesman *et al.* 2002).

Since P-gp is not expressed in all multidrug-resistant cells, a search for other efflux pumps led to the discovery of the multidrug-resistance associated protein 1 (MRP1, or ABCC1) (Cole *et al.* 1993). MRP1 is an ABC transporter similar to P-gp in structure, with the exception of an amino-terminal extension that contains five membrane-spanning domains attached to a P-gp-like core (Fig. 2). MRP1 recognizes neutral and anionic hydrophobic natural products, and transports glutathione, or other, conjugates of these drugs, or, in some cases (such as for vincristine) co-transportes unconjugated glutathione (Loe *et al.* 1998; Jedlitschky *et al.* 1996; Muller *et al.* 1994). The discovery of MRP1 stimulated a genomic search for homologues, leading to the discovery of eight additional members of the ABCC subfamily of transporters, six of which have been studied in some detail

(Borst *et al.* 2000). Like MRP1, some of these MRPs have the five-transmembrane amino-terminal extension (ABCC2, ABCC3 and ABCC6, also named MRP2, MRP3, and MRP6), whereas others do not. Several MRP family members transport drugs in model systems and therefore have the potential to confer drug resistance (Borst *et al.* 2000).

Some anticancer drugs, such as mitoxantrone, are poor substrates for MDR1 and MRP1. Selection for mitoxantrone resistance resulted in the identification of multidrug-resistant cells that produce a more distant member of the ABC transporter family, ABCG2, also known as MXR (mitoxantrone-resistance gene), BCRP (breast cancer resistance protein) or ABC-P (ABC transporter in placenta) (Miyake *et al.* 1999; Doyle *et al.* 1998; Allikmets *et al.* 1998). This transporter is thought to be a homodimer of two half-transporters, each containing an ATP-binding domain at the amino-terminal end of the molecule and six transmembrane segments (Fig. 2).

In Fig.2 a schematic representation of the structural features of the ABC transporters known to confer resistance is represented.

Other ABC family members have been associated with drug resistance. For example, the bile salt export protein (BSEP, also known as ABCB11) is expressed at high levels in liver cells, and in transfection experiments it confers low-level resistance to paclitaxel (Childs *et al.* 1998). MDR3 (sometimes called MDR2), a phosphatidylcholine FLIPPASE that is closely related to P-gp, normally transports phospholipids into bile, but can transport paclitaxel and vinblastine (Smit *et al.* 1993; Zhou *et al.* 1999; Borst *et al.* 2000). Furthermore, ABCA2 is overexpressed in estramustine-resistant cells (Laing *et al.* 1998; Vulevic *et al.* 2001). Estramustine is a nitrogen mustard derivative of oestradiol, so ABCA2, expressed intracellularly in endosomal/lysosomal vesicles, might participate in steroid transport (Gottesman *et al.* 2002). By their ability to transport nucleoside analogues, ABCC3/MRP3 and ABCC5/MRP5 are proteins that are thought to cause certain forms of drug resistance (Reid *et al.* 2003a). Finally, ABCC11/MRP8 has recently been associated with anti-cancer drug export (Guo *et al.* 2003; Szakács *et al.* 2004a).

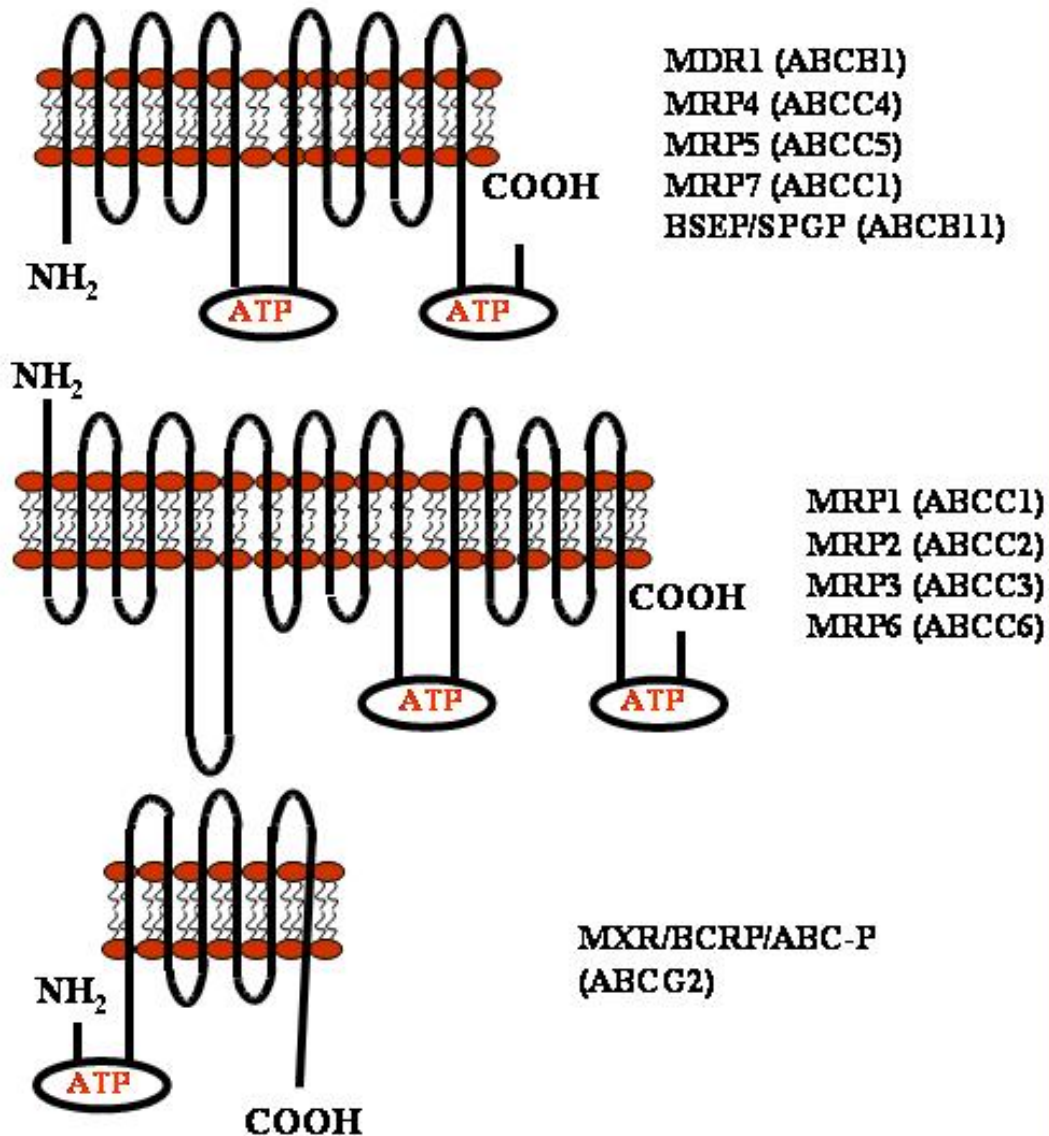


Figure 2. **Structures of ABC transporters known to confer drug resistance.**

ABC transporters such as MDR1 and MRP4 have 12 transmembrane domains and 2 ATP-binding sites. The structures of MRP1, 2, 3 and 6 are similar in that they possess 2 ATP-binding regions. They also contain an additional domain that is composed of 5 transmembrane segments at the amino-terminal end, giving them a total of 17 transmembrane domains. The half-transporter ABCG2 contains 6 transmembrane domains and 1 ATP-binding region. Half-transporters are thought to homodimerize or heterodimerize to function.

Although many ABC transporters have been identified as drug-resistance proteins, they are all expressed in normal tissues (Gottesman *et al.* 2002). ABC transporters have an important role in regulating central nervous system permeability. The brain is protected against blood-borne toxins by the blood-brain barrier, and the blood-cerebrospinal fluid barrier. At the level of the blood-brain barrier, P-gp, located on the luminal surface of endothelial cells, plays an important role in preventing the penetration of cytotoxins across the endothelium (Schinkel *et al.* 1996; Xie *et al.* 1999). MRP proteins such as MRP1 are localized to the basolateral membrane of the choroid plexus, where they serve to pump the metabolic waste products of blood-cerebrospinal fluid barrier into the blood (Rao *et al.* 1999). In a similar manner, ABC transporters seem to protect testicular tissue and the developing fetus, since P-gp and MRP1 transporters have been found to be expressed in testis (Gottesman *et al.* 2002). On the other hand, P-gp is also localized in placenta (Cordon-Cardo *et al.* 1990), as the half-transporter ABCG2 (Jonker *et al.* 2000; Maliepaard *et al.* 2001). MRP1 and other isoforms might also be involved in protecting fetal blood from toxic organic anions and in excreting glutathione/glucuronide metabolites into the maternal circulation (St-Pierre *et al.* 2000).

Whereas ABC transporters are expressed in the brain, testis and placenta to protect them from cytotoxins, the liver, gastrointestinal tract and kidney use these transporters to excrete toxins, thus protecting the entire organism. Examples are the presence of P-gp in the apical membranes of hepatocytes, where it transports toxins into bile (Schinkel *et al.* 1997), as well as the presence of MRP3 in the basolateral surface of hepatocytes, where it transports organic anions from liver back into the bloodstream (Scheffer *et al.* 2000). In addition, the ABC transporter MRP2 (cMOAT) has been found to be expressed on the apical surface of hepatocytes, where it transports bilirubin-glucuronide and other organic anions into bile (Konig *et al.* 1999). In the gastrointestinal tract, P-gp is localized in apical membranes of mucosal cells, where it extrudes toxins, forming a first line of defence (Gottesman *et al.* 2002). Additionally, P-gp actively secretes intravenously administered drugs into the gastrointestinal tract (Sparreboom *et al.* 1997). In contrast to P-gp, MRP1 is located in the basolateral membrane of mucosa cells, and therefore transports substrates into the interstitium and the bloodstream, rather than across the apical surface into the intestinal lumen (Evers *et al.* 1996). MRP2, on the other hand, is localized in the canalicular membrane of hepatocytes and the apical surface of epithelial cells, and has a primary role in the excretion of bilirubin-glucuronide. Studies indicated that MRP2 was capable of mediating drug efflux, suggesting that this transporter, like P-gp, might also regulate drug bioavailability (Dietrich *et al.* 2001).

2.2 Screening for ABC Transporters Involved in MDR

Tools, such as the oligo-based, cDNA-based microarrays or SAGE (Serial analysis of gene expression, Velculescu *et al.* 1995) are relevant methodologies to screen for multifactorial mechanisms of drug resistance. Although microarrays make possible the screening of thousands of genes in the same matrix, attempts aiming to address anticancer drug resistance have been biased in their interpretation by microarrays bearing a low number of ABC transporter superfamily probes (Lamendola *et al.* 2003).

At the beginning of my stage at the National Institutes of Health (NIH), in the laboratory directed by Dr M. Gottesman, I was involved in studies directed to the design and the application of a dedicated ABC-ToxChip. In this system, a comprehensive set of detoxifying genes was complemented with probes specifically matching 36 of the 48 ABC transporters. Instead of using the short 25-mer probe-technology (Affimetrix, Santa Clara, CA), not optimized for detecting infrequent transcripts, a combination of 70-mer oligo probes and 200-500 bp fragments was used. This strategy offers higher sensitivity due to the longer complementary sequence.

We used such a dedicated ABC-ToxChip to compare the transcriptional profiles of the parental prostate cancer cell line DU145 and its 9-nitro-camptothecin-selected derivative cell line RC0.1 (Annereau *et al.* 2004). Camptothecin derivatives such as CPT-11 (Irinotecan) or Hycamtin (Topotecan) are increasingly used in anti-tumor therapy against colon or lung cancers (Kudoh *et al.* 1998). 9-nitro-camptothecin has recently been used in phase II studies for pancreatic cancer and is now in phase III clinical trials (Pantazis *et al.* 2003). The camptothecin resistant cell line RC0.1 derived from the parental sensitive cell line DU145 by continuous exposure to the drug 9-nitro-camptothecin. Many factors, such as specific mutations in topoisomerase I gene and a general alteration of apoptotic regulation have been proposed to explain the phenotype of drug resistance in the prostate cancer cell line RC0.1 (Reinhold *et al.* 2003; Urasaki *et al.* 2001; Chatterjee *et al.* 2001).

Our results indicated that the resistance phenotype of RC0.1 cell line is accompanied by the differential expression of the ABC transporter ABCC2/MRP2, as well as that of enzymes regulating glutathione metabolism (Annereau *et al.* 2004). In fact, among the 20,000 genes, ABCC2/MRP2 shows a strong variation of the expression levels associated with 9-nitro-camptothecin resistance.

First named the canalicular multispecific organic anion transporter (cMOAT), ABCC2/MRP2 is a 190 kDa phosphoglycoprotein localized in the canalicular (apical) membrane of hepatocytes. It is involved in the transport of organic anions, including sulfated and glucuronidated bile salts. Overexpression of MRP2 has been suggested to confer resistance to anti-cancer drugs such as

cisplatin, anthracyclines, and methotrexate, and animal models have shown reduced hepatic transport of camptothecins (Horikawa *et al.* 2002).

We were also able to confirm the microarray results by quantitative real-time RT-PCR analyses. These showed that among the 47 ABC transporters, ABCC2/MRP2 is overexpressed in RC0.1 resistant cell line, whereas the expression of the other members of the superfamily was found to be unchanged (Annereau *et al.* 2004). The obtained results were confirmed by Western blot analyses as well (Annereau *et al.* 2004).

On the basis of these results, my research project was directed to the analysis of the role of the ABC transporter ABCC2/MRP2 in camptothecin resistance. To this purpose, experiments were performed to analyze the effects of MRP2 inhibition on the resistance phenotype of RC0.1 tumor cell line (see Results section).

Moreover, in the early phase of my stage at the NIH, I was involved in studies directed to determine which ABC transporters play a role in drug resistance of cancer cells. To this purpose, we characterized the expression profile of the 48 ABC transporters in a panel of cancer cells (Szakács *et al.* 2004a) whose molecular characteristics have been cataloged. We chose a panel of 60 human cancer cell lines (the NCI-60), which have been used by the Developmental Therapeutics Program (DTP) of the National Cancer Institute (NCI) to screen for more than 100,000 chemical compounds since 1990. Included among the 60 cell lines are leukemias, melanomas, and cancers of ovarian, breast, prostate, lung, renal, colon, and central nervous system. Patterns of drug activity across the cell lines and patterns of cell sensitivity across the set of tested drugs have been shown to contain detailed information on mechanisms of action and resistance (Paul *et al.* 1989; Weinstein *et al.* 1992). In addition to this pharmacological characterization, the NCI-60 cells have been more extensively profiled at the DNA, mRNA, protein and functional levels than any other set of cells in existence.

The main goal of this study was the identification of the relationship between ABC transporters expression levels and sensitivity to drugs or drug candidates. The addressed question was which of the ABC transporters do (and which do not) confer resistance or sensitivity to various classes of agents. To this purpose, the expression profile of the 48 ABC transporters in the NCI-60 cell lines was measured by real-time RT-PCR, since reproducible and quantitative correlations between expression and sensitivity were required (Szakács *et al.* 2004a). The results of RT-PCR analyses allowed the construction of a clustered image map (“heat map”) (Weinstein *et al.* 1997) that offers a visual summary of the patterns of ABC transporters expression across the 60 cell lines (Szakács *et al.* 2004a). Such image map is reported in Fig. 3. Quantitative analyses showed that the pattern of expression is mostly characteristic of the tissue of origin for melanoma cells, as 9 of the 10 melanoma cells cluster together (Szakács *et al.*

2004a). The database provides valuable information on the expression patterns of both known and currently uncharacterized ABC transporters (Szakács *et al.* 2004a). Some of them are expressed ubiquitously, whereas others are selectively expressed in particular cell types. Furthermore, the expression of ABC transporters appears to be independent of sequence-homology categories (Szakács *et al.* 2004a).

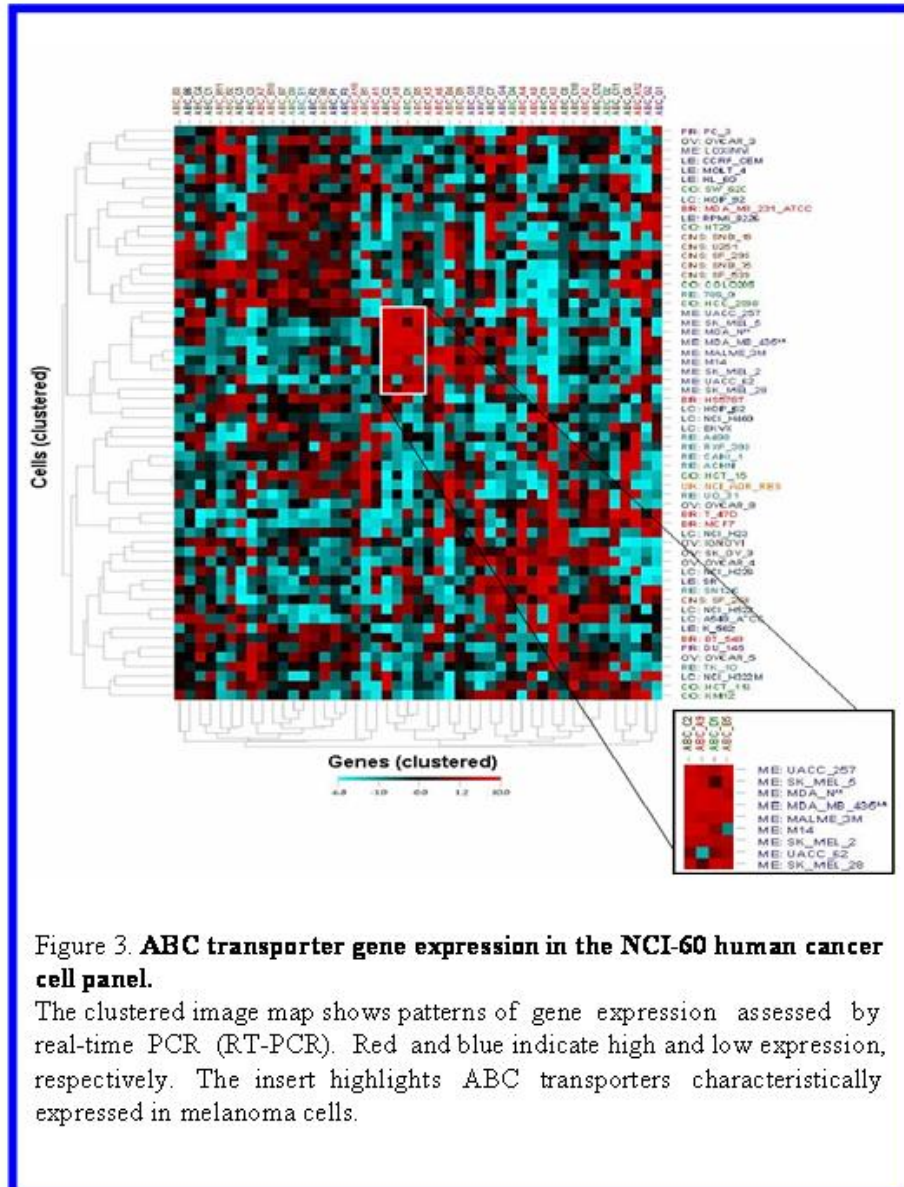


Figure 3. **ABC transporter gene expression in the NCI-60 human cancer cell panel.**

The clustered image map shows patterns of gene expression assessed by real-time PCR (RT-PCR). Red and blue indicate high and low expression, respectively. The insert highlights ABC transporters characteristically expressed in melanoma cells.

The identification of transported molecules should help to understand the physiological mechanisms and specificities of ABC transporters. By correlating the results of ABC transporters expression with the growth inhibitory profiles of 1,429 candidate anticancer drugs tested against the cells, transporters able to confer resistance to anticancer agents were identified (Szakács *et al.* 2004a). Pearson's correlation coefficients were calculated for a total of 68,592 relationships (48 genes x 1,429 compounds) (Szakács *et al.* 2004a). One striking result was the identification of at least one compound whose toxicity appears to be potentiated, rather than antagonized, by P-gp (ABCB1/MDR1) (Szakács *et al.* 2004a). Of the 1,429 compounds analyzed in the study, 28 were shown to be less active in cells that expressed large amounts of ABCC2/MRP2 (Szakács *et al.* 2004a). In order to verify this finding, dose-response curves of control and ABCC2-transfected cells were obtained upon treatment with one of these compound (NSC641281), available from DTP (Developmental Therapeutics Program). In sharp contrast to the control (sham-transfected) cells, ABCC2-overexpressing cells were found to be extremely resistant to NSC641281, reinforcing the suggestion that this compound is an ABCC2/MRP2 substrate (Szakács *et al.* 2004a).

My research project (see Aims of the study) was aimed at the identification of putative substrates for the ABC transporter ABCC2/MRP2. As shown in the Results section, prostaglandins were identified as potential substrates.

2.3 Prostaglandins, as a New Class of Compounds Interacting with ABC Transporters

Prostaglandins are key mediators in the regulation of many physiological processes. They are involved in inflammatory responses and tumorigenesis, and their synthesis and metabolism are tightly regulated (Funk 2001). The first step in prostaglandin synthesis is the production of arachidonic acid, which is released from membrane lipid primarily by cytosolic phospholipase A₂ (Funk 2001). Arachidonic acid is then oxidized to the intermediate prostaglandin H₂ (PGH₂) by PGH synthases, also known as cyclooxygenase (COX)-1 and -2, and the recently identified COX-3 (Warner and Mitchell 2002). These enzymes are known clinically as the targets of aspirin and other nonsteroidal anti-inflammatory drugs (NSAIDs) (Vane 2000).

Several recent studies have shown a link between COX-2 expression and carcinogenesis. Prostaglandins are overproduced by a variety of tumors, leading to the suggested prophylactic use of COX-2 inhibitors to decrease the incidence of colon cancer (Prescott and Fitzpatrick 2000; Gupta and Dubois 2001). After COX-mediated synthesis, PGH₂ is further converted by tissue-specific prostaglandin synthases into PGE₂, PGF_{2α}, PGD₂, prostacyclin, or thromboxane B₂, the biologically active molecules.

Prostaglandins are formed and secreted by most cells, and act as autocrine- or paracrine-signaling molecules. In many cases they exert their effects extracellularly via interaction with a family of G protein-coupled membrane receptors (Breyer and Breyer 2000), although some prostaglandins interact with the nuclear hormone receptor peroxisomal proliferator-activated receptor γ (PPAR γ) (Harris *et al.* 2002). The localized action of prostaglandins requires their efficient release, reuptake, and metabolism to initiate and terminate signaling. The uptake of prostaglandins is mediated by many organic anion transporters (OAT); one of the best characterized is the prostaglandin transporter (PGT) (Schuster 2002). It is thought to mediate prostaglandin uptake via an exchange mechanism, with lactate acting as the counter-ion (Chan *et al.* 2002). In contrast, the release of prostaglandins after their synthesis, a process essential for their activity, is still unknown. Although poorly membrane permeable, primary prostaglandins such as PGE₂ are widely assumed to diffuse passively from the cell.

However, it is known that the proinflammatory leukotriene LTC₄, a prostanoid, is transported by the multidrug resistance proteins MRP1 (Jedlitschky *et al.* 1994; Leier *et al.* 1994; Muller *et al.* 1994) and MRP2 (Cui *et al.* 1999). Besides MRP1^{-/-} mice show an impaired response to inflammatory stimuli, associated with decreased LTC₄ secretion (Wijnholds *et al.* 1997). Furthermore, the metabolically inactive glutathione conjugate of PGA₁ (PGA₁-GS) is transported by both MRP1 (Akimaru *et al.* 1996; Ishikawa *et al.* 1998; Evers *et al.*

1997) and MRP2 (Evers *et al.* 1998). MRP1 also transports the glutathione conjugate of the synthetic prostaglandin Δ^7 -PGA1 methyl ester (Akimaru *et al.* 1996). The primary prostaglandin PGE₂, however, was not found to be a substrate of MRP1 (Evers *et al.* 1997). A recent study showed that in inside-out membrane vesicles derived from insect cells or HEK 293 cells, the ABC transporter ABCC4/MRP4 catalyzes the time- and ATP- dependent uptake of prostaglandin E₁ (PGE₁) and PGE₂ (Reid *et al.* 2003b). In contrast, MRP1, MRP2, MRP3, and MRP5 do not transport PGE₁ or PGE₂. The MRP4-mediated transport of PGE₁ and PGE₂ displays saturation kinetics, with Km values of 2.1 and 3.4 μ M, respectively. Furthermore, PGF_{1 α} , PGF_{2 α} , PGA₁, and thromboxane B₂ are high-affinity inhibitors of MRP4 and so presumably substrates (Reid *et al.* 2003b). In the same way, several nonsteroidal anti-inflammatory drugs are potent inhibitors of MRP4 at concentrations that do not inhibit MRP1. In cells expressing the prostaglandin transporter PGT, the steady-state accumulation of PGE₁ and PGE₂ is reduced proportional to MRP4 expression (Reid *et al.* 2003b). Inhibition of MRP4 by an MRP4-specific RNA interference construct reversed this accumulation deficit (Reid *et al.* 2003b). Thus, MRP4 can release prostaglandins from cells and some nonsteroidal anti-inflammatory drugs, in addition to inhibiting prostaglandins synthesis, might also act by inhibiting this release.

Among prostaglandins, cyclopentenone prostaglandins, such as prostaglandin J₂ (PGJ₂), Δ^{12} -prostaglandin J₂ (Δ^{12} -PGJ₂), 15-deoxy- $\Delta^{12,14}$ -prostaglandin J₂ (15-d-PGJ₂), prostaglandin A₁ (PGA₁) and prostaglandin A₂ (PGA₂) influence a variety of cellular processes including growth and differentiation, gene expression, apoptosis and inhibition of inflammatory signaling pathways (Kliwer *et al.* 1995; Atsmon *et al.* 1990a; Honn and Marnett 1985; Clay *et al.* 2000; Clay *et al.* 1999; Forman *et al.* 1995; Rovin *et al.* 2002). 15-deoxy- $\Delta^{12,14}$ -prostaglandin J₂ (15-d-PGJ₂), a terminal product of prostaglandin D₂ metabolism, is among the most potent cyclopentenone prostaglandins. This prostaglandin has attracted considerable attention because of its antitumor activities including the ability to inhibit growth and induce apoptosis in several cancer cell lines (Clay *et al.* 2000; Clay *et al.* 1999; Harris and Phipps 2002; Eibl *et al.* 2001; Shimada *et al.* 2002; Padilla *et al.* 2002). Additionally, 15-d-PGJ₂ influences the expression of several genes and has anti-inflammatory effects (Kliwer *et al.* 1995; Yamazaki *et al.* 2002; Rossi *et al.* 2000; Straus *et al.* 2000; Ricote *et al.* 1998; Jiang *et al.* 1998). In addition to its potential pharmacological utility, the physiological relevance of 15-d-PGJ₂ is supported by recent findings showing that it is produced in cells and tissues including activated macrophages, where 15-d-PGJ₂ is made and secreted (Shibata *et al.* 2002) and human breast tissue (Badawi and Badr 2003). Its biological effects are mediated by both peroxisomal proliferator-activated receptor γ (PPAR γ)-independent and PPAR γ -dependent mechanisms (Clay *et al.* 1999; Forman *et al.* 1995; Rossi *et al.* 2000;

Straus *et al.* 2000; Shibata *et al.* 2002; Dussault and Forman 2000; Oliva *et al.* 2003).

Many PPAR γ -independent effects are believed to involve the formation of 15-d-PGJ₂/protein adducts (Rossi *et al.* 2000; Oliva *et al.* 2003; Castrillo *et al.* 2000; Cernuda-Morollon *et al.* 2001) via reactions between protein thiols and the α,β -unsaturated ketone on 15-d-PGJ₂ (Atsmon *et al.* 1990a; Atsmon *et al.* 1990b; Paumi *et al.* 2003; Bogaards *et al.* 1997). Formation of these adducts inactivates or modifies the function of the target protein resulting in the observed biological effects (Rossi *et al.* 2000; Oliva *et al.* 2003; Castrillo *et al.* 2000; Cernuda-Morollon *et al.* 2001). Indeed, the inhibition of cell proliferation by cyclopentenone prostaglandins has been attributed to the presence of this α,β -unsaturated carbonyl in a variety of tumor models (Atsmon *et al.* 1990b; Honn and Marnett 1985). Moreover, previous studies have indicated that this electrophilic center of 15-d-PGJ₂ and other cyclopentenone prostaglandins is a target for the Michael addition of glutathione (Atsmon *et al.* 1990a; Atsmon *et al.* 1990b; Bogaards *et al.* 1997; Ohno and Hirata 1993; Parker and Ankel 1992). 15-d-PGJ₂ is also a ligand for the nuclear receptor PPAR γ . Activation of PPAR γ by binding of this or other ligands facilitates PPAR γ /retinoid X receptor heterodimer formation, recruitment of transcriptional coeffectors, and binding of the PPAR γ /retinoid X receptor complex to its PPAR responsive elements (Kliwer *et al.* 1995; Forman *et al.* 1995; Dussault and Forman 2000; Kodera *et al.* 2000; Chawla *et al.* 2001; Krey *et al.* 1997). Consequently, ligand binding to PPAR γ is associated with the altered expression of a variety of genes including those involved in adipocyte differentiation, cell proliferation, and lipid and glucose homeostasis (Dussault and Forman 2000; Chawla *et al.* 2001; Hihi *et al.* 2002). PPAR γ is upregulated in cancer cells including those from colon and breast, and it has been suggested that the ligands of PPAR γ may be useful in the treatment of some cancers (Honn and Marnett 1985; Clay *et al.* 2000; Clay *et al.* 1999; Shimada *et al.* 2002; Padilla *et al.* 2002; Elstner *et al.* 1998). 15-d-PGJ₂ cytotoxicity and activation of PPAR γ -dependent transcription are attenuated by expression of the glutathione conjugate efflux transporters, MRP1/ABCC1 and MRP3/ABCC3 (Paumi *et al.* 2003). This attenuation is glutathione-dependent and is associated with the formation of the glutathione conjugate of 15-d-PGJ₂, 15-d-PGJ₂-SG, and its MRP-dependent efflux (Paumi *et al.* 2003).

These observations appear to be in agreement with a putative role of the ABC transporter ABCC2/MRP2 in the transport of cyclopentenone prostaglandins.

3. AIMS OF THE STUDY

The main goal of the present study was the analysis of the role played by the ABC transporter ABCC2/MRP2 in multidrug resistance (MDR).

In the first part of my study, experiments were performed to clarify the role of ABCC2/MRP2 in camptothecin resistance. The model of study was represented by the human prostate cancer cell line RC0.1, derived from the parental sensitive cell line DU145 by continuous exposure to the drug Rubitecan (9-nitro-camptothecin). 9-nitro-camptothecin is now in phase III clinical trials (Pantazis *et al.* 2003). Many factors have been proposed to explain the phenotype of drug resistance in the resistant cell line RC0.1 (Reinhold *et al.* 2003; Urasaki *et al.* 2001; Chatterjee *et al.* 2001). Since microarray analyses indicated high expression levels of MRP2 in RC0.1 cell line (Annereau *et al.* 2004), experiments were here performed to analyze the meaning of MRP2 overexpression associated with resistance. To this purpose, different strategies were used to inhibit this ABC transporter, such as the use of MK571, a compound that is known to strongly inhibit MRP2 by interacting with its substrate binding site (Chen *et al.* 1999), and RNA interference (RNAi) technology. In both cases, experiments were then performed to analyze the effects of MRP2 inhibition on the resistance phenotype of RC0.1 tumor cell line.

In the second part of my study, experiments were performed to analyze a putative involvement of ABCC2/MRP2 in the transport of cyclopentenone prostaglandins. Previous studies indicated 28 anticancer drugs as putative substrates of ABCC2/MRP2 (Szakács *et al.* 2004a). Experiments performed in the present study showed an effective involvement of MRP2 in their transport. The analysis of the chemical structures of the 28 identified MRP2 substrates indicated the presence of common structural features, such as a cyclopentanone ring, an element structurally related to the cyclopentenone ring of prostaglandins. This observation led us to assume a role of ABCC2/MRP2 in the transport of this class of prostaglandins. This hypothesis is in agreement with recent findings indicating the involvement of other ABC transporters in the transport of prostaglandins (Reid *et al.* 2003b; Paumi *et al.* 2003), and with the observation that the mechanism of prostaglandins release from cells is not completely understood. Cyclopentenone prostaglandins are known to influence a variety of cellular processes, such as growth and differentiation, gene expression, apoptosis and inhibition of inflammatory signaling pathways (Rovin *et al.* 2002; Forman *et al.* 1995; Kliewer *et al.* 1995). In order to verify the involvement of MRP2 in the transport of this class of biological molecules, experiments were performed to analyze the effects of cyclopentenone prostaglandins on the growth and the resistance phenotype of control (sham-transfected) and ABCC2-transfected cells.

4. MATERIALS AND METHODS

4.1 Cell Lines and Culture Conditions

DU145 cell line (Stone *et al.* 1978) and its 9-nitro-camptothecin-derivative RC0.1 cell line were a generous gift from Dr P. Pantazis (University of Miami, Coral Gables, FL). They were cultured in RPMI 1640 (Life Technologies, Gaithersburg, MD) medium. Resistance phenotype of RC0.1 cell line was maintained by passage in 9-nitro-camptothecin-containing medium (0.1 μ M) every three months.

Control and ABCC2-transfected Madin-Darby canine kidney cell lines (MDCKII) were a generous gift from Dr Balasz Sarkadi (Budapest). Control and MRP1-transfected human embryonic kidney cell lines (HEK 293) were a generous gift from Dr Suresh V. Ambudkar (NCI, NIH, Bethesda, USA) (Muller *et al.* 2002). These four cell lines were grown in Dulbecco's modified Eagle's medium (Life Technologies, Gaithersburg, MD).

MCF-7 and MCF-7MDR cell lines, available in Dr Gottesman's laboratory, were grown in Dulbecco's modified Eagle's medium (Life Technologies, Gaithersburg, MD). Resistance phenotype of MCF-7MDR cell line, due to P-gp overexpression, was maintained by culturing cells in colchicine-containing medium (60 ng/ml).

All of the cell lines were cultured in media supplemented with 10% fetal bovine serum (Hyclone Inc. Logan, UT), 2 mM L-glutamine (Life Technologies, Gaithersburg, MD), 50 Units/ml penicillin (Life Technologies, Gaithersburg, MD), and 50 μ g/ml streptomycin (Life Technologies, Gaithersburg, MD). Cells were grown at 37°C in a humidified atmosphere containing 5% CO₂/95% air. All of the cell lines were discarded after 3 months and new lines were obtained from frozen stocks.

4.2 Antibodies, Drugs and Chemicals

The antibodies used in the current study were the following: murine monoclonal antibody M₂-III-6 directed against an internal epitope COOH-terminal (aa 1339-1541) of human MRP2 protein (Alexis, San Diego, CA); murine monoclonal antibody C219 (Alexis, San Diego, CA) directed against human P-gp; murine polyclonal antibody directed against human and rat GAPDH (Research Diagnostic Inc., Flanders, NJ); horseradish peroxidase-conjugated goat antimouse immunoglobulin antibody (Jackson ImmunoResearch Laboratories, # IR-115-035-164).

The compounds designated by NSC numbers were obtained from the Drug Synthesis and Chemistry Branch, Developmental Therapeutics Program, Division of Cancer Treatment and Diagnosis, National Cancer Institute, National Institutes of Health, Bethesda, MD, USA. The compounds NSC641281, NSC645145, NSC618059 and NSC626878 were dissolved in dimethyl sulfoxide (DMSO) at the following concentrations: 52 mM (NSC641281), 260 mM (NSC645145), 213 mM (NSC618059) and 54 mM (NSC626878).

Colchicine, camptothecin and dimethyl sulphoxide (DMSO) were purchased from Sigma Chemical Co. (St. Louis, MO). The drug rubitecan (9-nitro-camptothecin) was purchased from LKT Laboratories (St. Paul, MN, # C0156). The compound MK571 was purchased from Alexis (San Diego, CA).

Cyclopentenone prostaglandins, such as prostaglandin J₂ (PGJ₂), Δ^{12} -prostaglandin J₂ (Δ^{12} -PGJ₂), 15-deoxy- $\Delta^{12,14}$ -prostaglandin J₂ (15-d-PGJ₂), prostaglandin A₁ (PGA₁) and prostaglandin A₂ (PGA₂) were purchased from Cayman Chemical (Ann Arbor, MI). They were dissolved in dimethyl sulfoxide (DMSO) at the following concentrations (as indicated by the manufacturer): 10 mg/ml (PGJ₂), 100 mg/ml (Δ^{12} -PGJ₂), 20 mg/ml (15-d-PGJ₂), 50 mg/ml (PGA₁), 50 mg/ml (PGA₂).

4.3 siRNA Preparation and Transfection

The 4 short interfering RNA (siRNA) sequences targeting human ABCC2/MRP2 corresponded to the following coding regions relative to the start codon:

- 1) 1560-1578 (5'-GAATCAAGATCCTGAAATA-3');
- 2) 3682-3700 (5'-GAACCTGACTGTCTTCTTT-3');
- 3) 1222-1240 (5'-TATCATGGCTTCTGTATAT-3');
- 4) 3115-3133 (5'-CTACGGAGCTCTGGGATTA-3').

The siRNA duplexes with the sense and antisense sequences represented in Table 1 were used.

Sequences of the 4 siRNA duplexes targeting human ABCC2/MRP2	
<u>siRNA duplex 1</u>	5'-GAAUCAAGA UCCUGAAA UAdTdT-3' (sense) 3'-dTdTTCUUAGUUCUAGGACUUUAU-5' (antisense)
<u>siRNA duplex 2</u>	5'- GAACCUGACUGUCUUCUUUdTdT-3' (sense) 3'-dTdTTCUUGGACUGACAGAAGAAA-5' (antisense)
<u>siRNA duplex 3</u>	5'-UAUCAUGGCUUCUGUAUAUdTdT-3' (sense) 3'-dTdTAAUAGUACCGAAAGACAUAUA-5' (antisense)
<u>siRNA duplex 4</u>	5'-CUACGGAGCUCUGGGAUUAdTdT-3' (sense) 3'-dTdTGAUGCCUCGAGACCCUAAU-5' (antisense)
Table1: Sequences of the 4 siRNA duplexes targeting the human ABC transporter ABCC2/MRP2. For each siRNA the sense and antisense sequences are represented.	

The siRNA sequence targeting *MDR1* corresponded to the coding region 79-99 (5'-AAGGAAAAGAAACCAACTGTC-3') relative to the start codon (Wu *et al.* 2003). The siRNA duplex with the following sense and antisense sequences was used:

5'-GGAAAAGAAACCAACUGUCdTdT-3' (sense) and
3'-dTdTCCUUUUCUUUGGUUGACAG-5' (antisense).

Cells of the different cell lines in exponential phase of growth were plated in six-well plates at a density of 5×10^5 cells/well and grown for 24 hours. The number of cells was chosen to allow the cells to be 30-50% confluent the day of transfection. At the time of plating and during the transfection, antibiotics were not added to the culture medium. Cells were then incubated for 24 hours at 37°C in a humidified 5% CO₂. After 24 hours, cells were transfected with siRNA (pool of 4 MRP2-specific siRNAs: 100 nM, 25 nM each; P-gp siRNA: 200 nM, as described by Wu *et al.* 2003) using oligofectamine and OPTI-MEM I serum-reduced medium (Invitrogen Life Technologies, Inc., Carlsbad, CA), according to the manufacturer's instructions. Briefly, oligofectamine reagent (3 µl) was diluted in serum-reduced medium to a final volume of 15 µl and incubated at room temperature for 5-10 minutes. Diluted oligofectamine was then mixed to diluted siRNA duplexes and incubated at room temperature for 15-20 minutes. Following the incubation, the solution was added to the cells, previously washed with serum-reduced medium. Cells were then incubated for 4 hours at 37°C in a humidified 5% CO₂. Following the incubation, serum was added to the cells without removing the transfection mixture. Silencing was examined 24-72 hours after the

transfection in the case of MRP2, and 24 hours after the transfection in the case of P-gp. Control cells were treated with oligofectamine and serum-reduced medium (mock).

4.4 Western Blot Analyses

Cells were washed twice with cold PBS containing a cocktail of proteases inhibitors (Roche Applied Science, Indianapolis, IN), scraped off the dishes, and collected by centrifugation at 500 x g for 10 minutes at 4°C. Cell pellets were then dissolved in a lysis buffer containing 10 mM Tris-HCl, pH 8.0, 0.1% Triton X-100 (v/v), 10 mM MgSO₄, 2 mM CaCl₂, 2 mM DTT, a cocktail of proteases inhibitors (Roche Applied Science, Indianapolis, IN) and 20 µg/ml micrococcal DNase (Sigma Chemical Co., St. Louis, MO). Samples were then incubated at 37°C for 5 minutes, quickly frozen in dry ice, thawed in cold water and sonicated in a bath sonicator (3 times for 1 minute, with 30 seconds intervals of incubation on ice). Protein concentration was determined using a Bradford assay (Bio-Rad, Hercules, CA). Samples were then mixed with Novex Tris-Glycine SDS sample buffer (Invitrogen, Carlsbad, CA). Identical amounts (50 µg of protein) of cell lysates were loaded on Novex 4–20% Tris-glycine gels (Invitrogen, Carlsbad, CA) and transferred to nitrocellulose membranes (Invitrogen, Carlsbad, CA) at 200 mAmps for 2 hours at 4°C. At this point, membranes were incubated in a blocking solution (20% non-fat milk in PBS buffer containing 0.5% Tween 20) at room temperature for 1 hour and washed with PBS buffer containing 0.5% Tween 20. Membranes were then incubated with a murine monoclonal anti-MRP2 antibody M₂-III-6 (Alexis, San Diego, CA) diluted 1:200, or a murine monoclonal anti-P-gp antibody C219 (Alexis, San Diego, CA) diluted 1:2000, or a murine polyclonal anti-GAPDH antibody (Research Diagnostic Inc., Flanders, NJ) diluted 1:2000. For details about antibodies see above. Primary antibodies were all diluted in PBS buffer containing 0.5% Tween 20 and 5% non-fat milk, and incubated with the membranes at room temperature overnight on a shaker. Membranes were then washed with PBS buffer containing 0.5% Tween 20 and incubated with a horseradish peroxidase-conjugated goat antimouse immunoglobulin antibody (Jackson ImmunoResearch Laboratories, # IR-115-035-164), diluted 1:5000 in PBS buffer containing 0.5% Tween 20 and 5% non-fat milk. Membranes were incubated with the secondary antibody for 1 hour at room temperature on a shaker. Detection by enzyme-linked chemiluminescence (enhanced chemiluminescence: ECL) was performed according to the manufacturer's instructions (Amersham, Piscataway, NJ).

4.5 Analysis of Drug Sensitivity

Cell survival was measured by the MTT [3-(4,5-Dimethylthiazol-2-yl)-2,5-diphenyltetrazolium] assay. Exponentially growing cells were trypsinized, harvested, and 5×10^3 cells in 100 μ l of culture medium were inoculated into each well of a 96 well plate. A different number of cells was plated just in the case of DU145 and RC0.1 cell lines. In fact, because of the differences in duplication time and size of the two cell lines, 1×10^3 cells (RC0.1) and 2.5×10^3 cells (DU145) in 100 μ l of culture medium were inoculated into each well of a 96 well plate, thus to reach equal levels of confluency (20-30%) after 24 hours. After overnight incubation, serially diluted drug was added in 100 μ l of culture medium to give the indicated final concentration. Cells were then incubated for 72 hours at 37°C in 5% CO₂. Following the incubation, the MTT assays were performed as indicated by the manufacturer (Molecular Probes, Eugene, OR).

Briefly, the medium was removed and 100 μ l of fresh medium red phenol-free (Iscove's Modified Dulbecco's Medium, Life Technologies, Gaithersburg, MD), containing 10 μ l of MTT (12 mM in PBS, Molecular Probes), were added to each well and the cells were incubated for an additional 4 hours at 37°C in 5% CO₂. After aspiration of the culture medium, the resulting formazan precipitate was dissolved with 150 μ l of isopropanol/0.1 N HCl. Plates were then placed on a shaker for 5 minutes in the dark and the formation of the soluble MTT purple dye was immediately monitored by measuring the optical density at 570 nm using a 96 well plate reader (SpectroMax 250, Molecular Devices Inc., city, state).

In order to examine the effects of the compounds MK571 and 15-d-PGJ₂, used as MRP2 inhibitors, cells were preincubated without or with MK571 (20 μ M), or 15-d-PGJ₂ (2.37 μ M) for 24 hours and then incubated with various concentrations of drugs in the presence and in the absence of MK-571 (20 μ M) or 15-d-PGJ₂ (2.37 μ M).

In order to assess whether siRNA-directed suppression of MRP2 sensitized RC0.1 resistant cells to camptothecins, mock-treated and si-RNA-treated cells were trypsinized 24 hours after the transfection, performed in 6 well plates, and transferred into 96 well plates. The same number of mock-treated and siRNA-treated cells (1×10^3) was inoculated into each well of a 96 well plate. Following overnight incubation, serially diluted drug was added in 100 μ l of culture medium to give the indicated final concentration. The drug (camptothecin or 9-nitro-camptothecin) was thus added to the culture medium 48 hours after the treatment with MRP2-specific siRNAs. After 72 hours from drug addition, MTT assays were performed as described above to evaluate cell viability.

Cell survival was expressed as the percentage of viable cells in the presence of the compound under test, with respect to control cultures grown in the

absence of the tested compound. The values reported in each figure represent the average of the values obtained in 3 independent experiments.

5. RESULTS AND DISCUSSION

5.1 Overexpression of the ABC Transporter ABCC2/MRP2 in the Resistant Tumor Cell Line RC0.1

In this study the human prostate resistant cancer cell line RC0.1, derived from the parental sensitive cell line DU145 by continuous exposure to 0.1 μ M rubitecan (9-nitro-camptothecin) (Chatterjee *et al.* 1996), was used. This cell line presents a peculiar profile of multidrug resistance (Reinhold *et al.* 2003), since it has been reported to be resistant to camptothecin (Oberlies and Kroll 2004) and its analogues, NB-506 (an inhibitor of topoisomerase I) (Meng *et al.* 2003) and cisplatin (Ho *et al.* 2003). RC0.1 cells have been reported to be also sensitive to drugs known to be exported by ABC transporters, such as ABCB1/MDR1 or ABCC1/MRP1 (Chatterjee *et al.* 2001).

Many factors have been proposed to explain the phenotype of drug resistance in RC0.1 cell line (Reinhold *et al.* 2003; Urasaki *et al.* 2001). Among them, the effects of specific mutations in topoisomerase I gene which would prevent the binding of camptothecin and its analogues, and a general alteration of apoptotic regulation. Topoisomerase I enzyme has recently been investigated as a new target for chemotherapy (Cabanillas 1999; Kantarjian 1999). In higher eukaryotes, it is an essential enzyme that catalyzes the relaxation of negative supercoils during DNA processing, including replication, transcription, and repair. The natural product camptothecin targets the topoisomerase I/DNA covalent complex, a catalytic intermediate, by reversibly blocking topoisomerase I-mediated religation of the DNA strand and release of free topoisomerase I (Hsiang *et al.* 1985). In the presence of camptothecin, topoisomerase I remains covalently linked to one strand of the DNA, and thus leaves the DNA as a single-stranded nicked DNA linked to the protein. These lesions are cytotoxic and trigger apoptotic cell death (Shao *et al.* 1999; Strumberg *et al.* 2000). However, it is worth noting that topoisomerase I mutations can explain resistance to camptothecin and its analogues in some experimental models (Pommier *et al.* 1999; Chen and Liu 1994; Beck *et al.* 1997; Nieves-Neira and Pommier 1999), but they have not been implicated in clinical resistance to camptothecins.

In order to compare mRNA expression profiles of DU145 and RC0.1 cells, microarray and quantitative RT-PCR analyses were performed (Annereau *et al.* 2004). The ABC transporter ABCC2/MRP2 was found to be overexpressed in the resistant cell line RC0.1, whereas the expression of other members of the ABC superfamily was found to be unchanged (Annereau *et al.* 2004). Since mRNA levels may not reflect protein expression, due to modulation of translation or inhibition of protein processing, MRP2 expression was analyzed also at the protein

level. To this purpose, total proteins were extracted from cells of both cell lines, DU145 and RC0.1, and analyzed by SDS-PAGE, followed by Western blot analyses with an anti-MRP2 antibody. The results indicated that the protein expression follows the pattern predicted by RNA analyses (Annereau *et al.* 2004). The ABC transporter MRP2 was found to be up-regulated in the resistant cell line, whereas the signal for MRP2 was not detectable in the case of the parental sensitive cell line DU145 (Fig. 4). In these experiments the use of an antibody able to recognize the housekeeping protein glyceraldehyde-3-phosphate dehydrogenase (GAPDH) allowed a direct comparison of the expression levels (Fig. 4).

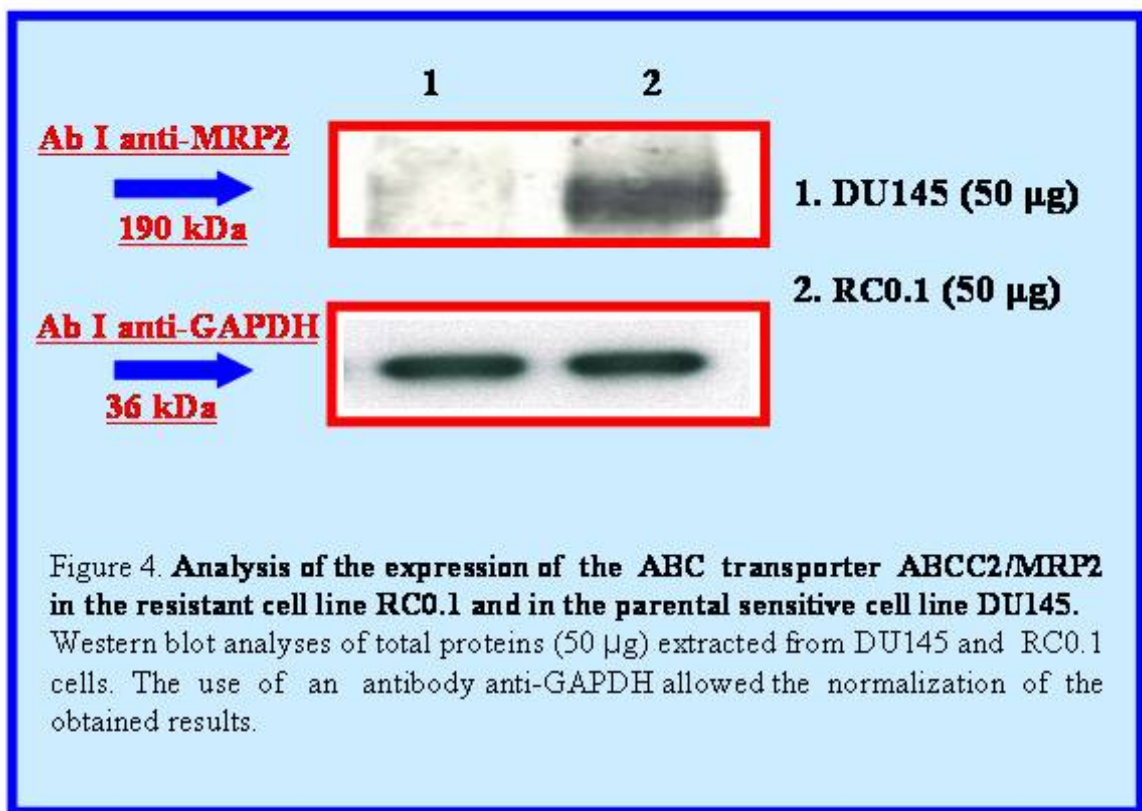
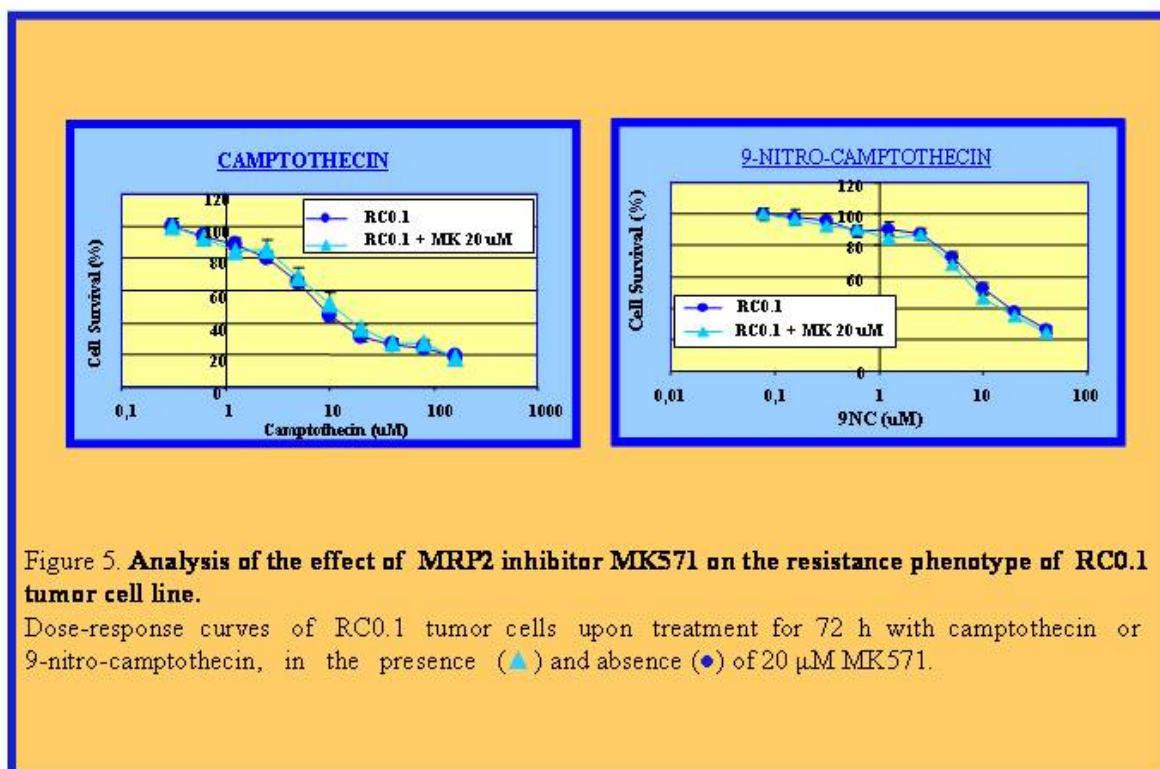


Figure 4. **Analysis of the expression of the ABC transporter ABCC2/MRP2 in the resistant cell line RC0.1 and in the parental sensitive cell line DU145.** Western blot analyses of total proteins (50 μg) extracted from DU145 and RC0.1 cells. The use of an antibody anti-GAPDH allowed the normalization of the obtained results.

5.2 Analysis of the Effect of the MDR-reversing Agent MK571 on the Resistance Phenotype of RC0.1 Tumor Cell Line

In order to establish the role of the ABC transporter MRP2 in maintaining the resistance phenotype of RC0.1 tumor cells, the cytotoxicity of the drug camptothecin and its derivative 9-nitro-camptothecin was evaluated in the presence of MK571, a compound that is known to strongly inhibit MRP2 by interacting with its substrate binding site (Chen *et al.* 1999). Dose-response curves of DU145 and RC0.1 cells were performed to examine the cytotoxic effect of MK571. When cells were incubated in the presence of MK571, it was found to be not toxic for either cell lines at a concentration of 20 μM (data not shown). Dose-response curves of DU145 and RC0.1 cells were then obtained upon treatment with increasing concentrations of the drugs (camptothecin or 9-nitro-camptothecin) in the presence and absence of 20 μM MK571. The results of the MTT assays are shown in Fig. 5. Unexpectedly, the presence of the inhibitor MK571 did not revert the resistance phenotype of RC0.1 tumor cells.



5.3 Inhibition of MRP2 Protein Expression by RNA Interference

An alternative strategy was used to evaluate the role of the ABC transporter MRP2 in the resistance phenotype of RC0.1 tumor cells to the drug 9-nitro-camptothecin. To this purpose, the expression of MRP2 was inhibited using the RNA interference (RNAi) technology. RNAi is a conserved biological response to double-stranded RNA fragments, which results in sequence-specific gene silencing (Hannon 2002). Physiologically, RNAi is initiated by specific double-stranded RNA (dsRNA) fragments generated by RNase III Dicer enzyme that is responsible for the processing of long dsRNAs into small interfering RNAs (siRNAs). These siRNAs are incorporated into a protein complex that recognizes and cleaves its target mRNAs (Nykanen *et al.* 2001) (Fig. 6). Introduction of dsRNAs into mammalian cells does not result in efficient Dicer-mediated generation of siRNAs and therefore does not induce RNAi (Ui-Tei *et al.* 2000). The requirement for Dicer in maturation of siRNAs can be bypassed by introducing synthetic 21-nucleotides siRNA duplexes that inhibit expression of transfected or endogenous genes in a variety of mammalian cells (Elbashir *et al.* 2001).

A pool of 4 specific siRNAs, whose sequence is shown in Fig. 7, was used to inhibit the expression of MRP2. Their homology to different regions of MRP2 mRNA sequence is indicated in Fig. 7.

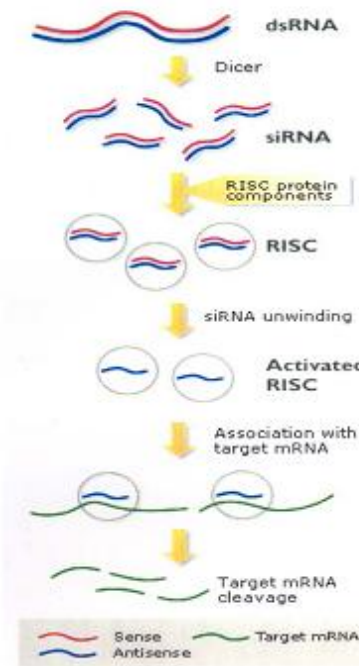


Figure 6. **Mechanism leading to RNA interference (RNAi) mediated gene silencing.**

Specific double-stranded RNA (dsRNA) fragments are generated by RNase III Dicer enzyme that is responsible for the processing of long dsRNAs into small interfering RNAs (siRNAs). These siRNAs are incorporated into a protein complex that recognizes and cleaves its target mRNAs.

```

1)      1      gaatcaagatcctgaaata 19
         |||
1560    gaatcaagatcctgaaata 1578

2)      1      gaacctgactgtcttcttt 19
         |||
3682    gaacctgactgtcttcttt 3700

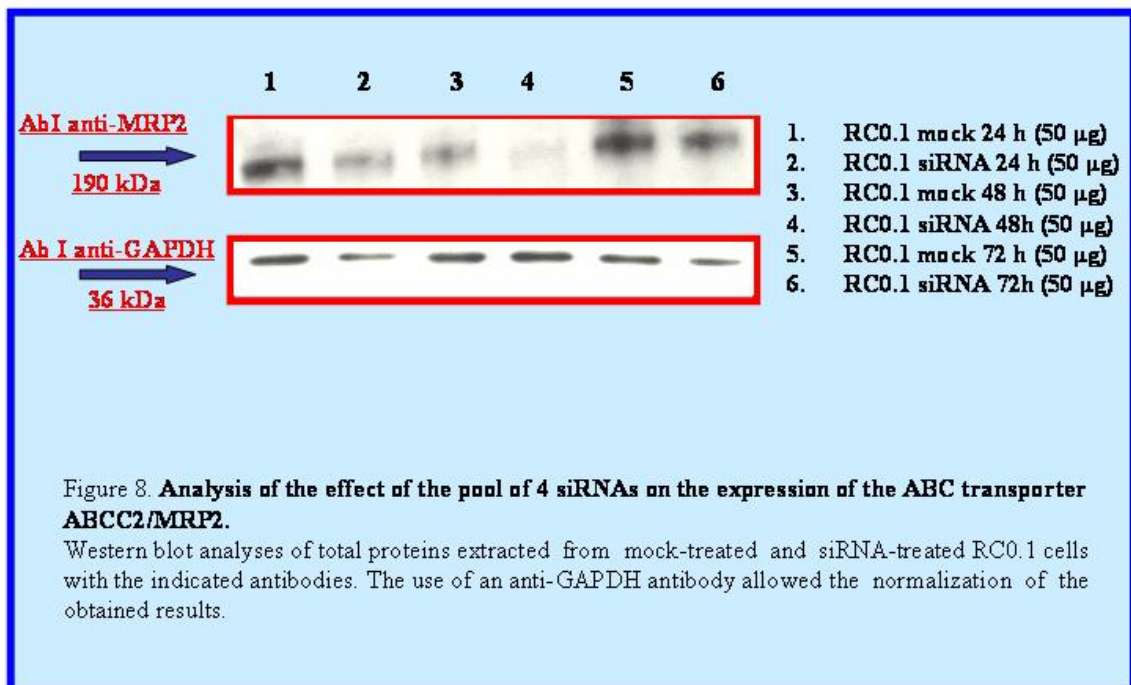
3)      1      tatcatggcttctgtatat 19
         |||
1222    tatcatggcttctgtatat 1240

4)      1      ctacggagctctgggatta 19
         |||
3115    ctacggagctctgggatta 3133

```

Figure 7. **Sequence of siRNA duplexes used to inhibit MRP2 expression.** Their homology to different MRP2 mRNA regions is indicated for each siRNA in the lower line of the duplex.

Both DU145 and RC0.1 tumor cells were transfected with the pool of 4 siRNAs, used at a concentration of 25 nM each. Following the transfection, the expression of the ABC transporter MRP2 was analyzed at the protein level. Total proteins were extracted and analyzed by SDS-PAGE, followed by Western blot analyses with an anti-MRP2 antibody. The results obtained are shown in Fig. 5. The expression of the ABC transporter MRP2 was found to be significantly inhibited in RC0.1 cells after 24 and 48 hours from the transfection as compared to the controls (mock-treated cells), with higher inhibition values at 48 hours. At 72 hours instead, the level of expression of MRP2 appeared to have been restored (Fig. 8). On the other hand, a signal for MRP2 was instead not detectable in DU145 cells (data not shown), as expected from MRP2 low expression levels in this cell line.



To further confirm the specificity of siRNA-mediated silencing of MRP2, experiments were performed to test the effects of the pool of 4 MRP2-specific siRNAs on the expression of the ABC transporter P-glycoprotein (P-gp), the product of the ABCB1 (or MDR1) gene. To this purpose, RNAi experiments were performed using the human breast cancer cell lines MCF-7 and MCF-7MDR. The resistant cell line MCF-7MDR, characterized by high levels of expression of P-gp, derived from the parental sensitive cell line MCF-7 by transduction with MDR1 cDNA (Clark *et al.* 1992). Both MCF-7 and MCF-7MDR tumor cells were transfected with the pool of 4 MRP2-specific siRNAs, used at a concentration of 25 nM each. Following the transfection, the expression of the ABC transporter P-gp was analyzed at the protein level after 24 hours from the treatment. Total proteins were extracted and analyzed by SDS-PAGE, followed by Western blot analyses with an anti-Pgp antibody. The results indicated that (see Fig. 9) the MRP2-specific siRNAs did not affect P-gp expression in MCF7-MDR cells. Thus, we can conclude that MRP2 is a specific target of the siRNAs pool, since the expression of the homologous protein P-gp was not affected by the treatment with these siRNAs. In order to have a positive control for this experiment, MCF-7 and MCF-7MDR cells were also transfected with a siRNA duplex known to inhibit the expression of P-gp (Wu *et al.* 2003). This siRNA was used at a concentration of 200 nM. Following the transfection, Western blot analyses were performed after 24 hours from the treatment, as described above. The expression of P-gp was found to decrease in siRNA-treated cells as compared to mock-treated cells (Fig. 9).

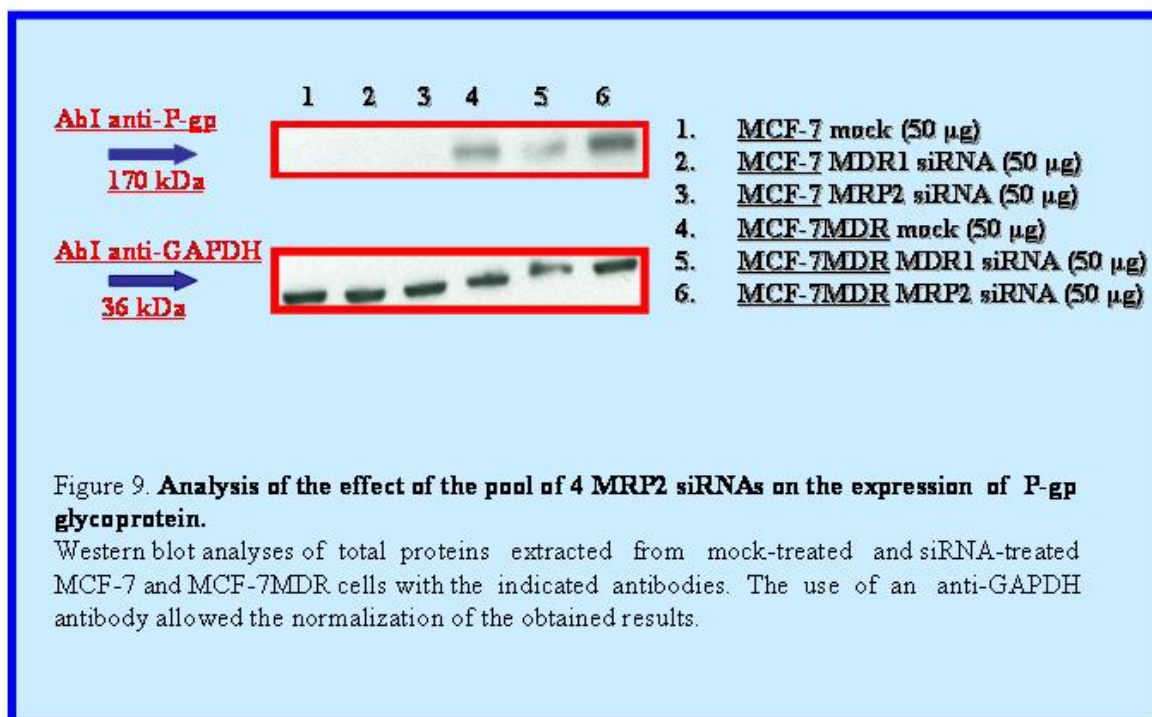


Figure 9. **Analysis of the effect of the pool of 4 MRP2 siRNAs on the expression of P-gp glycoprotein.**

Western blot analyses of total proteins extracted from mock-treated and siRNA-treated MCF-7 and MCF-7MDR cells with the indicated antibodies. The use of an anti-GAPDH antibody allowed the normalization of the obtained results.

5.4 Analysis of the Effects of siRNA-mediated MRP2 Silencing on the Resistance Phenotype of RC0.1 Tumor Cell Line

In order to assess whether siRNA-directed suppression of MRP2 sensitized RC0.1 resistant cells to the drug 9-nitro-camptothecin, the drug sensitivity of siRNA-treated RC0.1 cells was compared to that of the mock-treated cells. To this purpose, 48 hours after the treatment with MRP2-specific siRNAs, the drug (camptothecin or 9-nitro-camptothecin) was added to the culture medium. This time interval was chosen since at 48 hours the strongest inhibition of MRP2 expression was observed. After 72 hours from drug addition, MTT assays were performed to evaluate cell viability. The results of these experiments indicated that the resistance of RC0.1 cells to the drugs camptothecin and 9-nitro-camptothecin was not affected by silencing MRP2 expression (Fig. 10).

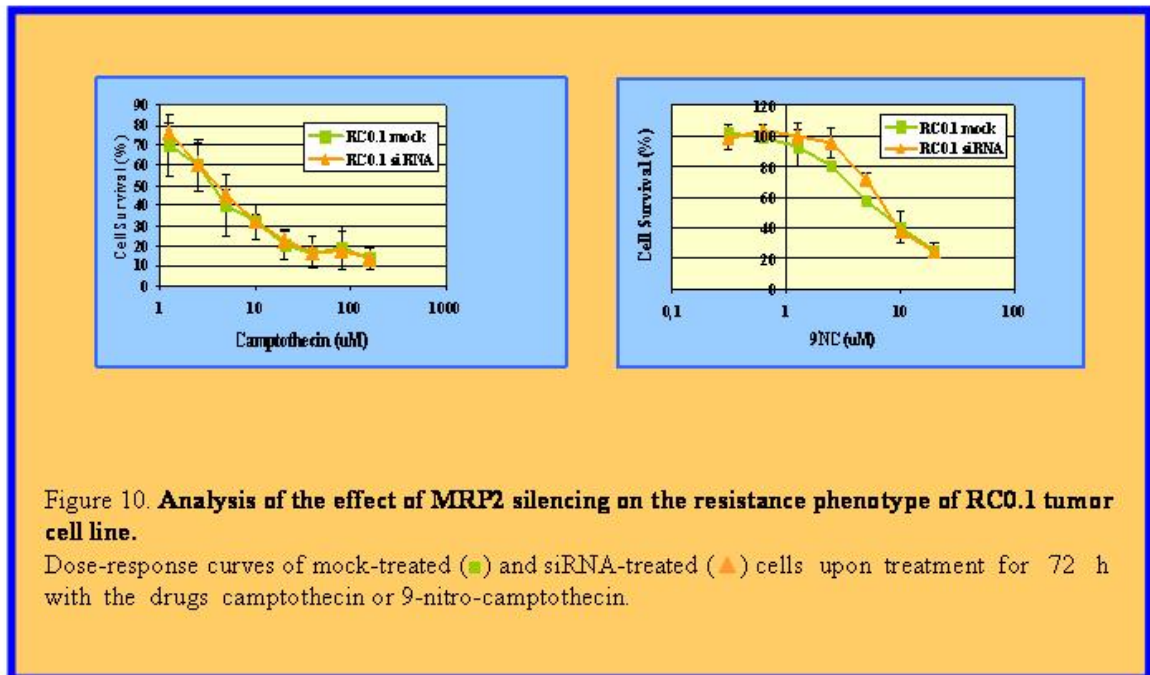


Figure 10. **Analysis of the effect of MRP2 silencing on the resistance phenotype of RC0.1 tumor cell line.**

Dose-response curves of mock-treated (■) and siRNA-treated (▲) cells upon treatment for 72 h with the drugs camptothecin or 9-nitro-camptothecin.

Thus, the results obtained from MRP2 inhibition experiments (Fig. 5), as well as from MRP2 silencing experiments (Fig. 10), indicated the absence of any correlation between the high expression levels of MRP2 in RC0.1 cell line and its resistance phenotype. We can speculate that the high expression levels of MRP2 possibly represent an early adaptation of cells to the drug, followed by the evolution of different resistance mechanisms, such as mutations in the topoisomerase I gene.

These observations are in agreement with the results obtained by microarray analyses, which indicated that mRNA expression profiles are significantly different in RC0.1 cells with respect to DU145 cells. In particular, these analyses indicated the overexpression of the enzyme gamma-glutamylcysteine synthetase (GSC), also known as glutamate cysteine ligase, in the resistant cell line RC0.1 (Annereau *et al.* 2004). GSC is a key enzyme in glutathione metabolism. In contrast, despite its general up-regulation in cancer cells, the expression of the enzyme glutathione S-transferase pi (GST-Pi), catalyzing the conjugation of glutathione to electrophilic carcinogens, was found to be significantly reduced in RC0.1 cells (Annereau *et al.* 2004). Since the ABC transporter MRP2 is known to transport GSH-S-conjugates (e.g., leukotriene C4 and 2,4-dinitrophenyl-S-GSH), oxidized glutathione (GSSG), glucuronide conjugates (e.g., glucuronidated bilirubin and bile salts), and sulfate conjugates of certain bile acids (e.g., 3-sulfatolithocholytaurine) (Muller *et al.* 1994), these observations seem to suggest a “metabolic switch” in RC0.1 cells responsible for the resistance phenotype.

5.5 Identification of New Substrates for the ABC Transporter ABCC2/MRP2

In previous studies we identified 28 anticancer drugs as putative substrates of the ABC transporter MRP2 (Szakács *et al.* 2004a). Four of these were available from DTP (Developmental Therapeutics Program) and named as follows: NSC641281; NSC645145; NSC618059; NSC626878. Their chemical structures are represented in Fig. 11.

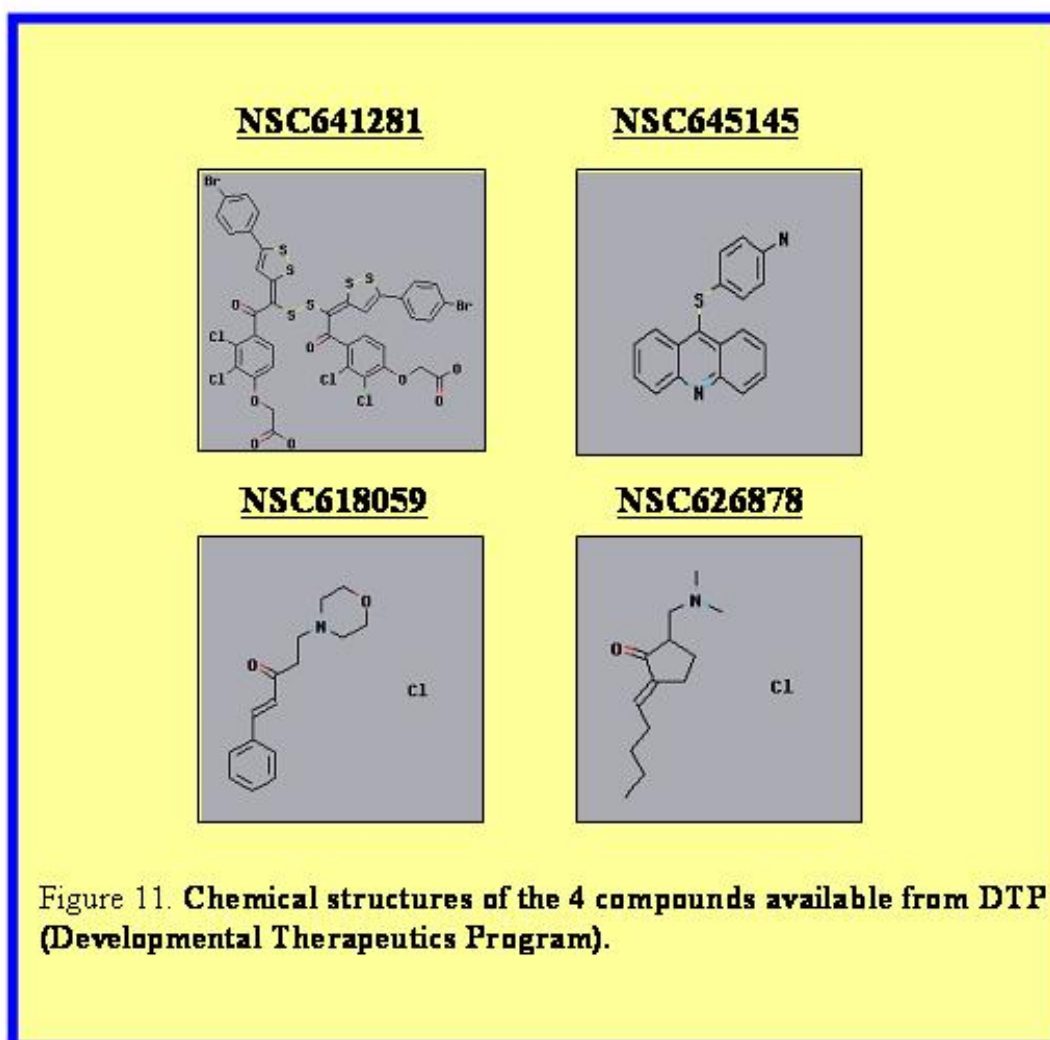


Figure 11. **Chemical structures of the 4 compounds available from DTP (Developmental Therapeutics Program).**

Dose-response curves of wild-type (MDCK parental) and ABCC2-transfected (MDCKII cMOAT) Madin-Darby canine kidney cells were obtained upon treatment with the four compounds. In all the experiments, ABCC2-overexpressing cells were found to be more resistant to the four drugs as compared to control cells, as indicated by the results of MTT assays (Fig. 12). This clearly indicated the involvement of the ABC transporter MRP2 in the transport of these drugs. The strongest evidence was obtained in the case of compound NSC641281, since ABCC2-overexpressing cells proved to be extremely resistant to this compound, reinforcing the suggestion that NSC641281 is an ABCC2/MRP2 substrate (Szakács *et al.* 2004a).

To test the specificity of the involvement of MRP2 in the transport of the four identified compounds, dose-response curves were performed using control (HEK 293 parental) and MRP1-transfected human embryonic kidney cells (HEK 293). ABCC1/MRP1 is an ABC transporter homologous to MRP2, belonging to the same subfamily (ABCC). Control and MRP1-transfected cells were found to be equally sensitive to compounds NSC641281, NSC645145 and NSC618059 (Fig. 10), suggesting that the efflux of these compounds is MRP1 independent, but specifically requires MRP2 involvement. However, MRP1-transfected cells were found to be slightly more resistant to compound NSC626878 as compared to control cells (Fig. 13). This suggested a putative role of MRP1 in the transport of this compound.

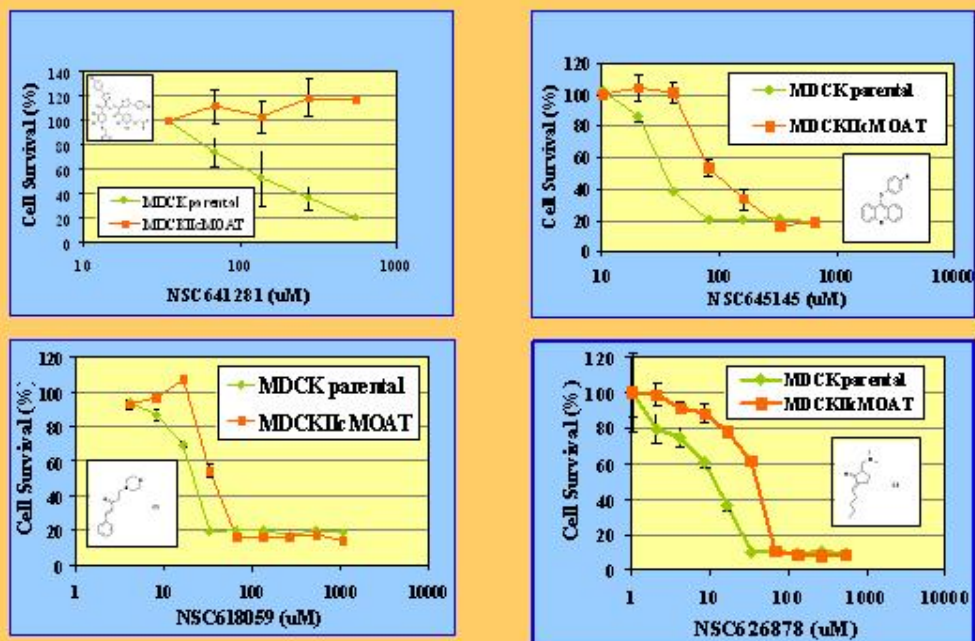


Figure 12. **Analysis of the effects of compounds NSC641281, NSC645145, NSC618059 and NSC626878 on the viability of control (MDCK parental) and MRP2-transfected (MDCKII cMOAT) cells.**

Dose-response curves of control (♦) and MRP2-transfected (■) cells upon treatment for 72 h with compounds NSC641281, NSC645145, NSC618059 and NSC626878. The chemical structure of each tested compound is reported in the correspondent panel.

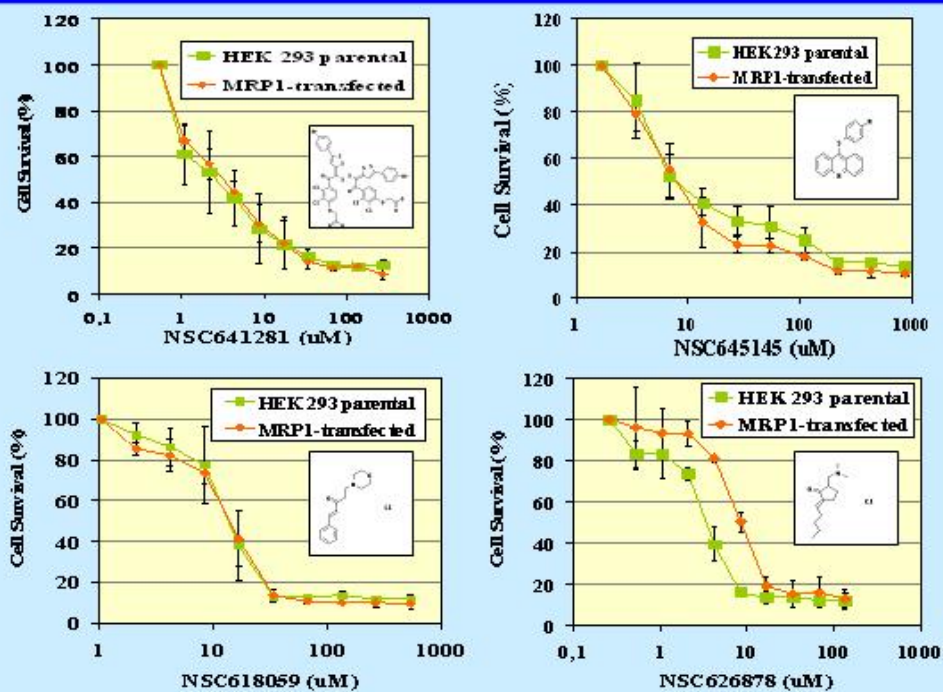
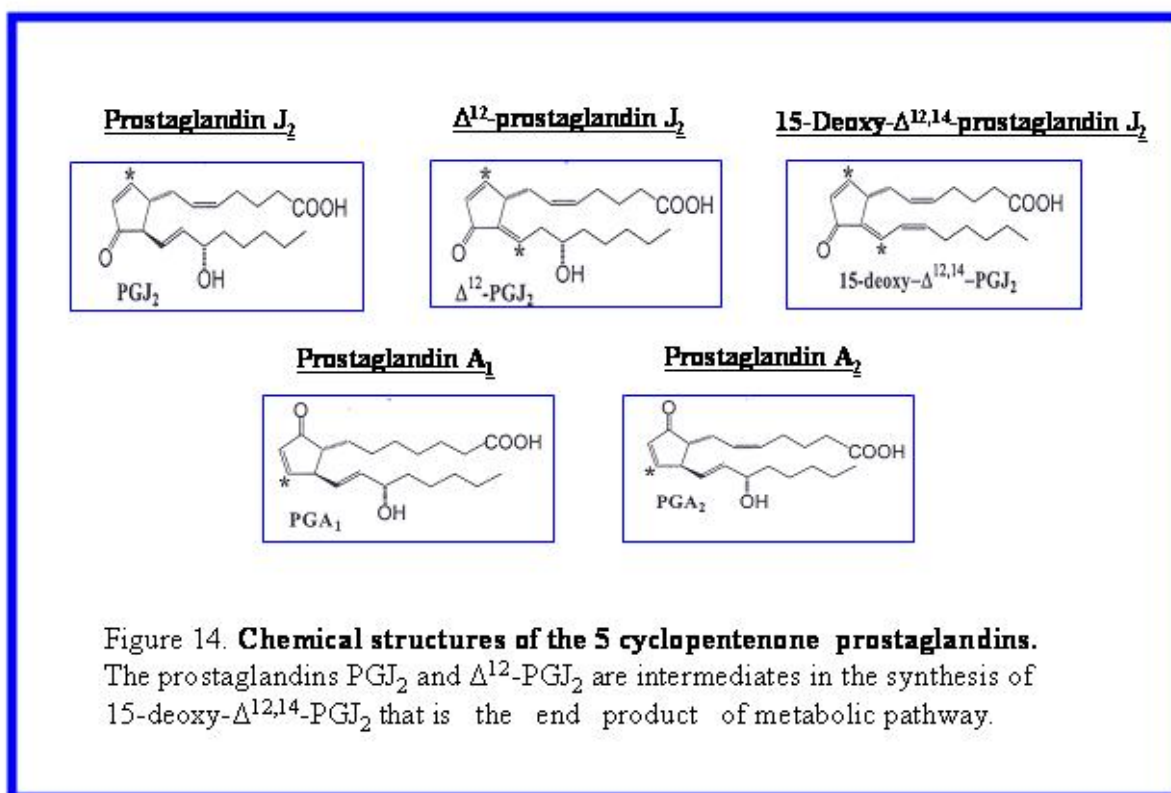


Figure 13. **Analysis of the effects of compounds NSC641281, NSC645145, NSC618059 and NSC626878 on the viability of control (HEK 293 parental) and MRP1-transfected cells.** Dose-response curves of control (■) and MRP1-transfected (●) HEK 293 cells upon treatment for 72 h with compounds NSC641281, NSC645145, NSC618059 and NSC 626878. The chemical structure of each tested compound is reported in the correspondent panel.

5.6 Identification of the Cyclopentenone Prostaglandin 15-Deoxy- $\Delta^{12,14}$ -Prostaglandin J_2 (15-d-PG J_2) as a New Substrate of the ABC Transporter MRP2

Cyclopentenone prostaglandins, such as prostaglandin J_2 (PG J_2), Δ^{12} -prostaglandin J_2 (Δ^{12} -PG J_2), 15-deoxy- $\Delta^{12,14}$ -prostaglandin J_2 (15-d-PG J_2), prostaglandin A_1 (PGA $_1$) and prostaglandin A_2 (PGA $_2$) influence a variety of cellular processes, including growth and differentiation, gene expression, apoptosis and inhibition of inflammatory signaling pathways (Rovin *et al.* 2002; Forman *et al.* 1995; Kliewer *et al.* 1995). The chemical structures of the 5 cyclopentenone prostaglandins are reported in Fig. 14.



The analysis of the chemical structures of the 28 predicted substrates of MRP2 evidenced common structural features. As shown in Fig. 15, 7 of the 28 predicted substrates of MRP2 share a common structural element, represented by a cyclopentanone ring, structurally related to the cyclopentenone ring of prostaglandins. These compounds are evidenced by a green box in Fig. 15.

Based on this observation, a role of MRP2 in the efflux of cyclopentenone prostaglandins was hypothesized.

In Fig. 15, the 4 compounds available from DTP (Developmental Therapeutics Program) are represented in red. Among them, NSC626878 is the only compound containing a cyclopentanone ring. This compound was also indicated as a putative substrate of both MRP1 and MRP2 (see above).

To test our hypothesis, dose-response curves of control (MDCK parental) and ABCC2-transfected (MDCKII cMOAT) cells were obtained upon treatment with the five above mentioned cyclopentenone prostaglandins. The results of the MTT assays are reported in Fig. 16. Control and MRP2-transfected cells were found to be equally sensitive to the cytotoxic action of Δ^{12} -prostaglandin J₂ (Δ^{12} -PGJ₂), prostaglandin A₁ (PGA₁) and prostaglandin A₂ (PGA₂). On the contrary, MRP2-overexpressing cells were found to be more resistant to prostaglandin J₂ (PGJ₂) and 15-deoxy- $\Delta^{12,14}$ -prostaglandin J₂ (15-d-PGJ₂) as compared to control cells (Fig. 13). Since PGJ₂ is an intermediate of the synthesis of 15-d-PGJ₂, the end product of the metabolic pathway (Straus and Glass 2001), the obtained results suggested a role of MRP2 in the transport of the cyclopentenone prostaglandin 15-d-PGJ₂.

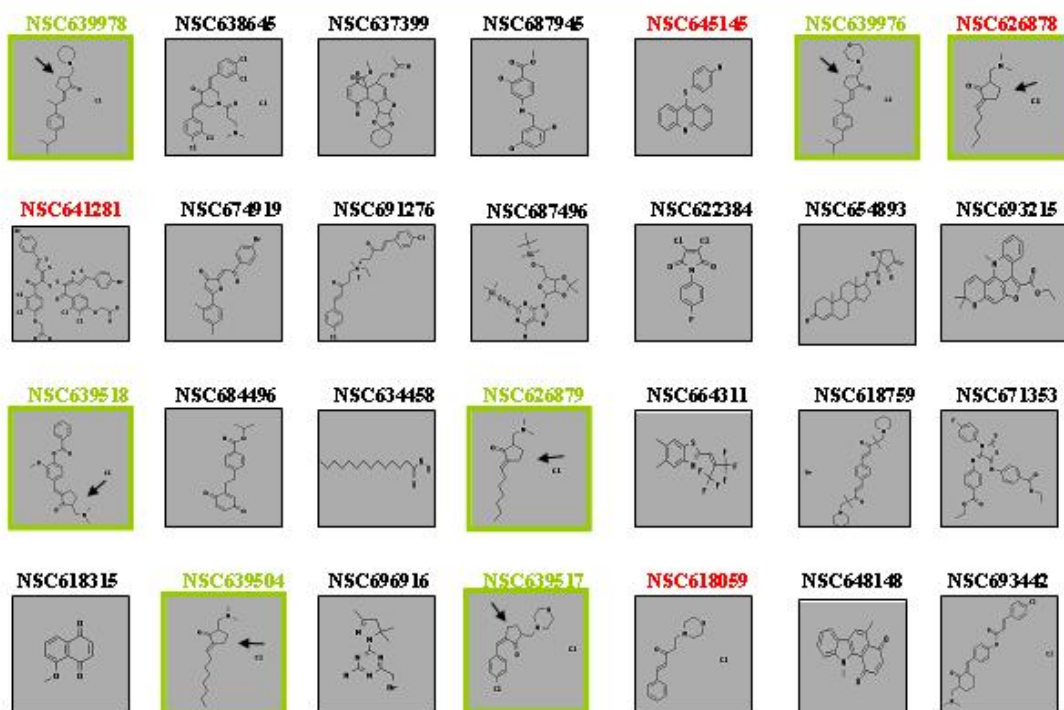


Figure 15. **Chemical structures of the 28 predicted MRP2 substrates.**

The compounds containing a cyclopentanone ring are included in a green box. Each cyclopentanone ring is indicated by a black arrow. The 4 compounds available from DTP are indicated in red.

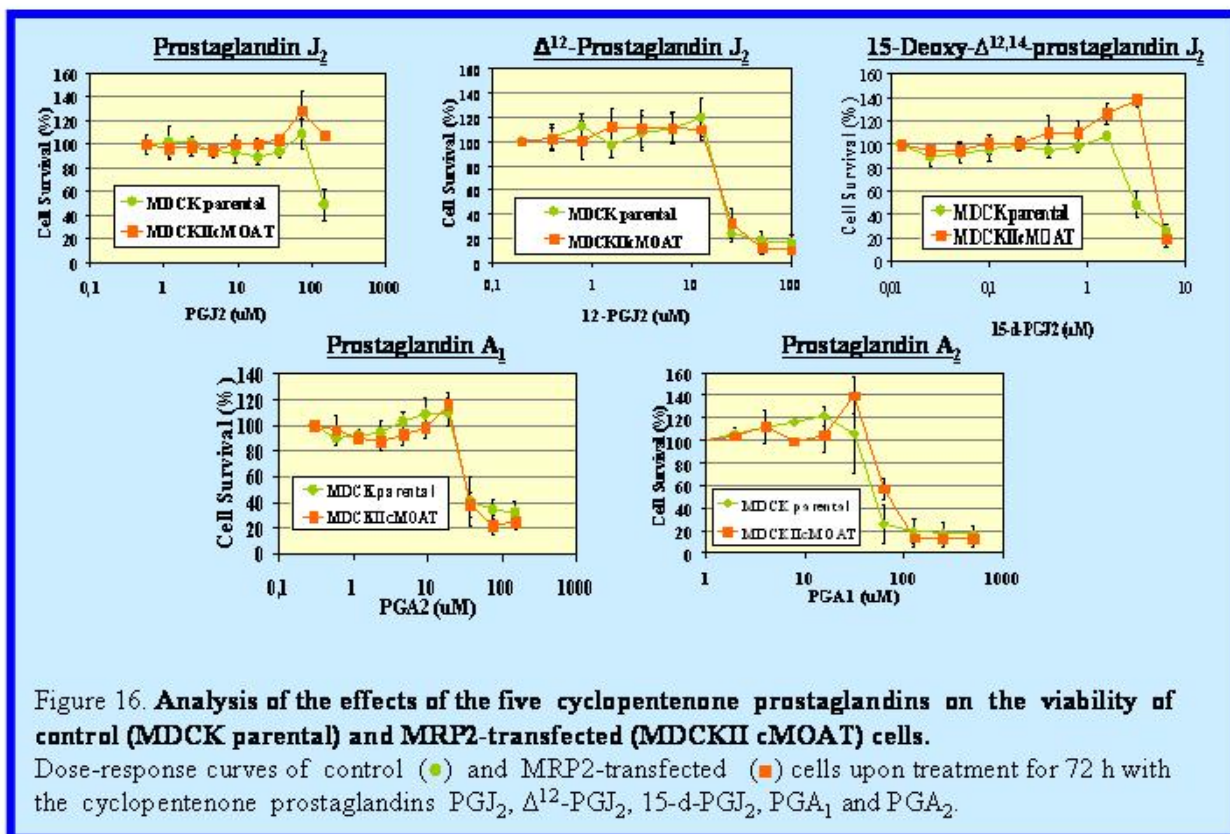
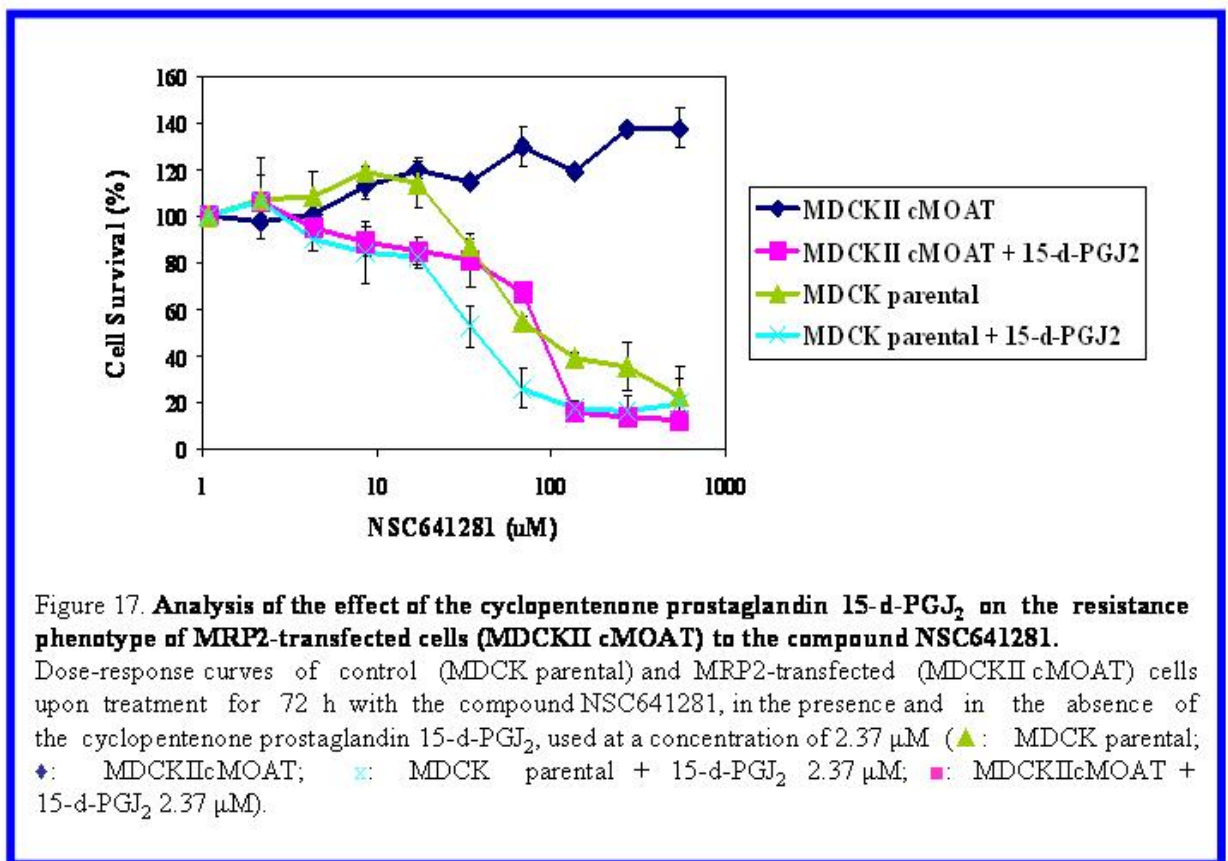


Figure 16. Analysis of the effects of the five cyclopentenone prostaglandins on the viability of control (MDCK parental) and MRP2-transfected (MDCKII cMOAT) cells. Dose-response curves of control (●) and MRP2-transfected (■) cells upon treatment for 72 h with the cyclopentenone prostaglandins PGJ₂, Δ¹²-PGJ₂, 15-d-PGJ₂, PGA₁ and PGA₂.

Further analyses were performed using the cyclopentenone prostaglandin 15-d-PGJ₂ as an inhibitor of the ABC transporter MRP2. To this purpose, control (MDCK parental) and MRP2-transfected (MDCKII cMOAT) cells were exposed to the identified MRP2 substrate NSC641281 (see above), in the absence and presence of 15-d-PGJ₂ at the highest concentration previously found to be not toxic for both cell lines (2.37 μM). In the presence of 15-d-PGJ₂ the resistance of MRP2-transfected cells (MDCKII cMOAT) to the drug NSC641281 was completely reverted, since they became as sensitive as control cells (Fig. 17).

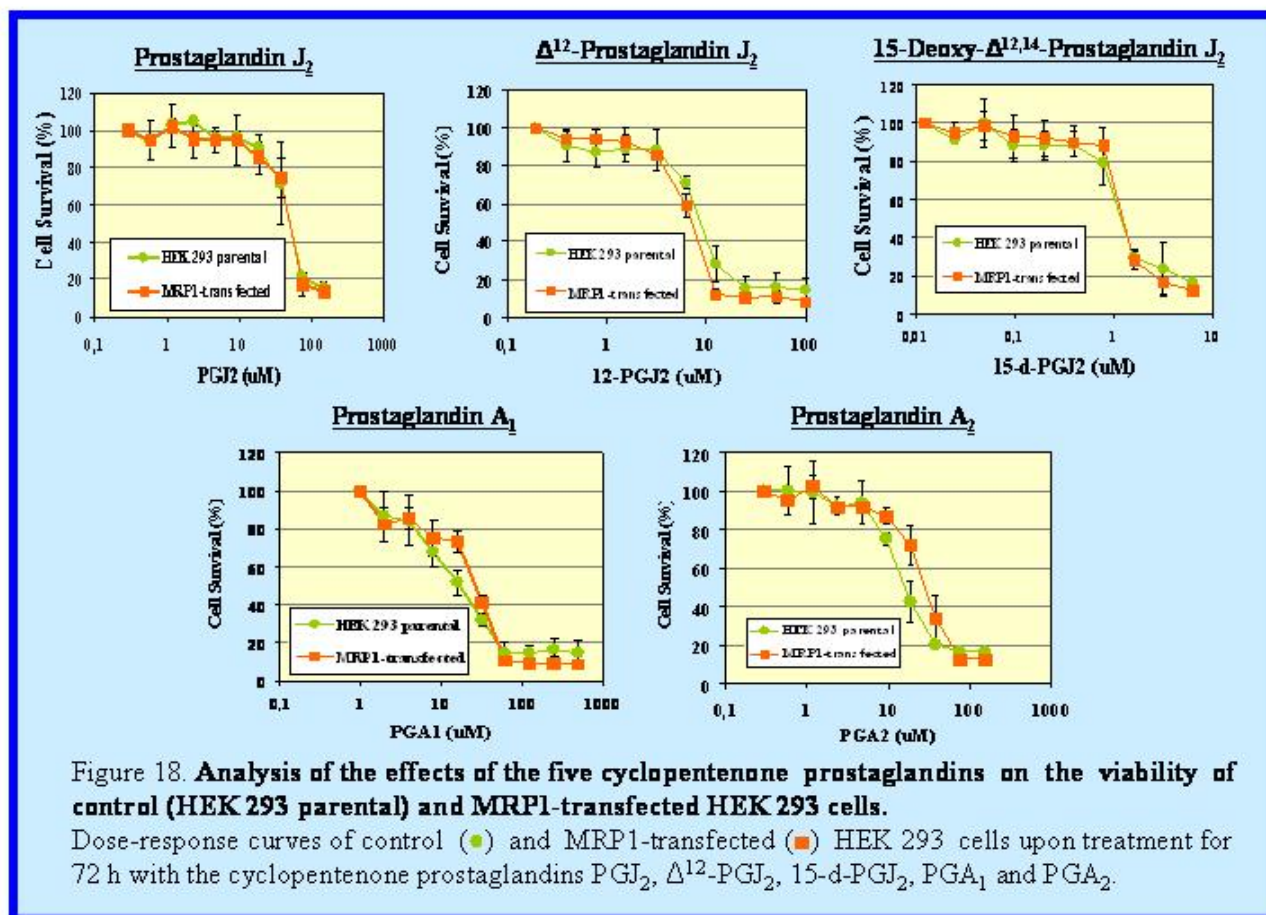
These results clearly indicated that compound NSC641281 and prostaglandin 15-d-PGJ₂ compete for the same target, MRP2. This is a clear evidence of a new role of MRP2 transporter, *i.e.* its involvement in the efflux of cyclopentenone prostaglandin 15-d-PGJ₂.



To test the specificity of the ABC transporter MRP2 in the transport of 15-d-PGJ₂, dose-response curves were performed using control (HEK 293 parental) and MRP1-transfected human embryonic kidney cells (HEK 293). As mentioned before, MRP1 is an ABC transporter belonging to the same subfamily (ABCC) of MRP2. Dose-response curves of control and MRP1-transfected HEK 293 cells were obtained upon treatment with the above mentioned cyclopentenone prostaglandins. Control and MRP1-transfected cells were found to be equally sensitive to the cytotoxic action of cyclopentenone prostaglandins (Fig. 18). These results allowed us to exclude a role of MRP1 in the transport of cyclopentenone prostaglandin 15-d-PGJ₂, which seems to be specifically related to MRP2.

However, it is worth noting that there is a discrepancy between these results and recent findings indicating that MRP1, as well as MRP3, are able to modulate the biological effects of 15-d-PGJ₂ in a glutathione-dependent manner (Paumi *et al.* 2003).

To this purpose, further experiments will be performed to clarify the role of the ABC transporter MRP1 in the transport of cyclopentenone prostaglandins.



6. CONCLUSIONS

In the first part of my study, the role of the ABC transporter ABCC2/MRP2 in camptothecin resistance was analyzed. Microarray analyses, performed with a novel ABC-ToxChip (Annereau *et al.* 2004), indicated high levels of MRP2 expression in the camptothecin-resistant prostate tumor cell line RC0.1, derived from the parental sensitive cell line DU145 by continuous exposure to the drug 9-nitro-camptothecin. Following this observation, experiments were here performed to clarify the role of MRP2 in the resistance phenotype of RC0.1 tumor cell line. Inhibition of this ABC transporter by specific RNA interference constructs or by the inhibitor MK571 did not revert the resistance phenotype of RC0.1 cell line. Thus, the obtained results demonstrated that MRP2 overexpression is not directly related to the resistance phenotype. This observation is in agreement with data indicating the presence of specific mutations in topoisomerase I gene and a general alteration of apoptotic regulation in the prostate cancer cell line RC0.1 (Reinhold *et al.* 2003; Urasaki *et al.* 2001; Chatterjee *et al.* 2001). We can speculate that more than one mechanism is involved in resistance phenotype of RC0.1 tumor cell line, and that the elevated expression of MRP2 represents only one of the adaptation mechanisms of cells to the drug.

By further experiments, I was able to identify a new physiological role of the ABC transporter ABCC2/MRP2, *i.e.* its involvement in the transport of the cyclopentenone prostaglandin 15-deoxy- $\Delta^{12,14}$ prostaglandin J₂ (15-d-PGJ₂). Among cyclopentenone prostaglandins, 15-d-PGJ₂ has attracted considerable attention because of its antitumor activities (Clay *et al.* 2000; Clay *et al.* 1999; Harris and Phipps 2002; Eibl *et al.* 2001; Shimada *et al.* 2002; Padilla *et al.* 2002).

Prostaglandins are thought to exit cells by passive diffusion, but such a mechanism is incompatible with their water solubility, which clearly suggests the necessity of an active process. In this contest, the idea of an involvement of ABC transporters in prostaglandins efflux is really interesting. Such an observation is in agreement with recent findings indicating that the ABC transporter MRP4 is involved in the efflux of prostaglandins PGE₁ and PGE₂ (Reid *et al.* 2003b), and that MRP1 and MRP3 are able to modulate the biological effects of 15-d-PGJ₂, in a glutathione-dependent manner (Paumi *et al.* 2003).

The results obtained in the present study clearly indicated a specific involvement of ABCC2/MRP2 in the transport of 15-d-PGJ₂, whereas other cyclopentenone prostaglandins appear not to interact with this ABC transporter. Such a result broadens the physiological substrate specificity of MRP2, and suggests a putative interaction between cyclopentone prostaglandins and other MRP subfamily members of ABC transporters.

BIBLIOGRAPHY

- Akamaru K, Kuo MT, Furuta K, Suzuki M, Noyori R, Ishikawa T. Induction of MRP/GS-X pump and cellular resistance to anticancer prostaglandins. *Cytotechnology* 1996;19:221-7.
- Allikmets R, Schriml LM, Hutchinson A, Romano-Spica V, Dean M. A human placenta-specific ATP-binding cassette gene (ABCP) on chromosome 4q22 that is involved in multidrug resistance. *Cancer Res* 1998;58:5337-9.
- Ambudkar SV, Dey S, Hrycyna CA, Ramachandra M, Pastan I, Gottesman, MM. Biochemical, cellular, and pharmacological aspects of the multidrug transporter. *Annu Rev Pharmacol Toxicol* 1999;39:361-98.
- Annereau JP, Szakács G, Tucker CJ, Arciello A, Cardarelli C, Collins J, Grissom S, Zeeberg B, Reinhold W, Weinstein J, Pommier Y, Paules RS, Gottesman MM. Analysis of ABC transporter expression in drug-selected cell lines by a microarray dedicated to multidrug resistance. *Mol Pharmacol* 2004;Epub ahead of print.
- Atsmon J, Freeman ML, Meredith MJ, Sweetman BJ, Roberts LJ 2nd. Conjugation of 9-deoxy-delta 9,delta 12(E)-prostaglandin D2 with intracellular glutathione and enhancement of its antiproliferative activity by glutathione depletion. *Cancer Res* 1990a;50:1879-85.
- Atsmon J, Sweetman BJ, Baertschi SW, Harris TM, Roberts LJ 2nd. Formation of thiol conjugates of 9-deoxy-delta 9,delta 12(E)-prostaglandin D2 and delta 12(E)-prostaglandin D2. *Biochemistry* 1990b;29:3760-5.
- Badawi AF, Badr MZ. Expression of cyclooxygenase-2 and peroxisome proliferator-activated receptor-gamma and levels of prostaglandin E2 and 15-deoxy-delta 12,14-prostaglandin J2 in human breast cancer and metastasis. *Int J Cancer* 2003;103:84-90.
- Beck WT, Khelifa T, Kusumoto H, Mo YY, Rodgers Q, Wolverson JS, Wang Q. Novel mechanisms of resistance to inhibitors of DNA topoisomerases. *Adv Enzyme Regul* 1997;37:17-26.
- Bogaards JJ, Venekamp JC, van Bladeren PJ. Stereoselective conjugation of prostaglandin A2 and prostaglandin J2 with glutathione, catalyzed by the human glutathione S-transferases A1-1, A2-2, M1a-1a, and P1-1. *Chem Res Toxicol* 1997;10:310-7.
- Borst P, Evers R, Kool M, Wijnholds J. A family of drug transporters: the multidrug resistance-associated proteins. *J Natl Cancer Inst* 2000;92:1295-302.
- Borst P, Zelcer N, van Helvoort A. ABC transporters in lipid transport. *Biochim Biophys Acta* 2000;1486:128-44.
- Breyer MD, Breyer RM. Prostaglandin E receptors and the kidney. *Am J Physiol Renal Physiol* 2000;279:F12-23.
- Cabanillas F. The role of topoisomerase-I inhibitors in the treatment of non-Hodgkin's lymphoma. *Semin Hematol* 1999;36:11-5.

Castrillo A, Diaz-Guerra MJ, Hortelano S, Martin-Sanz P, Bosca L. Inhibition of IKappa B kinase and IKappa B phosphorylation by 15-deoxy-Delta(12,14)-prostaglandin J(2) in activated murine macrophages. *Mol Cell Biol* 2000;20:1692-8.

Cernuda-Morollon E, Pineda-Molina E, Canada FJ, Perez-Sala D. 15-Deoxy-Delta 12,14-prostaglandin J2 inhibition of NF-kappaB-DNA binding through covalent modification of the p50 subunit. *J Biol Chem* 2001;276:35530-6.

Chan BS, Endo S, Kanai N, Schuster VL. Identification of lactate as a driving force for prostanoid transport by prostaglandin transporter PGT. *Am J Physiol Renal Physiol* 2002;282:F1097-102.

Chatterjee D, Schmitz I, Krueger A, Yeung K, Kirchhoff S, Krammer PH, Peter ME, Wyche JH, Pantazis P. Induction of apoptosis in 9-nitrocamptothecin-treated DU145 human prostate carcinoma cells correlates with de novo synthesis of CD95 and CD95 ligand and down-regulation of c-FLIP(short). *Cancer Res* 2001;61:7148-54.

Chatterjee D, Wyche JH, Pantazis P. Induction of apoptosis in malignant and camptothecin-resistant human cells. *Ann NY Acad Sci* 1996;803:143-56.

Chawla A, Repa JJ, Evans RM, Mangelsdorf DJ. Nuclear receptors and lipid physiology: opening the X-files. *Science* 2001;294:1866-70.

Chen AY, Liu LF. DNA Topoisomerases: essential enzymes and lethal targets. *Annu Rev Pharmacol Toxicol* 1994;94:194-218.

Chen CJ, Chin JE, Ueda K, Clark DP, Pastan I, Gottesman MM, Roninson IB. Internal duplication and homology with bacterial transport proteins in the mdr1 (P-glycoprotein) gene from multidrug-resistant human cells. *Cell* 1986;47:381-9.

Chen ZS, Kawabe T, Ono M, Aoki S, Sumizawa T, Furukawa T, Uchiumi T, Wada M, Kuwano M, Akijama SI. Effect of multidrug resistance-reversing agents on transporting activity of human canalicular multispecific organic anion transporter. *Mol Pharmacol* 1999;56:1219-28.

Childs S, Yeh RL, Hui D, Ling V. Taxol resistance mediated by transfection of the liver-specific sister gene of P-glycoprotein. *Cancer Res* 1998;58:4160-7.

Chin KV, Tanaka S, Darlington G, Pastan I, Gottesman MM. Heat shock and arsenite increase expression of the multidrug resistance (MDR1) gene in human renal carcinoma cells. *J Biol Chem* 1990;265:221-6.

Chin KV, Ueda K, Pastan I, Gottesman MM. Modulation of activity of the promoter of the human MDR1 gene by Ras and p53. *Science* 1992;255:459-62.

Clarke R, Currier S, Kaplan O, Lovelace E, Boulay V, Gottesman MM, Dickson RB. Effect of P-glycoprotein expression on sensitivity to hormones in MCF-7 human breast cancer cells. *J Natl Cancer Inst* 1992;84:1506-12.

Clay CE, Namen AM, Atsumi G, Willingham MC, High KP, Kute TE, Trimboli AJ, Fonteh AN, Dawson PA, Chilton FH. Influence of J series prostaglandins on

apoptosis and tumorigenesis of breast cancer cells. *Carcinogenesis* 1999;20:1905-11.

Clay CE, Namen AM, Fonteh AN, Atsumi G, High KP, Chilton FH. 15-deoxy-Delta(12,14)PGJ(2) induces diverse biological responses via PPARgamma activation in cancer cells. *Prostaglandins Other Lipid Mediat* 2000;62:23-32.

Cole SP, Bhardwaj G, Gerlach JH, Mackie JE, Grant CE, Almquist KC, Stewart AJ, Kurz EU, Duncan, AM, Deeley RG. Overexpression of a transporter gene in a multidrug-resistant human lung cancer cell line. *Science* 1992;258:1650-4.

Cordon-Cardo C, O'Brien JP, Boccia J, Casals D, Bertino JR, Melamed MR. Expression of the multidrug resistance gene product (P-glycoprotein) in human normal and tumor tissues. *J Histochem Cytochem* 1990;38:1277-87.

Cui Y, Konig J, Buchholz JK, Spring H, Leier I, Keppler D. Drug resistance and ATP-dependent conjugate transport mediated by the apical multidrug resistance protein, MRP2, permanently expressed in human and canine cells. *Mol Pharmacol* 1999;55:929-37.

Dean M, Rzhetsky A, Alliknets R. The human ATP-binding cassette (ABC) transporter superfamily. *Genome Res.* 2001;11:1156-66.

Dietrich CG, de Waart DR, Ottenhoff R, Schoots IG, Elferink RP. Increased bioavailability of the food-derived carcinogen 2-amino-1-methyl-6-phenylimidazo[4,5-b]pyridine in MRP2-deficient rats. *Mol Pharmacol* 2001;59:974-80.

Doyle LA, Yang W, Abruzzo LV, Krogmann T, Gao Y, Rishi AK, Ross DD. A multidrug resistance transporter from human MCF-7 breast cancer cells. *Proc Natl Acad Sci USA* 1998;95:15665-70.

Dussault I, Forman BM. Prostaglandins and fatty acids regulate transcriptional signaling via the peroxisome proliferator activated receptor nuclear receptors. *Prostaglandins Other Lipid Mediat* 2000;62:1-13.

Eibl G, Wenthe MN, Reber HA, Hines OJ. Peroxisome proliferator-activated receptor gamma induces pancreatic cancer cell apoptosis. *Biochem Biophys Res Commun* 2001;287:522-9.

Elbashir SM, Harborth J, Lendeckel W, Yalcin A, Weber K, Tuschl T. Duplexes of 21-nucleotide RNAs mediate RNA interference in cultured mammalian cells. *Nature* 2001;411:494-8.

Elstner, E, Muller C, Koshizuka K, Williamson EA, Park D, Asou H, Shintaku P, Said JW, Heber D, Koeffler HP. Ligands for peroxisome proliferator-activated receptor gamma and retinoic acid receptor inhibit growth and induce apoptosis of human breast cancer cells in vitro and in BNX mice. *Proc Natl Acad Sci USA* 1998;95:8806-11.

Evers R, Cnubben NH, Wijnholds J, van Deemter L, van Bladeren PJ, Borst P. Transport of glutathione prostaglandin A conjugates by the multidrug resistance protein 1. *FEBS Lett* 1997;419:112-6.

Evers R, Kool M, van Deemter L, Janssen H, Calafat J, Oomen LC, Paulusuma CC, Oude Elferink RP, Baas F, Schinkel AH, Borst P. Drug export activity of the human canalicular multispecific organic anion transporter in polarized kidney MDCK cells expressing cMOAT (MRP2) cDNA. *J Clin Invest* 1998;101:1310-9.

Evers R, Zaman GJ, van Deemter L, Jansen H, Calafat J, Oomen LC, Oude Elferink RP, Borst P, Schinkel AH. Basolateral localization and export activity of the human multidrug resistance-associated protein in polarized pig kidney cells. *J Clin Invest* 1996;97:1211-8.

Forman BM, Tontonoz P, Chen J, Brun RP, Spiegelman BM, Evans RM. 15-Deoxy-delta 12, 14-prostaglandin J2 is a ligand for the adipocyte determination factor PPAR gamma. *Cell* 1995;83:803-12.

Funk CD. Prostaglandins and leukotrienes: advances in eicosanoid biology. *Science* 2001;294:1871-5.

Godinot N, Iversen PW, Tabas L, Xia X, Williams DC, Dantzig AH, Perry WL 3rd. Cloning and functional characterization of the multidrug resistance-associated protein (MRP1/ABCC1) from the cynomolgus monkey. *Mol Cancer Ther* 2003;2:307-16.

Gottesman MM, Fojo T, Bates SE. Multidrug resistance in cancer: role of ATP-dependent transporters. *Nat Rev Cancer* 2002;2:48-58.

Guo Y, Kotova E, Chen ZS, Lee K, Hopper-Borge E, Belinsky MG, Kruh GD. MRP8 (ABCC11) is a cyclic nucleotide efflux pump and a resistance factor for fluoropyrimidines, 2'3'-dideoxycytidine and 9'-(2'-phosphonylmethoxyethyl)-adenine. *J Biol Chem* 2003;278:29509-14.

Gupta RA, Dubois RN. Colorectal cancer prevention and treatment by inhibition of cyclooxygenase-2. *Nat Rev Cancer* 2001;1:11-21.

Hannon GJ. RNA interference. *Nature* 2002;418:244-51.

Harris SG, Padilla J, Koumas L, Ray D, Phipps RP. Prostaglandins as modulators of immunity. *Trends Immunol* 2002;23:144-50.

Harris SG, Phipps RP. Prostaglandin D(2), its metabolite 15-d-PGJ(2), and peroxisome proliferator activated receptor-gamma agonists induce apoptosis in transformed, but not normal, human T lineage cells. *Immunology* 2002;105:23-34.

Hihi AK, Michalik L, Wahli W. PPARs transcriptional effectors of fatty acids and their derivatives. *Cell Mol Life Sci* 2002;59:790-8.

Ho YP, Au-Yeung SC, To KK. Platinum-based anticancer agents: innovative design strategies and biological perspectives. *Med Res Rev* 2003;23:633-55.

Honn KV, Marnett LJ. Requirement of a reactive alpha, beta-unsaturated carbonyl for inhibition of tumor growth and induction of differentiation by "A" series of prostaglandins. *Biochem Biophys Res Commun* 1985;129:34-40.

Horikawa M, Kato Y, Sugiyama Y. Reduced gastrointestinal toxicity following inhibition of the biliary excretion of irinotecan and its metabolites by probenecid in rats. *Pharm Res* 2002;19:1345-53.

Hsiang YH, Hertzberg R, Hecht S, Liu LF. Camptothecin induces protein-linked DNA breaks via mammalian DNA topoisomerase I. *J Biol Chem* 1985;260:14873-8.

Ishikawa T, Akimaru K, Nakanishi M, Tomokiyo K, Furuta K, Suzuki M, Noyori R. Anti-cancer-prostaglandin-induced cell-cycle arrest and its modulation by an inhibitor of the ATP-dependent glutathione S-conjugate export pump (GS-X pump). *Biochem J* 1998;336:569-76.

Jedlitschky G, Leier I, Buchholz U, Barnouin K, Kurz G, Keppler D. Transport of glutathione, glucuronate, and sulfate conjugates by the MRP gene-encoded conjugate export pump. *Cancer Res* 1996;56:988-94.

Jedlitschky G, Leier I, Buchholz U, Center M, Keppler D. ATP-dependent transport of glutathione S-conjugates by the multidrug resistance-associated protein. *Cancer Res* 1994;54:4833-6.

Jiang C, Ting AT, Seed B. PPAR-gamma agonists inhibit production of monocyte inflammatory cytokines. *Nature* 1998;391:82-6.

Jonker JW, Smit JW, Brinkhuis RF, Maliepaard M, Beijnen JH, Schellens JH, Schinkel AH. Role of breast cancer resistance protein in the bioavailability and fetal penetration of topotecan. *J Natl Cancer Inst* 2000;92:1651-6.

Kantarjian H. New developments in the treatment of acute myeloid leukaemia: focus on topotecan. *Semin Hematol* 1999;36:16-25.

Kliwer SA, Lenhard JM, Willson TM, Patel I, Morris DC, Lehmann JM. A prostaglandin J2 metabolite binds peroxisome proliferator-activated receptor gamma and promotes adipocyte differentiation. *Cell* 1995;83:813-9.

Kodera Y, Takeyama K, Murayama A, Suzawa M, Masuhiro Y, Kato S. Ligand type-specific interactions of peroxisome proliferator-activated receptor gamma with transcriptional coactivators. *J Biol Chem* 2000;43:33201-4.

Konig J, Nies AT, Cui Y, Leier I, Keppler D. Conjugate export pumps of the multidrug resistance protein (MRP) family: localization, substrate specificity, and MRP2-mediated drug resistance. *Biochim Biophys Acta* 1999;1461:377-94.

Krey G, Braissant O, L'Horsset F, Kalkhoven E, Perroud M, Parker MG, Wahli W. Fatty acids, eicosanoids, and hypolipidemic agents identified as ligands of peroxisome proliferator-activated receptors by coactivator-dependent receptor ligand assay. *Mol Endocrinol* 1997;11:779-91.

Kudoh S, Fujiwara Y, Takada Y, Yamamoto H, Kinoshita A, Ariyoshi Y, Furuse K, Fukuoka M. Phase II study of irinotecan combined with cisplatin in patients with previously untreated small-cell lung cancer. West Japan Lung Cancer Group. *J Clin Oncol* 1998;16:1068-74.

Laing NM, Belinsky MG, Kruh GD, Bell DW, Boyd JT, Barone L, Testa JR, Tew KD. Amplification of the ATP-binding cassette 2 transporter gene is functionally linked with enhanced efflux of estramustine in ovarian carcinoma cells. *Cancer Res* 1998;58:1332-7.

Lamendola DE, Duan Z, Yusuf RZ, Seiden MV. Molecular description of evolving paclitaxel resistance in the SKOV-3 human ovarian carcinoma cell line. *Cancer Res* 2003;63:2200-5.

Leier I, Jedlitschky G, Buchholz U, Cole SP, Deeley RG, Keppler D. The MRP gene encodes an ATP-dependent export pump for leukotriene C₄ and structurally related conjugates. *J Biol Chem* 1994;269:27807-10.

Loe DW, Deeley RG, Cole SP. Characterization of vincristine transport by the M_r 190,000 multidrug resistance protein (MRP): evidence for cotransport with reduced glutathione. *Cancer Res* 1998;58:5130-6.

Lowe SW, Ruley HE, Jacks T, Housman DE. p53-dependent apoptosis modulates the cytotoxicity of anticancer agents. *Cell* 1993;74:957-67.

Maliapaard M, Scheffer GL, Faneyte IF, van Gastelen MA, Pijnenborg AC, Schinkel AH, van De Vijver MJ, Scheper RJ, Schellens JH. Subcellular localization and distribution of the breast cancer resistance protein transporter in normal human tissues. *Cancer Res* 2001;61:3458-64.

Marino PA, Gottesman MM, Pastan I. Regulation of the multidrug resistance gene in regenerating rat liver. *Cell Growth Differ* 1990;1:57-62.

Meng LH, Liao ZY, Pommier Y. Non-camptothecin DNA topoisomerase I inhibitors in cancer therapy. *Curr Top Med Chem* 2003;3:305-20.

Miyake K, Mickley L, Litman T, Zhan Z, Robery R, Cristensen B, Brangi M, Greenberger L, Dean M, Fojo T, Bates SE. Molecular cloning of cDNAs which are highly overexpressed in mitoxantrone-resistant cells: demonstration of homology to ABC transport genes. *Cancer Res* 1999;59:8-13.

Muller M, Meijer C, Zaman GJ, Borst P, Scheper RJ, Mulder NH, de Vries EG, Jansen PL. Overexpression of the gene encoding the multidrug resistance-associated protein results in increased ATP-dependent glutathione S-conjugate transport. *Proc Natl Acad Sci USA* 1994;91:13033-7.

Muller M, Yong M, Peng XH, Petre B, Arora S, Ambudkar SV. Evidence for the role of glycosylation in accessibility of the extracellular domains of human MRP1 (ABCC1). *Biochemistry* 2002;41:10123-32.

Nieves-Neira W, Pommier Y. Apoptotic response to camptothecin and 7-hydroxystaurosporine (UCN-01) in the eight human breast cancer cell lines of the NCI anticancer drug screen: multifactorial relationship with topoisomerase I, protein kinase C, bcl-2 and caspase pathways. *Int J Cancer* 1999;82:396-404.

Nykanen A, Haley B, Zamore PD. ATP requirements and small interfering RNA structure in the RNA interference pathway. *Cell* 2001;107:309-21.

Oberlies NH, Kroll DJ. Camptothecin and taxol: historic achievements in natural products research. *J Nat Prod* 2004;67:129-35.

Ohno K, Hirata M. Characterization of the transport system of prostaglandin A₂ in L-1210 murine leukemia cells. *Biochem Pharmacol* 1993;46:661-7.

Oliva JL, Perez-Sala D, Castrillo A, Martinez N, Canada FJ, Bosca L, Rojas JM. The cyclopentenone 15-deoxy-delta 12,14-prostaglandin J2 binds to and activates H-Ras. *Proc Natl Acad Sci USA* 2003;100:4772-7.

Padilla J, Leung E, Phipps RP. Human B lymphocytes and B lymphomas express PPAR-gamma and are killed by PPAR-gamma agonists. *Clin Immunol* 2002;103:22-33.

Pantazis P, Han Z, Balan K, Wang Y, Wyche JH. Camptothecin and 9-nitro-camptothecin (9NC) as anti-cancer, anti-HIV and cell-differentiation agents. *Anticancer Res* 2003;23:3623-38.

Parker J, Ankel H. Formation of a prostaglandin A2-glutathione conjugate in L1210 mouse leukaemia cells. *Biochem Pharmacol* 1992;43:1053-60.

Paull KD, Shoemaker RH, Hodes L, Monks A, Scudiero DA, Rubinstein L, Plowman J, Boyd MR. Display and analysis of patterns of differential activity of drugs against human tumor cell lines: Development of mean graph and COMPARE algorithm. *J Natl Cancer Inst* 1989;81:1088-92.

Paumi CM, Wright M, Townsend AJ, Morrow CS. Multidrug resistance protein (MRP) 1 and MRP3 attenuate cytotoxic and transactivating effects of the cyclopentenone prostaglandin, 15-deoxy-Delta(12,14)prostaglandin J2 in MCF7 breast cancer cells. *Biochemistry* 2003;42:5429-37.

Pommier Y, Pourquier P, Urasaki Y, Wu J, Laco G. Topoisomerase I inhibitors: selectivity and cellular resistance. *Drug Resistance Update* 1999;2:307-18.

Prescott SM, Fitzpatrick FA. Cyclooxygenase-2 and carcinogenesis. *Biochem Biophys. Acta* 2000;1470:M69-78.

Ramachandra M, Ambudkar SV, Chen D, Hrycyna CA, Dey S, Gottesman MM, Pastan I. Human P-glycoprotein exhibits reduced affinity for substrates during a catalytic transition state. *Biochemistry* 1998;37:5010-9.

Rao VV, Dahlheimer JL, Bardgett ME, Snyder AZ, Finch RA, Sartorelli AC, Piwnicka-Worms D. Choroid plexus epithelial expression of MDR1 P-glycoprotein and multidrug resistance-associated protein contribute to the blood-cerebrospinal-fluid drug-permeability barrier. *Proc Natl Acad Sci USA* 1999;96:3900-5.

Reid G, Wielinga P, Zelcer N, De Haas M, Van Deemter L, Wijnholds J, Balzarini J, Borst P. Characterization of the transport of nucleoside analog drugs by the human multidrug resistance proteins MRP4 and MRP5. *Mol Pharmacol* 2003a;63:1094-103.

Reid G, Wielinga P, Zelcer N, van der Heijden I, Kuil A, de Haas M, Wijnholds J, Borst P. The human multidrug resistance protein MRP4 functions as a prostaglandin efflux transporter and is inhibited by nonsteroidal antiinflammatory drugs. *Proc Natl Acad Sci USA* 2003b;100:9244-9.

Reinhold WC, Kouros-Mehr H, Kohn KW, Maunakea AK, Lababidi S, Roschke A, Stover K, Alexander J, Pantazis P, Miller L, Liu E, Kirsch IR, Urasaki Y, Pommier Y, Weinstein JN. Apoptotic susceptibility of cancer cells selected for

camptothecin resistance: gene expression profiling, functional analysis, and molecular interaction mapping. *Cancer Res* 2003;63:1000-11.

Ricote M, Li AC, Willson TM, Kelly CJ, Glass CK. The peroxisome proliferator-activated receptor-gamma is a negative regulator of macrophage activation. *Nature* 1998;391:79-82.

Rossi A, Kapahi P, Natoli G, Takahashi T, Chen Y, Karin M, Santoro MG. Anti-inflammatory cyclopentenone prostaglandins are direct inhibitors of IKappaB kinase. *Nature* 2000;403:103-8.

Rovin BH, Wilmer WA, Lu L, Doseff AI, Dixon C, Kotur M, Hilbelink T. 15-Deoxy-Delta12,14-prostaglandin J2 regulates mesangial cell proliferation and death. *Kidney Int* 2002;61:1293-302.

Sauna ZE, Ambudkar SV. Characterization of the catalytic cycle of ATP hydrolysis by human P-glycoprotein. The two ATP hydrolysis events in a single catalytic cycle are kinetically similar but affect different functional outcomes. *J Biol Chem* 2001;276:11653-61.

Scheffer GL, Kool M, Heijn M, de Haas M, Pijnenborg AC, Wijnholds J, van Helvoort A, de Jong MC, Hooijberg JH, Mol CA, van der Linden M, de Vree JM, van der Valk P, Elferink RP, Borst P, Scheper RJ. Specific detection of multidrug resistance proteins MRP1, MRP2, MRP3, MRP5, and MDR3 P-glycoprotein with a panel of monoclonal antibodies. *Cancer Res* 2000;60:5269-77.

Schinkel AH, Mayer U, Wagenaar E, Mol CA, van Deemter L, Smit JJ, van der Valk MA, Voordouw AC, Spits H, van Tellingen O, Zijlmans JM, Fibbe WE, Borst P. Normal viability and altered pharmacokinetics in mice lacking mdr1-type (drug-transporting) P-glycoproteins. *Proc Natl Acad Sci USA* 1997;94:4028-33.

Schinkel AH, Wagenaar E, Mol CA, van Deemter L. P-glycoprotein in the blood-brain barrier of mice influences the brain penetration and pharmacological activity of many drugs. *J Clin Invest* 1996;97:2517-24.

Schuetz EG, Beck WT, Schuetz JD. Modulators and substrates of P-glycoprotein and cytochrome P4503A coordinately up-regulate these proteins in human colon carcinoma cells. *Mol Pharmacol* 1996;49:311-8.

Schuster VL. Prostaglandin transport. *Prostaglandins Other Lipid Mediat* 2002;68-69:633-47.

Senior AE, Bhagat S. P-glycoprotein shows strong catalytic cooperativity between the two nucleotide sites. *Biochemistry* 1998;37:831-6.

Shao RG, Cao CX, Zhang H, Kohn KW, Wold MS, Pommier Y. Replication-mediated, DNA damage by camptothecin induces phosphorylation of RPA by DNA-dependent protein kinase and dissociates RPA:DNA-PK complexes. *EMBO J* 1999;18:1397-406.

Shen DW, Goldenberg S, Pastan I, Gottesman MM. Decreased accumulation of [¹⁴C]carboplatin in human cisplatin-resistant cells results from reduced energy-dependent uptake. *J Cell Physiol* 2000;183:108-16.

Shen D, Pastan I, Gottesman MM. Cross-resistance to methotrexate and metals in human cisplatin-resistant cell lines results from a pleiotropic defect in accumulation of these compounds associated with reduced plasma membrane binding proteins. *Cancer Res* 1998;58:268-75.

Shibata T, Kondo M, Osawa T, Shibata N, Kobayashi M, Uchida K. 15-deoxy-delta 12,14-prostaglandin J2. A prostaglandin D2 metabolite generated during inflammatory processes. *J Biol Chem* 2002;227:10459-66.

Shimada T, Kojima Y, Yoshiura K, Hiraishi H, Terano A. Characteristics of the peroxisome proliferator activated receptor gamma (PPARgamma) ligand induced apoptosis in colon cancer cells. *Gut* 2002;50:658-64.

Smit JJ, Schinkel AH, Oude Elferink RP, Groen AK, Wagenaar E, van Deemter L, Mol CA, Ottenhoff R, van der Lugt NM, van Roon MA, *et al.* Homozygous disruption of the murine *mdr2* P-glycoprotein gene leads to a complete absence of phospholipid from bile and to liver disease. *Cell* 1993;75:451-62.

Sparreboom A, van Asperen J, Mayer U, Schinkel AH, Smit JW, Meijer DK, Borst P, Nooijen WJ, Beijnen JH, van Tellingen O. Limited oral bioavailability and active epithelial excretion of paclitaxel (Taxol) caused by P-glycoprotein in the intestine. *Proc Natl Acad Sci USA* 1997;94:2031-5.

Stone KR, Mickey DD, Wunderli H, Mickey GH, Paulson DF. Isolation of a human prostate carcinoma cell line (DU 145). *Int J Cancer* 1978;21:274-81.

St-Pierre MV, Serrano MA, Macias RI, Dubs U, Hoehli M, Lauper U, Meier PJ, Marin JJ. Expression of members of the multidrug resistance protein family in human term placenta. *Am J Physiol Regul Integr Comp Physiol* 2000;279:1495-503.

Straus DS, Glass CK. Cyclopentenone prostaglandins: new insights on biological activities and cellular targets. *Med Res Rev* 2001;21:185-210.

Straus DS, Pascual G, Li M, Welch JS, Ricote M, Hsiang CH, Sengchanthalangsy LL, Ghosh G, Glass CK. 15-deoxy-delta 12,14-prostaglandin J2 inhibits multiple steps in the NF-kappa B signaling pathway. *Proc Natl Acad Sci USA* 2000;97:4844-9.

Strumberg D, Pilon AA, Smith M, Hickey R, Malkas L, Pommier Y. Conversion of topoisomerase I cleavage complexes on the leading strand of ribosomal DNA into 5'-phosphorylated DNA double-strand breaks by replication runoff. *Mol Cell Biol* 2000;20:3977-87.

Synold TW, Dussault I, Forman, BM. The orphan nuclear receptor SXR coordinately regulates drug metabolism and efflux. *Nature Med* 2001;7:584-90.

Szakács G, Annereau JP, Lababidi S, Shankavaram U, Arciello A, Bussey KJ, Reinhold W, Guo Y, Kruh GD, Reimers M, Weinstein JN, Gottesman MM. Predicting drug sensitivity and resistance: profiling ABC transporter genes in cancer cells. *Cancer Cell* 2004a;6:129-37.

Szakács G, Chen GK, Gottesman MM. The molecular mysteries underlying P-glycoprotein-mediated multidrug resistance. *Cancer Biol Ther* 2004b ;3:382-4.

Thorgeirsson SS, Huber BE, Sorrell S, Fojo A, Pastan I, Gottesman MM. Expression of the multidrug-resistance gene in hepatocarcinogenesis and regenerating rat liver. *Science* 1987;236:1120-2.

Thottassery JV, Zambetti, GP, Arimori, K, Schuetz EG, Schuetz JD. p53-dependent regulation of MDR1 gene expression causes selective resistance to chemotherapeutic agents. *Proc Natl Acad Sci USA* 1997;94:11037-42.

Ui-Tei K, Zenno S, Mijata Y, Saigo K. Sensitive assay of RNA interference in *Drosophila* and Chinese hamster cultured cells using firefly luciferase gene as target. *FEBS Lett* 2000;479:79-82.

Urasaki Y, Laco GS, Pourquier P, Takebayashi Y, Kohlhagen G, Gioffre C, Zhang H, Chatterjee D, Pantazis P, Pommier Y. Characterization of a novel topoisomerase I mutation from a camptothecin-resistant human prostate cancer cell line. *Cancer Res* 2001;61:1964-9.

Vane JR. The fight against rheumatism: from willow bark to COX-1 sparing drugs. *J. Physiol. Pharmacol.* 2000;51:573-86.

Velculescu VE, Zhang L, Vogelstein B, Kinzler KW. Serial analysis of gene expression. *Science* 1995;270:484-7.

Vulevic B, Chen Z, Boyd JT, Davis W Jr, Walsh ES, Belinsky MG, Tew KD. Cloning and characterization of human adenosine 5'-triphosphate-binding cassette, sub-family A, transporter 2 (ABCA2). *Cancer Res* 2001;61:3339-47.

Warner TD, Mitchell JA. Cyclooxygenase-3 (COX-3): filling in the gaps toward a COX continuum? *Proc. Natl. Acad. Sci. USA* 2002;99:13371-3.

Weinstein JN, Kohn KW, Grever MR, Viswanadhan VN, Rubinstein LV, Monks AP, Scudiero DA, Welch L, Koutsoukos AD, Chiousa AJ, *et al.* Neural computing in cancer drug development: Predicting mechanism of action. *Science* 1992;258:447-51.

Weinsten JN, Myers TG, O'Connor PM, Friend SH, Fornace AJ Jr, Kohn KW, Fojo T, Bates SE, Rubinstein LV, Anderson NL, *et al.* An information-intensive approach to the molecular pharmacology of cancer. *Science* 1997;275:343-9.

Wijnholds J, Evers R, van Leusden MR, Mol CA, Zaman GJ, Mayer U, Beijnen JH, van der Valk M, Krimpenfort P, Borst P. Increased sensitivity to anticancer drugs and decreased inflammatory response in mice lacking the multidrug resistance-associated protein. *Nat Med* 1997;3:1275-9.

Wu H, Hait WN, Yang JM. Small interfering RNA-induced suppression of MDR1 (P-glycoprotein) restores sensitivity to multidrug-resistant cancer cells. *Cancer Res* 2003;63:1515-19.

Xie R, Hammarlund-Udenaes M, de Boer AG, de Lange EC. The role of P-glycoprotein in blood-brain barrier transport of morphine: transcortical

microdialysis studies in Mdr1a (^{-/-}) and Mdr1a (^{+/+}) mice. *Br J Pharmacol* 1999;128:563-8.

Yamazaki R, Kusunoki N, Matsuzaki T, Hashimoto S, Kawai S. Nonsteroidal anti-inflammatory drugs induce apoptosis in association with activation of peroxisome proliferator-activated receptor gamma in rheumatoid synovial cells. *J Pharmacol Exp Ther* 2002;302:18-25.

Zastawny RL, Salvino R, Chen J, Benchimol S, Ling V. The core promoter region of the P-glycoprotein gene is sufficient to confer differential responsiveness to wild-type and mutant p53. *Oncogene* 1993;8:1529-35.

Zhou Y, Gottesman MM, Pastan I. Studies of human MDR1-MDR2 chimeras demonstrate the functional exchangeability of a major transmembrane segment of the multidrug transporter and phosphatidylcholine flippase. *Mol Cell Biol* 1999;19:1450-9.

ACKNOWLEDGEMENTS

I thank Dr Renata Piccoli, my supervisor. She was really precious for me in every moment. She was always ready to give me advice, and she always supported me, even during my stage at the NIH.

I am really grateful to Dr Michael Gottesman for the opportunity he gave me to spend fifteen months in the Laboratory of Cell Biology. It was a great experience, which I will never forget in my life. I thank Dr Gottesman for his kindness, his constant support, and his valuable comments and suggestions.

I thank Dr Giancarlo Vecchio, coordinator of the Doctorate, for his kindness and valuable support.

I am grateful to Dr Giuseppe D'Alessio for his constant support and the opportunity he gave me to work on a very interesting project.

I thank Dr Claudia De Lorenzo. She was not only a good colleague, but first of all a precious friend. To work with her was really great and I learned a lot from her enthusiasm.

I thank Dr Jean-Philippe Annereau and Dr Gergely Szakács. Their help, advice and support were essential during my stage at the NIH.

I thank all my colleagues of the Laboratory of Cell Biology for their kindness and support.

I thank Dr Bensi Thea. Her friendship let me feel at home during my stage in the USA.

I thank Dr Sonia Di Gaetano, Dr Pasquale Buonanno and Dr Fulvio Guglielmi for their kindness and support during the last months.

Finally, but not at the end of the list, I thank Dr Elio Pizzo, a precious colleague, and my future husband. He waited for me and supported me in every moment during these years.

LIST OF PUBLICATIONS

- 1) Spalletti-Cernia D, Sorrentino R, Di Gaetano S, Arciello A, Garbi C, Piccoli R, D'Alessio G, Vecchio G, Laccetti P, Santoro M. Antineoplastic ribonucleases selectively kill thyroid carcinoma cells via caspase-mediated induction of apoptosis. *J Clin Endocrinol Metab.* 2003;88:2900-7.
- 2) De Lorenzo C, Arciello A, Cozzolino R, Palmer DB, Laccetti P, Piccoli R, D'Alessio G. A fully human antitumor immunoRNase selective for ErbB-2-positive carcinomas. *Cancer Res.* 2004;64:4870-4.
- 3) Szakács G, Annereau JP, Lababidi S, Shankavaram U, Arciello A, Bussey KJ, Reinhold W, Guo Y, Kruh GD, Reimers M, Weinstein JN, Gottesman MM. Predicting drug sensitivity and resistance: profiling ABC transporter genes in cancer cells. *Cancer Cell.* 2004;6:129-37.
- 4) Annereau JP, Szakács G, Tucker CJ, Arciello A, Cardarelli C, Collins J, Grissom S, Zeeberg B, Reinhold W, Weinstein J, Pommier Y, Paules RS, Gottesman MM. Analysis of ABC transporter expression in drug-selected cell lines by a microarray dedicated to multidrug resistance. *Mol Pharmacol.* 2004.[Epub ahead of print]

Antineoplastic Ribonucleases Selectively Kill Thyroid Carcinoma Cells Via Caspase-Mediated Induction of Apoptosis

DANIELA SPALLETTI-CERNIA, ROSANNA SORRENTINO, SONIA DI GAETANO, ANGELA ARCIELLO, CORRADO GARBI, RENATA PICCOLI, GIUSEPPE D'ALESSIO, GIANCARLO VECCHIO, PAOLO LACCETTI, AND MASSIMO SANTORO

Istituto di Endocrinologia ed Oncologia Sperimentale del Consiglio Nazionale delle Ricerche (CNR), Dipartimento di Biologia e Patologia Cellulare e Molecolare, Università di Napoli Federico II (D.S.-C., R.S., C.G., G.V., M.S.), 80131 Naples, Italy; Dipartimento di Chimica Biologica, Università di Napoli Federico II (S.D.G., A.A., R.P., G.D., P.L.), 80134 Naples, Italy; and Istituto di Biostrutture e Bioimmagini-CNR (S.D.G.), 80134 Naples, Italy

Bovine seminal ribonuclease (BS-RNase), a natural dimeric homolog of bovine pancreatic RNase (RNase A), and HHP2-RNase, an engineered dimeric form of human pancreatic RNase (HP-RNase), are endowed with powerful antitumor effects. Here we show that BS- and HHP2-RNases, but not monomeric RNase A, induce apoptosis of human thyroid carcinoma cell lines. RNase-induced apoptosis was associated with activation of initiation caspase-8 and -9. This was followed by activation of executioner caspase-3, leading to the proteolytic cleavage of poly(ADP-ribose) polymerase. The caspase inhibitor Z-Val-Ala-Asp-(OMe)-fluoromethylketone protected

thyroid cancer cells from BS-RNase-induced apoptosis. RNase-triggered apoptosis and caspase activation were accompanied by reduced phosphorylation of Akt/protein kinase B (PKB), a serine-threonine kinase that when phosphorylated is able to deliver survival signals to cancer cells. BS-RNase antitumor effects in nude mice were accompanied by caspase activation and apoptosis. Because of the high selectivity of apoptotic effects for malignant cells, BS- and HHP2-RNase are promising tools for the treatment of aggressive thyroid cancer. (*J Clin Endocrinol Metab* 88: 2900–2907, 2003)

APPROXIMATELY 20,000 NEW cases of thyroid carcinoma are diagnosed each year in the United States, and 1,300 patients die of the disease. The biological behavior of thyroid carcinoma varies from indolent microcarcinomas to poorly differentiated carcinoma, which is associated with significant morbidity and mortality, and anaplastic carcinoma, one of the most aggressive human malignancies. At diagnosis, most anaplastic carcinoma patients have distant metastases, primarily in lung, bone, and liver. Doxorubicin, alone or combined with cisplatin, is the most widely used therapeutic agent, but it does not improve survival in anaplastic carcinoma patients (1, 2). Thus, although radioactive iodine is beneficial in cases of differentiated tumors, more effective chemotherapeutic agents are needed for aggressive thyroid cancers.

Bovine seminal ribonuclease (BS-RNase) from bull semen and Onconase (Onconase is a registered trademark of Alfacell, Inc., Bloomfield, NJ) from frog eggs (*Rana pipiens*) are selectively toxic for cancer cells (3). BS-RNase, the only dimeric RNase in the vertebrate superfamily (for a review, see Ref. 4), is not toxic for normal cells grown *in vitro*, nor does it exert appreciable toxic effects when administered *in vivo* to experimental animals (5), whereas it is very cytotoxic

for a number of tumor cells of different origins (3). BS-RNase exerts remarkable antitumor effects in syngeneic and xenotransplant models (6), and antimetastatic activity (5). Onconase is currently being tested in phase II clinical trials (7). Conjugation of ribonucleases with polymers or antibodies results in increased stability and specificity. Onconase linked to a monoclonal antibody (anti-CD22) is a potent immunotoxin against B cell lymphoma (8).

The binding of BS-RNase to a component of the extracellular matrix (9, 10) or of Onconase to an unidentified cell surface receptor (11) is followed by endocytosis, translocation to the cytosol, degradation of RNA (rRNA or tRNA by BS-RNase and Onconase, respectively), and suppression of protein synthesis. The cytosolic ribonuclease inhibitor (cRI) tightly binds to internalized RNases, blocking their cytotoxic activity. Thus, only RNases that can evade cRI are capable of exerting a cytotoxic action (11–15). The resistance of BS-RNase to cRI inhibition depends on the dimeric structure of the enzyme (12, 13, 15). On the other hand, Onconase, the frog RNase, is inhibited by frog, but not mammalian, cRI.

We recently transformed human pancreatic RNase (HP-RNase), a monomeric noncytotoxic RNase, into a dimeric RNase (designated HHP-RNase). This was achieved by replacing four of its amino acid residues (Q28, K31, K32, and N34) with the corresponding residues (L28, C31, C32, and K34) from BS-RNase. HHP-RNase was selectively cytotoxic for malignant cell lines (16). A second generation dimeric mutant of HP-RNase, designated HHP2-RNase, obtained by introducing another mutation (E111G), was more cytotoxic

Abbreviations: BS-, Bovine seminal; cRI, cytosolic ribonuclease inhibitor; fmk, fluoromethylketone; HDF, human diploid fibroblasts; HP-, human pancreatic; PARP, poly(ADP-ribose) polymerase; PI3K, phosphoinositide 3-kinase; pNA, *p*-nitroanilide; RNase, ribonuclease; zVADfmk, Z-Val-Ala-Asp-(OMe)-fluoromethylketone; Akt/PKB, protein kinase B.

than HHP-RNase (17). Given their human origin, HP-RNase dimeric variants are very promising anticancer agents because their effects are less likely to be curtailed by the host immune response.

Onconase and RC-RNase (a cytotoxic ribonuclease from *Rana catesbeiana*) promote apoptosis of HeLa (18) and MCF-7 breast cancer cells (19), respectively, and BS-RNase induces apoptosis of human neuroblastoma (20) and thyroid tumor cells (16, 21, 22). Two major apoptotic pathways, triggered by mitochondria and cell surface receptors, respectively, have been identified. The mitochondrial pathway is involved in the apoptotic response to DNA-damaging agents, for example, conventional cancer chemotherapeutics and radiation (for a review, see Ref. 23). Caspases, aspartate-specific cysteine proteases, are key effectors of apoptosis (for a review, see Ref. 24). The initiation caspase of mitochondria-driven apoptosis is caspase-9; the initiation caspase of the cell surface-triggered apoptosis is caspase-8. In turn, caspase-8 and -9 directly activate executioner caspase-3 (for a review, see Ref. 24).

We have studied BS-RNase- and HHP2-RNase-induced apoptosis in four thyroid carcinoma cell lines. Our results demonstrate that the two RNases kill thyroid carcinoma cells by engaging both the mitochondrial and the cell surface-initiated apoptotic machinery and suggest that Akt/protein kinase B (PKB) is a target of apoptotic RNase cell signaling.

Materials and Methods

RNases

BS-RNase was purified from bovine seminal vesicles as reported previously (25). HHP2-RNase was generated and purified as previously described (17). RNase A was purchased from Sigma-Aldrich Corp. (St. Louis, MO).

Cell lines

NPA and ARO cells (26), a gift from J. A. Fagin, derive from human papillary and anaplastic thyroid carcinomas, respectively. CAL62 (27), a gift from J. Giovanni, and KAT4 (28), a gift from K. B. Ain, were established from human thyroid anaplastic carcinomas. All of these cell lines are tumorigenic when injected into nude mice (26–28). HDF are normal human diploid fibroblasts, and they were gifts from P. Dotto and C. Missero. All cell lines were grown in DMEM supplemented with 10% fetal calf serum (Life Technologies, Inc., Paisley, PA), penicillin (50 U/ml), and streptomycin (50 µg/ml; Sigma-Aldrich Corp.).

Analysis of apoptosis

For fluorescence microscopy analysis, 10^4 cells were plated on coverglasses in 24-well plates. Twenty-four hours after plating, RNases were added to a final concentration of 1.8 µM. Seventy-two hours later, adherent cells and those present in the medium were fixed for 20 min in 3.7% formaldehyde, washed in PBS, permeabilized for 5 min in 0.1% Triton X-100, and stained for 30 min with Hoechst 33258 (Sigma-Aldrich Corp.) at a concentration of 0.5 µg/ml in PBS. The stained cells were observed under an epifluorescent microscope (Axiovert 2, Carl Zeiss, New York, NY) interfaced with the image analyzer software KS300 (Carl Zeiss), and photographed.

For a time-dependent analysis of apoptotic DNA fragmentation, cells were plated in 96-well plates (1×10^3 /well in 100 µl medium). After 24 h, each RNase was added to the culture medium (to a final concentration of 1.8 µM) for times ranging from 15 min to 72 h. Apoptosis was measured in quadruplicate samples using the Cell Death Detection ELISA Plus kit (Roche, Mannheim, Germany). This photometric sandwich enzyme immunoassay determines cytoplasmic histone-associated DNA fragments (mono- and oligonucleosomes) upon induction of cell death.

Briefly, a mixture of biotin-labeled antihistone and peroxidase-conjugated anti-DNA antibodies was added to the cell lysates and placed in a streptavidin-coated microtiter plate. During incubation, the antihistone antibody binds to the histone component of the apoptotic nucleosomes and simultaneously captures the immunocomplex to the streptavidin-coated plates via its biotinylation. Meanwhile, the anti-DNA antibody reacts with the DNA component of the nucleosomes. The amount of nucleosomes was determined spectrophotometrically at 405 nm with 2,2'-azino-bis(3-ethylbenzthiazoline-6-sulfonic acid) as a substrate of peroxidase (Microplate reader, Bio-Rad Laboratories, Inc., Munich, Germany).

Determination of caspase activation

Cells were treated with RNases for various times. At the end of each treatment, caspases-3, -8, and -9 activities were tested with colorimetric protease assay kits (Alexis Biochemicals, San Diego, CA), in which the chromophore *p*-nitroanilide (pNA) is detected spectrophotometrically (at 400 or 405 nm) after cleavage from the labeled substrate. The caspase-3/ CPP32, the Flice/caspase-8, and the caspase-9/Mch6 kits assay the activity of caspase-3, which recognizes the Asp-Glu-Val-Asp (DEVD) sequence; the activity of caspase-8, which recognizes the Ile-Glu-Thr-Asp (IETD) sequence; and the activity of caspase-9, which recognizes the Leu-Glu-His-Asp (LEHD) sequence, respectively. The increase in caspase activity was determined by comparing the absorbance of pNA from a treated sample *vs.* an untreated control. The results from three independent experiments were averaged for each time point.

Caspase inhibitors

Caspase inhibitors (Alexis Biochemicals, San Diego, CA) irreversibly bind to the caspase active sites because the peptide recognition sequence is linked to a fluoromethylketone (fmk). To increase cell permeability, their aspartic acid residues are esterified with methyl groups. Z-Val-Ala-Asp-(OMe)-fluoromethylketone (zVADfmk; 50 µM; added every 24 h) was used as a general upstream caspase inhibitor for the *in vivo* DNA fragmentation assay. Z-Ile-Glu-Thr-Asp(OMe)-fluoromethylketone, Z-Leu-Glu(OMe)-His-Asp(OMe)-fluoromethylketone, and Z-Asp(OMe)-Glu(OMe)-Val-Asp(OMe)-fluoromethylketone (to a final concentration of 10 µM) were used as caspase-8, -9, and -3 selective inhibitors, respectively.

Immunoblot

Protein lysates (100 µg) were electrophoresed through 7.5% sodium dodecyl sulfate-polyacrylamide gel, transferred to Immobilon membranes (Bio-Rad Laboratories, Inc.), and analyzed by immunoblot. Antipoly-(ADP-ribose) polymerase (anti-PARP) antibodies (1:2000) were purchased from Roche Molecular Biochemicals. Anti-Akt and antiphospho-Akt (Ser⁴⁷³), specific for the active Akt phosphorylated at serine 473, antibodies were obtained from Cell Signaling (Beverly, MA). Immunoreactive bands were visualized using the enhanced chemiluminescence detection reagents (Amersham Pharmacia Biotech, Arlington Heights, IL) according to the manufacturer's protocol.

Tumorigenicity in nude mice

ARO cells (2×10^6 /mouse) were inoculated sc into the right dorsal portion of 6-wk-old male BALB/c *ν/ν* mice (The Jackson Laboratory, Bar Harbor, ME). BS-RNase (20 µg/g body weight) or vehicle (PBS) was injected in the peritumor area starting 1 d after cell implantation for a total of six injections (at 72-h intervals). Tumors were harvested 14 d after cell implantation and weighed. Apoptotic rate and caspase-9 and -3 activity were measured as described above. No mouse showed signs of wasting or other signs of toxicity. Animals were maintained at the Dipartimento di Biologia e Patologia Cellulare e Molecolare Animal Facility. All manipulations were performed under isoflurane gas anesthesia and were conducted in accordance with Italian regulations for experimentation on animals.

Statistical analysis

A *t* test was used to evaluate the statistical significance of the results. Analyses were performed with the BMDP New System statistical pack-

age version 1.0 for Microsoft Corp. Windows (BMDP Statistical Software, Los Angeles, CA).

Results

BS-RNase and HHP2-RNase induce apoptosis of thyroid carcinoma cells

We previously demonstrated that dimeric RNases (16) are very cytotoxic for NPA, a highly tumorigenic human thyroid carcinoma cell line. To identify the mode of thyroid cell death, we treated NPA cells and HDF with BS-RNase and HHP2-RNase. Noncytotoxic RNase A and HP-RNase were used as controls. After treatment (1.8 μ M for 72 h), cells were examined for the presence of apoptotic nuclear bodies by fluorescence microscopy after Hoechst 33258 staining. Cells were cytopun to analyze both adherent and detached cells; the experiments were performed in triplicate; at least 200 cells were counted for each assay. BS-RNase and HHP2-RNase treatment caused relevant apoptosis of NPA cells (25–30 \pm 5%); apoptotic cells showed typical condensed chromatin and apoptotic bodies (Fig. 1A). In contrast, apoptosis was not detected (<2%) with RNase A (Fig. 1A) or HP-RNase (not shown). More importantly, apoptosis was not detected (<5%) in HDF cells treated with BS-RNase or HHP2-RNase (data not shown and see below).

PARP cleavage, a sensitive marker of caspase-mediated apoptosis, resulted in the disappearance of the 116-kDa full-size PARP band (p116PARP) monitored by Western blot. p116PARP levels decreased in NPA cells after 24 h of BS-RNase treatment (Fig. 1B); after 72 h, most of the full-size PARP had disappeared. Differently, BS-RNase treatment did not affect the amount of p116PARP in HDF cells (Fig. 1B).

We used an ELISA-based assay to quantitate apoptosis. As shown in Fig. 1C, apoptotic nucleosomes were detected after treatment of NPA cells with both cytotoxic ribonucleases; the greatest effects occurred at 24 h (BS-RNase) and 48 h (HHP2-RNase). As expected, apoptotic nucleosomes were not detected in HDF cells (Fig. 1C). To determine whether these findings also applied to other thyroid carcinoma cell lines, we measured apoptosis in highly tumorigenic anaplastic ARO, CAL62, and KAT4 cells after treatment for various times. These anaplastic cell lines were even more sensitive than NPA cells to the proapoptotic effects of HHP2-RNase (Fig. 2) and BS-RNase (not shown).

BS-RNase and HHP2-RNase trigger caspase cascades in thyroid cancer cells

To assess the role of caspases in RNase-induced apoptosis, we analyzed the kinetics of caspase activation in the four

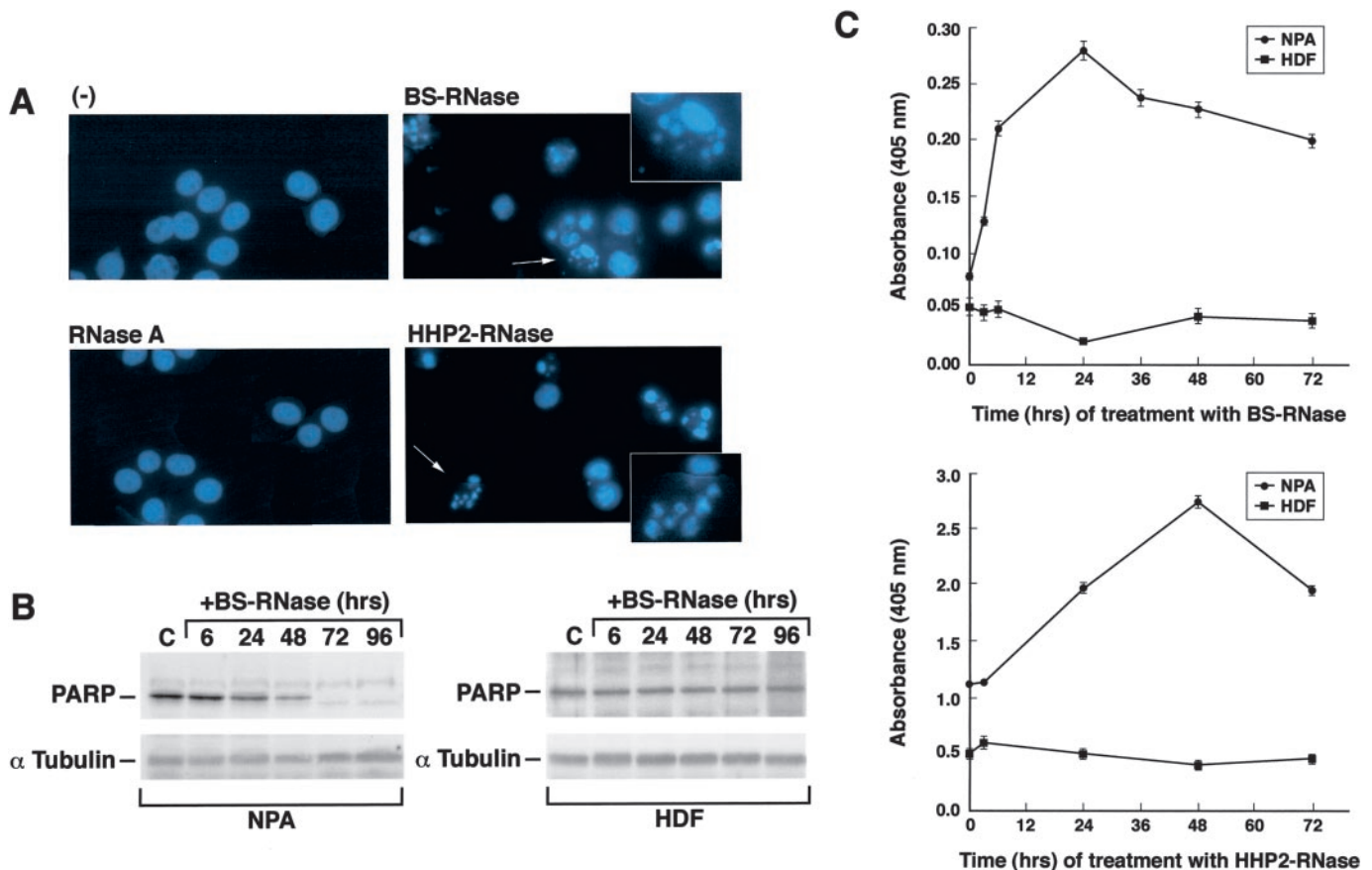


FIG. 1. NPA cell apoptosis induced by cytotoxic RNases. A, NPA cells were exposed for 72 h to the indicated RNases or were left untreated (–). Cells were fixed and stained with Hoechst 33258 to reveal nuclear signs of apoptosis and photographed ($\times 360$). Insets, Apoptotic nuclei ($\times 2400$). B, NPA and HDF cells were treated with BS-RNase for the indicated times. Protein lysates were immunoblotted with anti-PARP and antitubulin for normalization. C, NPA and HDF cells were treated with the indicated RNases for times ranging from 15 min to 72 h. At the end of each treatment, DNA fragmentation was measured with the Cell Death Detection ELISA Plus kit. Values are the mean \pm SD of quadruplicate determinations of three independent experiments.

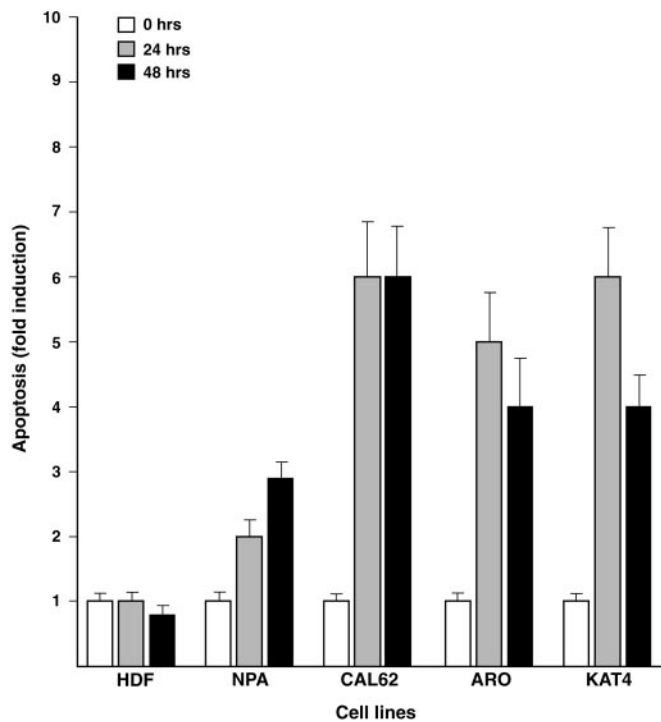


FIG. 2. DNA fragmentation of thyroid carcinoma cells treated with HHP2-RNase. The various cell lines were treated with HHP2-RNase for 0, 24, or 48 h. At the end of each treatment, DNA fragmentation was measured with the Cell Death Detection ELISA Plus kit. Values are expressed as the fold increase in apoptosis and are the mean \pm SD of quadruplicate determinations of three independent experiments.

thyroid cancer cell lines using substrates specific for caspase-8, -9, and -3. In these assays the spectrophotometric detection of pNA chromophore, cleaved from the specific synthetic substrate, is a measure of caspase activity. Selective inhibitors of the three caspases served as a control of specificity. Caspase-8 activity increased significantly at 5 min and peaked at 30 min in NPA cells treated with BS-RNase (Fig. 3A). Its activity slowly declined thereafter, but was still significantly enhanced at 48 h. Similar kinetics were observed in HHP2-RNase-treated NPA cells (Fig. 3A). The extent of caspase-8 activation in the three anaplastic cell lines was, on the average, even greater than that in NPA cells (Fig. 3A). Caspase-9 activity began to increase at 6 h and peaked at 24 h in BS-RNase-treated NPA cells, whereas it peaked at 3–6 h after treatment with HHP2-RNase in all four cancer cell lines (Fig. 3B). Consistent with its downstream role, caspase-3 activity started to increase later than caspase-8 and -9 activities, with a peak at 24–48 h depending on the RNase tested and on the cell line (Fig. 3C). There was no caspase activation in HDF cells treated with either BS-RNase or HHP2-RNase. No apoptosis was detected in cells treated with RNase A.

A general caspase inhibitor protects thyroid cancer cells from BS-RNase-induced cell death

If RNase-induced apoptosis is a caspase-dependent process, DNA fragmentation should be partially or fully prevented in cells cotreated with RNases and caspase inhibitors.

To address this question, we cotreated NPA cells with BS-RNase and zVADfmk (to a final concentration of 50 μ M), a general upstream inhibitor of caspases. The inhibitor was replenished daily when the treatment exceeded 24 h. zVADfmk significantly decreased RNase-induced DNA fragmentation (Fig. 4). Similarly, HHP2-RNase-induced apoptosis of CAL62 cells was significantly decreased by zVADfmk treatment (not shown). However, apoptosis was reduced, but not abrogated, upon caspase inhibition.

Cytotoxic RNases decrease Akt/PKB phosphorylation

The serine/threonine protein kinase Akt/PKB (hereafter Akt) has emerged as a key factor in tumorigenesis (29). Akt is a downstream effector of phosphoinositide 3-kinase (PI3K). Amplification of PI3K and Akt family genes, loss of function mutations of the *PTEN* phosphatase (which negatively regulates the PI3K/Akt pathway), and gain of function mutations of upstream activators of Akt (*e.g.* oncogenic *ras* and receptor tyrosine kinases) are frequent features of human cancer, including thyroid carcinomas (30–32). Akt affects such important cancer cell functions as growth and survival. In particular, by phosphorylating Bad and caspase-9, Akt obstructs caspase activation and protects cancer cells from apoptosis (29). We examined Akt activation by immunoblot with antibodies specific for the activated form of Akt phosphorylated at serine 473 in NPA and Cal62 thyroid cancer cells treated with HHP2-RNase. RNase treatment caused a slow, but significant, decrease in Akt activation levels; at 24 h of treatment, Akt phosphorylation was approximately 3-fold lower than that in untreated cells, as measured by phosphorimaging (Fig. 5).

In vivo BS-RNase antitumor effects are associated with induction of apoptosis

We determined whether the proapoptotic effects of RNases could be detected *in vivo* in mice bearing tumors induced by thyroid neoplastic cells. Nude mice were inoculated with 2×10^6 ARO cells sc. Starting 24 h after cells injection, five mice were treated with six injections (at 72-h intervals) of BS-RNase (20 μ g/g body weight) in the peritumoral area. Another group of five control mice was treated with PBS. Consistent with *in vitro* cytotoxic effects of BS-RNase, the average tumor weight of RNase-treated animals was 0.06 ± 0.01 g, whereas untreated tumors reached 0.4 ± 0.02 g 14 d after cell injection. Tumor tissues were harvested, and apoptotic rate and caspase activation were measured as described above. As shown in Fig. 6, apoptosis was significantly ($P = 0.02$) increased (>8-fold) in tumors treated with BS-RNase compared with vehicle-treated tumors. Moreover, the activity of downstream caspase-9 and -3 increased significantly ($P = 0.02$ and $P = 0.009$, respectively) in tumors treated with BS-RNase.

Discussion

Cytotoxic RNases are a nonmutagenic alternative to conventional DNA-damaging cancer therapy. We show that BS-RNase and HHP2-RNase readily kill thyroid carcinoma cells by apoptosis. No apoptosis was observed

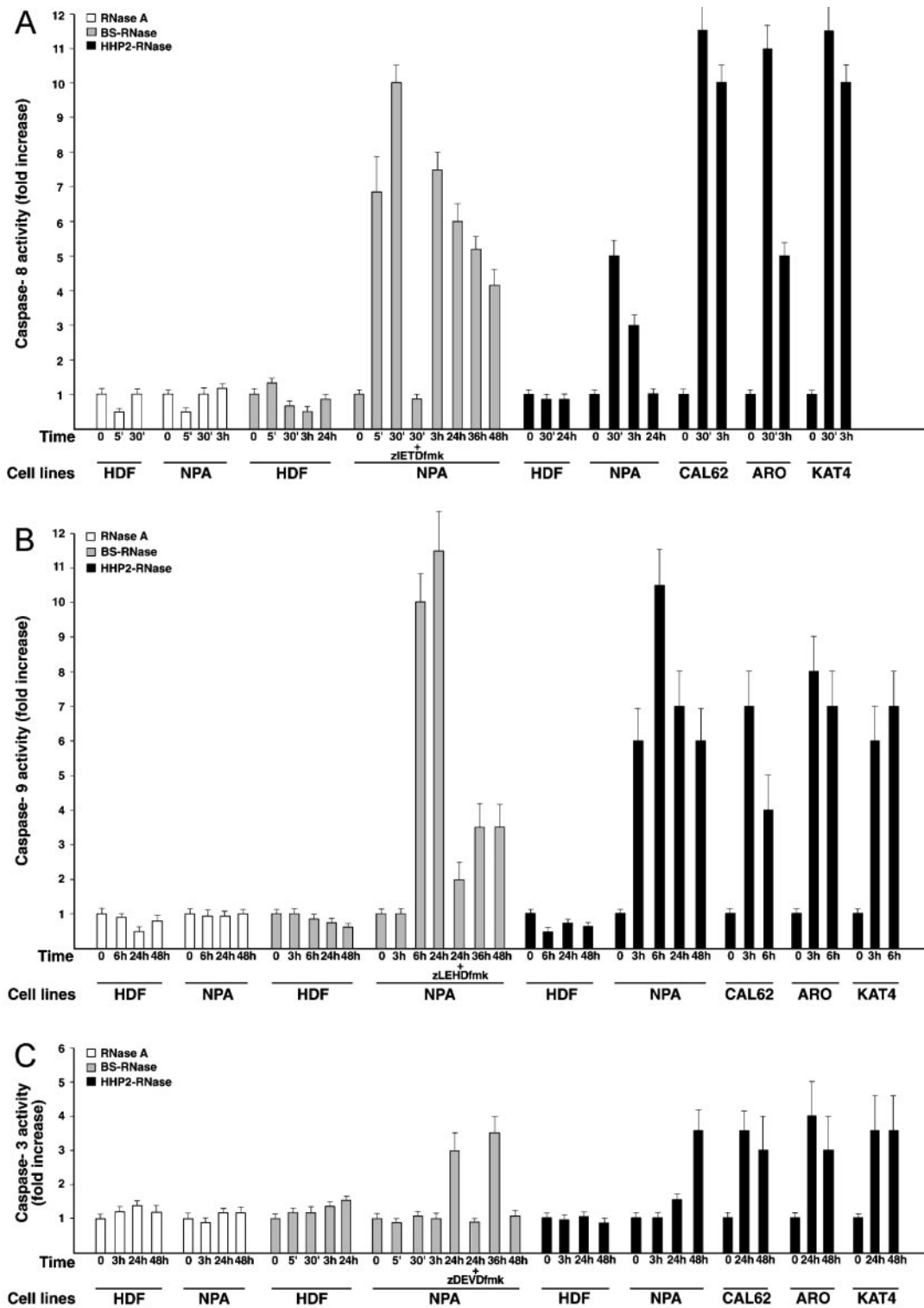


FIG. 3. Caspase activation. Time course of caspase-8 (A), caspase-9 (B), and caspase-3 (C) substrate hydrolysis in cells exposed to RNases. Caspase activity was also measured in the presence of the caspase-8 inhibitor Z-Ile-Glu-Thr-Asp(OMe)-fluoromethylketone (zIETDfmk), the caspase-9 inhibitor Z-Leu-Glu(OMe)-His-Asp(OMe)-fluoromethylketone (zLEHDfmk), or the caspase-3 inhibitor Z-Asp(OMe)-Glu(OMe)-Val-Asp(OMe)-fluoromethylketone (zDEVDfmk) to prove specificity. Each point represents the mean \pm SD of three determinations from three independent experiments.

when the same cells were treated with monomeric RNases. Furthermore, no apoptosis was observed upon RNase treatment of normal human diploid fibroblasts, which con-

firms the selectivity of cytotoxic RNases for malignant cells. Importantly, induction of apoptosis was also observed when tumors induced by thyroid carcinoma cells in

nude mice were treated *in vivo* with BS-RNase. The thyroid carcinoma cell lines studied lack functional p53 (26, 33) (Spalletti-Cernia, D., unpublished observations) and are thus resistant to chemotherapeutic drugs such as doxorubicin. Consequently, by inducing cell death regardless

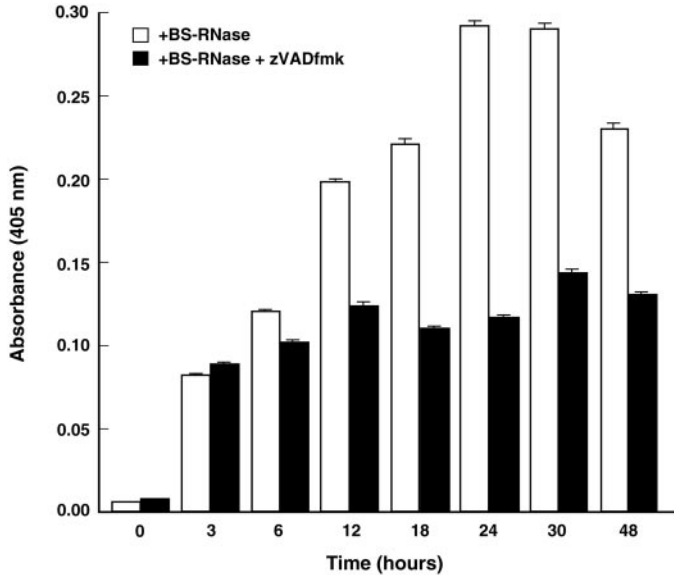


FIG. 4. BS-RNase-mediated NPA cell apoptosis depends on caspase activation. Cells growing in 96-well plates were either untreated (time zero) or treated with BS-RNase for different times without (□) or with (■) zVADfmk. Apoptosis was measured as the mean ± SD of quadruplicate determinations of three independent experiments with the Cell Death Detection ELISA Plus kit.

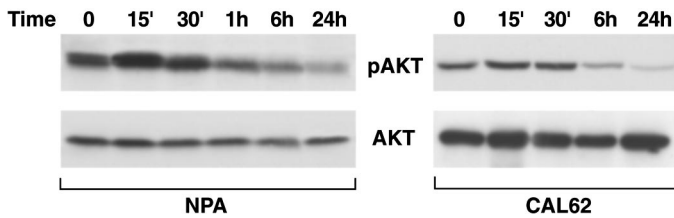


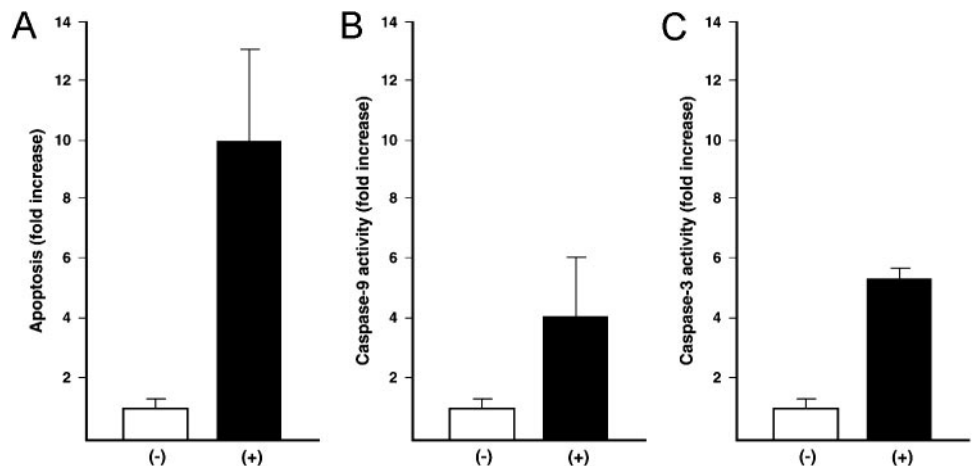
FIG. 5. RNase-mediated apoptosis is accompanied by reduced Akt phosphorylation. NPA and CAL62 cells were treated with HHP2-RNase for the indicated times. Protein lysates were immunoblotted with antiphospho-Akt (pAKT) and anti-Akt for normalization.

of p53 status, cytotoxic RNases have an advantage over current therapeutic protocols for advanced human thyroid carcinomas that frequently carry inactivated p53 (26).

Both BS-RNase and HHP2-RNase induced robust caspase activation in the carcinoma cells. RNase-mediated apoptosis was dependent on caspase activation, and cell treatment with zVADfmk significantly reduced DNA fragmentation. However, the constant presence of apoptotic cells despite zVADfmk probably indicates that other pathways, in addition to caspase activation, transduce the apoptotic signals of RNases. The kinetics of caspase activation after RNase treatment of thyroid cancer cells are consistent with a model in which caspase-8 activation is an upstream event, followed by activation of caspase-9 and then caspase-3. Caspase-8 mediates cytochrome *c* release from mitochondria by activating Bid (a proapoptotic Bcl-2 family member) that, in turn, triggers caspase-9 activation (34). Alternatively, caspase-9 may be activated independently of caspase-8. Whatever the case, the capability of BS- and HHP2-RNases of inducing two distinct caspase cascades probably accounts for their pronounced proapoptotic effect and may hinder the development of resistance of cancer cells.

Caspase-8 is typically activated by the engagement of cell surface proteins of the TNF receptor superfamily, such as Fas. Neoplastic thyroid cells are killed by caspase-8, whereas they are resistant to FasL (35). This is probably due to short-lived protein inhibitor(s) acting upstream from caspase-8, because treatment with protein synthesis inhibitors rescues sensitivity to Fas ligand (35). We did not detect Fas or Fas ligand overexpression after cell treatment with RNases (not shown). However, it is feasible that cytotoxic RNases act downstream from Fas in neoplastic thyroid cells by blocking the synthesis of the putative caspase-8 inhibitor(s). Our results differ from those of Iordanov and colleagues (19), who found activation of caspase-9, -3, and -7, but not of caspase-8, upon treatment of HeLa cells with Onconase. These discrepancies may be due to the different phenotypes of the cell lines and the different RNases used. The mode of RNase delivery may also determine which caspase cascades are activated. Indeed, although we simply added RNase to the culture medium, exploiting the natural capability of cancer cells to internalize cytotoxic RNases, Iordanov and colleagues (19)

FIG. 6. *In vivo* induction of apoptosis by BS-RNase. Nude mice were inoculated with 2×10^6 ARO cells sc and treated with six injections of BS-RNase or PBS as a control. Tumor tissues from RNase-treated (+) and PBS-treated (-) mice were harvested, and triplicate determinations of apoptotic rate with the Cell Death Detection ELISA Plus kit (A) and caspase-9 (B) and -3 (C) activation were performed. The mean ± SD are shown.



used lipofectin-mediated delivery of Onconase. Lipofectin treatment is very efficient because it skips one of the rate-limiting steps in RNase action, *i.e.* transport across the cell membrane. However, it might have perturbed the normal engagement of the RNase with the cell surface, thus modifying the caspase response.

The very rapid caspase-8 activation in thyroid cancer cells (starting as early as 5 min post-RNase and peaking at 30 min) suggests that either the cellular routing (membrane binding-endocytosis-cytosolic penetration-RNA hydrolysis-translation inhibition) of RNases is very rapid, or that RNases trigger intracellular signaling events soon after being engaged at the cell surface.

Cellular RNA degradation is probably a key step in the process of RNase-mediated cell death. Although the inhibition of protein synthesis *per se* could lead to apoptosis, evidence suggests that RNase-induced cell death does not entirely result from the inhibition of protein synthesis. Indeed, inhibitors of protein synthesis, such as cycloheximide, require much higher levels of translational inhibition, and they do so with slower kinetics compared with RNases. Thus, it is likely that apoptosis results not only from protein synthesis inhibition, but also from cell signaling events such as c-Jun N-terminal kinase activation (36) or Akt dephosphorylation (this paper). The therapeutic specificity of RNases remains enigmatic. Endocytosis or cellular routing rates of RNases may differ between malignant and nonmalignant cells. Alternatively, malignant cells might be more sensitive than normal cells to the toxic effects of RNA hydrolysis. Whatever the case, we show that there is a major difference between malignant and normal cells upstream from the cellular events leading to apical caspases (-8 and -9) activation. In addition, our data suggest that the down-modulation of Akt is at least one of the mechanisms leading to thyroid cell death.

Because they obstruct Akt, which is frequently activated in thyroid cancer, and because they kill thyroid cancer cells regardless of p53 status, BS-RNase and HHP2-RNase are promising novel chemotherapeutic agents for aggressive thyroid cancers.

Acknowledgments

We are grateful to Jean Ann Gilder (Scientific Communication) for editing the text. We thank Paola Ferraro and Salvatore Sequino for animal manipulations and animal care.

Received March 11, 2002. Accepted February 28, 2003.

Address all correspondence and requests for reprints to: Dr. Massimo Santoro, Istituto di Endocrinologia ed Oncologia Sperimentale del CNR, Via S. Pansini 5, 80131 Naples, Italy. E-mail: masantor@unina.it.

This work was supported by the Associazione Italiana per la Ricerca sul Cancro; the Italian Ministry of Instruction, University, and Research; the Italian Ministry of Health; and a fellowship from the European Community-European Social Fund-FSE (to D.S.C.).

D.S.-C. and R.S. are recipients of a fellowship from the BioGeM scar.l. (Biotecnologia e Genetica Molecolare nel Mezzogiorno d'Italia) Consortium.

References

- Hedinger C, Williams ED, Sobin LH 1989 The WHO histological classification of thyroid tumors: a commentary on the second edition. *Cancer* 63:980–911
- Rosai J, Carcangiu ML, DeLellis RA 1992 Atlas of tumor pathology: tumors of the thyroid gland, 3rd Ser. Washington DC: Armed Force Institute of Pathology

- Youle JR, D'Alessio G 1997 Antitumor RNases. In: D'Alessio G, Riordan JF, eds. *Ribonucleases: structures and functions*. New York: Academic Press; 491–514
- D'Alessio G, Di Donato A, Mazzarella L, Piccoli R 1997 Seminal ribonuclease: the importance of diversity. In: D'Alessio G, Riordan JF, eds. *Ribonucleases: structures and functions*. New York: Academic Press; 383–423
- Laccetti P, Spalletti-Cernia D, Portella G, De Corato P, D'Alessio G, Vecchio G 1994 Seminal ribonuclease inhibits tumor growth and reduces the metastatic potential of Lewis lung carcinoma. *Cancer Res* 54:4253–4256
- Matousek J 2001 Ribonucleases and their antitumor activity. *Comp Biochem Physiol C Toxicol Pharmacol* 129:175–191
- Mikulski SM, Costanzi JJ, Vogelzang NJ, McCachren S, Taub RN, Chun H, Mittelman A, Panella T, Puccio C, Fine R, Shogen K 2002 Phase II trial of a single weekly intravenous dose of ranpirnase in patients with unresectable malignant mesothelioma. *J Clin Oncol* 20:274–81
- Newton DL, Hansen HJ, Mikulski SM, Goldenberg DM, Rybak SM 2001 Potent and specific antitumor effects of an anti-CD22-targeted cytotoxic ribonuclease: potential for the treatment of non-Hodgkin lymphoma. *Blood* 97: 528–535
- Mastronicola MR, Piccoli R, D'Alessio G 1995 Key extracellular and intracellular steps in the antitumor action of seminal ribonuclease. *Eur J Biochem* 230:242–249
- Bracale A, Spalletti-Cernia D, Mastronicola MR, Castaldi F, Mannucci R, Nitsch L, D'Alessio G 2002 Essential stations in the intracellular pathway of cytotoxic bovine seminal ribonuclease. *Biochem J* 362:553–560
- Wu Y, Mikulski SM, Ardelt W, Rybak SM, Youle RJ 1993 A cytotoxic ribonuclease. Study of the mechanism of Onconase cytotoxicity. *J Biol Chem* 268:10686–10693
- Kim JS, Soucek J, Matousek J, Raines RT 1995 Mechanism of ribonuclease cytotoxicity. *J Biol Chem* 270:31097–31102
- Murthy BS, De Lorenzo C, Piccoli R, D'Alessio G, Sirdeshmukh R 1996 Effects of protein RNase inhibitor and substrate on the quaternary structures of bovine seminal RNase. *Biochemistry* 35:3880–3885
- Leland PA, Staniszewski KE, Kim BM, Raines RT 2001 Endowing human pancreatic ribonuclease with toxicity for cancer cells. *J Biol Chem* 276:43095–43102
- Antignani A, Naddeo M, Cubellis MV, Russo A, D'Alessio G 2001 Antitumor action of seminal ribonuclease, its dimeric structure, and its resistance to the cytosolic ribonuclease inhibitor. *Biochemistry* 40:3492–3496
- Piccoli R, Di Gaetano S, De Lorenzo C, Grauso M, Monaco C, Spalletti-Cernia D, Laccetti P, Cinatl J, Matousek J, D'Alessio G 1999 A dimeric mutant of human pancreatic ribonuclease with selective cytotoxicity toward malignant cells. *Proc Natl Acad Sci USA* 96:7768–7773
- Di Gaetano S, D'Alessio G, Piccoli R 2001 Second generation antitumor human RNase: significance of its structural and functional features for the mechanism of antitumor action. *Biochem J* 358:241–247
- Iordanov MS, Ryabinina OP, Wong J, Dinh TH, Newton DL, Rybak SM, Magun BE 2000 Molecular determinants of apoptosis induced by the cytotoxic ribonuclease Onconase: evidence for cytotoxic mechanisms different from inhibition of protein synthesis. *Cancer Res* 60:1983–1994
- Hu C-CA, Tang C-HA, Wang J-J 2001 Caspase activation in response to cytotoxic *Rana catesbeiana* ribonuclease in MCF-7 cells. *FEBS Lett* 503:65–68
- Cinatl Jr J, Cinatl J, Kotchetkov R, Vogel JU, Woodcock BG, Matousek J, Pouckova P, Kornhuber B 1999 Bovine seminal ribonuclease selectively kills human multidrug-resistant neuroblastoma cells via induction of apoptosis. *Int J Oncol* 15:1001–1009
- Laccetti P, Portella G, Mastronicola MR, Russo A, Piccoli R, D'Alessio G, Vecchio G 1992 In vivo and in vitro growth-inhibitory effect of bovine seminal ribonuclease on a system of rat thyroid epithelial transformed cells and tumors. *Cancer Res* 52:4582–4586
- Kotchetkov R, Cinatl J, Krivtchik AA, Vogel JU, Matousek J, Pouckova P, Kornhuber B, Schwabe D, Cinatl Jr J 2001 Selective activity of BS-RNase against anaplastic thyroid cancer. *Anticancer Res* 21:1035–1042
- Hansen R, Oren M 1997 p53; from inductive signal to cellular effect. *Curr Opin Genet Dev* 7:46–51
- Earnshaw WC, Martins LM, Kaufmann SH 1999 Mammalian caspases; structure, activation, substrates and functions during apoptosis. *Annu Rev Biochem* 68:383–424
- D'Alessio G, Di Donato A, Piccoli R, Russo A 2001 Seminal ribonuclease: procedures for the preparation of natural and recombinant enzyme, of its quaternary isoforms, of monomeric forms; an assay for the selective cytotoxicity of the enzyme. *Methods Enzymol* 341:248–263
- Fagin JA, Matsuo K, Karmakar A, Chen DL, Tang SH, Koeffler HP 1993 High prevalence of mutations of the p53 gene in poorly differentiated human thyroid carcinomas. *J Clin Invest* 91:179–84
- Gioanni J, Zanghellini E, Mazeau C, Zhang D, Courdi A, Farges M, Lambert JC, Duplay H, Schneider M 1991 Characterization of a human cell line from an anaplastic carcinoma of the thyroid gland. *Bull Cancer* 78:1053–1062
- Ain KB, Tofiq S, Taylor KD 1996 Antineoplastic activity of taxol against human anaplastic thyroid carcinoma cell lines *in vitro* and *in vivo*. *J Clin Endocrinol Metab* 81:3650–3653

29. **Testa JR, Bellacosa A** 2001 AKT plays a central role in tumorigenesis. *Proc Natl Acad Sci USA* 98:10983–10985
30. **Ringel MD, Hayre N, Saito J, Saunier B, Schuppert F, Burch H, Bernet V, Burman KD, Kohn LD, Saji M** 2001 Overexpression and overactivation of Akt in thyroid carcinoma. *Cancer Res* 61:6105–6111
31. **Bruni P, Boccia A, Baldassarre G, Trapasso F, Santoro M, Chiappetta G, Fusco A, Viglietto G** 2000 PTEN expression is reduced in a subset of sporadic thyroid carcinomas: evidence that PTEN-growth suppressing activity in thyroid cancer cells mediated by p27^{kip1}. *Oncogene* 19:3146–3155
32. **Weng LP, Gimm O, Kum JB, Smith WM, Zhou XP, Wynford-Thomas D, Leone G, Eng C** 2001 Transient ectopic expression of PTEN in thyroid cancer cell lines induces cell cycle arrest and cell type-dependent cell death. *Hum Mol Genet* 10:251–258
33. **Blagosklonny MV, Giannakakou P, Wojtowicz M, Romanova LY, Ain KB, Bates SE, Fojo T** 1998 Effects of p53-expressing adenovirus on the chemosensitivity and differentiation of anaplastic thyroid cancer cells. 83:2516–22
34. **Sellers WR, Fisher DE** 1999 Apoptosis and cancer drug targeting. *J Clin Invest* 104:1655–1661
35. **Mitsiades N, Poulaki V, Tseleni-Balafouta S, Koutras DA, Stamenkovic I** 2000 Thyroid carcinoma cells are resistant to FAS-mediated apoptosis but sensitive tumor necrosis factor-related apoptosis-inducing ligand. *Cancer Res* 60:4122–4129
36. **Iordanov MS, Wong J, Newton DL, Rybak SM, Bright RK, Flavell RA, Davis RJ, Magun BE** 2000 Differential requirement for the stress-activated protein kinase/c-Jun NH₂-terminal kinase in RNA damage-induced apoptosis in primary and in immortalized fibroblasts. *Mol Cell Biol Res Commun* 4:122–128

A Fully Human Antitumor ImmunoRNase Selective for ErbB-2-Positive Carcinomas

Claudia De Lorenzo,¹ Angela Arciello,¹ Rosanna Cozzolino,¹ Donald B. Palmer,² Paolo Laccetti,¹ Renata Piccoli,¹ and Giuseppe D'Alessio¹

¹Department of Biological Chemistry, University of Naples Federico II, Naples, Italy, and ²Department of Veterinary Basic Sciences, The Royal Veterinary College, University of London, London, United Kingdom

ABSTRACT

We report the preparation and characterization of a novel, fully human antitumor immunoRNase (IR). The IR, a human RNase and fusion protein made up of a human single chain variable fragment (scFv), is directed to the ErbB-2 receptor and overexpressed in many carcinomas. The anti-ErbB-2 IR, named hERB-hRNase, retains the enzymatic activity of the wild-type enzyme (human pancreatic RNase) and specifically binds to ErbB-2-positive cells with the high affinity ($K_d = 4.5$ nM) of the parental scFv. hERB-hRNase behaves as an immunoprototoxin and on internalization by target cells becomes selectively cytotoxic in a dose-dependent manner at nanomolar concentrations. Administered in five doses of 1.5 mg/kg to mice bearing an ErbB-2-positive tumor, hERB-hRNase induced a dramatic reduction in tumor volume. hERB-hRNase is the first fully human antitumor IR produced thus far, with a high potential as a poorly immunogenic human drug devoid of nonspecific toxicity, directed against ErbB-2-positive malignancies.

INTRODUCTION

Immunotherapy is of great interest today as an effective strategy to manage cancer and as an alternative to chemotherapy. The Food and Drug Administration has approved several monoclonal antibodies as therapeutic agents to manage tumors, and an increasing number are undergoing clinical evaluation (1). Examples of approved antibodies are humanized or human-mouse chimeric monoclonal antibodies, such as anti-ErbB-2 trastuzumab (Herceptin) and anti-CD20 rituximab (Rituxan), widely used against breast cancer and non-Hodgkin's lymphoma, respectively (2). To enhance their clinical potential, antibodies also have been coupled to cytotoxic agents or radionuclides (3).

Immunotoxins (ITs), made up of antibodies or miniantibodies [single chain variable fragment (scFv)] fused to toxins, have been proposed as anticancer drugs during the past 2 decades (4, 5). These chimeric proteins combine the potent toxicity of toxins with the antigen specificity of antibodies. However, the murine nature of the immunomoiety, the plant or bacterial nature of the toxin moieties, and their high toxicity have greatly limited the therapeutic potential of ITs (6, 7), especially because of the occurrence of vascular leak syndrome (8–10). Although the development of humanized antibodies has alleviated some of these effects, the toxins themselves remain a problem.

An alternative, more recent strategy in anticancer immunotherapy is that based on immunoconjugates in which an RNase substitutes for the toxin (11). Mammalian RNases are not toxic to cells unless internalized; thus, these fusion proteins are not ITs but rather immunoprototoxins. We have proposed (12) to call them immunoRNases (IRs). IRs have been prepared with various RNases, each fused to a monoclonal antibody raised against cell receptors (12–15). However,

the IRs prepared thus far have a limited interest for immunotherapy, given the nonhuman origin of the antibody moiety used and the choice of the targeted receptors, such as the epidermal growth factor or the transferrin receptor (16, 17).

Because of its preferential expression in tumor cells (18) and its extracellular accessibility, an attractive target for immunotherapy is ErbB-2, a transmembrane tyrosine kinase receptor that is overexpressed on many carcinoma cells of different origin (19, 20), with a key role in the development of malignancy (21, 22). Furthermore, activated ErbB-2 is readily internalized, an event that can be mimicked by an antibody directed toward the receptor. Thus, an anti-ErbB-2 antibody can deliver an RNase into ErbB-2-overexpressing tumor cells. Such a strategy has been successfully tested using a murine scFv fused to a human RNase (12).

The use of antibody and RNase moieties of human origin for the preparation of fully human IRs is highly desirable to obtain effective and tumor-selective but also immunocompatible immunoagents.

Fully human scFvs recently have been generated with the phage display technology through the expression of large repertoires of antibody variable regions on filamentous phages after their fusion to a phage coat protein (23–25). Taking advantage of this powerful technique, we have isolated a novel human anti-ErbB-2 scFv (26) from a large phage display library (23) through a double-selection strategy performed on live cells. This scFv specifically binds to ErbB-2-positive cells, inhibits receptor autophosphorylation, is internalized in target cells, and strongly inhibits their proliferation (26).

We report here the construction and characterization of a fully human antitumor IR made up of the available human anti-ErbB-2 scFv (26) and a human RNase, which we have termed hERB-hRNase. This IR, to our knowledge the first human IR to be produced, may prove to be a valuable anticancer agent for therapy of ErbB-2-overexpressing carcinomas.

MATERIALS AND METHODS

Antibodies and Cell Cultures. The antibodies used in the current study were the following: murine monoclonal antibody 9E10 directed against the myc tag protein (27), the IgG fraction from a rabbit anti-human pancreas RNase (HP-RNase) antiserum (Igtech, Salerno, Italy) purified by affinity chromatography of the antiserum on protein A-Sepharose CL-4B (Amersham Pharmacia Biotech, Piscataway, NJ), horseradish peroxidase-conjugated anti-His antibody (Qiagen, Valencia, CA), horseradish peroxidase-conjugated goat antirabbit immunoglobulin antibody (Pierce, Rockford, IL), horseradish peroxidase-conjugated rabbit antimouse immunoglobulin antibody (Pierce), and FITC-conjugated sheep antirabbit immunoglobulin antibody (Dako, Glostrup, Denmark).

The MDA-MB361 (provided by Dr. N. Normanno, Cancer Institute of Naples, Italy) and the SKBR3 cell lines from human breast tumor and the A431 cell line from human epidermoid carcinoma (American Type Culture Collection, Manassas, VA) were cultured in RPMI 1640 (Life Technologies, Rockville, MD). The MDA-MB453 cell line from human breast tumor (a gift of H. C. Hurst, ICRF, London, UK) and the TUBO cell line from a BALB-neu T mouse-derived mammary lobular carcinoma (provided by Dr. G. Forni, University of Turin, Italy) were grown in DMEM (Life Technologies). Media were supplemented with 10% fetal bovine serum (20% for TUBO cells), 50 units/ml penicillin, and 50 μ g/ml streptomycin (all from Life Technologies).

Received 11/28/03; revised 4/6/04; accepted 5/17/04.

Grant support: AIRC (Associazione Italiana per la Ricerca sul Cancro), Italy, and by MIUR (Ministero dell'Università e della Ricerca Scientifica e Tecnologica), Italy.

The costs of publication of this article were defrayed in part by the payment of page charges. This article must therefore be hereby marked *advertisement* in accordance with 18 U.S.C. Section 1734 solely to indicate this fact.

Requests for reprints: Giuseppe D'Alessio, Department of Biological Chemistry, University of Naples Federico II, via Mezzocannone 16, 80134 Naples, Italy. Phone: 39-081-253-4731; Fax: 39-081-552-1217; E-mail: dalessio@unina.it.

Construction of the Chimeric cDNA Encoding hERB-hRNase. A cDNA coding for HP-RNase (28) was engineered by two successive PCRs. Upstream primers (termed A and B) were used to incorporate the *NotI* restriction site at the 5' end and a spacer sequence, whereas a downstream primer (C) was used to introduce a *NotI* site at the 3' end. In the first reaction, primers B and C were used. The oligonucleotide B sequence (5'-GGCCCGAAGGCGGCAGCAAAGAATCTAGAGCTAAAAA-3') encodes the COOH-terminal half of the spacer; the oligonucleotide C sequence (5'-ATAAGAATGCGGCCGCA-GAGTCTTCAACAGACG-3') contains the *NotI* restriction site. In the second reaction, primers A and C were used. Oligonucleotide A (5'-ATAAGAATGCGGCCGCAAGCGGCCCGGAAGGCGG-3') encodes the N-terminal half of the spacer preceded by the *NotI* site sequence. The PCR fragment then was digested with *NotI* (New England Biolabs, Beverly, MA) and cloned into the corresponding site of pHEN2 vector (29) downstream to the sequence encoding the available human anti-ErbB-2 scFv (26). The correct directional insertion of the RNase gene in the *NotI* site was assessed by PCR using the forward primer A in combination with a reverse oligonucleotide corresponding to a vector sequence positioned downstream to the *NotI* site (5'-TGAATTT-TCTGTATGAGG-3').

Sequence analyses confirmed the expected DNA sequence. The assembled gene then was cloned in a T7 promoter-based *Escherichia coli* expression vector (pET22b+).

Expression and Purification of hERB-hRNase. Cultures of *E. coli* BL21 (DE3), previously transformed with the recombinant pET22b(+) expression vector, were grown at 37°C in LB medium containing 50 µg/ml ampicillin until the exponential phase was reached. The expression of soluble IR (henceforth called hERB-hRNase) was induced by addition of isopropyl-β-D-thiogalactopyranoside to a final concentration of 1 mM in the cell culture, which then was grown at room temperature overnight. Cells were harvested by centrifugation at 6000 rpm for 15 min, and the periplasmic extract was obtained as described previously (26) and incubated with the 4-mercapto-ethyl-pyridine HyperCel matrix (BioSeptra, Cergy-Saint-Christophe, France) for 2 h at room temperature. After extensive washes with 50 mM Tris-HCl (pH 8.0), two additional wash steps were performed: the first with H₂O and the second with 25 mM sodium caprylate in 50 mM Tris-HCl (pH 8.0). The 4-mercapto-ethyl-pyridine HyperCel resin then was equilibrated in 50 mM Tris-HCl (pH 8.0) before elution of the protein with 50 mM sodium acetate (pH 4.0). The sample was immediately adjusted to pH 7.0, diluted with B-PER buffer (Pierce), and loaded on an immobilized-metal affinity chromatography column using a cobalt-chelating resin (TALON; Clontech, Palo Alto, CA) to achieve further purification. Wash and elution steps were performed according to the manufacturer's recommendations. The purity of the final preparation was evaluated by SDS-PAGE, followed by Coomassie staining and Western blot analysis with anti-HP-RNase immunoglobulins, followed by goat anti-rabbit horseradish peroxidase-conjugated IgG.

RNase Activity Assays. RNase activity was tested as described previously (30) on yeast RNA (8 mg/ml). RNase zymograms, carried out on SDS-PAGE electropherograms, were performed as described previously (31).

Binding Assays. ErbB-2-positive SKBR3, MDA-MB361, MDA-MB453, and TUBO cells and ErbB-2-negative A431 control cells, harvested in non-enzymatic dissociation solution (Sigma, St. Louis, MO), were washed and transferred to U-bottomed microtiter plates (1 × 10⁵ cells/well). After blocking with PBS containing 6% BSA, the plates were incubated with purified immunoagents in ELISA buffer (PBS/BSA 3%) for 90 min. After centrifugation and removal of supernatants, pelleted cells were washed twice in 200 µl of ELISA buffer, resuspended in 100 µl of the same buffer, and incubated for 1 h with either rabbit anti-HP-RNase IgG (for the detection of hERB-hRNase) or with murine anti-myc monoclonal antibody (for scFv detection), followed by peroxidase-conjugated anti-rabbit or antimouse IgG (Pierce), respectively, according to the source of the primary antibody. After 1 h, the plates were centrifuged, washed with ELISA buffer, and reacted with 3,3',5,5'-tetramethylbenzidine (Sigma). Binding values were determined from the absorbance at 450 nm and reported as the mean of at least three determinations (SD ≤ 5%).

Internalization of hERB-hRNase. Cells grown on coverslips to 60% confluency were incubated with the immunoagent (20 µg/ml) for 16 h at 37°C. Cells then were washed, fixed, and permeabilized as described elsewhere (26). Intracellular IR was detected with a rabbit anti-HP-RNase antibody, followed

by FITC-conjugated sheep anti-rabbit antibody. Optical confocal sections were taken using a confocal microscope (LSM 510; Zeiss, Oberkochen, Germany).

Cytotoxicity Assays. Cells were seeded in 96-well plates (150 µl/well); SKBR3, MDA-MB361, TUBO, and MDA-MB453 cells were seeded at a density of 1.5 × 10⁴/well, and A431 cells were seeded at a density of 5 × 10³/well. Cell survival was expressed as percentage of viable cells in the presence of the protein under test, with respect to control cultures grown in the absence of the protein.

Stability of the IR. The stability of hERB-hRNase was determined by incubating the protein at a concentration of 0.04 mg/ml in either human or murine serum at 37°C for 24 or 48 h. At the end of incubation the samples were tested using the analytical tests described previously.

In Vivo Antitumor Activity. All of the experiments were performed with 6-week-old female BALB/cAnNCrIBR mice (Charles River Laboratories, Wilmington, MA). TUBO cells (5 × 10⁵) were suspended in 0.2 ml sterile PBS and injected s.c. (day 0) in the right paw. At day 10, tumors were clearly detectable (at least 15 mm³ in volume). At day 11, hERB-hRNase, dissolved in PBS, was administered five times at 72-h intervals peritumorally or i.p. to two groups of five mice at doses of 1.5 mg/kg of body weight. Equimolar doses of native HP-RNase or anti-ErbB-2 scFv were administered peritumorally to other two groups as controls. Another group of control animals was treated with identical volumes of sterile PBS. At day 45, blood samples were taken and tested to obtain the main hematologic parameters. During the treatment period, tumor volumes (V) were measured and calculated using the formula of rotational ellipsoid $V = A \times B^2/2$ (A is axial diameter and B is rotational diameter). All of the mice were maintained at the animal facility of the Department of Cellular and Molecular Biology and Pathology, University of Naples Federico II. The experiments on animals described here were conducted in accordance with accepted standards of animal care and the Italian regulations for the welfare of animals used in studies of experimental neoplasia. The School of Medicine Institutional Committee on animal care approved the study.

RESULTS

Construction and Purification of hERB-hRNase. The anti-ErbB-2 fully human IR was prepared as follows: the cDNA encoding HP-RNase was amplified by two successive PCRs (see "Materials and Methods"), which added a spacer sequence encoding a peptide of 11 residues designed to separate the RNase (28) and scFv moieties in the fusion protein. The resulting product was cloned in the expression vector pHEN2 (29), downstream to the sequence encoding the available human anti-ErbB-2 scFv (26), and in *NcoI/NotI* sites. The resulting construct encoding the IR, named hERB-hRNase, is shown in Fig. 1. It includes a 15-residue linker made up of glycine and serine residues (SSGGGGSGGGSGGS) interposed between V_H and V_L chains, an 11-residue spacer (AAASGGPEGGS) inserted between the antibody fragment and the RNase, and a COOH-terminal hexahistidine tag. The chimeric cDNA was fully sequenced and re-cloned in a T7 promoter-based *E. coli* expression vector (pET22b+) equipped with a pel B signal sequence for expression of hERB-hRNase as a soluble protein in the periplasmic space.

Characterization of hERB-hRNase. The purified IR was analyzed by Western blot analysis with an anti-His and an anti-HP-RNase

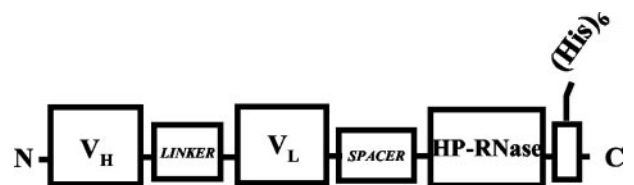


Fig. 1. Schematic representation of the human immunorNase hERB-hRNase. V_H and V_L, the variable domains of heavy and light chains, respectively, of the anti-ErbB-2 single chain variable fragment (scFv); LINKER, the 15-residue junction peptide SS(G₄S)₂GGS; SPACER, the peptide AAASGGPEGGS connecting the scFv and the RNase moieties; HP-RNase, human pancreatic RNase; and (His)₆, a 6-residue His tag.

antibody. By both analyses, an immunoreactive band of the expected size, approximately M_r 46,000, was visualized (Fig. 2).

The fusion protein then was tested for enzymatic activity by a zymogram developed using yeast RNA as a substrate. As illustrated in Fig. 2, a single active band was detectable, corresponding to the size of hERB-hRNase. The ribonucleolytic activity of the purified IR was further tested with the acid-insoluble RNA precipitation assay (30), by which the chimeric protein was found to have a specific activity of 950 ± 25 units/nmol. This result was confirmed for several preparations of the recombinant fusion protein. Because the specific activity of wild-type HP-RNase is $\sim 1100 \pm 20$ units/nmol, we can conclude that the chimeric protein retains $\sim 90\%$ of the activity of the parental RNase molecule.

The ability of hERB-hRNase to specifically recognize ErbB-2 was evaluated by ELISA, performed as described in "Materials and Methods," using SKBR3 cells from human breast cancer, which express high levels of ErbB-2. As a control we used A431 cells from human epidermoid carcinoma, which express the receptor at low levels. The results, shown in Fig. 3, indicate that the IR binds with high affinity to SKBR3 cells, whereas no significant binding to A431 cells was detected. The apparent binding affinity of hERB-hRNase for the ErbB-2 receptor (*i.e.*, the concentration corresponding to half-maximal saturation) was found to be 4.5 nM, almost identical to that obtained with the parental scFv (4 nM; see Fig. 3).

These results demonstrate that the antibody and RNase moieties maintain their biological functions in the chimeric protein.

Internalization of hERB-hRNase by SKBR3 Cells. It has been reported that the human anti-ErbB-2 scFv, previously isolated in our laboratory, undergoes receptor-mediated endocytosis in SKBR3 cells

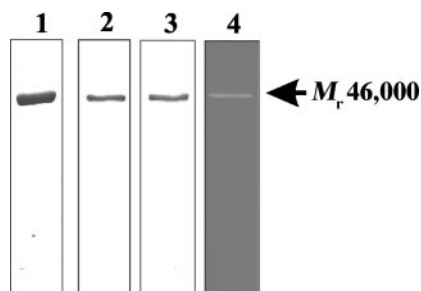


Fig. 2. SDS-PAGE analyses of purified hERB-hRNase. Lane 1, hERB-hRNase eluted from the cobalt-chelating affinity chromatography (Coomassie Blue staining); Lanes 2 and 3, Western blot analyses of the sample as in Lane 1 using anti-human pancreatic-RNase IgGs (Lane 2) or an anti-His antibody (Lane 3); Lane 4, zymogram of the sample as in Lane 1 using yeast RNA as a substrate.

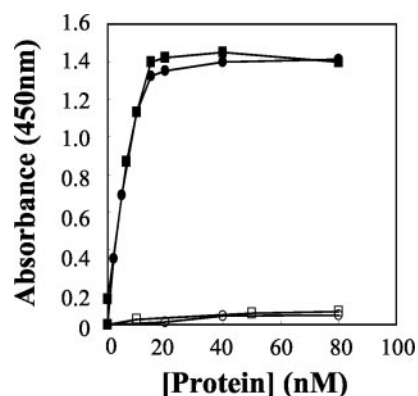


Fig. 3. Binding tests of hERB-hRNase to ErbB-2-positive (SKBR3) and ErbB-2-negative (A431) cell lines. SKBR3 cells (black symbols) and A431 cells (white symbols) were tested by ELISA with hERB-hRNase (squares) or with the anti-ErbB-2 single chain variable fragment (circles) as a control.

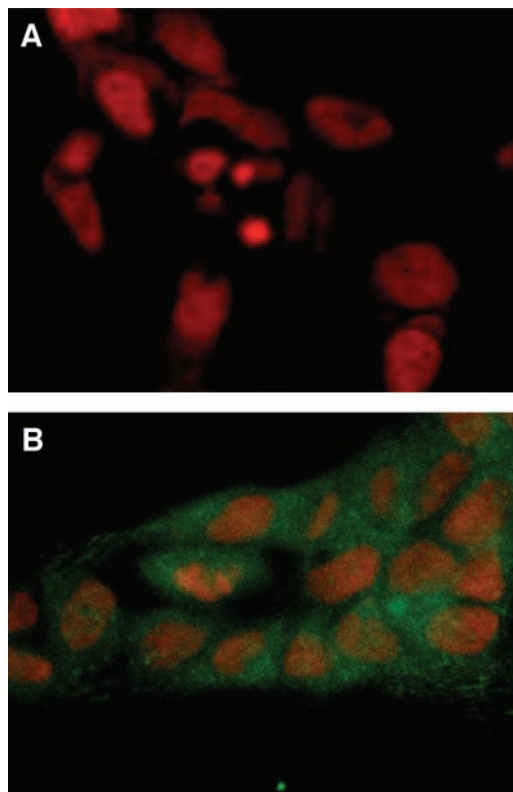


Fig. 4. Internalization of hERB-hRNase in SKBR3 cells as visualized by confocal microscopy. Cells were incubated in the absence (A) or in the presence of the immunorNase for 16 h (B); magnification 1:200.

(26). To test whether the scFv in the fusion protein could provide a useful vehicle to deliver the RNase into the cytosol, tumor target cells were incubated with hERB-hRNase for 16 h at 37°C. After extensive washes, cells were fixed and permeabilized as described previously (26). Internalized IR was visualized with anti-HP-RNase antibody, followed by sheep antirabbit FITC-conjugated antibody. As shown in Fig. 4, a strong intracellular staining was visualized (Fig. 4B) by confocal microscopy.

Cytotoxic Effects of hERB-hRNase on Tumor Cells. The purified hERB-hRNase then was tested for its effects on ErbB-2-positive and ErbB-2-negative cell survival. For the latter cell type, A431 cells from human epidermoid carcinoma were used; as antigen-positive cells, we used SKBR3, MDA-MB361, and MDA-MB453 derived from human breast carcinomas and TUBO cells from a BALB-neu T mouse-derived mammary lobular carcinoma (32). Cells were plated in the absence or in the presence of increasing concentrations of hERB-hRNase, and after a 72-h incubation, cell survival was measured by counting trypan blue-excluding cells.

As shown in Fig. 5, hERB-hRNase was found to be selectively cytotoxic in a dose-dependent manner on all of the antigen-positive cell lines tested. The values of IC_{50} (*i.e.*, the concentration capable of reducing cell viability by 50%) were found to be 12.5, 47, 52, and 60 nM for SKBR3, MDA-MB361, MDA-MB453, and TUBO cells, respectively. When the IR was tested on A431 control cells, no effects on their proliferation were observed (see Fig. 5). Moreover, no effects on cell survival were detected when native HP-RNase was tested on ErbB-2-positive cells at concentrations up to 1 μ M (*i.e.*, at doses of RNase up to 20-fold higher than the highest dose of RNase present in the IR samples tested on the cell cultures). These results indicate that (a) the RNase moiety in the IR has no effect on cell proliferation unless driven inside the cells by the immune moiety; and (b) hERB-

hRNase is able to finely discriminate between target and nontarget cells and to specifically induce the death of target cells.

The stronger cytotoxicity of hERB-hRNase on SKBR3 and MDA-MB361 cells compared with that observed on MDA-MB453 cells could be related to their different level of ErbB-2, reported to be sixfold lower in the latter cells (12, 33). By ELISA we confirmed a lower level of ErbB-2 immunoreactivity in MDA-MB453 cells compared with SKBR3 and MDA-MB361 cells and found a similar low ErbB-2 content on TUBO cells (data not shown). These results indicate that there is a positive correlation between the expression levels of ErbB-2 on a particular cell type, the extent of binding of hERB-hRNase to those cells, and their sensitivity to its cytotoxic action.

Stability of hERB-hRNase. The stability of immunoagents at 37°C is a critical factor for their potential as therapeutic agents. The stability of hERB-hRNase in human or murine serum at 37°C for up to 48 h was analyzed by monitoring its integrity as a protein and as functional bioeffector. Following an incubation in serum for 24 or 48 h at 37°C, the percentage of undegraded and enzymatically active IR was determined by Western blot analysis with anti-His tag antibody and zymogram analyses, respectively. By using a Phosphorimager, the intensity of the electrophoretic bands obtained with treated hERB-hRNase was expressed as the percentage of the signal given by the untreated protein. We found that after 24 or 48 h, the percentage of undegraded and enzymatically active hERB-hRNase was $100 \pm 5\%$.

The binding properties of the IR after incubation in serum were assessed by ELISA on ErbB-2-positive cells and expressed as the concentration corresponding to half-maximal saturation. It was found that the protein incubated in human or murine serum conserved a value of half-maximal saturation of 5 nM, virtually identical to that measured for the protein before incubation (see above).

Finally, hERB-hRNase was found to fully retain its cytotoxic activity after incubation at 37°C for up to 48 h. The IC_{50} values of the incubated samples tested on SKBR3 cells (see above) were within $\pm 10\%$ of the values measured before incubation.

These results clearly indicate that the IR is stable under the examined physiologic-like conditions.

In Vivo Antitumor Activity of hERB-hRNase. For *in vivo* studies, the ErbB-2-positive tumor cell line TUBO of murine origin (see above) was used. As shown in Fig. 6, the hERB-hRNase treatment of mice bearing TUBO tumors with five doses of 1.5 mg/kg of hERB-hRNase injected peritumorally induced a dramatic reduction (86%) in tumor volume. Similar results were obtained when the protein was administered systemically by i.p. injections. This suggests that the protein is stable in the bloodstream and is able to permeate tumor masses. Contrarily, the anti-ErbB-2 scFv and native HP-RNase injected peritumorally showed no significant effects on tumor growth (see Fig. 6). During the treatment period, the animals did not show

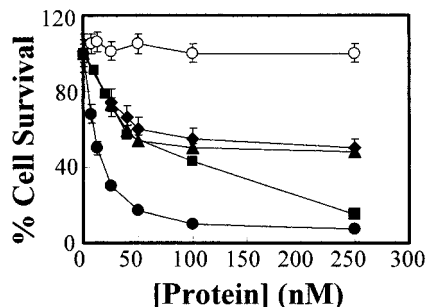


Fig. 5. Effects of hERB-hRNase on cell survival. Dose-response curves of SKBR3 (●), MDA-MB361 (■), MDA-MB453 (▲), TUBO (◆), and A431 cell lines (○) on treatment for 72 h with hERB-hRNase.

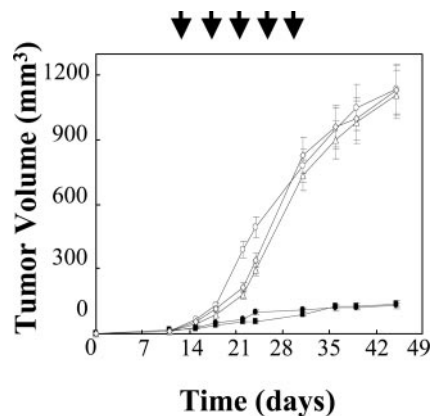


Fig. 6. *In vivo* suppression of tumor growth by hERB-hRNase. Tumor growth was followed in mice inoculated s.c with 5×10^5 TUBO mammary carcinoma cells. Treated animals were injected i.p. (●) or in the peritumoral area (■) with hERB-hRNase at doses of 1.5 mg/kg body weight. Control animals were treated with sterile PBS solution (◇), equimolar doses of the anti-ErbB-2 single chain variable fragment (△), or human pancreatic-RNase (○) administered peritumorally. Injections were repeated five times at 72-h intervals as indicated by the arrows.

signs of wasting or other visible signs of toxicity. Their main hematologic parameters were those of normal mice (data not shown).

DISCUSSION

Immunotherapy has been demonstrated to be a valuable approach in anticancer therapy. As previously indicated, ITs directed to cell surface molecular targets have been shown to have a therapeutic potential. However, they also have limitations, mainly represented by nonspecific toxicity related to vascular leak syndrome and by the immunogenicity of their bacterial or plant toxins (8–10).

To circumvent these problems, IRs (*i.e.*, chimeric proteins made up of RNases fused to an antireceptor antibody or scFv) have been prepared (13–15). These IRs were cytotoxic to tumor cells at nanomolar concentrations. However, the choice of epidermal growth factor or transferrin receptors as targets for the antibody, as well as the murine origin of the antibodies used, sets a limit in the use of these reagents as therapeutic drugs.

ErbB-2 is an attractive tumor target because of its specific localization on many tumor cells of different origin, its extracellular accessibility, and its high expression levels in many carcinomas (19, 20). Furthermore, its high expression in carcinomas has been reported to be a clear sign of negative prognosis (21, 22).

Here, we report the construction, characterization, and antitumor activity of the first fully human IR targeting the ErbB-2 receptor. In this novel fusion protein, named hERB-hRNase, the human scFv and human RNase moieties preserve their biological actions. In contrast with previous reports (11), the IR activity as an RNase is nearly that of the native, free enzyme. Likewise, the IR binds to target cells as selectively and effectively as the parental, free scFv.

As for the RNase fused in the IR construct, it is mandatory, for assigning to the IR the role and the action of an immunoprototoxin, that the RNase *per se* is not a cytotoxic agent. Our work has shown that the HP-RNase used in hERB-hRNase is not *per se* a cytotoxic agent, neither *in vivo* nor *in vitro*, but becomes cytotoxic on internalization. This may not be surprising because it has been reported that when nontoxic RNases, such as RNase A, are artificially introduced into frog oocytes, they become powerful cytotoxic agents (34).

It is the ability of the parental scFv to be internalized by ErbB-2-overexpressing cells fully preserved in the fusion protein, which allows the RNase to enter the cytosol and kill target cells.

It should be noted that the scFv alone was found to inhibit the

proliferation of SKBR3 cells with an IC₅₀ value of 200 nM (26). This indicates that the IR, for which an IC₅₀ value of 12.5 nM was obtained, is a more effective anticancer agent. This result can only be attributed to the additional toxic action of the internalized RNase because the RNase alone has no effect on cell viability.

It may be of interest that hHERB-hRNase has been found to be stable for at least 48 h when incubated at 37°C in human or murine serum. This feature of the IR adds to its potential as a promising antitumor drug. Even more interesting are the results of *in vivo* assays of hHERB-hRNase antitumor action carried out on mice inoculated with TUBO ErbB-2-positive tumor cells, which produce tumors similar to the alveolar-type human lobular mammary carcinomas (35). These experiments proved that low doses of hHERB-hRNase also are effective *in vivo*. Treatment of mice inoculated with TUBO cells with only five doses of IR (1.5 mg/kg body weight) administered either peritumorally or systemically strongly inhibited the growth of TUBO tumors in mice. Such effect again can be attributed to the fusion protein as a whole because the two moieties, the anti-ErbB-2 scFv and HP-RNase, when administered separately to mice bearing the same tumor, were not found to be effective in inhibiting tumor growth.

To our knowledge, hHERB-hRNase is to date the first fully human IR to be constructed and tested with satisfactory results *in vitro* and *in vivo*. Its fully human nature, combined with its stability and its selective cytotoxic action on target cells, could make it a precious tool in the therapy of human mammary carcinomas.

ACKNOWLEDGMENTS

We thank Dr. Giancarlo Vecchio for valuable comments and suggestions.

REFERENCES

- Brekke OH, Sandlie I. Therapeutic antibodies for human diseases at the dawn of the twenty-first century. *Nat Rev Drug Discov* 2003;2:52–62.
- Milenic DE. Monoclonal antibody-based therapy strategies: providing options for the cancer patient. *Curr Pharm Des* 2002;8:1749–64.
- Allen TM. Ligand-targeted therapeutics in anticancer therapy. *Nat Rev Cancer* 2002;2:750–63.
- Pastan I, FitzGerald D. Recombinant toxins for cancer treatment. *Science* 1991;254:1173–7.
- Reiter Y, Pastan I. Recombinant Fv immunotoxins and Fv fragments as novel agents for cancer therapy and diagnosis. *Trends Biotechnol* 1998;16:513–20.
- Weiner LM, O'Dwyer J, Kitson J, et al. Phase I evaluation of an anti-breast carcinoma monoclonal antibody 260F9-recombinant ricin A immun conjugate. *Cancer Res* 1989;49:4062–7.
- Schindler J, Sausville E, Messmann R, Uhr JW, Vitetta ES. The toxicity of deglycosylated ricin A chain-containing immunotoxins in patients with non-Hodgkin's lymphoma is exacerbated by prior radiotherapy: a retrospective analysis of patients in five clinical trials. *Curr Opin Oncol* 2001;13:168–75.
- Schnell R, Vitetta E, Schindler J, et al. Treatment of refractory Hodgkin's lymphoma patients with an anti-CD25 ricin A-chain immunotoxin. *Leukemia* 2000;14:129–35.
- Soler-Rodríguez AM, Ghetie MA, Oppenheimer-Marks N, Uhr JW, Vitetta ES. Ricin A-chain and ricin A-chain immunotoxins rapidly damage human endothelial cells: implications for vascular leak syndrome. *Exp Cell Res* 1993;206:227–34.
- Baluna R, Vitetta ES. An *in vivo* model to study immunotoxin-induced vascular leak in human tissue. *J Immunother* 1999;22:41–7.
- Rybak SM, Newton DL. Natural and engineered cytotoxic ribonucleases: therapeutic potential. *Exp Cell Res* 1999;253:325–35.
- De Lorenzo C, Nigro A, Piccoli R, D'Alessio G. A new RNase-based immun conjugate selectively cytotoxic for ErbB2-overexpressing cells. *FEBS Lett* 2002;516:208–12.
- Zewe M, Rybak SM, Dubel S, et al. Cloning and cytotoxicity of a human pancreatic RNase immunofusion. *Immunotechnology* 1997;3:127–36.
- Suwa T, Ueda M, Jinno H, et al. Epidermal growth factor receptor-dependent cytotoxic effect of anti-EGFR antibody-ribonuclease conjugate on human cancer cells. *Anticancer Res* 1999;19:4161–5.
- Stocker M, Tur MK, Sasse S, Krussmann A, Barth S, Engert A. Secretion of functional anti-CD30-angiogenin immunotoxins into the supernatant of transfected 293T-cells. *Protein Expr Purif* 2003;28:211–9.
- Christensen ME. The EGF receptor system in head and neck carcinomas and normal tissues. Immunohistochemical and quantitative studies. *Dan Med Bull* 1998;45:121–34.
- Moos T, Morgan EH. Transferrin and transferrin receptor function in brain barrier systems. *Cell Mol Neurobiol* 2000;20:77–95.
- Ishida T, Tsujisaki M, Hanzawa Y, et al. Significance of erbB-2 gene product as a target molecule for cancer therapy. *Scand J Immunol* 1994;39:459–66.
- Slamon DJ, Godolphin W, Jones LA, et al. Studies of the HER-2/neu proto-oncogene in human breast and ovarian cancer. *Science* 1989;244:707–12.
- Klapper LN, Kirschbaum MH, Sela M, Yarden Y. Biochemical and clinical implications of the ErbB/HER signaling network of growth factor receptors. *Adv Cancer Res* 2000;77:25–79.
- Graus-Porta D, Beerli RR, Daly JM, Hynes NE. ErbB-2, the preferred heterodimerization partner of all ErbB receptors, is a mediator of lateral signaling. *EMBO J* 1997;16:1647–55.
- Lohrisch C, Piccart M. HER2/neu as a predictive factor in breast cancer. *Clin Breast Cancer* 2001;2:129–35.
- Griffiths AD, Williams SC, Hartley O, et al. Isolation of high affinity human antibodies directly from large synthetic repertoires. *EMBO J* 1994;13:3245–60.
- Vaughan TJ, Williams AJ, Pritchard K, et al. Human antibodies with sub-nanomolar affinities isolated from a large non-immunized phage display library. *Nat Biotechnol* 1996;14:309–14.
- Sheets MD, Amersdorfer P, Finner R, et al. Efficient construction of a large nonimmune phage antibody library: the production of high-affinity human single-chain antibodies to protein antigens. *Proc Natl Acad Sci USA* 1998;95:6157–62.
- De Lorenzo C, Palmer DB, Piccoli R, Ritter MA, D'Alessio G. A new human antitumor immunoreagent specific for ErbB2. *Clin Cancer Res* 2002;8:1710–9.
- Evan GI, Lewis GK, Ramsay G, Bishop JM. Isolation of monoclonal antibodies specific for human c-myc proto-oncogene product. *Mol Cell Biol* 1985;5:3610–6.
- Russo N, de Nigris M, Ciardiello A, Di Donato A, D'Alessio G. Expression in mammalian cells, purification and characterization of recombinant human pancreatic ribonuclease. *FEBS Lett* 1993;333:233–7.
- Nissim A, Hoogenboom HR, Tomlinson IM, et al. Antibody fragments from a "single pot" phage display library as immunochemical reagents. *EMBO J* 1994;13:692–8.
- Bartholeyns J, Wang D, Blackburn P, Wilson G, Moore S, Stein WH. Explanation of the observation of pancreatic ribonuclease activity at pH 4.5. *Int J Pept Protein Res* 1977;10:172–5.
- Blank A, Sugiyama RH, Dekker CA. Activity staining of nucleolytic enzymes after sodium dodecyl-sulfate-polyacrylamide gel electrophoresis: use of aqueous isopropanol to remove detergent from gels. *Anal Biochem* 1982;120:267–75.
- Rovero S, Amici A, Carlo ED, et al. DNA vaccination against rat her-2/Neu p185 more effectively inhibits carcinogenesis than transplantable carcinomas in transgenic BALB/c mice. *J Immunol* 2000;165:5133–42.
- Merlin JL, Barberi-Heyob M, Bachmann N. *In vitro* comparative evaluation of trastuzumab (Herceptin) combined with paclitaxel (Taxol) or docetaxel (Taxotere) in HER2-expressing human breast cancer cell lines. *Ann Oncol* 2002;13:1743–8.
- Saxena SK, Rybak SM, Winkler G, et al. Comparison of RNases and toxins upon injection into *Xenopus* oocytes. *J Biol Chem* 1991;266:21208–14.
- Di Carlo E, Diodoro MG, Boggio K, et al. Analysis of mammary carcinoma onset and progression in HER-2/neu oncogene transgenic mice reveals a lobular origin. *Lab Invest* 1999;79:1261–9.

Predicting drug sensitivity and resistance: Profiling ABC transporter genes in cancer cells

Gergely Szakács,^{1,4,*} Jean-Philippe Annereau,^{1,4} Samir Lababidi,² Uma Shankavaram,² Angela Arciello,¹ Kimberly J. Bussey,² William Reinhold,² Yanping Guo,³ Gary D. Kruh,³ Mark Reimers,² John N. Weinstein,² and Michael M. Gottesman^{1,*}

¹Laboratory of Cell Biology

²Laboratory of Molecular Pharmacology, Center for Cancer Research, NCI, NIH, Bethesda, Maryland, 20892

³Medical Science Division, Fox Chase Cancer Center, Philadelphia, Pennsylvania 19111

⁴These authors contributed equally to this work.

*Correspondence: szakacs@mail.nih.gov, mgottesman@nih.gov

Summary

For analysis of multidrug resistance, a major barrier to effective cancer chemotherapy, we profiled mRNA expression of the 48 known human ABC transporters in 60 diverse cancer cell lines (the NCI-60) used by the National Cancer Institute to screen for anticancer activity. The use of real-time RT-PCR avoided artifacts commonly encountered with microarray technologies. By correlating the results with the growth inhibitory profiles of 1,429 candidate anticancer drugs tested against the cells, we identified which transporters are more likely than others to confer resistance to which agents. Unexpectedly, we also found and validated compounds whose activity is potentiated, rather than antagonized, by the MDR1 multidrug transporter. Such compounds may serve as leads for development.

Introduction

The ABC (ATP binding cassette) family of membrane transport proteins includes the best-known mediators of resistance to anticancer drugs. In particular, MDR (multidrug resistance) pumps ABCB1 (MDR1-P-gp), ABCC1-MRP1, and ABCG2-MXR (Gottesman et al., 2002; Cole et al., 1992; Borst et al., 2000; Deeley and Cole, 1997; Litman et al., 2001) actively extrude many types of drugs from cancer cells, thereby conferring resistance to those agents. More broadly, the ABC transporters appear to have evolved to defend the cell through recognition and energy-dependent removal of a large variety of natural toxic agents (Sarkadi et al., 1996). Their functional significance is suggested by the observation that they form one of the largest protein families, found in various cellular membranes of organisms from bacteria to mammals. Based on sequence homology, 48 different ABC transporters (grouped into seven subfamilies ranging from A to G) have been defined in the human genome. Their functions range from export of cholesterol (ABCA1) to regulation of chloride current (ABCC7-CFTR), and they play roles in the absorption, distribution, and excretion of pharmacological compounds.

Despite these generalizations, relatively little is known about

the functions of most members of the family. Given the high degree of similarity of ABC sequences, however, it seems plausible that additional members may also be drug exporters and may thus be associated with decreased sensitivity of cancer cells to chemotherapy. To explore that proposition, we wanted to characterize ABC gene expression in a set of cancer cells whose responses to a large number of compounds are known and whose molecular characteristics have been cataloged. The natural choice was a panel of 60 human cancer cell lines (the NCI-60) used by the Developmental Therapeutics Program (DTP) of the National Cancer Institute (NCI) to screen >100,000 chemical compounds since 1990. Included among the 60 are leukemias, melanomas, and cancers of ovarian, breast, prostate, lung, renal, colon, and central nervous system origin. Patterns of drug activity across the cell lines and patterns of cell sensitivity across the set of tested drugs have been shown to contain detailed information on mechanisms of action and resistance (Paull et al., 1989; Weinstein et al., 1992). In addition to this pharmacological characterization, the NCI-60 cells have been more extensively profiled at the DNA, mRNA, protein, and functional levels than any other set of cells in existence. Therefore, if we were to measure their expression of ABC transporters, it would be possible to link ABC transport function to

SIGNIFICANCE

Multidrug resistance of tumors is frequently associated with decreased cellular accumulation of anticancer drugs and elevated expression of ABC transporters such as MDR1. At present, relatively little is known about the substrate specificities of most ABC transporters. Here, we present a pharmacogenomic approach, in which we correlate expression profiles of all 48 human ABC transporters with patterns of drug activity in the NCI-60 cell lines. The findings are used to identify candidate substrates for several ABC transporters, as well as compounds whose toxicities are potentiated by ABCB1-MDR1. The gene expression database will serve as a high-quality "time capsule" that can be mined to generate new hypotheses and to illuminate additional features of ABC transporters and their functional relationships with other molecules.

a variety of other molecular, physiological, and pharmacological features of the cells.

We wished to focus, in particular, on the relationship between ABC expression levels and sensitivity to drugs or drug candidates, asking which of the transporters do (and which do not) confer resistance or sensitivity to various classes of agents. Previous transcript expression profiling of the NCI-60 using cDNA arrays of >9000 elements (Scherf et al., 2000) and Affymetrix Hu6800 oligonucleotide chips (Staunton et al., 2001) proved useful for identification of patterns and molecular biomarkers. However, those studies had three major limitations with reference to the ABC transporters: (1) only 15 and 11 of the 48 transporters were represented in the cDNA and oligonucleotide arrays, respectively; the total combined coverage was only 17 of 48, and the mean correlation between the two sets for the 9 transporters represented in both was only +0.43; (2) in part because of limited sensitivity, 64.2% and 58.5% of the values were undetectable above background for the cDNA and oligonucleotide arrays, respectively; and (3) crosshybridization among close family members could be expected, especially with the cDNA arrays, but also with the oligonucleotide arrays insofar as they were not designed with central focus on the ABC transporters. Since reproducible, quantitative correlations between expression and sensitivity were required for our study, we chose to measure transcript expression by the "gold standard" method, quantitative real-time RT-PCR, rather than the less sensitive, less specific microarray technology. Finding such correlations (and confirming them in follow-up studies) demonstrates the important role of ABC transporters in the drug resistance of cancer cells. One striking result was the identification of at least one compound whose toxicity appears to be potentiated, rather than antagonized, by ABCB1 (MDR1).

Results and discussion

Forty-eight ABC proteins are coded by the human genome (see <http://nutrigene.4t.com/humanabc.htm> for a comprehensive database). Figure 1 shows a clustered image map ("heat map") (Weinstein et al., 1997) that offers a visual summary of the patterns of ABC transporter expression across the 60 cell lines. The complete RT-PCR results on the 48 ABC transporters (47 determined in this work and one previously reported [Prades et al., 2002]) are presented in Supplemental Table S1 at <http://www.cancer.org/cgi/content/full/6/2/129/DC1>. A 49th ABC gene, ABCC13, is predicted to encode a nonfunctional protein (Yabuuchi et al., 2002) and therefore is not included in this study. Quantitative analysis showed that the pattern of expression is most characteristic of tissue of origin for melanoma (9 of the 10 melanoma cells cluster together on the dendrogram). The one melanoma line not found in the melanoma cluster (LOX-IMVI) is amelanotic and undifferentiated and has been shown to lack transcripts characteristic of melanoma (Stinson et al., 1992). MDA-MB435 and MDA-N were originally thought to be from breast cancer, but their appearance within the melanoma cluster is consistent with strong molecular profile evidence that they are melanoma-derived or at least melanoma-like (Scherf et al., 2000; Ellison et al., 2002; Ross et al., 2000). MDA-N is an ERBB2 transfectant of MDA-MB435. CNS (5/6), renal (5/8), and ovarian (4/6) cells tend to form clusters, whereas the leukemia, colon, lung, breast, and prostate cancer cell lines do not cluster well by tissue of origin. Overall, the coherence by tissue

of origin is moderate (see Supplemental Table S2), as indicated by a κ statistic of 0.46 (with two-tailed 95% confidence interval = 0.33–0.60). Interestingly, the two luminal, estrogen receptor-positive breast lines (T47D and MCF7) cluster together.

This database provides valuable information on the expression patterns of both known and currently uncharacterized ABC transporters. Some of them are expressed ubiquitously (e.g., ABCC1), whereas others are selectively expressed in particular cell types (e.g., ABCB5 in melanoma-derived cells; see inset in Figure 1 and Supplemental Table S3). Langmann et al. (2003) found high expression of ABCA2 in brain, ABCA3 in lung, and ABCB1 and ABCC4 in kidney. When analyzed by Monte Carlo permutation *t* test, our data show that ABCA2 is ubiquitously expressed throughout the 60 lines ($p > 0.61$ for each of the nine tissues of origin), whereas ABCA3 is selectively expressed ($p = 0.039$) in H522M, A549, and EKVX (all of them lung cancer lines). ABCB1 is indeed selectively expressed in the renal cancer cell lines ($p = 0.0059$). However, ABCC4 is only moderately expressed in those cells ($p > 0.145$ for each of the nine tissues of origin). This apparent discrepancy with respect to the results of Langman et al. may be due to heterogeneity of the human tissue samples used in that study, or may reflect distinctive characteristics of the cancer cells. The distribution of ABC transporters on the gene dendrogram appears to be independent of sequence-homology categories. ABCB2 and ABCB3, known to function as heterodimeric components of the ER transport system for peptide antigen presentation, are found in different clusters, suggesting that their reported coordinate expression is disrupted in the cancer cells. Conversely, ABCG5 and ABCG8, which also form a heterodimer, show the expected concordance in expression pattern across the 60 cells (see Figure 1).

Correlation of ABC transporter mRNA levels with drug resistance

In a previous study using cDNA microarrays, the 60 cell lines were found to cluster reasonably well by tissue of origin on the basis of expression patterns determined for a broad range of genes, but they did not cluster as well on the basis of patterns of drug sensitivity (Scherf et al., 2000). Furthermore, there was only a modest correspondence between the two clusterings. Hence, cell clusters in the present study that appear similar for both ABC transporter expression and drug activity patterns are particularly interesting. Clusters such as that consisting of ACHN, UO-31, HCT15, and NCI-ADR-RES fall into that category. Not surprisingly, ABCB1 (i.e., MDR1) is highly expressed in those cells.

Since ABCB1 (MDR1-Pgp) extrudes molecules from the cell, the activity patterns of its substrates across the 60 cell lines are expected to be negatively correlated with its pattern of expression (Shoemaker, 2000; Lee et al., 1994). Figure 2 indicates that such is indeed the case for a set of 118 compounds with putatively known mechanisms of action (Weinstein et al., 1992). Reported substrates (e.g., geldanamycin, paclitaxel and its analogs, doxorubicin and vinblastine, and bisantrene [Lee et al., 1994]), indicated by blue bars, show striking inverse correlations, whereas compounds not transported by MDR1 (e.g., hydroxyurea, camptothecins, methotrexate, and 5-fluorouracil) are invariably found to be noncorrelated or positively correlated (red bars). Of the 118 compounds, only two inversely correlated drugs, an anthrapyrazole-derivative (NSC 355644, $r = -0.36$) and Baker's soluble antifol (NSC 139105, $r = -0.3$), have not

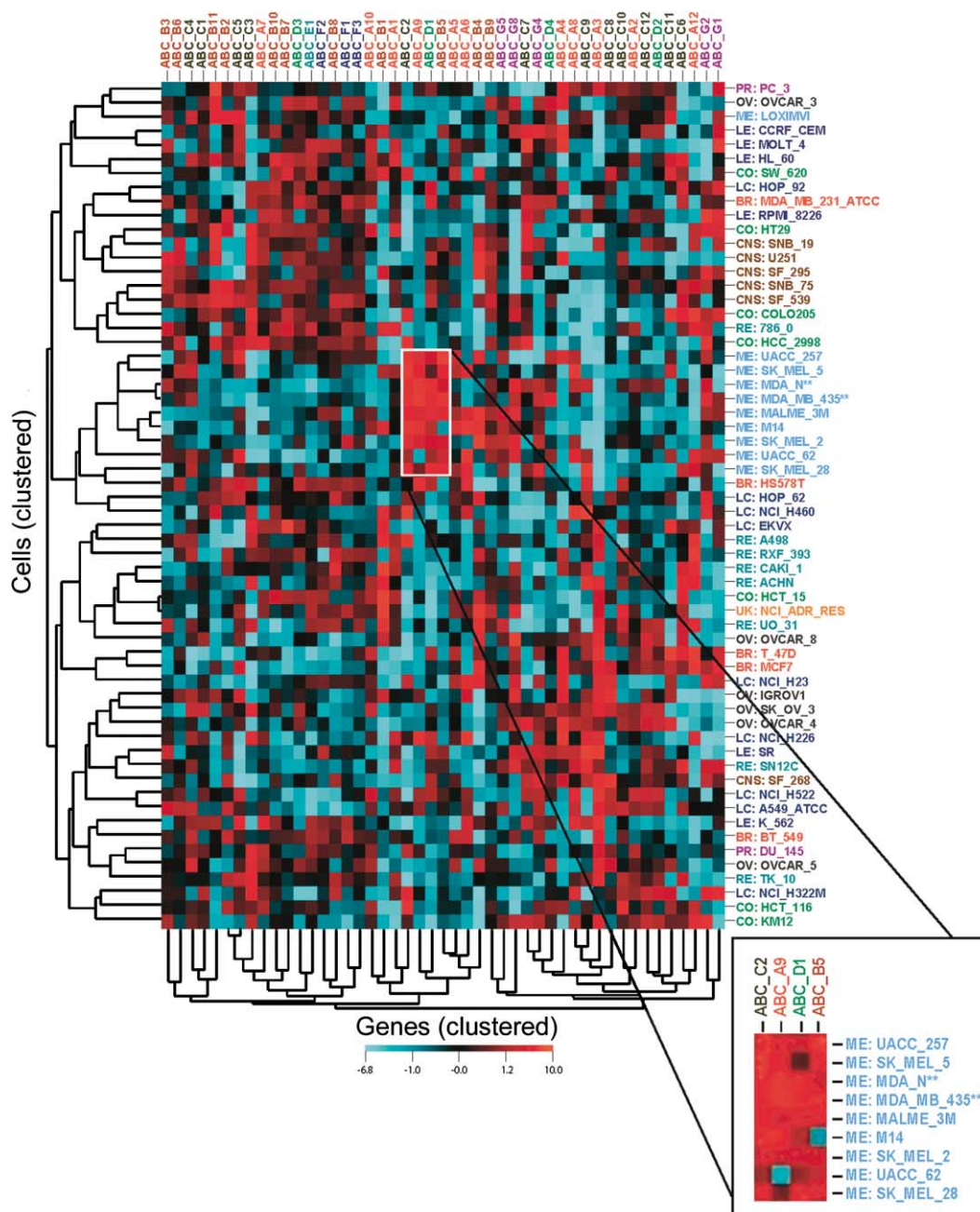


Figure 1. ABC transporter gene expression in the NCI-60 human cancer cell panel

The clustered image map shows patterns of gene expression assessed by real-time RT-PCR. Red and blue indicate high and low expression, respectively. The hierarchical clustering on each axis was done using the average-linkage algorithm with $1-r$ as the distance metric, where r is the Pearson's correlation coefficient, after subtracting row and column means. The inset highlights ABC transporters characteristically expressed in melanoma cells. For more details, see Supplemental Table S3.

previously been established as MDR1 substrates (black bars). However, resistance to Baker's antifol is reversed by verapamil, a potent inhibitor of MDR1 transport, suggesting that it is indeed an MDR1 substrate (Gupta et al., 1988).

To identify additional compounds that show significant inverse correlation with the expression of ABCB1, we extended the analysis to a larger data set containing the activity patterns of 1,429 compounds (Scherf et al., 2000). Since the measured

distribution of ABCB1 was heavily right-skewed (i.e., a small number of the cell lines expressed high levels of ABCB1 transcript), we were concerned that the correlations obtained might be based on the relationship of drug activity to MDR1 expression in only a subset of the cell types. Therefore, we also computed bootstrap distributions (based on 10,000 bootstrap samples) of all correlations to obtain estimates of variability and confidence intervals with stringent significance levels. The 18 compounds

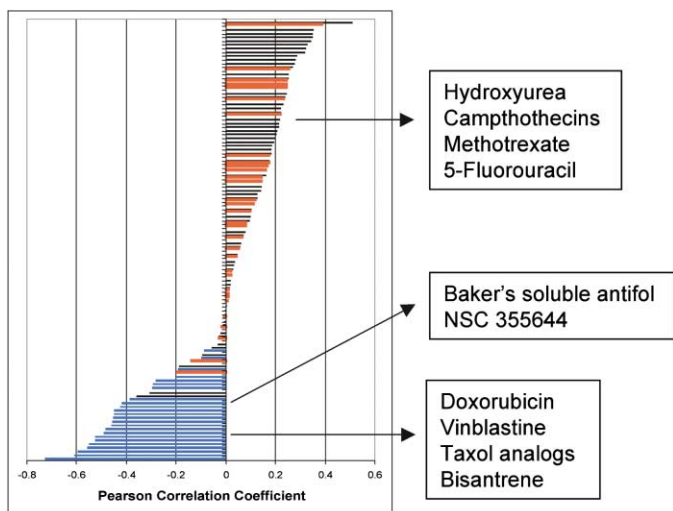


Figure 2. Relationship between drug sensitivity and ABCB1 expression in the NCI-60 for a set of 118 drugs of putatively known mechanism of action

Blue bars indicate known ABCB1 substrates; red bars indicate compounds shown in previous studies not to be substrates of ABCB1; black bars indicate compounds for which data were not available from the literature. The drug names listed at the top and bottom are commonly used, representative agents from the classes shown by red and blue bars.

that survived this statistical screening share structural features (large size, polyaromatic backbone, amphipathic character) with the well-known MDR1 substrates (Rabow et al., 2002; Supplemental Figure S1 at <http://www.cancercell.org/cgi/content/full/6/2/129/DC1>). NSC 328426 (phyllanthoside), NSC 259968 (Bouvardin), and NSC 156625 (Coralyn) have been tested in various laboratories and shown to interact with MDR1 (Lee et al., 1994; Gupta et al., 1988). The rest have not previously been implicated in MDR1-mediated resistance.

Evidence that correlations predict drug resistance due to ABC transporters

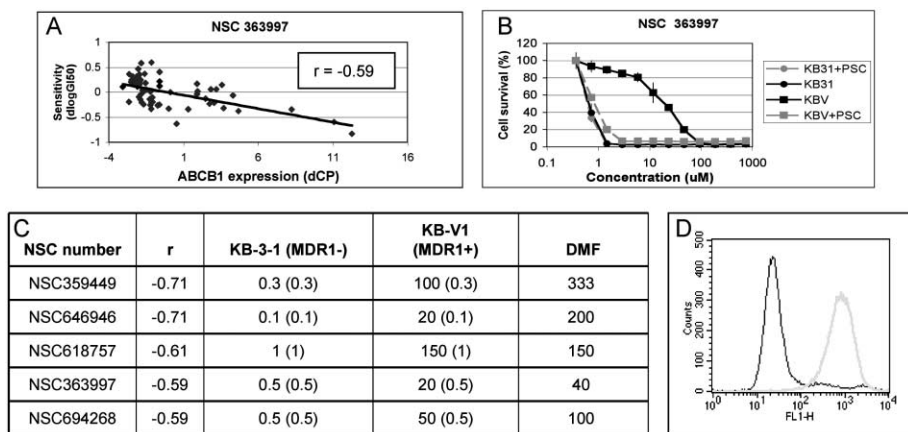
To test whether our approach using the NCI-60 does, in fact, identify new substrates, we used the MTT assay to test all top-scoring compounds that were available from DTP for follow-up experiments. KB-3-1, a human carcinoma cell line, and KB-V1, a multidrug resistant derivative of KB-3-1 that overexpresses MDR1-P-gp (Shen et al., 1986), were used for the tests. Figure 3 shows a typical result. When compared with the parental line, KB-V1 cells proved resistant to NSC 363997. PSC 833, an MDR1 antagonist, reversed the resistance, providing evidence that the observed resistance was linked to P-gp function. Further experiments showed that KB-V1 cells were 30- to 300-fold less sensitive than KB-3-1 cells to all 6 compounds available for study. This resistance of KB-V1 cells was invariably reversible by PSC 833. The intrinsic fluorescence of one of the compounds, NSC 634791, allowed us to measure the effect of MDR1 activity on its export from cells. Following incubation with NSC 634791 for 10 min at 37°C, MDR1-positive cells contained less of the fluorescent compound than did the parental KB-3-1 cell line (Figure 3). The decreased accumulation was completely reversible by addition of PSC 833 (which had no effect on the parental cells), further corroborating the hypothesis that NSC 634791 is an MDR1 substrate.

These results support the idea that correlation of ABCB1 expression with activity patterns in the 60 cell lines can be used to identify potential ABCB1 substrates among the >100,000 compounds tested at the NCI (Alvarez et al., 1995; Izquierdo et al., 1996; Bates et al., 1994; Wu et al., 1992). The chemical properties of inversely correlated compounds may also help define the "common pharmacophore" of the structurally dissimilar MDR1 substrates (Scala et al., 1997; Pajeva and Wiese, 2002; Blower et al., 2002).

ABC proteins transport a wide variety of compounds through the lipid bilayer, and identification of transported molecules should help us understand the physiological mechanisms and specificities of the transporters. To identify which ABC transporters and substrates may play roles in drug resistance of cancer cells, we calculated Pearson's correlation coefficients for a total of 68,592 relationships (48 genes \times 1429 compounds; Supplemental Table S5) using bootstrap analysis with 10,000 iterations. The analysis yielded 131 highly inverse-correlated gene-drug pairs (Supplemental Table S6), sufficiently highly correlated in the negative sense that none of their 10,000 bootstrap samples were positively correlated. This list suggests that several ABC transporters of unknown function can, in fact, influence response of cells to treatment. Assuming functional relationship, the compounds are predicted to be substrates of the respective ABC transporters. To verify this hypothesis, we performed independent followup experiments in defined systems for the most interesting correlative findings. As examples, we will describe here the results for two transporter drug pairs, one involving ABCC2-MRP2, the other involving ABCC11.

The ABCC (MRP) subfamily is comprised of nine members that transport structurally diverse lipophilic anions and function as drug efflux pumps (Kruh and Belinsky, 2003). ABCC2-MRP2 is a canalicular efflux pump with a role in the hepatobiliary excretion of bilirubin glucuronide as well as numerous pharmaceuticals. ABCC11, a recently identified member of the superfamily, has been shown to mediate the ATP-dependent transport of cyclic nucleotides and confer resistance to certain nucleotide analogs (Guo et al., 2003). Of the 1429 compounds analyzed in this study, 14 were shown by the stringent bootstrap criterion described above to be less active in cells that expressed large amounts of ABCC2. One of these compounds was available from DTP for followup testing (Figure 4A). One compound was less active in the presence of large amounts of ABCC11 (Figure 4C, Supplemental Figure S1, and Supplemental Table S6). To verify whether these highly significant negative correlations indicate functional relationships, in which ABCC2 and ABCC11 protect the cells by exporting the related compounds, we compared control cells with ABCC2-transfected or ABCC11-transfected derivatives in MTT assays. In sharp contrast to the control (sham-transfected) cells, the ABCC2-overexpressing MDCKII cells proved extremely resistant to NSC 641281, reinforcing the suggestion that NSC 641281 is an ABCC2-MRP2 substrate (Figure 4B). Similarly, ABCC11-transfected LLC-PK1 cells were 2- to 3-fold more resistant to NSC 671136 than were control, sham-transfected cells (Figure 4D), suggesting that ABCC11-mediated resistance can extend to types of compounds other than nucleotide analogs.

The real-time RT-PCR database and analytical approach presented here thus provide an unbiased method for discovering the substrate specificities of known, as well as yet uncharacterized, members of the superfamily. Activity profiles



in $\mu\text{moles/liter}$. The effect of the MDR1-P-gp inhibitor PSC 833 on IC_{50} values in KB-V1 cells is expressed as a dose modifying factor, $\text{DMF} = (\text{IC}_{50})_{\text{PSC833}} / (\text{IC}_{50})_{\text{parental}}$, where $(\text{IC}_{50})_{\text{PSC833}}$ is the value obtained in the presence of the inhibitor.

D: Accumulation of the intrinsically fluorescent compound NSC 634791 in MDR1-overexpressing KB-V1 cells. Representative histograms show the green fluorescence of cells after incubation with $1.74 \mu\text{M}$ NSC 634791 for 10 min at 37°C in the presence (gray) or absence (black) of $2 \mu\text{M}$ PSC 833.

of the 18 ABCB1 substrates were very strongly correlated with expression of the transporter. In contrast, the other two molecules considered to be “MDR transporters,” ABCC1 (MRP1) and ABCG2 (MXR or BCRP), were more weakly correlated with a smaller number of compounds, which did not include known substrates. The lack of the expected correlations may partially be explained by the statistical limitations of the correlative approach: the sample size ($n = 60$), the experimental uncertainty, and the fact that multiple tests of significance are being done simultaneously may contribute to false negative predictions (hence, the “multiple testing” corrections we describe in the text and Experimental Procedures). There are also biological limitations: first, as is the case for almost all transcript profiling studies, there remains uncertainty about the relationship between mRNA and protein expression, and the relationship of both to function. As indicated in Supplemental Table S8 and Supplemental Figure S2 at <http://www.cancer.org/cgi/content/full/6/2/129/DC1>, a comparison of the mRNA and protein expression profiles for ABCB1 and ABCG2, respectively, indicates that, at least for those two transporters, the real-time RT-PCR and protein expression data correlate quite well. Second, correlation does not imply causality. Third, there might be functionally relevant differences between the RNA messages that are not detected by RT-PCR measurements. That is, the 60 cells may contain splice variants or SNPs that influence the substrate specificities of the transporters (Imai et al., 2002; Honjo et al., 2002). Fourth, cofactors (e.g., conjugating enzymes) or transporters (e.g., ABCC1) may be expressed discordantly in the 60 cells. Fifth, the ubiquitous and consistent expression of certain ABC transporters (e.g., ABCC1) makes it difficult to detect functional relationships through correlations. Finally, the presence of MDR1 may mask the contribution of less potent transporters of the same compounds. The somewhat surprising correlation of compounds with the expression of ABCD1, a peroxisomal half-transporter associated with adrenal leukodystrophy (Mosser et al., 1993) (Supplemental Table S6), is probably a consequence of the inverse correlation between the expression of ABCD1 and ABCB1 ($r = -0.48$, see also Figure 1 and Supplemental Table S1). Compounds showing inverse correlation with

Figure 3. Verification of novel ABCB1 substrates by studies following up on NCI-60 correlations

A: Scatter plot showing the correlation (r) of ABCB1 expression with sensitivity of the 60 cells to NSC 363997 ($r = -0.59$; 99.99% two-tailed bootstrap confidence interval -0.8488 to -0.1130).

B: MTT assay dose-response curves for treatment of KB-3-1 parental cancer cells and the selected resistant variant KBV1 with increasing concentrations of NSC 363997. The dashed lines indicate the same, but in the presence of $2 \mu\text{M}$ inhibitor PSC 833 (for KB-3-1, the solid and dashed lines overlap). Values are means \pm SEM for representative experiments performed in triplicate.

C: Summary of further, analogous cytotoxicity assays performed using the other five available compounds. Concentrations resulting in 50% cell death (IC_{50}) in the absence and presence (values in parentheses) of $2 \mu\text{M}$ PSC 833 are shown

ABCD1-expression are therefore likely to be positively correlated with ABCB1 expression (Supplemental Table S5).

Positive correlations identify compounds potentiated by ABCB1

The positive correlation between activity and ABCB1 expression for some of the compounds in Supplemental Table S5 suggests that those compounds can inhibit growth of the cancer cells more strongly if MDR1 is overexpressed. For some transporters, including MDR1, several high positive correlations between gene expression and drug sensitivity are higher than would be expected by random sampling from a distribution of no real underlying correlations (in the case of MDR1, for the top 10 positive correlations, the Benjamini-Hochberg procedure [Reiner et al., 2003] estimates on average 3 false positive predictions). Thus the toxicity of at least some of the compounds increases systematically with higher MDR1 expression in the NCI-60. To investigate that possibility, we used the MTT assay and the KB-3-1/KB-V1 cell pair to test the top-scoring compound that was available from DTP (Figure 5A). Figure 5B shows that KB-V1 cells are 4- to 5-fold more sensitive than the parental KB-3-1. The finding that PSC 833 completely reversed sensitivity of KB-V1 cells to NSC 73306 strongly suggests that the increased sensitivity is due to the function of MDR1, not to other, nonspecific properties of the KB-V1 cells.

To substantiate further that the observed potentiation of NSC 73306 was not due to nonspecific factors arising during the generation of KB-V1, we repeated the MTT assays using HeLa-transfectants in which human *MDR1* is under tetracycline control. In these cells, addition of tetracycline suppresses transcription of *MDR1* mRNA, and, over a period of a few days, MDR1 disappears from the cells, providing a near-isogenic model for well-controlled experiments (Aleman et al., 2003). Figure 5C shows that the MDR1-expressing cells (MDR1-On) are 2- to 4-fold more sensitive than are MDR1-Off cells, providing strong evidence that the increased sensitivity to NSC 73306 is mediated by MDR1 function. Interestingly, NSC 73306 does not block MDR1-mediated transport of other molecules (data not shown), suggesting that it might avoid the well-documented

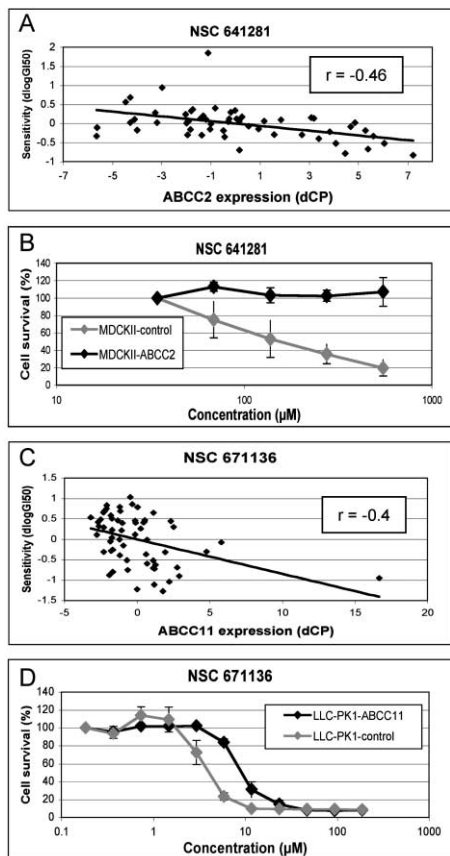


Figure 4. Prediction from the NCI-60 data of new substrates for ABCC2-MRP2 and ABCC11-MRP8, then validation of the predictions by MTT assay

A: Scatter plot showing the correlation (r) of ABCC2 expression with sensitivity of the 60 cells to NSC 641281 ($r = -0.46$; 99.99% two-tailed bootstrap confidence interval -0.7987 to -0.0440).

B: Dose-response curves for treatment of sham-transfected and ABCC2-transfected MDCKII dog kidney cells with NSC 641281. The ABCC2-expressing cells showed no signs of toxicity even at maximal concentrations.

C: Scatter plot showing the correlation (r) of ABCC11 expression with sensitivity of the 60 cells to NSC 671136 ($r = -0.4$; 99.99% two-tailed bootstrap confidence interval -0.6726 to -0.0141). Note: removal of the single, high-expressing cell line (T47D) from the analysis does not significantly reduce the observed correlation ($r = -0.38$; 99.99% confidence interval -0.7233 to -0.03915).

D: Dose-response curves for treatment of sham-transfected and ABCC11-transfected LLC-PK1 non-small cell lung cancer cells with NSC 671136.

side effects observed in clinical trials of “classical” MDR1 inhibitors (Kellen, 2003). Possible explanations for the increased (colateral) sensitivity of otherwise resistant cells include ATP depletion (Kabanov et al., 2003) and altered activity of enzymes that influence the toxicity of the compound (Bergman et al., 2003). The results reported in this section suggest that the pharmacogenomic approach presented here can be exploited to discover such MDR1-potentiated compounds, which may serve as leads for development of novel anticancer agents to treat resistant disease. Studies are underway to characterize other positively correlated compounds and to elucidate their mechanisms of action.

Conclusions

This work demonstrates correlations between expression of ABC transporters and response to cytotoxic drugs, confirmed

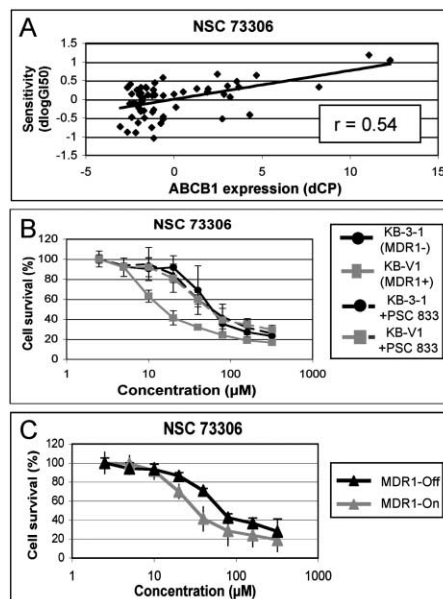


Figure 5. Prediction from the NCI-60 data, followed by independent verification, that the toxicity of NSC 73306 is potentiated, rather than inhibited, by expression of ABCB1

A: Scatter plot showing positive correlation ($r = +0.54$; 95% confidence interval 0.259 to 0.713) of ABCB1 expression with sensitivity of the 60 cell lines to NSC 73306.

B: Dose-response curves indicating that selected resistant KBV1 cells are approximately 4-fold more sensitive to NSC 73306 than are the parental KB-3-1 cells in an MTT assay. Dashed lines indicate the corresponding results in the presence of 2 μ M PSC 833, which completely abolished the heightened sensitivity of KBV1.

C: Dose-response to NSC 73306 of KB HeLa cells expressing MDR1 under tetracycline control. Cells were grown in the absence (MDR1-On) or presence (MDR1-Off) of 2 μ g/ml tetracycline for at least seven days before starting the MTT assay. Cell surface expression and function of MDR1 were verified prior to the assay by staining with anti-MDR1 monoclonal antibody (MRK-16) and by performing a functional assay based on MDR1-controlled accumulation of the fluorescent dye Calcein (Homolya et al., 1996) (data not shown). The MTT assay showed an approximately 2-fold higher sensitivity to NSC 73306 with upregulation of MDR1-P-gp. Values are means \pm SEM of triplicate measurements.

in all tested cases by evidence of resistance or sensitivity in cell lines transfected with the appropriate ABC transporters. Although in some cases the levels of resistance were relatively low, ample evidence indicates that even low (2- to 4-fold) levels of drug resistance can have a significant impact on the clinical efficacy of anticancer treatment (Gottesman et al., 2002). Animal models have also demonstrated decreased responsiveness to chemotherapy in xenografts of a KB line selected for low levels of in vitro resistance (Horton et al., 1988). For many anticancer drugs, toxic-to-therapeutic ratios are low and, therefore, even a small increase in cell-based resistance can hamper chemotherapy.

The importance to cancer therapy of circumventing MDR is evident (Sikic, 1999). Even precisely targeted anticancer drugs are subject to mechanisms of resistance. The real-time RT-PCR database presented here provides a means to identify (1) ABC transporters whose expression confers drug resistance, (2) compounds that retain activity in cells that express MDR proteins, (3) compounds that are exported by MDR proteins, and

(4) drugs that exploit hidden vulnerabilities of MDR cells. Here, we have summarized some initial conclusions from analyses to date. More importantly, however, the database will serve for many years as a high-quality “time capsule” that can be mined by ourselves and others to illuminate additional features of the ABC transporters and their complex functional relationships with other molecules. In particular, these gene expression profiles will aid studies of the physiological function of the many ABC transporters whose mechanisms remain to be characterized.

Experimental procedures

Purification of RNA

Using the RNeasy kit (Qiagen) according to the manufacturer's instructions, as described previously (Scherf et al., 2000), we purified total RNA from stocks of the cell lines used in the DTP screen. Aliquots of the RNA were stored at -70°C . The quality (purity and integrity) of the RNA samples was assessed using an Agilent 2100 Bioanalyzer with the RNA 6000 NanoLabChip reagent set (Agilent Technologies) and by assessing the ribosomal RNA bands on a native agarose gel. The RNA was quantitated using a spectrophotometer.

Quantitative RT-PCR

Expression levels of 47 ABC transporters were measured by real-time quantitative RT-PCR using the LightCycler RNA Amplification SYBR Green kit and a LightCycler machine (Roche Biochemicals, Indianapolis, IN). Specific oligonucleotide probes were designed for each of the ABC transporters using DNASTar Primer Select (DNASTAR Inc.), and they were then synthesized at Lofstrand Laboratories (Gaithersburg, MD). When possible, the amplicons were designed to encompass exon-intron boundaries to avoid amplification of genomic DNA. The sequence of ABCA13 was not known when we assembled the PCR primers. Data reporting ABCA13 expression (Supplemental Table S1 at <http://www.cancercell.org/cgi/content/full/6/2/129/DC1>) were taken from Prades et al., 2002. Since the Syber Green assay detects accumulation of double-stranded DNA, we selected those primers (from a battery consisting of about 200 primers) that amplified a single product of the correct size. A list of the primers and corresponding gene reference/accession numbers for the ABC proteins is shown in Supplemental Table S7. RT-PCR was carried out on 150 ng total RNA, in the presence of 250 nM specific primers. Following reverse transcription (20 min at 55°C), the PCR reaction consisted of 45 cycles of denaturation (15 s at 95°C), annealing (30 s at 58°C), and elongation (30 s at 72°C). No-template (water) reaction mixtures were prepared as negative controls.

Data processing

During the PCR amplification, fluorescence emission was measured and recorded in real time by the LightCycler. Crossing point values were calculated, using the LightCycler software package, by the Fit Points analysis method, with baseline fluorescence set at 1. The SyberGreen assay measures accumulation of double-stranded products, and the appearance of primer dimers limits quantitation at high cycle numbers. The specificity of amplified products was verified by melting-curve analysis and agarose gel electrophoresis (not shown). The raw results were expressed as number of cycles to reach the crossing point. If the desired product was not detected, the corresponding value was adjusted to crossing points indicating no expression. To assess the contribution of experimental artifacts, selected cell lines were assessed in replicate. The average pairwise correlation of replicate expression profiles was 0.96. The reproducibility of the measurements was further confirmed by cluster analyses, which showed that replicates clustered tightly together (data not shown).

Since the expression levels of housekeeping genes (glyceraldehyde-3-phosphate dehydrogenase [GAPDH], Porphobilinogen Deaminase [PBGD], tyrosine 3-monooxygenase/tryptophan 5-monooxygenase activation protein, and zeta polypeptide [YWHAZ]) were found to be highly variable among the 60 cell lines (not shown; however, see Vandesompele et al., 2002), they were not used as controls, and data were normalized with respect to the mean expression of the transporters (excluding ABCA13). Finally, the values were mean-centered and multiplied by -1 to indicate expression values

with reference to the mean expression of each ABC transporter across the 60 cell lines.

Drug database

More than 100,000 chemical compounds have been tested in the NCI-60 screen by the Developmental Therapeutics Program. For this study, we focused on a subset consisting of 118 compounds whose mechanisms of action are putatively classifiable (Weinstein et al., 1992) and a larger set of 1400 compounds that have been tested multiple times and whose screening data met quality control criteria described elsewhere (Scherf et al., 2000). Both sets are available at <http://discover.nci.nih.gov>. The two were combined to form a joint dataset that included 1429 compounds.

Statistical analysis

The statistical analyses were performed using the SAS software package, v8.2 (SAS Institute Inc, Cary, NC), and the R package (www.r-project.org). Two-dimensional agglomerative hierarchical cluster analysis, with average linkage algorithm and distance metric $1-r$, where r is the Pearson correlation coefficient, was performed using the CIMminer tool (<http://discover.nci.nih.gov>) to group the 60 cell lines as well as 47 ABC transporters based on the expression profiles. The resulting matrix of numbers was displayed in clustered image map form (Weinstein et al., 1997) as Figure 1.

To determine quantitatively how well the 47 genes cluster the cell lines by their tissues of origin, we used a statistical method developed by S. Lababidi (unpublished data). In that method, the κ statistic is used to indicate how well the observed clusters correspond to the nine tissue-of-origin classifications. For that calculation, one cell line, UK: NCI-ADR-RES, was excluded because it did not clearly fit into any of the usual categories.

To identify which genes are, on average, significantly over- or underexpressed in cells from a given tissue of origin (in comparison with the rest of the cell lines), we used Monte Carlo permutation t tests with 10,000 iterations to compare, for each tissue, the within-tissue mean and the mean over all of the other tissue types (this approach avoids the assumption of normality and is suitable for small sample sizes).

To narrow down the list of candidates based on correlation of the gene expression data for 48 ABC transporters and the extended list of 1429 drug activities measured in 60 cell lines (both centered around zero across the cell lines as well as across the expression values or the drug activities, respectively), we calculated the 95% bootstrap confidence intervals of Pearson correlation coefficients for all of the possible relationships (a total of $48 \times 1429 = 68,592$ correlation coefficients). The bootstrap confidence intervals were calculated using the empirical percentiles method with balanced resampling of 10,000 iterations (Chernick, 1999). Balanced resampling forces each observation to appear exactly a number of times equal to the total number of iterations. By bootstrap resampling, we avoided parametric assumptions about the distributions of the variables and incorporated possible non-normal distributional characteristics. For 10,000 bootstrap iterations with 95% confidence interval, the component of resampling error has a standard error of no more than 0.002. In recognition of the multiple testing problem we preferred a stringent critical value of $p = 0.0001$. To control the overall false positive rate, we used both a step-down procedure (Westfall and Young, 1993) and a step-up procedure (Reiner et al., 2003) to adjust for multiple testing of all 47 genes simultaneously. In the Benjamini-Hochberg procedure, the p values are computed in the standard way by permutation, assuming that all distributions are exchangeable: the number of values in the permuted data with correlations over a threshold, divided by the number of compounds and by the number of permutations. We calculated the minimum FDR (q value) at which each compound would be declared using the step-up procedure for positively correlated test statistics (again true because all correlations being compared are computed against the same ABC gene). In this procedure, the first q value for the largest correlation is the Bonferroni-corrected p value for that gene; then further q values are calculated as $q_j = \max(p_j^*1429/j, q_{-1})$. This procedure limits the expected proportion of false positives in the list $1, \dots, j$ to at most q_j .

Drugs and chemicals

The compounds designated here by NSC numbers were obtained from the Drug Synthesis and Chemistry Branch, Developmental Therapeutics Program, Division of Cancer Treatment and Diagnosis, National Cancer Institute. Colchicine and dimethyl sulfoxide (DMSO) were purchased from

Sigma Chemical Co. (St. Louis, MO), and PSC 833 was provided by Novartis Pharmaceuticals Corp. (East Hanover, NJ).

Analysis of drug sensitivity

Cell survival was measured by the MTT (3-[4,5-Dimethylthiazol-2-yl]-2,5-diphenyltetrazolium) assay. Cells were seeded in 100 μ l medium at a density of 5000 cells/well in 96-well plates, and serially diluted drug (with or without 2 μ M PSC 833) was added the following day in 100 μ l medium to give the indicated final concentration. Cells were then incubated for 72 hr at 37°C in 5% CO₂, and the MTT assay was performed following the manufacturer's instructions (Molecular Probes, Eugene, OR).

Efflux assay

Trypsinized cells were washed twice in phosphate-buffered saline (PBS). 5 \times 10⁵ cells were preincubated for 5 min at 37°C in Iscove's Modified Dulbecco's Medium (Quality Biologicals, Gaithersburg, MD) with 0.5% dimethyl sulphoxide (DMSO), with or without 2 μ M PSC 833. NSC 634791 was then added to a final concentration of 1.74 μ M, and the cells were incubated for 10 min at 37°C, then sedimented by centrifugation, and resuspended in PBS. Green fluorescence intensity was measured using a FACS Calibur flow cytometer equipped with a 488 nm argon laser (Becton Dickinson Biosciences, San Jose, CA, USA). Acquisition of events was stopped at 10,000.

Acknowledgments

We thank Balázs Sarkadi for the MDCKII cell lines. We thank the staff of NCI DTP for generation of the pharmacological database used in this study and George Leiman for editorial assistance. This work was supported by the National Institutes of Health.

Received: March 12, 2004

Revised: June 7, 2004

Accepted: June 21, 2004

Published: August 23, 2004

References

- Aleman, C., Annereau, J.P., Liang, X.J., Cardarelli, C.O., Taylor, B., Yin, J.J., Aszalos, A., and Gottesman, M.M. (2003). P-glycoprotein, expressed in multidrug resistant cells, is not responsible for alterations in membrane fluidity or membrane potential. *Cancer Res.* 63, 3084–3091.
- Alvarez, M., Paull, K., Monks, A., Hose, C., Lee, J.S., Weinstein, J., Grever, M., Bates, S., and Fojo, T. (1995). Generation of a drug resistance profile by quantitation of mdr-1/P-glycoprotein in the cell lines of the National Cancer Institute Anticancer Drug Screen. *J. Clin. Invest.* 95, 2205–2214.
- Bates, S.E., Zhan, Z., Dickstein, B., Lee, J.S., Scala, S., Fojo, A.T., Paull, K., and Wilson, W. (1994). Reversal of multidrug resistance. *Prog. Clin. Biol. Res.* 389, 33–37.
- Bergman, A.M., Pinedo, H.M., Talianidis, I., Veerman, G., Loves, W.J., van der Wilt, C.L., and Peters, G.J. (2003). Increased sensitivity to gemcitabine of P-glycoprotein and multidrug resistance-associated protein-overexpressing human cancer cell lines. *Br. J. Cancer* 88, 1963–1970.
- Blower, P.E., Yang, C., Fligner, M.A., Verducci, J.S., Yu, L., Richman, S., and Weinstein, J.N. (2002). Pharmacogenomic analysis: Correlating molecular substructure classes with microarray gene expression data. *Pharmacogenomics J.* 2, 259–271.
- Borst, P., Evers, R., Kool, M., and Wijnholds, J. (2000). A family of drug transporters: The multidrug resistance-associated proteins. *J. Natl. Cancer Inst.* 92, 1295–1302.
- Chernick, M.R. (1999). *Bootstrap Methods: A Practitioner's Guide*. (New York: John Wiley & Sons, Inc.).
- Cole, S.P., Bhardwaj, G., Gerlach, J.H., Mackie, J.E., Grant, C.E., Almquist, K.C., Stewart, A.J., Kurz, E.U., Duncan, A.M., and Deeley, R.G. (1992).

Overexpression of a transporter gene in a multidrug-resistant human lung cancer cell line. *Science* 258, 1650–1654.

Deeley, R.G., and Cole, S.P. (1997). Function, evolution and structure of multidrug resistance protein (MRP). *Semin. Cancer Biol.* 8, 193–204.

Ellison, G., Klinowska, T., Westwood, R.F., Docter, E., French, T., and Fox, J.C. (2002). Further evidence to support the melanocytic origin of MDA-MB-435. *Mol. Pathol.* 55, 294–299.

Gottesman, M.M., Fojo, T., and Bates, S.E. (2002). Multidrug resistance in cancer: Role of ATP-dependent transporters. *Nat. Rev. Cancer* 2, 48–58.

Guo, Y., Kotova, E., Chen, Z.S., Lee, K., Hopper-Borge, E., Belinsky, M.G., and Kruh, G.D. (2003). MRP8, ATP-binding cassette C11 (ABCC11), is a cyclic nucleotide efflux pump and a resistance factor for fluoropyrimidines 2',3'-dideoxycytidine and 9'-(2'-phosphonylmethoxyethyl) adenine. *J. Biol. Chem.* 278, 29509–29514.

Gupta, R.S., Murray, W., and Gupta, R. (1988). Cross resistance pattern towards anticancer drugs of a human carcinoma multidrug-resistant cell line. *Br. J. Cancer* 58, 441–447.

Homolya, L., Hollo, M., Muller, M., Mechetner, E.B., and Sarkadi, B. (1996). A new method for a quantitative assessment of P-glycoprotein-related multidrug resistance in tumour cells. *Br. J. Cancer* 73, 849–855.

Honjo, Y., Morisaki, K., Huff, L.M., Robey, R.W., Hung, J., Dean, M., and Bates, S.E. (2002). Single-nucleotide polymorphism (SNP) analysis in the ABC half-transporter ABCG2 (MXR/BCRP/ABCP1). *Cancer Biol. Ther.* 1, 696–702.

Horton, J.K., Houghton, P.J., and Houghton, J.A. (1988). Relationships between tumor responsiveness, vincristine pharmacokinetics and arrest of mitosis in human tumor xenografts. *Biochem. Pharmacol.* 37, 3995–4000.

Imai, Y., Nakane, M., Kage, K., Tsukahara, S., Ishikawa, E., Tsuruo, T., Miki, Y., and Sugimoto, Y. (2002). C421A polymorphism in the human breast cancer resistance protein gene is associated with low expression of Q141K protein and low-level drug resistance. *Mol. Cancer Ther.* 1, 611–616.

Izquierdo, M.A., Shoemaker, R.H., Flens, M.J., Scheffer, G.L., Wu, L., Prather, T.R., and Scheper, R.J. (1996). Overlapping phenotypes of multidrug resistance among panels of human cancer-cell lines. *Int. J. Cancer* 65, 230–237.

Kabanov, A.V., Batrakova, E.V., and Alakhov, V.Y. (2003). An essential relationship between ATP depletion and chemosensitizing activity of Pluronic block copolymers. *J. Control. Release* 91, 75–83.

Kellen, J.A. (2003). The reversal of multidrug resistance: An update. *J. Exp. Ther. Oncol.* 3, 5–13.

Kruh, G.D., and Belinsky, M.G. (2003). The MRP family of drug efflux pumps. *Oncogene* 22, 7537–7552.

Langmann, T., Mauerer, R., Zahn, A., Moehle, C., Probst, M., Stremmel, W., and Schmitz, G. (2003). Real-time reverse transcription-PCR expression profiling of the complete human ATP-binding cassette transporter superfamily in various tissues. *Clin. Chem.* 49, 230–238.

Lee, J.S., Paull, K., Alvarez, M., Hose, C., Monks, A., Grever, M., Fojo, A.T., and Bates, S.E. (1994). Rhodamine efflux patterns predict P-glycoprotein substrates in the National Cancer Institute drug screen. *Mol. Pharmacol.* 46, 627–638.

Litman, T., Druley, T.E., Stein, W.D., and Bates, S.E. (2001). From MDR to MXR: New understanding of multidrug resistance systems, their properties and clinical significance. *Cell. Mol. Life Sci.* 58, 931–959.

Mosser, J., Douar, A.M., Sarde, C.O., Kioschis, P., Feil, R., Moser, H., Poustka, A.M., Mandel, J.L., and Aubourg, P. (1993). Putative X-linked adrenoleukodystrophy gene shares unexpected homology with ABC transporters. *Nature* 361, 726–730.

Pajeva, I.K., and Wiese, M. (2002). Pharmacophore model of drugs involved in P-glycoprotein multidrug resistance: Explanation of structural variety (hypothesis). *J. Med. Chem.* 45, 5671–5686.

Paull, K.D., Shoemaker, R.H., Hodes, L., Monks, A., Scudiero, D.A., Rubinstein, L., Plowman, J., and Boyd, M.R. (1989). Display and analysis of patterns of differential activity of drugs against human tumor cell lines: Develop-

- ment of mean graph and COMPARE algorithm. *J. Natl. Cancer Inst.* **81**, 1088–1092.
- Prades, C., Arnould, I., Annilo, T., Shulenin, S., Chen, Z.Q., Orosco, L., Triunfol, M., Devaud, C., Maintoux-Larois, C., Lafargue, C., et al. (2002). The human ATP binding cassette gene ABCA13, located on chromosome 7p12.3, encodes a 5058 amino acid protein with an extracellular domain encoded in part by a 4.8-kb conserved exon. *Cytogenet. Genome Res.* **98**, 160–168.
- Rabow, A.A., Shoemaker, R.H., Sausville, E.A., and Covell, D.G. (2002). Mining the National Cancer Institute's tumor-screening database: Identification of compounds with similar cellular activities. *J. Med. Chem.* **45**, 818–840.
- Reiner, A., Yekutieli, D., and Benjamini, Y. (2003). Identifying differentially expressed genes using false discovery rate controlling procedures. *Bioinformatics* **19**, 368–375.
- Ross, D.T., Scherf, U., Eisen, M.B., Perou, C.M., Rees, C., Spellman, P., Iyer, V., Jeffrey, S.S., Van de Rijn, M., Waltham, M., et al. (2000). Systematic variation in gene expression patterns in human cancer cell lines. *Nat. Genet.* **24**, 227–235.
- Sarkadi, B., Muller, M., and Hollo, Z. (1996). The multidrug transporters—proteins of an ancient immune system. *Immunol. Lett.* **54**, 215–219.
- Scala, S., Akhmed, N., Rao, U.S., Paull, K., Lan, L.B., Dickstein, B., Lee, J.S., Elgemeie, G.H., Stein, W.D., and Bates, S.E. (1997). P-glycoprotein substrates and antagonists cluster into two distinct groups. *Mol. Pharmacol.* **51**, 1024–1033.
- Scherf, U., Ross, D.T., Waltham, M., Smith, L.H., Lee, J.K., Tanabe, L., Kohn, K.W., Reinhold, W.C., Myers, T.G., Andrews, D.T., et al. (2000). A gene expression database for the molecular pharmacology of cancer. *Nat. Genet.* **24**, 236–244.
- Shen, D.W., Cardarelli, C., Hwang, J., Cornwell, M., Richert, N., Ishii, S., Pastan, I., and Gottesman, M.M. (1986). Multiple drug-resistant human KB carcinoma cells independently selected for high-level resistance to colchicine, adriamycin, or vinblastine show changes in expression of specific proteins. *J. Biol. Chem.* **261**, 7762–7770.
- Shoemaker, R.H. (2000). Genetic and epigenetic factors in anticancer drug resistance. *J. Natl. Cancer Inst.* **92**, 4–5.
- Sikic, B.I. (1999). Modulation of multidrug resistance: A paradigm for translational clinical research. *Oncology* **13**, 183–187.
- Staunton, J.E., Slonim, D.K., Collier, H.A., Tamayo, P., Angelo, M.J., Park, J., Scherf, U., Lee, J.K., Reinhold, W.O., Weinstein, J.N., et al. (2001). Chemosensitivity Prediction by Transcriptional Profiling. *Proc. Natl. Acad. Sci. USA* **12**, 10787–10792.
- Stinson, S.F., Alley, M.C., Kopp, W.C., Fiebig, H.H., Mullendore, L.A., Pittman, A.F., Kenney, S., Keller, J., and Boyd, M.R. (1992). Morphological and immunocytochemical characteristics of human tumor cell lines for use in a disease-oriented anticancer drug screen. *Anticancer Res.* **12**, 1035–1053.
- Vandesompele, J., De Preter, K., Pattyn, F., Poppe, B., Van Roy, N., De Paepe, A., and Speleman, F. (2002). Accurate normalization of real-time quantitative RT-PCR data by geometric averaging of multiple internal control genes. *Genome Biol.* **3**, RESEARCH0034.
- Weinstein, J.N., Kohn, K.W., Grever, M.R., Viswanadhan, V.N., Rubinstein, L.V., Monks, A.P., Scudiero, D.A., Welch, L., Koutsoukos, A.D., Chiausa, A.J., et al. (1992). Neural computing in cancer drug development: Predicting mechanism of action. *Science* **258**, 447–451.
- Weinstein, J.N., Myers, T.G., O'Connor, P.M., Friend, S.H., Fornace, A.J., Jr., Kohn, K.W., Fojo, T., Bates, S.E., Rubinstein, L.V., Anderson, N.L., et al. (1997). An information-intensive approach to the molecular pharmacology of cancer. *Science* **275**, 343–349.
- Westfall, P.H., and Young, S.S. (1993). *Resampling-Based Multiple Testing: Examples and Methods for p-value Adjustment* (New York: Wiley).
- Wu, L., Smythe, A.M., Stinson, S.F., Mullendore, L.A., Monks, A., Scudiero, D.A., Paull, K.D., Koutsoukos, A.D., Rubinstein, L.V., Boyd, M.R., et al. (1992). Multidrug-resistant phenotype of disease-oriented panels of human tumor cell lines used for anticancer drug screening. *Cancer Res.* **52**, 3029–3034.
- Yabuuchi, H., Takayanagi, S., Yoshinaga, K., Taniguchi, N., Aburatani, H., and Ishikawa, T. (2002). ABC13, an unusual truncated ABC transporter, is highly expressed in fetal human liver. *Biochem. Biophys. Res. Commun.* **6**, 410–417.

Molecular Pharmacology
July 12, 2004

Analysis of ABC transporter expression in drug-selected cell lines by a microarray dedicated to multidrug resistance

Jean-Philippe Annereau,^{1,2} Gergely Szakács,¹ Charles J. Tucker, Angela Arciello, Carol Cardarelli, Jennifer Collins, Sherry Grissom, Barry Zeeberg, William Reinhold, John Weinstein, Yves Pommier, Richard S. Paules, and Michael M. Gottesman

Laboratory of Cell Biology, National Cancer Institute, NIH, Bethesda, Maryland (J-P.A., G.S., A.A., C.C., M.M.G.); NIEHS Microarray Group, National Institute of Environmental Health Sciences, Research Triangle Park, North Carolina (C.J.T., J.C., S.G., R.S.P.); Laboratory of Molecular Pharmacology, National Cancer Institute, NIH, Bethesda, Maryland (B.Z., W.R., J.W., Y.P.)

Running Title: Microarray platform to study drug resistant cells

Address correspondence to: Michael M. Gottesman, Laboratory of Cell Biology,
National Cancer Institute, NIH, 37 Convent Drive, Room 2108, Bethesda, MD 20892-
4256. Email: mgottesman@nih.gov

Text pages: 33

Number of tables: 2 (plus 6 supplemental)

Number of figures: 2

Number of references: 43

Number of words: Abstract: 211

Introduction: 727

Discussion: 1208

ABBREVIATIONS: MDR, Multidrug Resistance, MRP2 Multidrug resistance associated protein 2; BSO, L-buthionine-[S,R]-sulfoximine; DTNB, 5,5'-Dithiobis 2-nitrobenzoic acid; CPT, Camptotecin; 9NC, 9-nitro-Camptothecin; SAGE, Serial Analysis of Gene Expression; GO, Gene Ontology; HUGO, Human Genome.

ABSTRACT

The discovery of the multidrug resistance protein 1 (MDR1), an ATP-binding cassette transporter able to transport many anticancer drugs, represents a clinically relevant breakthrough in multidrug resistance. Although the overexpression of ABC transporters such as P-gp/ ABCB1, MRP1/ABCC1 or MXR/ABCG2 appears to be a major cause of failure in the treatment of cancer, acquired resistance to multiple anticancer drugs may also be multifactorial, involving alteration of detoxification processes, apoptosis, DNA repair, drug uptake, and overexpression of further ABC transporters. We created a microarray platform to evaluate relative levels of transcriptional activation among genes involved in various mechanisms of resistance. In the ABC-ToxChip, a comprehensive set of genes important in toxicological responses (2,200 cDNA probes together with ~18,000 oligonucleotide probes) are complemented with probes specifically matching ABC transporters as well as oligos representing 18,000 unique human genes. By comparing the transcriptional profiles of KB-3-1 and DU-145 cells to resistant derivatives selected in colchicine (KB-8-5), and 9-nitro-camptothecin (RCO.1), respectively, we demonstrate that ABC transporters (ABCB1/MDR1 and ABCC2/MRP2, respectively) show dramatic overexpression, whereas the glutathione S-transferase gene (GST-Pi) shows the strongest decrease among the 20,000 genes studied. The results were confirmed by quantitative RT-PCR and immunohistochemistry. These results suggest that custom-made, dedicated microarrays will be helpful to elucidate mechanisms leading to anticancer drug resistance.

INTRODUCTION

Mechanisms leading to multidrug resistance (MDR) include increased drug efflux (Shen et al., 1986a; Gottesman et al., 2002), decreased drug uptake (Shen et al., 2000), recruitment of drug-processing and metabolizing enzymes (Schuetz et al., 1996), conjugating enzymes (Goto et al., 2002), alteration of the DNA repair activity, reduction of cell susceptibility to apoptosis (Reinhold et al., 2003), and mutation of specific drug targets (Urasaki et al., 2001). *In vitro* selected cell lines most likely utilize more than just one of the pathways cited above (Gottesman et al., 2002).

Tools, such as the oligo-based, cDNA-based microarrays or SAGE (Serial Analysis of Gene Expression, Velculescu et al., 1995) are relevant methodologies to screen for multifactorial mechanisms of drug resistance. However, microarray technology has several inherent problems that hamper definitive interpretation. Typical problems with the current technology include the necessity of validation by complementary technology such as further microarray analyses or RT-PCR (Lee et al., 2003). The lack of sensitivity could also prevent the detection of infrequent transcripts (Evans et al., 2002) and lead to biased conclusions. In research aiming at the elucidation of mechanisms underlying acquired drug resistance, the shortcomings of arrays available at the time of our study originated from the low representation of genes of interest and the general lack of specificity of the probes. This is especially true for the ABC (ATP Binding Cassette) superfamily, which has 48 members sharing high sequential similarity with highly divergent functions and/or specificities.

Like endogenous and exogenous toxic compounds, anti-cancer drugs diffuse through the cell membrane. One of the most interesting features of ABC transporters is that these proteins can transport many substrates across the membrane, including anti-cancer drugs, ions and peptides. MDR1 or P-gp was the first ABC transporter found to confer MDR in resistant tumor samples and *in vitro* selected cell lines (Shen et al., 1986b). Using cell lines selected in various anti-cancer drugs, overexpression of further ABC transporters, such as ABCC1-MRP1 (Cole et al., 1992), and ABCG2- MXR-BCRP (Miyake et al., 1999; Doyle et al., 1998) were clearly shown to be associated with drug export and resistance. In experiments performed *in vitro*, other members, such as ABCA2 and ABCB4 (MDR3) were shown to actively transport cytotoxic drugs (Laing et al., 1998; Smith et al., 2000). Among the members of the MRP (ABCC) subfamily, MRP2 (ABCC2, cMOAT) transports GSH-S-conjugates (e.g., leukotriene C4 and 2,4-dinitrophenyl-S-GSH), oxidized GSH (GSSG), glucuronide conjugates (e.g., glucuronidated bilirubin and bile salts), and sulfate conjugates of certain bile acids (e.g., 3-sulfatolithocholytaurine), (Muller et al., 1994). By their ability to transport nucleoside analogues, ABCC3-MRP3 and ABCC5-MRP5 are proteins that are thought to cause certain forms of drug resistance (Reid et al., 2003). Recently, ABCC11-MRP8 has also been associated with anti-cancer drug export (Guo et al., 2003; Szakács et al., 2004).

Although microarrays make possible the screening of thousands of genes in the same matrix, attempts aiming to address anticancer drug resistance have been biased in their interpretation by microarrays bearing a low number of ABC transporter superfamily probes (Lamendola et al., 2003). Here, we report the design and the application of a dedicated ABC-ToxChip, in which we complemented a comprehensive

set of detoxifying genes with probes specifically matching ABC transporters. Instead of using the short 25-mer probe-technology (Affymetrix, Santa Clara, CA), not optimized for detecting infrequent transcripts, we printed a combination of longer 70-mer oligo probes and 200-500 bp fragments, offering higher sensitivity due to the longer complementary sequences.

Camptothecin (CPT) derivatives such as CPT-11 (Irinotecan) or Hycamtin (Topotecan) are increasingly used in anti-tumor therapy against colon or lung cancers (Kudoh et al., 1998). 9-Nitro-camptothecin (9NC) has recently been used in phase II studies for pancreatic cancer and is now in phase 3 clinical trials (Pantazis et al., 2003). Many factors, such as specific mutations in topoisomerase I, complemented by a general alteration of apoptotic regulation, have been proposed to explain the phenotype of camptothecin resistance in a prostate cancer cell line (RCO.1) selected for resistance to 9NC (Reinhold et al., 2003; Urasaki et al., 2001; Chatterjee et al., 2001). To specifically address the role of detoxifying enzymes and ABC transporters in camptothecin resistance, we compared the transcriptional profiles of the parental prostate cancer DU145 cells and their 9NC-selected derivative cell line, RCO.1. Here, we show that in RCO.1 cells, 9NC resistance is accompanied by the differential expression of ABCC2-MRP2 and enzymes regulating glutathione metabolism.

Materials and Methods

Taq polymerase and RT-PCR reagents were from Invitrogen (Carlsbad, CA). Reagents for quantitative RT-PCR were from Roche. Inc. (Indianapolis, IN). High-density microarrays were printed in the NIEHS facility. 9NC (Ref. C0156) was purchased from LKT laboratories (St. Paul, MN).

Cell Lines and Cell Culture. DU-145 and its 9NC-selected derivative, RCO.1 cell lines were a generous gift from Dr. P. Pantazis (University of Miami, Coral Gables, FL). Cells were cultured in RPMI (Invitrogen) supplemented with 10% tetracycline-approved FBS (Hyclone Inc. Logan, UT), and 2mM L-glutamine by Quality Biological, Inc., (Gaithersburg, MD) at 37°C with 5% CO₂. Resistance to camptothecin analogs of RCO.1 was maintained with passage in camptothecin-containing media (0.1 µM) every three months.

RNA Preparation. Total RNA was purified as described in Reinhold et al. (2003). For the preparation of the RNA used in the microarray analysis or RT-PCR, cells were cultured in non-selective media.

Microarray Design. A 20K Human Oligo/cDNA hybrid Chip, printed at NIEHS (NIEHS Microarray Group, National Institute of Environmental Health Sciences) was used for gene expression profiling experiments. The chip contained three categories of probes:

1. 96 ABC-specific probes (matching 36 ABC transporters), consisting of either cDNA probes developed in-house or oligo-probes obtained from Operon Technologies

(Qiagen, Valencia, CA). To create the cDNA-probes, we performed PCR amplifications using specific primers on full-length cDNA sequences (ABCB1-MDR1, ABCC1-MRP1, ABCC2-MRP2, ABCG2-MXR, ABCC7-CFTR and ABCB11) or on cDNA prepared from cells rich in a given transporter (unpublished data). We used a blast-based algorithm to increase specificity: first, we aligned the targeted transporter with members of its own subfamily to locate a candidate region representing minimal overlap. Specificity was then verified by blasting the candidate sequence against the whole non-redundant human database. The probes synthesized by RT-PCR were TA cloned (Invitrogen), as detailed in Table 1. ABC transporters are named using the HGNC nomenclature (<http://nutrigene.4t.com/humanabc.htm>). When more than one probe was used for an ABC transporter, the probe name was chosen to match the closest Ref-Seq entry from the NCBI (i.e., ABCC3 (NM-003786, AJ294547.1, AJ294559.1, AJ294558.1)). The closest exon matching the probe sequence is indicated in Table 1.

2. 2,200 probes matching genes important in toxicological responses (cDNA clones from the NIEHS ToxChip version 3.0 (Nuwaysir et al., 1999)). The NIEHS set contains approximately 2,200 known human genes involved in pathways such as response to estrogens, polycyclic aromatic hydrocarbons, peroxisome proliferators, DNA damage, and oxidant stress, as well as genes involved in apoptosis, cell cycle, tumor suppression, signal transduction and transcription.

3. 18,000 genome-wide 70mer probes obtained from Operon Technologies (Qiagen, Valencia, CA). A complete listing of the two sets (Human Oligo gene-set and the Human TOX V1.0-set) printed on the ABC-ToxChip is available at <http://dir.niehs.nih.gov/microarray/annereau/home.htm>.

Gene Representation on the Microarray. The gene ontology classification (<http://www.geneontology.org/#ontologies>) annotates each gene in three categories: Molecular Function, Biological Process and Cellular Component. To search the Gene Ontology (GO) reference for each gene represented on our microarray, we used the human genome annotation (HUGO) reference converted from the Gene Accession number by the Source data base (<http://genome-www5.stanford.edu/cgi-bin/SMD/source/sourceSearch>) and the MatchMiner database (<http://discover.nci.nih.gov/matchminer/html/index.jsp>). Extraction of the GO annotation starting keyword entry was performed on the QuickGO server at EBI (<http://www.ebi.ac.uk/ego/>).

Microarray Spotting. The oligonucleotides were resuspended in ArrayIt Spotting Solution Plus buffer (Telechem, San Jose, CA) and spotted at a concentration of 40 μ M onto poly-L-lysine coated glass slides using a modified, robotic DNA arrayer (Beecher Instruments, Bethesda, MD). The spotting was performed in an environmentally controlled chamber with a temperature of 25°C at 40% relative humidity. After printing, the arrays were cross linked in a Stratalinker at a power of 300 millijoules and blocked with succinic anhydride/1-methyl-2-pyrrolidinone (protocol available at: <http://dir.niehs.nih.gov/microarray/methods.htm>)

Microarray Hybridizations. Each total RNA sample (25 μ g) was labeled with Cyanine 3 (Cy3) or Cyanine 5 (Cy5)-conjugated dUTP (Amersham, Piscataway, NJ) by

a reverse transcription reaction using the reverse transcriptase, SuperScript II (Invitrogen, Carlsbad, CA), and the primer, Oligo dT (Amersham, Piscataway, NJ). The fluorescently-labeled cDNAs were mixed and hybridized simultaneously on the microarray chip. Each RNA pair was hybridized to a total of 4 arrays employing a fluor reversal accomplished by labeling the control sample with Cy3 in 2 hybridizations and with Cy5 in the other 2 hybridizations. After hybridization, arrays were washed with Telechem wash buffers A, B, and C (Telechem International Inc., Sunnyvale, CA) for 2, 5, and 5 minutes respectively. The hybrid chips were scanned with an Agilent Scanner (Agilent Technologies, Wilmington, DE) using independent laser excitation of the two fluorors at 532 and 635 nm wavelengths for the Cy3 and Cy5 labels, respectively. Results are available at <http://dir.niehs.nih.gov/microarray/annereau/home.htm>.

Microarray Outlier Filtering. Raw pixel intensity images were analyzed using ArraySuite v2.0 extensions of the IPLab's image processing software package (Scanalytics, Fairfax, VA). This program uses methods that were developed and previously described by Chen et al. (2002) to locate targets on the array, measure local background for each target and subtract it from the target intensity value, and to identify differentially expressed genes using a probability-based method. The data were filtered with a cut-off at the intensity level just above the buffer blank measurement values to remove genes having one or more intensity values in the background range. After pixel intensity determination and background subtraction, the ratio of the intensity of the treated cells to the intensity of the control was calculated. The ratio intensity data from all probes on the Human Oligo chip was used to fit a probability distribution to the ratio

intensity values. The resulting probability distribution was used to calculate a 95% confidence interval for the ratio intensity values. Genes having normalized ratio intensity values outside this interval were considered to show significant differential expression.

Statistical Analysis and Filtering the Outliers. For each of the 4 replicate arrays for each sample, lists of differentially expressed genes at 95% confidence levels were created and deposited into the NIEHS MAPS database (Bushel et al., 2001). Genes that indicated fluorescence bias or high variation were not considered for further analysis. Assuming that the replicate hybridizations are independent, a calculation using the binomial probability distribution indicated that the probability of a single gene appearing on this list when there was no real differential expression was <0.00048 . The entire dataset is available at <http://dir.niehs.nih.gov/microarray/annereau/home.htm>.

Identification of Relevant Biological Processes. The GoMiner software, which can be downloaded at the LMB/NCI web site (discover.nci.nih.gov) offers a newly implemented feature—the ability to point out a biological process that has been altered. The algorithm uses Gene Ontology entries found in the outlier list as well as all the GO entries available on the chip. The Gene Ontology database lists three structured, controlled vocabularies (ontologies) that describe gene products in terms of their associated biological processes, cellular components and molecular functions in a species-independent manner. The GO entries are hierarchically linked, thus allowing pooling and construction of cluster genes of crossed pathways. The bias in the gene

representation (only a part of the genome is represented on the chip) could potentially lead to misleading conclusions. To evaluate the statistical weight of each emerging cluster, we have used the updated version of GoMiner that is now able to process multiple comparison analyses (Zeeberg et al., 2003, <http://discover.nci.nih.gov>). The statistical relevance of a candidate process found to be altered with drug resistance is therefore calculated in comparison to the overall processes that could be theoretically identified.

Quantitative RT-PCR. Real time PCR was performed with a Light Cycler RNA SYBR Green kit (Roche Biochemicals, Indianapolis, IN). The reaction was in a 20 μ l final volume with 0.150 μ g of purified total RNA, 4 μ l PCR mix provided by the manufacturer, 4 μ l $MgCl_2$ (25 mM), 2.5 μ l of each primer (2 μ M), 0.4 μ l of enzyme mix and DEPC- H_2O . Optimized and specific primers were designed to produce a unique band for the 47 ABC transporters (Szakács et al., 2004). The reverse transcriptase (RT) reaction was performed at 55°C for 20 min. cDNA generated by the RT step was denatured at 95°C for 20 sec. Amplification of the cDNA was achieved in 45 cycles of 95°C, 5 sec; 58°C, 10 sec; 72°C, 13 sec. Fluorescence was recorded during the elongation phase at 72°C.

Western Blots. Following SDS-Page electrophoresis on 6% acrylamide SDS-Page gels (Invitrogen, Carlsbad, CA), samples (50 μ g) were electro-blotted on nitrocellulose membranes (Invitrogen). Membranes were saturated with a 10%, fat-free milk solution (Giant Foods, Inc., Landover, MD), and then incubated overnight in the presence of an

anti-MRP2 primary antibody (M-8316, Sigma, St-Louis, MO) at 1:1000 dilution. An HRP-conjugated secondary antibody (anti-rabbit Goat IgG (Jackson ImmunoResearch Laboratories, Inc., West Grove, PA) was applied for 1 hour at 1:2000 dilution. ECL was purchased from Amersham (Pharmacia Biotech, Inc., Little Chalfond Bucks, UK).

For GAPDH and GST-Pi, 12% SDS-Page gels were used (Invitrogen). Primary antibodies were anti-GAPDH RDI-TRK-5G4-6C5 (Research Diagnostic Inc., Flanders, NJ) at 1:1000 dilution and anti-GST-P IgG1 at 1:1000 dilution (BD Biosciences Pharmingen, San Diego, CA). The secondary antibody was Goat-IgG anti-IgG Mouse HRP-conjugated (Jackson ImmunoResearch Laboratories, # IR-115-035-164) at 1:2000 dilution.

Results

Creation of a Hybrid cDNA/Oligo ABC-ToxChip to Study Drug Resistance.

The ABC-ToxChip is a dedicated microarray to study the drug resistance of cancer cells. The platform contains three distinct sets of probes (Fig. 1A). The first set of probes targets 36 ABC transporters (70-mer oligonucleotides, and cDNA probes). Specificity and sensitivity was ensured by targeting each transporter with multiple probes (Table 1). Since multidrug resistance can be regarded as a detoxification problem, we also applied the TOX-probes (Nuwaysir et al., 1999) that cover known detoxification genes involved in response to estrogens, polycyclic aromatic hydrocarbons, peroxisome proliferators, DNA damage and oxidant stress, as well as genes involved in apoptosis, cell cycle, tumor suppression, signal transduction and transcription. To reduce the problem of sequence reliability encountered in commercially available cDNA clones (Knight et al, 2001), the probes (200-500 bp) of the TOX-set were derived from sequence-verified plasmids originally compiled at the National Institute of Environmental Health Sciences (NIEHS). To avoid the risk of a biased analysis inherent to highly specialized microarrays, we completed the chip with 18,000 probes (GEN-set) targeting the human transcriptome (Operon Inc., Alameda, CA). To overcome the qualitative errors found on various platforms and to rule out possible cross-hybridization, we verified the specificity of the cDNA and 70-mer oligo sequences by extensive *in silico* analysis (not shown).

Of the 18,398 probes represented by 16,329 oligo probes and 2069 cDNA probes matching a valid gene reference, 11,813 were annotated with HUGO references,

using the Source / Matchminer databases (Zeeberg et al., 2003). The cDNA, or detoxification set has 1,394 probes with valid GO annotations, of which 1,152 are also represented in the GEN-set. The distribution of gene ontology entries proves that the cDNA set is indeed enriched in genes related to detoxification processes. For example, genes related to drug stress and DNA repair are highly represented in the cDNA TOX set (1.3% and 3.3% of the total genes, respectively), as compared to the GEN-set (0.3% and 0.6%, respectively).

Validation of the ABC-ToxChip Using an Established Model of Resistance.

To identify markers of resistance or sensitivity to colchicine, we compared two cell lines using the ABC-ToxChip. KB-8-5 cells were derived from parental KB-3-1 cells by selection in colchicine (Akiyama et al., 1985). RNA samples from the two cell lines were reverse transcribed, labeled with Cy3/Cy5 and hybridized to 4 ABC-ToxChip slides. After filtering the data for the most reliably differentially expressed genes with a statistical confidence of 95%, the comparison revealed 241 statistically significant variations (Table S1). Among the four cross-labeled experiments, 98 hits (40.6%) appeared in all 4 replicate scans. The rest (59.4%) were significant in only 3 of the 4 replicate slides.

In total we identified 13 differentially expressed genes associated with colchicine resistance with a ratio above 2.7 (Fig. 1C). Among the 20,000 genes, ABCB1/P-gp showed the highest variation (10-fold fluorescence ratio) associated with colchicine resistance. Closely related members of the same subfamily (ABCB2-3-4) showed only moderate (about 2-fold) changes, presumably due to cross-hybridization, confirming the improved specificity of our dedicated microarray for ABC transporters. To verify the

patterns of ABC-expression detected by the microarray analysis, we measured the expression of 47 ABC transporters by real time RT-PCR. The analysis confirms that ABCB1 (MDR1) shows the largest variation among the ABC transporters, while the expression of the other members is virtually unchanged (Fig. 1B). Comparison of KB-3-1 cells to KB-C1, a derivative showing extreme resistance (1 ug/ml) of colchicine showed the highest change in the expression of the same genes (log2ratio of 6.32 and -4.2 for ABCB1/MDR1 and GST-Pi, respectively, data not shown).

Increased expression of MDR1 (ABCB1) and the glycoprotein hormone subunit (GPH) was revealed by several independent probes (#M29447, #M37723 and #S70585, #W86681 for GPH and ABCB1, respectively). The list of further upregulated genes include Interleukin 8, MHC-I, COX-2 and the Interferon stimulated protein, while GST-Pi, Calcium-binding protein A10, Voltage gated sodium channel and EGF-like domain 5 are markedly downregulated in KB-8-5 cells as compared to the sensitive cell line. We used the information provided by HUGO to process the *ab initio* and hypothesis free GoMiner algorithm to detect biological processes that are represented by the differentially expressed genes and could possibly explain mechanisms leading to colchicine resistance.

Among 241 statistically significant outlier genes (see Materials and Methods), we identified 125 unique HUGO entries (52%). Since the dedicated design of the microarray can introduce a bias in analysis, with, for example, an overrepresented class of detoxifying genes printed, we evaluated the significance of the results in the light of the global representation of the GO ontology annotation entries. The GoMiner analysis indicates that expression of genes found to be altered by selection for colchicine

resistance is linked to antigen presentation and carbohydrate metabolism ($P < 0.0001$). In Table S2, we present the statistically relevant biological processes that can be associated with colchicine resistance. In Table S3, we present the genes that belong to the altered gene ontology categories related to antigen presentation, carbohydrate metabolism, transport and oxydoreduction.

Application of the ABC-ToxChip to Study 9-nitro-camptothecin Resistance.

We next turned our attention to RCO.1, a prostate cell line selected in 9NC, where mechanisms leading to the resistant phenotype have not been fully understood. This cell line was created by selecting parental DU-145 cells in 0.1 μM 9-nitro-camptothecin (Urasaki et al., 2001). RCO.1 presents a unique profile of multidrug resistance with a selective resistance to camptothecin analogs, NB-506 (an inhibitor of topoisomerase I) and cisplatin, while being sensitive to drugs known to be exported by ABCB1-MDR1 or ABCC1-MRP1 (Chatterjee et al., 2001). Several laboratories have attempted to elucidate this atypical profile of resistance: a mutation of topoisomerase I, preventing the binding of camptothecin analogs (Chatterjee et al., 2001) and an alteration of the apoptotic pathway (Chatterjee et al., 2001; Reinhold et al., 2003) have been proposed as explanations. However, an exhaustive analysis of ABC transporters or genes involved in detoxification has not been reported to date. To explore the role of ABC transporters and other detoxifying genes in 9NC resistance, we compared the mRNA expression profiles of DU-145 and RCO.1 cells using the ABC-ToxChip. Total cellular RNA was extracted from both cell lines. Since the phenotype of acquired 9NC resistance is stable without the pressure of selection, RNA was collected from cells cultured in drug-free medium. Microarray experiments were performed as described

previously for the KB cells. To control for labeling differences, reactions were carried out in quadruplicate, and the fluorescent dyes were switched.

The list of the most significant differentially expressed genes is shown in Figure 1C and in Table S4. Among the 20,000 genes, ABCC2-MRP2 shows one of the highest variations associated with 9NC resistance. First named the canalicular multispecific organic anion transporter (cMOAT), ABCC2-MRP2 is a 190-kDa phosphoglycoprotein localized in the canalicular (apical) membrane of hepatocytes. It is involved in the transport of organic anions, including sulfated and glucuronidated bile salts. Overexpression of MRP2 has been suggested to confer resistance to anti-cancer drugs such as cisplatin, anthacyclines, and methotrexate, and animal models have shown reduced hepatic transport of camptothecins (Horikawa et al., 2002).

Gamma-glutamylcysteine synthetase (GCS), also known as glutamate cysteine ligase, a key enzyme in glutathione metabolism, was coordinately up-regulated with MRP2, in keeping with the findings that MRP2 exports glutathione conjugates (Paulusma et al., 1996). In contrast, despite its general up-regulation in cancer cells, the expression of GST-Pi, catalyzing the conjugation of glutathione to electrophilic carcinogens, was significantly reduced in RCO.1 cells, as it was in the colchicine-selected KB cells.

Additional changes which might contribute to the pattern of drug resistance in RCO.1 cells were also observed. The up-regulation of various histones in the selected cells may provide means for the cells to adapt to the 9NC-mediated DNA insult. Further changes associated with drug resistance include reduction in the tumor-associated antigen L6 (transmembrane super family 4 or TM6). TM6 is also found to be down-

regulated in cisplatin-resistant cells (KB/cDDP) (Higuchi et al., 2003), indicating that the loss of TM6 expression is potentially associated with resistance to camptothecin and cisplatin. Of the genes presented in Table S4, the decreased expression of GST-Pi, NKT4 and Interleukin-4 in RCO.1 cells was also observed by an independent microarray analysis (Table 2), which however failed to detect the overexpression of ABCC2-MRP2.

Although 85 of the 125 outliers (68%) have a HUGO reference, the GoMiner algorithm did not suggest specific biological processes to be significantly linked to camptothecin resistance. (See tables S5 and S6 for the biological processes and their associated genes linked to camptothecin resistance.)

We next sought to determine whether the differential expression of ABCC2-MRP2 and GST-Pi could be confirmed by quantitative RT-PCR. The results show that among the 47 ABC transporters, ABCC2-MRP2 is overexpressed in the resistant cell line, while the expression of the other members is unchanged (Fig. 2A). Since mRNA levels may not reflect protein expression, due to modulation of translation or inhibition of protein processing, we analyzed the expression of MRP2 and GSTPi at the protein level. Fig. 2C shows that the protein expression of these two genes follows the pattern predicted by the RNA analyses: In the RCO.1 cells, GST-Pi is down-regulated and ABCC2-MRP2 is up-regulated as compared to the parental line.

Discussion

In this report, we present a new microarray design and analysis to study multifactorial drug resistance. We have designed and synthesized probes to match 36 of the 48 ABC transporters to print them on a platform enriched in genes involved in detoxification, as well as a general set of 18,000 human gene probes (the ABC-ToxChip). To increase at the same time sensitivity and specificity for genes involved in drug resistance, we combined on the same chip both cDNA and oligos probes. This approach provides an example of how existing microarray platforms may be modified to target a gene family with high sensitivity and specificity to study multidrug resistance of cancer. In this study, we confirm that overexpression of ABCB1 is a principal component of the genetic changes underlying colchicine resistance. KB-8-5 cells express ABCB1-MDR1 at a moderate level, comparable to that found in clinical samples. We had made several earlier attempts to identify the molecular signature of colchicine resistance, using a 9K cDNA microarray platform (UniGemV2, Advanced Technology Center, NIH, Gaithersburg, MD). The UniGemV2 chip failed to identify the overexpression of ABCB1-MDR1 and suggested, incorrectly, that the main outlier is ABCB2, a protein closely related to ABCB1 (not shown). ABCB2-TAP1 is a component of the ER transport system for peptide antigen presentation and is not believed to play a role in the efflux of cytotoxic compounds, and, in fact, was not actually overexpressed in KB-8-5 cells.

Analysis of a prostate cancer cell line (RCO.1) indicated the potential role of ABCC2/MRP2 in 9NC resistance. Previous studies have shown that the resistance of RCO.1 cells was also due to a mutation in the Topoisomerase 1 gene (Urasaki et al.,

2001) and to a defect in apoptosis pathways (Reinhold et al, 2003; Chatterjee et al., 1996), suggesting that resistance to camptothecin is multifactorial. Previous attempts to elucidate mechanisms leading to camptothecin resistance included microarray analyses of parental DU145 cells and RCO.1 cells (Reinhold et al., 2003), using a UniGem microarray. Despite the high expression of ABCC2/MRP2 in the resistant cells (Fig. 1C), its overexpression wasn't detected in these earlier studies. Taken together, these findings suggest that the specific targeting of ABC transporters in dedicated, custom-made arrays may improve the specificity and sensitivity of earlier generation microarrays. Typical shortcomings of microarray platforms may be attributed to imperfect clone annotation as well as the lack of specificity of probes targeted at overlapping or homologous sequences of closely related proteins, such as ABCB1 and ABCB2. These considerations prompted us to create our own, dedicated microarray platform. In order to ensure specificity, we designed probes uniquely matching the target transporters. The ABC-ToxChip analysis of cells selected in colchicine and 9NC demonstrate the elevated expression of ABCB1 and ABCC2, respectively. Since gene expression levels obtained by even the most carefully designed microarrays must be validated by independent methods, we also designed specific primers for the human ABC transporters (Szakács et al, 2004). The quantitative RT-PCR data confirmed the pattern of ABC transporter expression and suggested that there are no further ABC transporters differentially expressed in the cells analyzed in this study. Through the systematic analysis of ABC transporters and other genes of detoxification, our data provide novel information about the effect of 9NC selection on gene expression.

While the GoMiner algorithm did not identify major biological processes linked to 9NC resistance, the list of differentially expressed genes may provide some insight into mechanisms underlying (or accompanying) resistance. An interesting example is Radixin, which is overexpressed in the 9NC selected cell line. Radixin belongs to the ERM (Ezrin-Radixin-Myosin) protein complex, and is involved in localization of integral membrane proteins. Radixin $-/-$ mice have Dubin-Johnson-like symptoms (Kikuchi et al, 2002), because MRP2 is not properly localized to the plasma membrane.

The coordinated expression of phase II (conjugating) and phase III (efflux) systems has been shown to improve cellular detoxification (Morrow et al., 2000). We found significant changes in the expression of two glutathione metabolism-related genes. GST-Pi is involved in coupling electrophilic drugs to reduced glutathione, and GCS is the rate-limiting enzyme for glutathione synthesis. Neither GST-Pi mRNA nor the protein is detectable in the resistant cell line. This observation is striking given the association of high GST-Pi levels found in several resistant tumors and cell lines (Liu et al., 2001; Tew, 1994). In contrast, gamma glutamate cysteine synthetase (GCS) is overexpressed in the camptothecin resistant cells, as shown both by oligo and cDNA probes (see Fig. 1C). The changes in GST-Pi, GCS and ABCC2 expression suggest a putative “metabolic switch” necessary for resistance. As shown in Fig. 2B, these enzymes play a role in the pathway of glutathione-mediated detoxification. Consistently, two further genes belonging to the “Cysteine metabolism” ontology group (Table S4) show differential expression (cystathionine gamma-lyase and glutamate cyteine-ligase, Table S6).

Camptothecin resistance has been associated with the elevated expression of ABCG2-MXR (Brangi et al., 1999), which was observed in a sub-line of the human ovarian cancer cell line, A2780, selected against an analog of camptothecin: DX-8951f (van Hattum et al., 2002). Our results do not show elevated ABCG2 expression in RCO.1 cells, and suggest that ABCC2 may be involved in part of the resistant phenotype. Consistent with our findings, previous studies have reported MRP2 as a detoxifying transporter for camptothecin in animal models (Arimori et al., 2003) and cell lines transfected with antisense MRP2 (Koike et al., 1997). Since resistance of RCO.1 against 9NC was shown to be partially mediated by mutations in topoisomerase I, we speculate that the elevated expression of ABCC2 may play a role during the initial steps of the selection process. This early adaptation may provide the background for the evolution of further resistance mechanisms, such as mutation of topoisomerase 1 or loss of the expression of other topoisomerase(s) 1 genes (Urasaki et al., 2001).

Retroviral transfer of ABCC1 (MRP1) has been shown to result in decreased intracellular glutathione levels and increased sensitivity to BSO (Rappa et al., 2003). Furthermore, *in vitro* reversal of MRP1-mediated resistance and *in vivo* potentiation of the cytotoxicity of doxorubicin in MRP1-overexpressing tumors by BSO were previously reported (Rappa et al., 2003). In an analogous fashion, consistent with the capacity of ABCC2 to export glutathione conjugates (Konig et al., 1999), RCO.1 cells also proved hypersensitive to BSO treatment (data not shown). It is conceivable that the coordinated expression of MRP2 and GCS occur as the cells adapt to the cytotoxic stress. Since the maintenance of glutathione levels is critical for the survival of the

cells, overexpression of GCS may represent an adaptive response compensating for the loss of intracellular glutathione in the RCO.1 cells.

In conclusion, we have used a novel ABC-ToxChip to show the overexpression of two ABC transporters in two different cellular models of drug resistance. In both cases, ABC transporter overexpression occurs at the level of transcription and is prominent when compared to the pattern of expression of 18,000 other genes. Our results reinforce our interest in following the expression of ABC transporters as specific markers of acquired drug resistance. The ABC-ToxChip should be a helpful tool to assess the role of ABC transporters, and how their expression is linked to other detoxification genes in various pathophysiological processes, such as drug resistance, not only in tissue culture models, but in clinical samples as well.

Acknowledgments

We would like to thank Dr. Pantazis for the generous gift of the RCO.1 cell lines.
We are also grateful to George Leiman for editorial assistance.

References

- Akiyama S, Fojo A, Hanover JA, Pastan I, and Gottesman, MM (1985) Isolation and genetic characterization of human KB cell lines resistant to multiple drugs. *Somat Cell Mol Genet* **11**: 117-126.
- Arimori K, Kuroki N, Hidaka M, Iwakiri T, Yamsaki K, Okumura M, Ono H, Takamura N, Kikuchi M, and Nakano M (2003) Effect of P-glycoprotein modulator, cyclosporin A, on the gastrointestinal excretion of irinotecan and its metabolite SN-38 in rats. *Pharm Res* **20**:910-917.
- Brangi M, Litman T, Ciotti M, Nishiyama K, Kohlhagen G, Takimoto C, Robey R, Pommier Y, Fojo T, and Bates SE (1999) Camptothecin resistance: role of the ATP binding cassette (ABC) half-transporter, mitoxantrone-resistance (MXR), and potential for glucuronidation in MXR-expressing cells. *Cancer Res* **59**:5938-5946.
- Bushel PR, Hamadeh H, Bennett L, Sieber S, Martin K, Nuwaysir EF, Johnson K, Reynolds K, Paules RS, and Afshari CA (2001) MAPS: a microarray project system for gene expression experiment information and data validation. *Bioinformatics* **17**:564-565.
- Chatterjee D, Schmitz I, Krueger A, Yeung K, Kirchhoff S, Krammer PH, Peter ME, Wyche JH, and Pantazis P (2001) Induction of apoptosis in 9-nitrocamptothecin-treated DU145 human prostate carcinoma cells correlates with de novo synthesis of CD95 and CD95 ligand and down-regulation of c-FLIP(short). *Cancer Res* **61**:7148-7154.

- Chen Y, Kamat V, Dougherty ER, Bittner ML, Meltzer PS, Trent JM (2002) Ratio statistics of gene expression levels and applications to microarray data analysis. *Bioinformatics* **18**:1207-1215.
- Cole SP, Bhardwaj G, Gerlach JH, Mackie JE, Grant CE, Almquist KC, Stewart AJ, Kurz EU, Duncan AM, and Deeley RG (1992) Overexpression of a transporter gene in a multidrug-resistant human lung cancer cell line. *Science* **258**:1650-1654.
- Doyle LA, Yang W, Abruzzo LV, Krogmann T, Gao Y, Rishi AK, and Ross DD (1998) A multidrug resistance transporter from human MCF-7 breast cancer cells. *Proc Natl Acad Sci USA* **95**:15665-15670. Erratum in: *Proc Natl Acad Sci USA* **96**:2569, 1999.
- Evans SJ, Datson NA, Kabbaj M, Thompson RC, Vreugdenhil E, De Kloet ER, Watson SJ, and Akil H (2002) Evaluation of Affymetrix Gene Chip sensitivity in rat hippocampal tissue using SAGE analysis. *Eur J Neurosci* **16**:409-413.
- Goto S, Kamada K, Soh Y, Ihara Y, and Kondo T (2002) Significance of nuclear glutathione S-transferase pi in resistance to anti-cancer drugs. *Jpn J Cancer Res* **93**:1047-1056.
- Gottesman MM, Fojo T, and Bates SE (2002) Multidrug resistance in cancer: role of ATP-dependent transporters. *Nat Rev Cancer* **2**:48-58.
- Guo Y, Kotova E, Chen ZS, Lee K, Hopper-Borge E, Belinsky MG, and Kruh GD (2003) MRP8 (ABCC11) is a cyclic nucleotide efflux pump and a resistance factor for fluoropyrimidines, 2'3'-dideoxycytidine and 9'-(2'-phosphonylmethoxyethyl)-adenine. *J Biol Chem* **278**:29509-29514.
- Higuchi E, Oridate N, Furuta Y, Suzuki S, Hatakeyama H, Sawa H, Sunayashiki-Kusuzaki K, Yamazaki K, Inuyama Y, and Fukuda S (2003) Differentially expressed

- genes associated with CIS-diamminedichloroplatinum (II) resistance in head and neck cancer using differential display and CDNA microarray. *Head Neck* **25**:187-193.
- Horikawa M, Kato Y, Sugiyama Y (2002) Reduced gastrointestinal toxicity following inhibition of the biliary excretion of irinotecan and its metabolites by probenecid in rats. *Pharm Res* **19**:1345-1353.
- Kikuchi S, Hata M, Fukumoto K, Yamane Y, Matsui T, Tamura A, Yonemura S, Yamagishi H, Keppler D, Tsukita S, and Tsukita S (2002) Radixin deficiency causes conjugated hyperbilirubinemia with loss of Mrp2 from bile canalicular membranes. *Nat Genet* **31**:320-325.
- Knight J (2001) When the chips are down. *Nature* **410**:860-861.
- Koike K, Kawabe T, Tanaka T, Toh S, Uchiuni T, Wada M, Akiyama S, Ono M, Kuwano M (1997) A canalicular multispecific organic anion transporter (cMOAT) antisense cDNA enhances drug sensitivity in human hepatic cancer cells. *Cancer Res* **57**:5475-9.
- Konig J, Nies AT, Cui Y, Leier I, and Keppler D (1999) Conjugate export pumps of the multidrug resistance protein (MRP) family: localization, substrate specificity, and MRP2-mediated drug resistance. *Biochim Biophys Acta* **1461**:377-394.
- Kudoh S, Fujiwara Y, Takada Y, Yamamoto H, Kinoshita A, Ariyoshi Y, Furuse K, and Fukuoka M (1998) Phase II study of irinotecan combined with cisplatin in patients with previously untreated small-cell lung cancer. West Japan Lung Cancer Group. *J Clin Oncol* **16**:1068-1074.
- Laing NM, Belinsky MG, Kruh GD, Bell DW, Boyd JT, Barone L, Testa JR and Tew KD (1998) Amplification of the ATP-binding cassette transporter 2 gene is functionally

linked with enhanced efflux of estramustine in ovarian carcinoma cells. *Cancer Res* **58**:1332–1337.

Lamendola DE, Duan Z, Yusuf RZ, and Seiden MV (2003) Molecular description of evolving paclitaxel resistance in the SKOV-3 human ovarian carcinoma cell line. *Cancer Res* **63**:2200-2205.

Lee JK, Bussey KJ, Gwadry FG, Reinhold W, Riddick G, Pelletier SL, Nishizuka S, Szakacs G, Annereau JP, Shankavaram U, Lababidi S, Smith LH, Gottesman MM, Weinstein JN (2003) Comparing cDNA and oligonucleotide array data: concordance of gene expression across platforms for the NCI-60 cancer cells. *Genome Biol* **4**: R82.

Liu J, Chen H, Miller DS, Saavedra JE, Keefer LK, Johnson DR, Klaassen CD, and Waalkes MP (2001) Overexpression of glutathione S-transferase II and multidrug resistance transport proteins is associated with acquired tolerance to inorganic arsenic. *Mol Pharmacol* **60**: 302-309.

Miyake K, Mickley L, Litman T, Zhan Z, Robey R, Cristensen B, Brangi M, Greenberger L, Dean M, Fojo T, and Bates SE (1999) Molecular cloning of cDNAs which are highly overexpressed in mitoxantrone-resistant cells: demonstration of homology to ABC transport genes. *Cancer Res* **59**:8-13.

Morrow CS, Smitherman PK, and Townsend AJ (2000) Role of multidrug-resistance protein 2 in glutathione S-transferase P1-1-mediated resistance to 4-nitroquinoline 1-oxide toxicities in HepG2 cells. *Mol Carcinog* **29**:170-8.

Muller M, Meijer C, Zaman GJ, Borst P, Scheper RJ, Mulder NH, de Vries EG, and Jansen PL (1994) Overexpression of the gene encoding the multidrug resistance-

- associated protein results in increased ATP-dependent glutathione S-conjugate transport. *Proc Natl Acad Sci USA* **91**:13033-13037.
- Nuwaysir EF, Bittner M, Trent J, Barrett JC, and Afshari CA (1999) Microarrays and toxicology: the advent of toxicogenomics. *Mol Carcinog* **24**:153-159.
- Pantazis P, Han Z, Balan K, Wang Y, and Wyche JH (2003) Camptothecin and 9-nitrocamptothecin (9NC) as anti-cancer, anti-HIV and cell-differentiation agents. Development of resistance, enhancement of 9NC-induced activities and combination treatments in cell and animal models. *Anticancer Res* **23**:3623-3638.
- Paulusma CC, Bosma PJ, Zaman GJ, Bakker CT, Otter M, Scheffer GL, Scheper RJ, Borst P, and Oude Elferink RP (1996) Congenital jaundice in rats with a mutation in a multidrug resistance-associated protein gene. *Science* **271**:1126-1128.
- Rappa G, Gamcsik MP, Mitina RL, Baum C, Fodstad O, Lorico A (2003) Retroviral transfer of MRP1 and gamma-glutamyl cysteine synthetase modulates cell sensitivity to L-buthionine-S,R-sulphoximine (BSO): new rationale for the use of BSO in cancer therapy. *Eur J Cancer* **39**:120-128.
- Reid G, Wielinga P, Zelcer N, De Haas M, Van Deemter L, Wijnholds J, Balzarini J, and Borst P (2003) Characterization of the transport of nucleoside analog drugs by the human multidrug resistance proteins MRP4 and MRP5. *Mol Pharmacol* **63**:1094-1103.
- Reinhold WC, Kouros-Mehr H, Kohn KW, Maunakea AK, Lababidi S, Roschke A, Stover K, Alexander J, Pantazis P, Miller L, Liu E, Kirsch IR, Urasaki Y, Pommier Y, and Weinstein JN (2003) Apoptotic susceptibility of cancer cells selected for

camptothecin resistance: gene expression profiling, functional analysis, and molecular interaction mapping. *Cancer Res* **63**:1000-1011.

Schuetz EG, Beck WT, and Schuetz JD (1996) Modulators and substrates of P-glycoprotein and cytochrome P4503A coordinately up-regulate these proteins in human colon carcinoma cells. *Mol Pharmacol* **49**:311-318.

Shen DW, Fojo A, Chin JE, Roninson IB, Richert N, Pastan I, and Gottesman MM (1986a) Human multidrug-resistant cell lines: increased *mdr1* expression can precede gene amplification. *Science* **232**:643-645.

Shen DW, Cardarelli C, Hwang J, Cornwell M, Richert N, Ishii S, Pastan I, and Gottesman MM (1986b) Multiple drug-resistant human KB carcinoma cells independently selected for high-level resistance to colchicine, adriamycin, or vinblastine show changes in expression of specific proteins. *J Biol Chem* **261**:7762-7770.

Shen DW, Goldenberg S, Pastan I, and Gottesman MM (2000) Decreased accumulation of [¹⁴C]carboplatin in human cisplatin-resistant cells results from reduced energy-dependent uptake. *J Cell Physiol* **183**:108-116.

Smith AJ, van Helvoort A, van Meer G, Szabo K, Welker E, Szakacs G, Varadi A, Sarkadi B, and Borst P (2000) MDR3 P-glycoprotein, a phosphatidylcholine translocase, transports several cytotoxic drugs and directly interacts with drugs as judged by interference with nucleotide trapping. *J Biol Chem* **275**:23530-23539.

Szakács G, Annereau J-P, Lababidi S, Shankavaram U, Arciello A, Bussey KJ, Reinhold W, Guo Y, Kruh GD, Reimers M, Weinstein JN, and Gottesman MM (2004)

Predicting drug sensitivity and resistance: Profiling ABC transporter genes in cancer cells. *Cancer Cell* in press.

Tew RD (1994) Glutathione-associated enzymes in anticancer drug resistance. *Cancer Res* **54**:4313-4320.

Urasaki Y, Laco GS, Pourquier P, Takebayashi Y, Kohlhagen G, Gioffre C, Zhang H, Chatterjee D, Pantazis P, and Pommier Y (2001) Characterization of a novel topoisomerase I mutation from a camptothecin-resistant human prostate cancer cell line. *Cancer Res* **61**:1964-1969.

van Hattum AH, Hoogsteen IJ, Schluper HM, Maliepaard M, Scheffer GL, Scheper RJ, Kohlhagen G, Pommier Y, Pinedo HM, and Boven E (2002) Induction of breast cancer resistance protein by the camptothecin derivative DX-8951f is associated with minor reduction of antitumour activity. *Br J Cancer* **87**:665-672.

Velculescu VE, Zhang L, Vogelstein B, and Kinzler KW (1995) Serial analysis of gene expression. *Science* **270**:484-487.

Zeeberg BR, Feng W, Wang G, Wang MD, Fojo AT, Sunshine M, Narasimhan S, Kane DW, Reinhold WC, Lababidi S, Bussey KJ, Riss J, Barrett JC, and Weinstein JN (2003) GoMiner: a resource for biological interpretation of genomic and proteomic data. *Genome Biol* **4**:R28.

Notes:

This work was supported by the National Institutes of Health.

¹J-P. Annereau and G. Szakács contributed equally to this work.

²Present address for J-P. Annereau: Laboratoire de Biologie Moléculaire et Structurale, Batiment 23B, Institut de Chimie des Substances Naturelles, Centre National de la Recherche Scientifique, 1 avenue de la Terrasse, 91198 Gif Sur Yvette, France

TABLE 1

ABC probes printed on the ABC-ToxChip

Probe ^a	ABC transporter ^b	Gene bank identifier ^c	Matching exon	Probe ^a	ABC transporter ^b	Gene bank identifier ^c	Matching exon
OLIGO	ABCA1	NM-005502.1		OLIGO	ABCC3	NM-003786.2	
cDNA	ABCA1	XM-050009.5		cDNA	ABCC3	AJ294547.1	exon 3
OLIGO	ABCA2	AF178941.1		cDNA	ABCC3	AJ294559.1	exons 20-23
OLIGO	ABCA3	NM-001089.1		cDNA	ABCC3	AJ294558.1	exon 19
cDNA	ABCA3	XM-028843.2		cDNA	ABCC3	NM-020038.1	
OLIGO	ABCA4	NM-000350.1		OLIGO	ABCC4	NM-005845.1	
cDNA	ABCA4	Y15644.1	exon 10	cDNA	ABCC4	XM-036453.1	
cDNA	ABCA4	Y15676.1	exon 42	cDNA	ABCC4	AF071203.1	
cDNA	ABCA5	NM-018672.1		cDNA	ABCC4	U66686.1	
cDNA	ABCA5	XM-057257.3		cDNA	ABCC4	AF071202.1	
OLIGO	ABCA8	NM-007168.1		OLIGO	ABCC5	NM-005688.1	
cDNA	ABCA12	NM-015657.1		cDNA	ABCC5	BC007229.1	
OLIGO	ABCB1	NM-000927.2		cDNA	ABCC5	AF146074.1	
cDNA	ABCB1	M29426.1	exon 4	cDNA	ABCC5	AB005659.1	
cDNA	ABCB1	M37723.1	exon 6	cDNA	ABCC5	XM-002914.6	
cDNA	ABCB1	XM-029059.2		OLIGO	ABCC6	NM-001171.2	
cDNA	ABCB1	M29447.1	exon 28	cDNA	ABCC6	AF076622.1	
OLIGO	ABCB2	NM-000593.2		cDNA	ABCC6	AF168791.1	
cDNA	ABCB2	U07198.1	exon 4,	cDNA	ABCC6	NM-001171.2	
cDNA	ABCB2	S70260.1		OLIGO	ABCC7	NM-000492.2	
cDNA	ABCB2	NM-000593.3		cDNA	ABCC7	M55109.1	exon 4
OLIGO	ABCB3	NM-000544.2		cDNA	ABCC7	M55032.1	exon 19
cDNA	ABCB3	XM-165824.1		cDNA	ABCC7	XM-004980.4	
OLIGO	ABCB4	NM-018850.1		OLIGO	ABCC8	NM-000352.2	
cDNA	ABCB4	XM-167466.1		OLIGO	ABCC9	NM-005691.1	
cDNA	ABCB5	XM-166496.1		cDNA	ABCC11	NM-032583.2	
OLIGO	ABCB6	NM-005689.1		cDNA	ABCC12	NM-033226.1	
cDNA	ABCB6	BC000559.1		OLIGO	ABCD1	NM-000033.2	
cDNA	ABCB6	XM-050891.4		cDNA	ABCD1	BC025358.1	
OLIGO	ABCB7	NM-004299.2		OLIGO	ABCD2	NM-005164.1	
cDNA	ABCB7	XM-032877.2		OLIGO	ABCD3	NM-002858.2	
OLIGO	ABCB8	XM-032165.2		cDNA	ABCD3	BC009712.1	
cDNA	ABCB8	XM-032165.5		OLIGO	ABCD4	NM-005050.1	
OLIGO	ABCB10	NM-012089.1		cDNA	ABCD4	NM-020326.1	
cDNA	ABCB10	XM-001871.4		OLIGO	ABCE1	NM-002940.1	
OLIGO	ABCB11	NM-003742.1		cDNA	ABCE1	XM-003555.9	
OLIGO	ABCC1	NM-019902.1		OLIGO	ABCF1	NM-001090.1	
cDNA	ABCC1	AF022824.1	exon 2	cDNA	ABCF1	BC016772.1	
cDNA	ABCC1	AF022826.1	exon 4	OLIGO	ABCF2	XM-039075.1	
cDNA	ABCC1	AF022830.1	exon 8	cDNA	ABCF2	BC001661.1	
cDNA	ABCC1	AF022853.1	exon 31	cDNA	ABCF3	NM-018358.1	
cDNA	ABCC1	AJ003198.1		OLIGO	ABCG1	NM-004915.2	
cDNA	ABCC1	NM-019902.1		cDNA	ABCG1	XM-032950.3	
cDNA	ABCC1	AF022830.1	exon 8	OLIGO	ABCG2	NM-004827.1	
OLIGO	ABCC2	XM-050760.1		cDNA	ABCG2	XM-032424.1	
cDNA	ABCC2	AJ132306.1	exon 23	cDNA	ABCG2	AF098951.2	
cDNA	ABCC2	AJ245627.1	exon 26	cDNA	ABCG4 lo	XM-012099.8	
cDNA	ABCC2	U63970.1		cDNA	ABCG8	NM-022437.1	

^aOligo indicates that the probe is a single-stranded, 70 mer oligonucleotide; cDNA indicates the probe is a fragment of double-stranded DNA amplified by PCR.

^bABC transporters are named using the HGNC nomenclature (<http://nutrigene.4t.com/humanabc.htm>).

^cThe probes are named after the closest matching RefSeq entries (National Center for Biotechnology Information (NCBI), e.g., C3 (NM-003786, AJ294547.1, AJ294559.1, AJ294558.1). The exon most closely matching the sequence is indicated.

TABLE 2

Differentially expressed genes identified by two independent microarray analyses (ATC-DU-145 versus RCO.1)

Clone ID	HCNG reference	Gene description	Ratio R/S ^a Reinhold et al., 2003	Ratio R/S ^a Present study ^b
266146	CYP24A1	Cytochrome P450 XXIV	12.66	NA (1.91)
429091	H2A1	Histone 2A like protein (H2A-I)	6.93	NA (2.70)
376370		EGR-Early Growth response protein	5.22	1.94(NA)
209156	DAD1	Defender against cell death	2.29	NA (1.91)
774710	GSTP1	Glutathione-S-transferase Pi	0.12	0.12 (0.03)
810859	NK4	Natural killer cells protein-4	0.13	NA (0.25)
328692	IL8	Interleukin 8	0.13	NA (0.26)
840683	CIN	Cytokine inducible nuclear protein	0.23	NA (0.45)

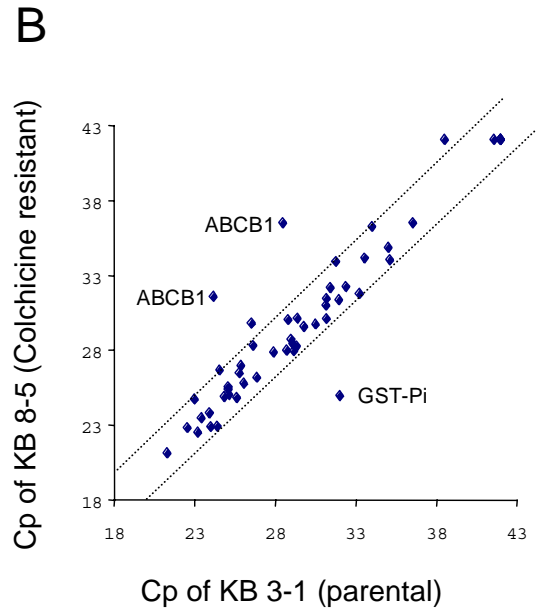
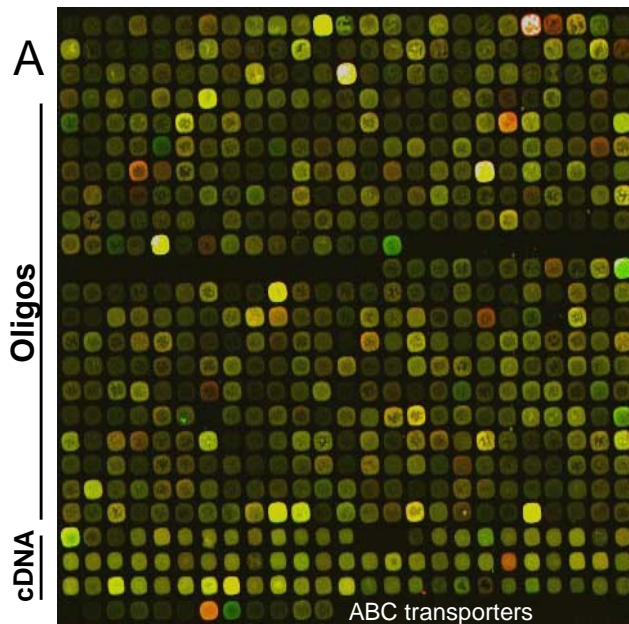
^aRelative expression, resistant versus sensitive (R/S)

^bRelative expression based on oligo and cDNA probes. Results based on cDNA probes are shown in parentheses. NA, not applicable.

Figure Legends

Fig. 1. Creation and application of the ABC-ToxChip. A, Details of a scan of the ABC-ToxChip . The section shown is one of the 32 blocks printed. The platform has 4 x 8 such blocks, each containing 625 (25 x 25) slots, yielding in total 20,000 probe-slots available for printing. The upper part of the block contains the oligo-set, and the lower part bears the cDNA probes matching the detoxification set. The probes specifically matching the ABC transporters are printed in the lowest row. B, Quantitative RT-PCR to follow transcriptional changes of ABC transporters and GST-Pi. Crossing point values of amplification for 47 ABC transporters and GST-Pi in the two samples are shown in a scatter plot. Deviations greater than 2 cycles are considered significant. Results demonstrate activation of MDR1 and downregulation of GST-Pi with colchicine resistance. C, Significant outliers (>2.7 fold) identified by the microarray experiments. ABC transporters appear as major outliers in both analyses, suggesting their strong contribution to the MDR phenotype. Genes where the variation was confirmed by more than one probe are indicated in grey. Arrows point out the most drastic changes discussed in this paper (i.e. GST and ABC transporters). OL and cD refer to oligo and cDNA probes, respectively. n defines the number of experiments (out of 4 replicates) where gene expression is found significantly altered. C.R. (calibrated ratio) indicates the fold of difference of expression between the resistant cell line versus the parental cell line.

Fig. 2. Overexpression of ABCC2 and downregulation of GST-Pi with 9NC selection. A, Confirmation of the overexpression of ABCC2, and down-regulation of GST-Pi with 9NC selection by quantitative RT-PCR. Crossing point values of amplification for 47 ABC transporters and GST-Pi in the two samples are shown in a scatter plot. B, Illustration of the role of ABCC2, GST and GCS in the glutathione-related detoxification pathway. The concentration of glutathione is regulated by its metabolism (GSH–GSX, GSH-GSSG) and biosynthesis, catalyzed by GST and GCS, respectively, and the activity of ABCC2. C, Correlation between the mRNA and protein levels. The symbols S and R correspond to the sensitive (ATC-DU-145) and resistant cell line (RCO.1), respectively. The signal for GST-Pi in the resistant cell line was below the level of detection.



C KB-3-1 versus KB-8-5

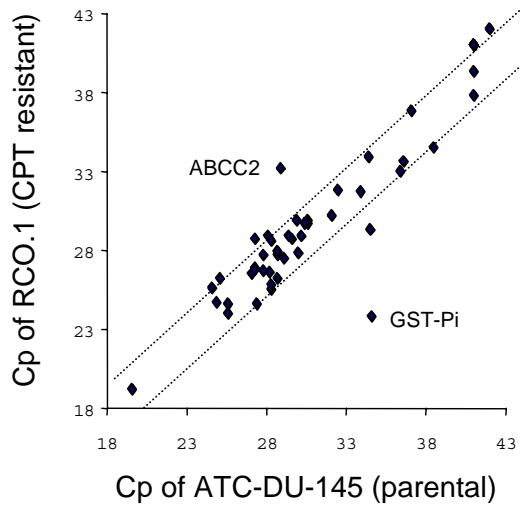
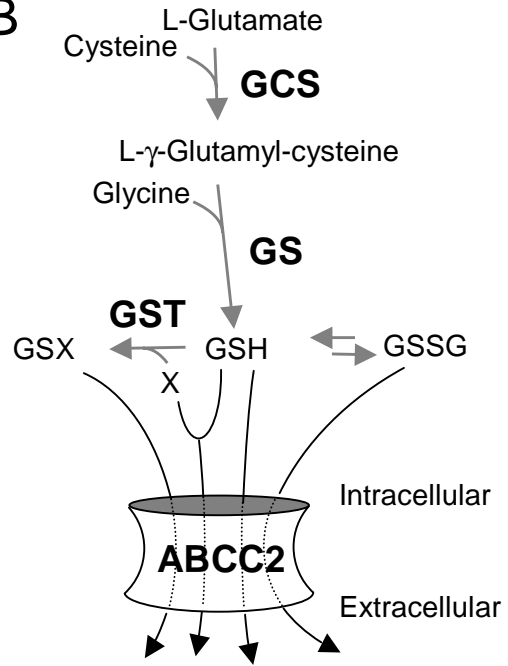
Gene ID	n	Description of up-regulated genes	C.R.
OL M29447	3	Human P-glycoprotein [MDR1] gene, exon 28	44.8
OL S70585	4	Glycoprotein hormone, alpha polypeptide	13.5
cD W86681	4	Glycoprotein hormone, alpha polypeptide	13
OL M37723	3	Human MDR1/P-glycoprotein gene, exon 6	11.3
OL M29426	3	Human P-glycoprotein [MDR1] gene, exon 4	9.39
cD W45324	4	Interleukin 8	7.19
OL X15422	3	Mannose-binding lectin 2	4.5
OL X58536	4	Major histocompatibility complex, class I, C	3.86
OL AF071596	4	Immediate early response 3	3.83
OL M80469	4	MHC class I HLA-J gene, exons 1-8	3.74
OL M12758	4	MHC class I HLA-A24 gene, exons 4,6-8	3.19
cD R80217	4	Cyclo oxygenase 2	2.99
OL M13755	4	Interferon stimulated protein	2.98

Gene ID	n	Description of down-regulated genes	C.R.
OL M38591	3	S100 calcium-binding protein A10	0.37
cD AA040702	4	Phosphoglycerate mutase 1 [brain]	0.36
OL AF225985	3	Sodium channel, voltage-gated, type I	0.36
cD R33755	4	Glutathione-S-transferase-Pi	0.35
OL AB011542	3	EGF-like-domain, multiple 5	0.35
OL U12472	3	Glutathione-S-transferase-Pi	0.06

ATC-DU-145 versus RCO.1

Gene ID	n	Description of up-regulated genes	C.R.
OL U70312	3	EGF-like repeats and discoidin-like domains 3	12.50
OL AJ132306	4	HSA132306 MRP2 gene, exon 23**	12.32
cD 376184	4	Insulin-like growth factor binding protein 3	6.88
OL M38591	4	S100 calcium-binding protein A10	5.79
cD 308366	3	Folate receptor 1	5.13
OL J02763	4	S100 calcium-binding protein A6	4.65
OL X60484	3	H4 histone family, member E	4.37
OL U00598	4	Aldo-keto reductase family 1, member C2	4.27
OL AB032261	4	Stearyl-CoA desaturase	4.07
OL U28369	3	Sema domain, immunoglobulin domain 3B	3.90
cD M30704	4	Amphiregulin	3.35
cD 203721	4	Glutamate cysteine ligase, catalytic	3.01
OL M76231	3	Sepiapterin reductase	2.96
OL X05908	4	Annexin A 1	2.82

Gene ID	n	Description of down-regulated genes NCBI	C.R.
OL Y11307	3	Cysteine-rich, angiogenic inducer, 61	0.36
OL X04741	3	Ubiquitin carboxyl-terminal esterase L1	0.35
cD 110503	4	Fos Related Antigen 1	0.35
cD 484963	4	Metallothionein from cadmium treated cells	0.33
OL M24283	3	Intercellular adhesion, human rhinovirus receptor	0.32
OL M90657	4	Transmembrane 4 super family member 1	0.32
OL S52784	3	Cystathionase	0.31
cD 328692	4	Interleukin 8	0.26
OL AJ270993	4	Homeobox B6	0.25
OL M59807	3	Natural killer cell transcript 4	0.25
OL X16172	4	Human HOX-2.5 gene for homeodomain protein	0.17
cD 136235	4	Glutathione-S-transferase-Pi	0.12
OL U12472	4	Glutathione-S-transferase-Pi	0.03

A**B****C**